Fakultät für Medizin
Institut für Virologie

Generation and characterization of novel human monoclonal antibodies directed against the hepatitis B virus

Lisa Sophia Wolff

Vollständiger Abdruck der von der Fakultät für Medizin der Technischen Universität München zur Erlangung des akademischen Grades eines

Doktors der Naturwissenschaften (Dr. rer. nat.)

genehmigten Dissertation.

Vorsitzender: Prof. Dr. Dirk Busch

Prüfende/-r der Dissertation:

1. Prof. Dr. Ulrike Protzer
2. Prof. Dr. Aphrodite Kapurniotu

Die Dissertation wurde am 30.06.2020 bei der Technischen Universität München eingereicht und durch die Fakultät für Medizin am 01.12.2020 angenommen.

Table of contents

Abstract

Although an effective, prophylactic vaccine is available, 257 million people worldwide are chronically infected with the hepatitis B virus (HBV). This represents a major health concern. These people are at risk to develop liver cirrhosis and hepatocellular carcinoma. Current standard therapies only suppress the viral replication, but fail to eradicate the infection completely. This is due to the viral replication template, the covalently closed circular DNA (cccDNA) of HBV, which remains in the nucleus of infected cells. A broad HBV-specific immune response seems to be essential for virus control, but in chronic HBV infection both, T cells as well as B cells are absent or functionally impaired. This is believed to be due to the continuous high load of circulating hepatitis B surface antigen (HBsAg). Therefore, new immunotherapeutic approaches are needed that aim at the restoration of the patients' immune response in order to detect and eliminate HBV infected cells.

High titer serum antibodies against HBsAg are associated with resolution of an HBV infection. Thus, the application of HBV-specific antibodies represents an interesting and promising immunotherapeutic approach. Antibodies in polyclonal hepatitis B immunoglobulin preparations are already used clinically for the prevention from infection. However, the therapeutic use of antibodies, in order to support the defective B-cell response in chronically infected humans is so-far limited. This is due to the high production cost for polyclonal sera and the limited availability of potent binders.

In order to overcome this lack of suitable binders, the overall aim of this study was to generate novel, fully human recombinant monoclonal antibodies against HBsAg from single memory B cells. Therefore, first, the frequency of HBV-specific memory B cells in peripheral blood of healthy, vaccinated individuals was estimated using the ELISpot technique. It detected a frequency of 0.01% of HBsAg-specific B cells in PBMC. This was low but sufficient to continue with B-cell isolation. Following that, three baits for the selective isolation of HBV-specific B cells with flow cytometry were evaluated. The data revealed that Alexa647-SVPs, HBsAg-Alexa594 and HBsAg-biotin could be used for HBV-specific B-cell sorting. These baits were then used to isolate antigen-specific memory B cells. In a next step, the isolated B cells were cultured either in the presence of Epstein-Barr virus or on CD40L-expressing feeder cells to promote the outgrowth of antibody secreting cells. However, B-cell

cultures did not result in stable B-cell lines secreting HBsAg-specific antibodies. Thus, these cells could not be used to develop recombinant monoclonal antibodies (mAbs). In parallel, single cell sorting with the different HBV-baits and subsequent antibody cloning was established. Using this, 76 monoclonal antibodies were generated and evaluated for HBsAg-specificity. However, only nine were antigen-specific, but among those two 4D06 and 4D08 indicated strong antigen reactivity.

In the second part of this thesis, the two newly generated monoclonal antibodies 4D06 and 4D08 were structurally and functionally characterized. Initially, 4D06 and 4D08 were transiently expressed in HEK293 cells and purified from cell culture supernatant. Purified mAbs revealed high antigen affinity determined by ELISA with EC_{50} values in the nanomolar range. The analysis of the antibody epitopes indicated a conformation dependent epitope for 4D06, whereas 4D08 seemed to recognize a linear epitope. However, the exact location still needs to be determined. Furthermore, the neutralization capacity of both mAbs was investigated. 4D06 and 4D08 indicated a concentration dependent broad neutralization capacity against HBV genotypes A-H, with 4D06 being superior to 4D08. The strongest neutralization capacity was shown against HBV genotype A. In contrast, the neutralization of genotype B was least efficient. Nevertheless, 4D06 as well as 4D08 were classified as broadly neutralizing monoclonal antibodies. In addition, both mAbs were capable of capturing soluble HBsAg from HBV-infected cells, indicating the potential to not only prevent HBV infection by blocking the virus attachment, but also to be used after an infection occurred. Besides antigen binding, the antibody effector function was assessed. The data indicated that the Fc region of both was preferentially recognized by Fc gamma receptor III (CD16), which is expressed on the surface of reporter cells and human NK cells.

Taken together, the present study shows that high affinity broadly neutralizing, fully human monoclonal antibodies against HBsAg can be generated from single HBV-specific memory B cells of healthy HBV-vaccinated volunteers. On the basis of these data, 4D06 and 4D08 should be characterized further in *in vivo* studies to enable a more detailed understanding of their function for a potential therapeutic application.

Zusammenfassung

Trotz der Verfügbarkeit eines effektiven, prophylaktischen Impfstoffs sind weltweit etwa 257 Millionen Menschen chronisch mit dem Hepatitis B Virus (HBV) infiziert. Dies stellt ein großes Gesundheitsproblem dar. Menschen mit chronischer Hepatitis B haben ein erhöhtes Risiko an Leberzirrhose und hepatozellulärem Karzinom zu erkranken, für welches es bislang nur unzureichende Behandlungsmöglichkeiten gibt. Nur selten wird das Virus mit Hilfe von aktuell zugelassenen Therapeutika eliminiert, da diese die virale kovalent geschlossene zirkuläre DNA (cccDNA) in infizierten Zellen nicht beseitigen. Die cccDNA verbleibt im Zellkern der infizierten Hepatozyten und kann nach Beendigung der antiviralen Therapie als viral Replikationsvorlage zur Wiederherstellung des Virus dienen. Um das Virus kontrollieren zu können ist eine breite HBV-spezifische Immunantwort notwendig. In Patienten mit chronischer HBV Infektion fällt jedoch auf, dass sowohl virus-spezifische T-Zellen als auch B-Zellen nicht vorhanden oder funktional eingeschränkt sind. Als Ursachen wird eine hohe und ständige Stimulation der Zellen durch das Hepatitis B Oberflächen Antigen (HBsAg) gesehen. Neue immuntherapeutische Ansätze versuchen daher die Immunantwort des Patienten wiederherzustellen, um virus-infizierte Zellen zu identifizieren und zu eliminieren.
Ein hoher Serumtiter von HBsAg-spezifischen Antikörpern steht in direktem Zusammenhang mit der Ausheilung einer HBV Infektion. Daher stellt die Anwendung von HBV-spezifischen Antikörpern zur immuntherapeutischen Behandlung chronischer Hepatitis B einen interessanten und vielversprechenden Ansatz dar. Antiköper in polyklonalen Immunglobulin-Präparationen werden bereits sehr erfolgreich zur Prävention der Infektion verwendet. Im Gegensatz dazu, ist die therapeutische Anwendung bislang eher begrenzt. Dies liegt insbesondere an den hohen Kosten für die Herstellung von polyklonalen Serumpräparaten, aber auch daran, dass geeignete Antigenbinder fehlen.

Ziel dieser Dissertation war es daher, dem Fehlen solcher Binder entgegen zu treten, in dem neue, vollständig humane, rekombinante monoklonale Antikörper entwickelt wurden, welche gegen HBsAg gerichtet sind. Als Ausgangsmaterial sollten einzelne B-Gedächtniszellen verwendet werden. Dazu wurde zunächst die Häufigkeit von HBV-spezifischen B-Gedächtniszellen im peripheren Blut gesunder

und geimpfter Spender mittels ELISpot untersucht. Es konnte eine Frequenz von 0,01% an HBsAg-spezifischen B-Zellen in mononukleären Zellen des peripheren Blutes bestimmt werden, welche als ausreichend für die spätere Isolation dieser Zellen erachtet wurde. Im nächsten Schritt wurden drei Köder zur gezielten Isolierung der antigen-spezifischen B-Zellen mittels Durchflusszytometrie untersucht. Alle drei Köder, Alexa647-SVPs, HBsAg-Alexa594 und HBsAg-biotin zeigten eine selektive Bindung und konnten zur Identifizierung der HBV-spezifischen B-Zellen verwendet werden. Im Anschluss wurden die Köder verwendet um antigen-spezifische B-Zellen mittel Zellsortierung zu isolieren. Die isolierten B-Zellen wurde entweder in Anwesenheit von Epstein-Barr Virus oder in Gegenwart von CD40L-exprimierenden Nährzellen kultiviert. Leider konnten nach der Kultur keine HBsAg-spezifischen Antikörper im Zellkulturüberstand nachgewiesen werden. Somit konnten diese Zellen nicht zur Erzeugung neuer Antikörper verwendet werden.

Parallel dazu wurden antigen-spezifische B-Zellen direkt nach der Isolierung mittel Einzelzellsortierung lysiert und deren mRNA genutzt um rekombinante Antikörper zu klonieren. Insgesamt wurden 76 neue Antikörper generiert. In der anschließenden Spezifitätsbestimmung mittels ELISA wurde jedoch festgestellt, dass lediglich neun Antikörper reaktiv gegen HBsAg waren. Zwei Antikörper, 4D06 und 4D08 zeigten dabei eine sehr starke Reaktion.

Im zweiten Teil der Dissertation wurden die beiden neuen rekombinanten HBV-spezifischen Antikörper 4D06 und 4D08 hinsichtlich ihrer strukturellen und funktionalen Eigenschaften charakterisiert. Hierzu wurden die Antikörper zunächst in HEK293 Zellen transient exprimiert und anschließend aus dem Zellkulturüberstand gereinigt. Die Affinität der Antikörper wurde mittels ELISA abgeschätzt. Für beide Antikörper wurden EC_{50}-Werte im nanomolaren Bereich ermittelt welche mit einer hohen Affinität für HBsAg korrelieren. Die weitere strukturelle Untersuchung ergab, dass der Antikörper 4D06 ein konformationelles Epitop erkennt, wohin gegen für 4D08 ein lineares Epitop ermittelt wurde. Die genaue Position der Epitope konnte jedoch nicht bestimmt werden. Hinsichtlich der Funktionalität wiesen beide Antikörper eine konzentrationsabhängige, breit neutralisierende Kapazität gegenüber der untersuchten HBV Genotypen A-H auf. Am besten wurde Genotyp A neutralisiert wohingegen die Neutralisationsfähigkeit am schwächsten gegenüber Genotyp B war. Neben der Antigenbindefähigkeit wurde auch die Effektorfunktion der Antikörper

untersucht. Es konnte gezeigt werden, dass die Fc Regionen beider Konstrukte bevorzugt von Fc gamma Rezeptor III (CD16) erkannt werden, welches durch die Aktivierung von Reporterzellen und humanen natürlichen Killerzellen gezeigt werden konnte.

Zusammenfassend zeigt die vorliegende Dissertation, dass hoch affine, breit neutralisierende humane monoklonale Antikörper gegen HBsAg aus einzelnen HBV-spezifischen B-Gedächtniszellen des peripheren Blutes entwickelt werden können. Für eine potentielle therapeutische Anwendung der Antikörper 4D06 and 4D08 sind jedoch noch weitere Charakterisierungsstudien nötig, um ein besseres Verständnis über deren Funktion zu erhalten.

Abbreviations

AA	amino acid
ADCC	antibody dependent cell cytotoxicity
ADCP	antibody dependent cellular phagocytosis
ADCs	antibody drug conjugates
Alexa594	Alexa Fluor 594
Alexa647	Alexa Fluor 647
ALL	acute lymphocytic leukemia
APCs	antigen presenting cells
ASCs	antibody secreting cells
BCR	B cell receptor
BFA	brefeldin A
BiTEs	bi-specific T cell engager antibodies
bp	base pair
Bregs	regulatory B cells
BSA	bovine serum albumin
bsAbs	bi-specific antibodies
CAR	chimeric antigen receptor
cccDNA	covalently closed circular DNA
CD	cluster of differentiation
cDNA	complementary DNA
CDRs	complementarity determining regions
C_H	constant heavy chain
CHB	chronic hepatitis B
C_L	constant light chain
CMV	cytomegalovirus
CTLA-4	cytotoxic T-lymphocyte associated protein-4
ctrl	control
CV	column volume
D	diversity
DCs	dendritic cells
DMEM	Dulbecco’s Modified Eagle Medium

DMSO	dimethyl sulfoxide
DNA	deoxyribonucleic acid
EBV	Epstein-Barr Virus
EDTA	ethlenediaminetetraacetic acid
EL	elution
ELISA	Enzyme-linked immunosorbant assay
ELISpot	Enzyme-linked immune spot assay
EMA	European Medicine Agency
EpCAM	Epithelial cell adhesion molecule
ER	endoplasmic reticulum
ETV	entecavir
FACS	fluorescence activated cell sorting
Fc	fragment crystallizable
FcγRs	Fc gamma receptors
FcRL5	Fc receptor like protein 5
FcRs	Fc receptors
FCS	fetal calf serum
FDA	Food and Drug Administration
FL	flow through
FMO	fluorescence minus one
FR	framework region
GCs	germinal centers
h	hours
HBc	HBV core protein
HBeAg	hepatitis B e antigen
HBIg	hepatitis B immunoglobulins
HBsAg	hepatitis B surface antigen
HBV	hepatitis B virus
HBV Env	HBV envelope protein
HBx	HBV X protein
HCC	hepatocellular carcinoma
HCV	hepatitis C virus
HDV	hepatitis delta virus

Hep	heparin
HIV	human immunodeficiency virus
HRP	horseradish peroxidase
HSPG	heparin sulfate proteoglycan
IFNγ	interferon gamma
IFNs	interferons
Ig	immunoglobulin
IgD	immunoglobulin D
IgE	immunoglobulin E
IgG	immunoglobulin G
IgM	immunoglobulin M
IL	interleukin
IL-10	interleukin 10
IL-12	interleukin 12
IL-18	interleukin 18
IL-2	interleukin 2
IL-4	interleukin 4
ISRE	interferon stimulated response elements
IU	international units
J	joining
KIR	killer Ig-like receptor
L	liter
LCLs	lymphoblastoid cell lines
mA	milliamps
mAb	monoclonal antibody
mAbs	monoclonal antibodies
MVBs	multivesicular bodies
MFI	Mean Fluorescence Intensity
mg	milligram
MHC	major histocompatibility complex
MHR	major hydrophilic region
min	minutes
Mip1b	macrophage proinflammatory protein 1 beta

mL	milliliter
MOI	multiplicity of infection
mRNA	messenger RNA
n.d.	not determined
NAPs	nucleic acid polymers
neg. ctrl	negative control
ng	nanogram
NK cells	natural killer cells
nm	nanometer
nM	nanomolar
NTCP	sodium taurocholate cotransporting polypeptide
NUCs	nucleos(t)ide analogues
OD	optical density
ORF	open reading frame
PBMC	peripheral blood mononuclear cells
PBS	phosphate buffered saline
PCR	polymerase chain reaction
PD-1	programmed cell death protein 1
PD-L1	PD Ligand 1
PE	phycoerytrin
PEG	polyethylene glycol
Peg-IFNα	pegylated interferon alpha
PEI	Paul Ehrlich Institute
Pen/Strep	penicillin / streptomycin
pgRNA	pre-genomic RNA
pos. ctrl.	positive control
PrP	prion protein gene
PRR	pattern recognition receptors
qPCR	quantitative PCR
rcDNA	relaxed circular DNA
RIG-I	retinoic acid inducible gene-I
RNA	ribonucleic acid
RNAse	ribonuclease

rpm	rounds per minute
RT	room temperature
RT-PCR	reverse transcriptase PCR
s	seconds
scFv	single chain fragment variable
SD	standard deviation
SDS-PAGE	sodium dodecyl sulfate polyacrylamide gel electrophoresis
SVP(s)	subviral particle(s)
T	temperature
TCR	T cell receptor
TGF-β	transforming growth factor beta
TLRs	Toll-like receptors
TMB	3,3',5,5''-tetramethylbenzidine
TNFα	tumor necrosis factor alpha
U	units
V	variable
V_H	variable heavy chain
V_L	variable light chain
µg	microgram
µL	microliter

1 Introduction

1.1 Hepatitis B Virus Infection

Hepatitis B is a potentially life-threatening liver infection that can cause an acute or chronic disease. Although an effective, prophylactic vaccine is available, worldwide approximately 257 million individuals are chronically infected with hepatitis B virus (HBV). These humans are at risk of developing liver cirrhosis and hepatocellular carcinoma (HCC). In 2015, more than 800,000 humans died in consequence of HBV-associated diseases (World Health Organization, 2019).

1.1.1 Hepatitis B Virus structure and replication cycle

The hepatitis B virus belongs to the family of *Hepadnaviridae*. It is an enveloped virus with a partially double stranded DNA genome and was first described 1970 by *Dane et al.* (Dane et al., 1970). Nine HBV genotypes (A-I) and four serotypes (*adw*, *ayw*, *adr*, *ayr*) with a different distribution worldwide are currently known (Kramvis, 2014). HBV genotypes A-E were estimated to cause 96% of chronic infections worldwide. Among these, infections with genotype C are most frequent (Velkov et al., 2018). The virus has a high tropism for hepatocytes and a narrow host range, as it only infects humans and chimpanzees (Wieland, 2015). Infectious virions (Dane particles) have a spherical, double-shelled shape and are 40-42 nm in diameter.

The HBV genome is a partially double stranded relaxed circular DNA (rcDNA) of about 3.2 kb length. Together with the HBV polymerase, a reverse transcriptase, it is surrounded by the viral capsid, which consists of 180-240 copies of HBV core proteins (HBc) (Seeger & Mason, 2015; Wynne et al., 1999). Host cell lipids and three variants of viral envelope proteins (HBV Env) make up the viral envelope, which covers the nucleocapsid. All HBV Env proteins share the same C-terminal domain, but differ in their N-terminal part, due to different start codons for protein translation. The small (S) envelope protein, a 226 amino acids long protein is made up of the C-terminal S-domain. The medium (M) HBV Env protein carries the S-domain and an addition of 55 amino acids, the preS2-domain. A further addition of 107 amino acids is defined as preS1-domain, which forms together with the S- and preS2-domain the large (L) HBV Env protein (Figure 1) (Seeger & Mason, 2015). All three proteins are transmembrane proteins, with certain parts exposed to the cytosol

or the lumen and a complex three-dimensional structure that is stabilized by several disulfide bonds (Bruss, 2004; Suffner et al., 2018).

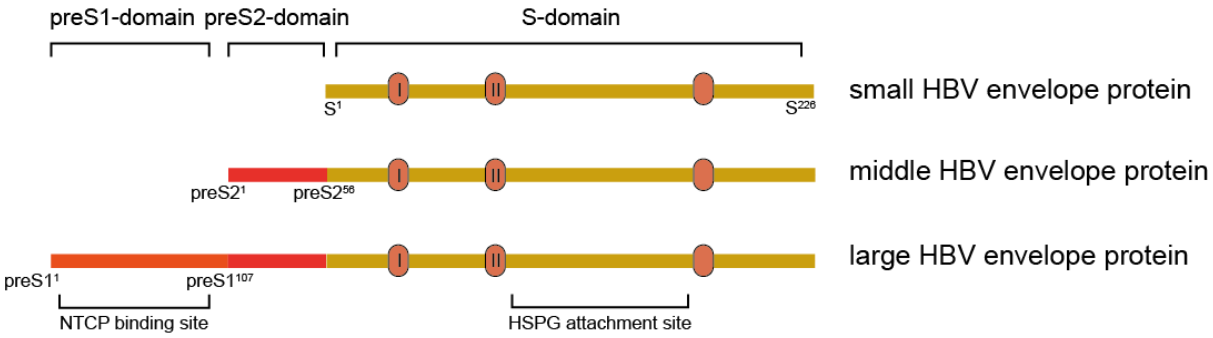

Figure 1. Illustration of S-, preS2- and preS1-domains of HBV envelope proteins
Small HBV envelope (HBV Env) proteins contain 226 amino acid S-domain (yellow), including several transmembrane domains and the heparan sulfate proteoglycan (HSPG) attachment site; the middle HBV Env proteins have a N-terminal extinction of 56 amino acids, the preS2-domain (red); Large Env proteins consists of a further N-terminal addition, the preS1-domain with 107 amino acids. It contains the NTCP binding site. Scheme adapted from (Cao et al., 2019)

The viral replication cycle is depicted in Figure 2. The first attachment of virions with hepatocytes is mediated by an unspecific binding to heparan sulfate proteoglycans (HSPG). Afterwards, specific binding to the cellular receptor sodium taurocholate cotransporting polypeptide (NTCP) occurs (Yan et al., 2012). In a next step, the virus is endocytosed and the envelope fuses with the endosomal membrane, which leads to the release of the viral capsid into the cytosol. The capsid is then transported to the nucleus, where the rcDNA of HBV is imported. With support of the host cell repair machinery, the rcDNA is repaired to form the covalently closed circular DNA (cccDNA) of HBV. cccDNA serves as the viral replication template, from which viral mRNAs are transcribed and consequently viral proteins are translated. In addition to HBc and HBV Env proteins, the HBV X (HBx) protein and the hepatitis B e antigen (HBeAg) are translated. While the HBeAg is secreted and has immunoregulatory function, the HBx protein serves as enhancer for viral transcription and is believed to play an important role in the progression to HBV-associated HCC (Levrero & Zucman-Rossi, 2016; D. Milich & Liang, 2003; Seeger & Mason, 2015). A pre-genomic RNA (pgRNA) is also transcribed, which is, upon binding to the HBV polymerase packed into viral capsids. Upon encapsidation, the polymerase reverse transcribes the pgRNA into rcDNA (Seeger & Mason, 2015).

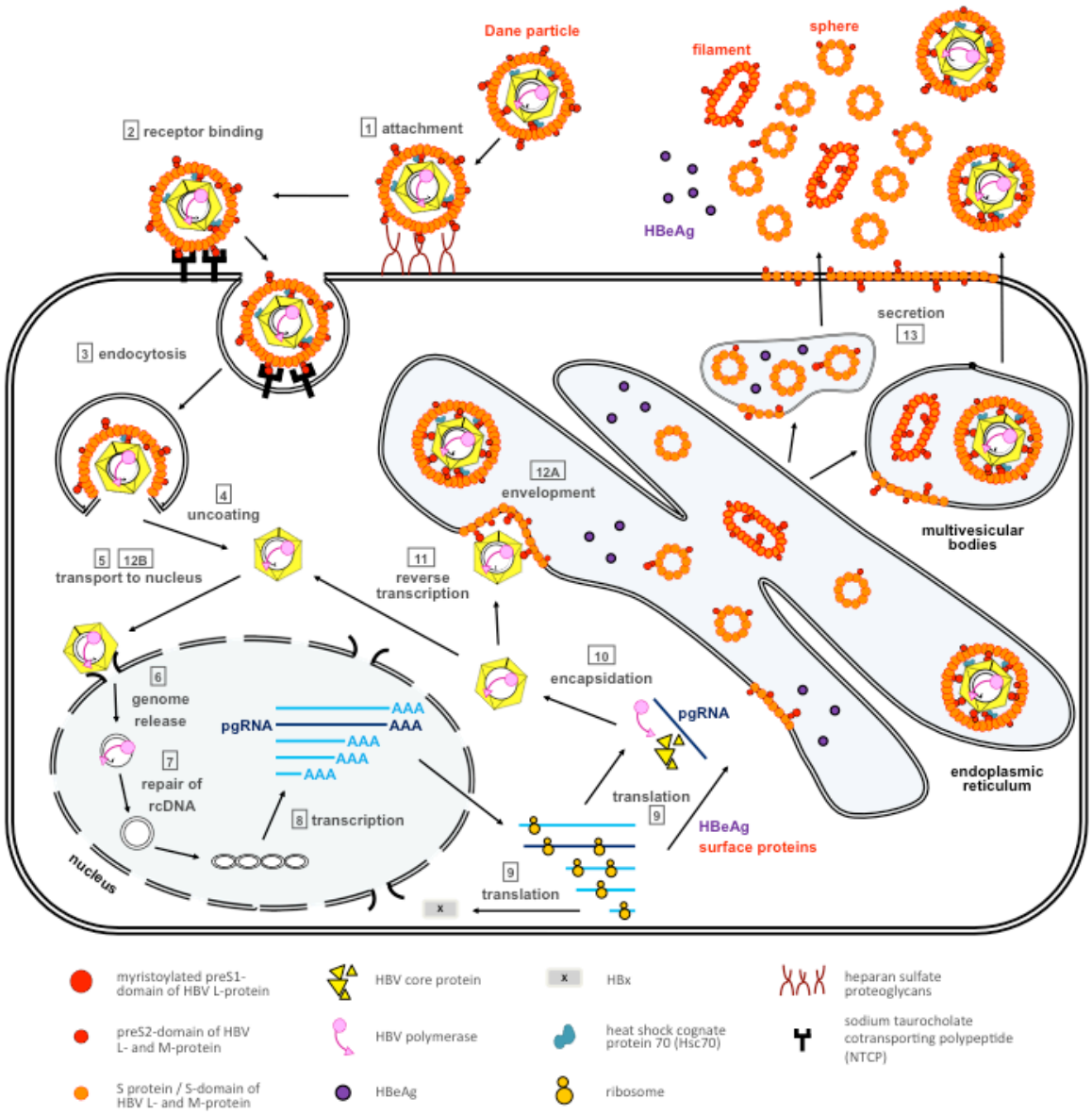

Figure 2. Hepatitis B Virus replication cycle
(1) Upon first attachment via heparan sulfate proteoglycans, (2) HBV binds to the cellular receptor sodium taurocholate cotransporting polypeptide. (3) The virus is endocytosed and fusion of the virus envelope with the endosomal membrane (4) releases the nucleocapsid in the cytosol. (5) The capsid is transported to the nucleus and (6) rcDNA is imported. (7) In the nucleus, rcDNA is repaired to form cccDNA, which serves as replication template to transcribe viral mRNAs (8). (9) Upon protein translation, (10) pgRNA and HBV polymerase are encapsidated. (11) After rcDNA formation by reverse transcription, the viral capsid can either be reimported to the nucleus (12b) or is enveloped (12a) by envelope proteins small (S), middle (M) and large (L). The formation of multivesicular bodies, allows the secretion of new infectious particles from the cell (13). Empty subviral particles (filaments or spheres), as well as HBeAg are also released. Besides the formation of the viral envelope, HBV Env proteins S, M, and L can additionally end up on the surface of infected cells. Scheme adapted from (Ko et al., 2017).

From now on, the viral capsids can take two routes. On the one hand, the capsid can be recycled and is shuttled back to the nucleus and rcDNA is imported similar to new

incoming viral capsids, to constantly stabilize the pool of cccDNA. On the other hand, the capsid can be enveloped at the endoplasmic reticulum (ER) and virions can be released from the cell via the formation of multivascular bodies (MVBs) (Seeger & Mason, 2015; Watanabe et al., 2007). Besides DNA containing infectious particles, HBV has the ability to secrete massive amounts of so-called subviral particles (SVPs). These are empty non-infectious rcDNA-free particles of spherical or filamentous form. SVPs can be detected in the blood of patients as soluble hepatitis B surface antigen (HBsAg). Spheres are secreted via the ER secretory pathway, while the filaments seem to be released via the MVB pathway (Jiang et al., 2015; Patient et al., 2009; Seeger & Mason, 2015; Watanabe et al., 2007). Furthermore, fusion of cell membrane with MVBs may also explain, how viral envelope proteins end up on the surface of infected hepatocytes (Safaie et al., 2016).

1.1.2 Course of HBV infection

1.1.2.1 Acute versus chronic infection

Infection with HBV can take two clinical routes. One is the acute, self-limiting course of infection that is seen in 90% of adults who will become infected. It is usually an asymptomatic infection, but in rare cases it can lead to fulminant hepatitis, associated with acute liver failure and death (World Health Organization, 2019). The other outcome of HBV infection is the chronic course of infection, which persists and is defined by the presence of HBsAg for more than six months in blood or serum of patients (Cornberg et al., 2011). The risk of progressing from acute to chronic infection is closely age related. 95% of infants and young children, mostly infected via vertical transmission at birth from their HBV-positive mothers, develop the chronic form. This is in contrast to only 5% of adults. Besides vertical transmission, HBV can be transmitted via blood, blood products or unprotected sexual contact (Peeridogaheh et al., 2018).

For virus clearance a strong interplay of the innate and adaptive immune response is needed (Guidotti & Chisari, 2006). The acute HBV infection is characterized by a strong and multispecific T- and B-cell response (Chisari et al., 2010; A. Tan et al., 2015). T cells produce antiviral cytokines and co-stimulate B cells which then secrete antibodies against different viral proteins (Maini et al., 1999; D. R. Milich et al., 1987; Thimme et al., 2003). Antibodies directed against HBV Env proteins (anti-HBs) do not only clear antigens and viruses from the circulation, but are also capable of

preventing re-infection (Neumann-Haefelin & Thimme, 2018). Although HBV itself is a non-cytopathic virus, the host immune response induces inflammation and liver damage (Guidotti & Chisari, 2006). In contrast, in chronic HBV carriers, the immune response is impaired. HBV-specific T cells are only detected in very low frequency and are functionally exhausted (Boni et al., 2007). HBV-specific B cells, are present, but defective and do not produce high affinity neutralizing antibodies (Burton et al., 2018; Salimzadeh et al., 2018). This is why patients with a weak immune system (due to immunosuppressive chemotherapy or immunodeficiency) are at high risk for developing chronic hepatitis B (CHB) (Cornberg et al., 2011). In addition, the constant weak ongoing immune response is associated with continuous hepatocyte destruction and regeneration and thus can lead to liver fibrosis, cirrhosis and HCC (Guidotti & Chisari, 2006).

1.1.2.2 HBV-associated liver cirrhosis and HCC

Hepatocellular carcinoma (HCC) has become the fourth most common cause of cancer related deaths worldwide and 80% of global HCC cases are related to chronic HBV and hepatitis C virus (HCV) infection (J. D. Yang et al., 2019). With regard to HBV infection, at least three molecular mechanisms are proposed for the development of HCC: The first is related to the constant inflammation and regeneration of hepatocytes, which promotes cellular DNA synthesis and cell division in order to counterbalance the loss of hepatocytes due HBV-specific T-cell killing (Guidotti & Chisari, 2006). The second mechanism relies on the integration of viral DNA into the host cell genome. Integration of the HBV genome into the cellular genome is found in 80-95% of HCC cases and can lead to disruption of gene expression (Peeridogaheh et al., 2018). This may lead to the activation of proto-oncogenes or the inactivation of tumor suppressor genes, resulting in increased cell growth and finally in the onset of hepatocarcinogenesis due to the accumulation of mutations (An et al., 2018). Lastly, the expression of viral proteins, especially the HBx and HBV Env proteins have been suggested to be an important trigger for the development of HBV-related HCC (Guidotti & Chisari, 2006). HBx is a regulatory protein that can directly act on chromatin function and transcription and thereby lead to silencing of tumor suppressor genes and chromosomal instability (Jung et al., 2007; Levrero & Zucman-Rossi, 2016). HBV Env proteins can accumulate in the endoplasmic reticulum (ER) membrane, which may lead to ER

stress, DNA damage and genomic instability (Levrero & Zucman-Rossi, 2016; Pollicino et al., 2014).

1.1.3 Prophylaxis and current treatment options

1.1.3.1 Active and passive immunization

HBV infection can efficiently be prevented by prophylactic vaccination with recombinant HBsAg. The recombinant vaccine was first introduced in 1986 and is recommended for all infants and particularly for those born in regions of high endemic such as Africa and South East Asia. Furthermore, it is recommended for every person who is at risk for instance health care workers (World Health Organization, 2019). Upon vaccination, protective anti-HBs antibodies are induced, that are capable of preventing from infection in more than 95% of vaccinated individuals (World Health Organization, 2019). Besides the active immunization with the HBV vaccine, also passive immunization with Hepatitis B immunoglobulins preparations (HBIg) is possible. HBIg is derived from plasma of donors with high anti-HBs titers and can be given to unvaccinated people as post-exposure prophylaxis, to infants born from infected mothers to prevent vertical transmission and to patients after liver transplantation to avoid re-infection (Terrault et al., 2018). Prevention of mother-to-child transmission has been shown to be highly effective, when a combination of active and passive immunization is applied (Wong et al., 1984).

1.1.3.2 Current therapeutic options for chronic HBV infection and HCC

While the prophylactic vaccine is very efficient in preventing infection, the current treatment options for chronic HBV infection are limited with regard to a complete virus clearance. Currently there are two treatment strategies available, which is the therapy with pegylated interferon alpha (Peg-IFNα) or nucleos(t)ide analogues (NUCs). Peg-IFNα modulates the innate immune response, has direct antiviral effect and can thereby induce stable HBV suppression. However, the frequency of patients that achieve HBsAg loss and virus clearance is low and Peg-IFNα treatment can be accompanied by severe side effects (European Association for the Study of the Liver. Electronic address & European Association for the Study of the, 2017; Fanning et al., 2019; Perrillo, 2009). NUCs selectively inhibit the viral polymerase, which results in reduced virion production and an efficient suppression of the viral

replication. Viral protein production, especially of HBV Env proteins, is not affected and subviral particle secretion is maintained (Liang et al., 2015). At present there are six EMA-approved NUCs available (lamivudine, adefovir dipivoxil, entecavir (ETV), telbivudine, tenofovirdisoproxil fumarate and tenofovir alafenamide), which are well tolerated, but differ in their barrier against HBV drug resistance (European Association for the Study of the Liver. Electronic address & European Association for the Study of the, 2017). In contrast to Peg-IFNα, which is a finite therapy, NUCs have to be taken for years in order to achieve undetectable serum HBV DNA or loss of serum HBsAg (Locarnini et al., 2015; Seto et al., 2016).

Although both therapeutic options suppress the viral replication, improve hepatic function and can prevent from progression to cirrhosis and HCC, they mostly fail in eradicating HBV completely (Liang et al., 2015). This is due to the intranuclear pool of cccDNA, which is hardly targeted and can serve as replication template, upon treatment discontinuation and thus can result in rebound of viremia. Therefore, the current goal of therapy is a “functional cure”. This is a clinical status defined by the sustained loss of serum HBsAg, with or without the seroconversion of anti-HBs antibodies and undetectable viral DNA (Revill et al., 2019). At present, only less than 10% of patients chronically infected with HBV achieve this (Kim et al., 2014; Zoulim & Durantel, 2015). Consequently, new strategies are needed to prevent from reoccurrence of infection upon treatment cessation by targeting the HBV cccDNA in infected hepatocytes.

Prognosis is poor for patients with chronic HBV infection that develop HCC. At early stages of HCC, liver transplantation and hepatic resection are curative options with an overall survival rate of at least 70% (Raza & Sood, 2014). However, most patients with HCC are diagnosed late and thus surgical resection is restricted. For more advanced stages of HCC, the standard of care is sorafenib treatment (Villanueva, 2019). Sorafenib is a tyrosine kinase inhibitor, inhibiting angiogenesis and tumor cell proliferation (Llovet et al., 2008; Raza & Sood, 2014). Unfortunately, sorafenib therapy only prolongs survival by several months (Llovet et al., 2008). Currently, several further treatment options are under investigation, but have so far not resulted in improved survival compared with sorafenib (Villanueva, 2019).

This shows once more that there is not only a need of developing effective treatment options for HCC, but also the high importance of HBV elimination as one major cause for HCC development.

1.2 Adaptive and innate immunity

The immune system protects humans from several dangerous threats including infections with pathogens such as bacteria, viruses and fungi. Additionally, it helps to detect and eliminate malignant cells. Immune responses can be divided into the innate and the adaptive branch. Both work closely together to eliminate a pathogen. The innate arm is usually the first line of response. It is not specific to a particular antigen and involves innate mediators such as cytokines, natural killer cells (NK) and phagocytic cells. Adaptive responses are highly specific, but take longer to be established as these depend on the development of lymphocytes with various specificities. T cells or T lymphocytes provide cell-mediated immune responses and are capable of direct killing of infected cells, while B cells or B lymphocytes mediate the humoral response, by secreting antibodies that can capture antigens in the circulation (Biron, 2016; Murphy & Weaver, 2017).

1.2.1 Innate immunity

When infection occurs, the innate immune response is immediately capable of recognizing a pathogen (or danger) and thus mediating protection. Innate receptors, so-called pattern recognition receptors (PRR), recognize certain determinants expressed by pathogens, infected or stressed cells. Toll-like receptors (TLRs) that are present in endosomes and cytosolic receptors such as retinoic acid inducible gene-I (RIG-I) are most relevant in viral infections as they are capable of detecting viral RNAs or DNAs. Upon recognition, a cascade of events is activated leading to the expression of type I interferons (IFNs) and pro-inflammatory cytokines such as tumor necrosis factor alpha (TNFα), interleukin 12 (IL-12) or interleukin 18 (IL-18). These are secreted from infected cells and can be recognized by their receptors on the surface of NK cells, dendritic cells (DCs) or monocytes/macrophages. Type-I-IFN-receptor-triggering induces intracellular signaling and the activation of interferon stimulated response elements (ISRE). This in turn drives the transcription of protein products that can either directly impact on the viral replication and spread or have an indirect effect as immune regulators (Biron, 2016; Murphy et al., 2012).

NK cells can directly induce killing of infected cells via the release of cytotoxic mediators such as granzyme and perforin or via the secretion of IFNγ and TNFα. This process is tightly regulated and depends on the expression and crosslinking of activating receptors on the NK-cell surface with its ligands on the target cell. NK cells use Fc (fragment crystallizable) receptors, FcγRIII, to recognize Fc regions of antibodies that bind infected cells, to mediate antibody dependent cell cytotoxicity (ADCC). Furthermore, other receptors such as killer Ig-like receptor (KIR), NKG2D and NKp-46 can trigger the activation of NK cells upon recognition of specific ligands, such as viral proteins expressed on the surface of infected cells. Besides the receptor-mediated activation, recognition of type I IFNs or pro-inflammatory cytokines can also directly activate NK cells. NK-cell stimulation not only causes killing of target cells, but also leads to NK-cell proliferation (Biron, 2016; Murphy & Weaver, 2017).

Monocytes and macrophages limit viral spread via antigen uptake and phagocytosis. DCs are antigen-presenting cells (APCs) that take up antigens and present molecules via major histocompatibility complex (MHC) class I or II to T cells leading to T-cell activation. In addition, both also secrete cytokines IL-12 and IL-18 that activate NK cells (Biron, 2016; Fanning et al., 2019). The presentation of antigens via MHC class molecules by APCs together with the secretion of specific cytokines can also trigger the induction of the adaptive immune response.

Innate immunity during HBV infection

HBV acts like a stealth virus and mostly stays undetected by the innate immune system. This is due to some specific strategies to evade immune recognition: First, the viral replication template, the HBV cccDNA, is hidden in the nucleus and thereby escapes from being detected by the innate DNA sensing cellular machinery (Wieland & Chisari, 2005). Second, the viral mRNAs are polyadenylated and capped, looking like normal cellular transcripts. Third, the new transcripts are protected in nucleocapsids in the cytoplasm (Carlo Ferrari, 2015).

Furthermore, HBV seems to actively inhibit the innate immune response by blocking the production of type I IFNs. HBV polymerase and HBx proteins have been shown to interfere with IRF3/IRF7 and RIG-I, thus blocking IFN signaling (Carlo Ferrari, 2015; A. Tan et al., 2015). Moreover, HBV dampens the function of several innate

immune cells. NK cells usually immediately produce IFNγ and TNFα when recognizing virus-infected cells, but upon HBV infection their activation and effector function is suppressed. In patients with acute HBV infection, NK-cell activation only becomes detectable once the viral load has decreased (A. Tan et al., 2015). In the setting of chronic HBV infection, the role of NK cells is two-sided: On the one hand, their functionality is inhibited by immunosuppressive cytokines interleukin 10 (IL-10) and transforming growth factor beta (TGFβ). On the other hand, NK cells seem to play an important role in the HBV-induced liver damage as large numbers of activated intrahepatic NK cells release cytotoxic perforin/granzyme and mediate hepatocyte apoptosis (Maini & Peppa, 2013).

1.2.2 T-cell mediated adaptive immunity

Unlike the innate immune response, the adaptive immune response is highly specific and takes longer to be induced. T and B cells are the major cell types responsible for the induction and expression of adaptive immunity. Both have genetically rearranged and highly diverse antigen receptors conferring specificity. T cells carry a T-cell receptor (TCR) on their surface, which is composed of an α– and a β-chain generated via a process called V(D)J-gene recombination. The TCR recognizes peptides with certain length, bound to a special groove on the surface of MHC molecules. CD4 T cells carry TCRs that recognize peptides with 8-11 amino acids presented on MHC class II molecules, while CD8 T cells have TCRs detecting peptides of 10-30 amino acids length presented on MHC class I molecules (Murphy & Weaver, 2017). CD4 T cells act as helper cells, providing B cells and CD8 T cells with additional signals to induce proliferation upon antigen recognition on APCs. CD8 T cells are cytotoxic T cells that can mediate immune response upon activation via the secretion of cytokines such as IFNγ and TNFα. These cytokines then stimulate other immune cells to participate in the immune response. Furthermore, similar to NK cells, cytotoxic T cells can secrete perforin and granzyme and induce target cell lysis. Upon activation, T cells undergo clonal expansion and consequently enhance the immune response (E. John Wherry & Masopust, 2016).

Besides the expression of activating receptors, T cells also express inhibitory molecules on their surface, which limits their activation. For instance, activated CD8 T cells express programmed cell death protein 1 (PD-1) making them susceptible for inhibition. PD-1 can be recognized by programmed cell death ligand 1 (PD-L1)

expressed on other immune cells, virus infected cells or tumor cells. If several inhibitory molecules are expressed in combination, CD8 T cells are considered as functionally exhausted, which can be a consequence of continuous stimulation with antigens (E. J. Wherry & Kurachi, 2015).

1.2.2.1 T-cell response in HBV infection

The T-cell response seems to be the most important factor in the outcome of HBV infection. In individuals with acute HBV infection, the HBV-specific T-cell response is multi-specific, strong and polyclonal (A. Tan et al., 2015). Both CD4 and CD8 T cells are activated upon recognition of viral antigens presented by APCs. CD8 T cells are recruited into the liver and induce viral clearance either by the non-cytolytic mechanism, secreting IFNγ and TNFα or by the lysis of infected cells, inducing liver damage (Guidotti et al., 1999; Lucifora et al., 2014; Maini et al., 2000). CD4 T cells boost the HBV-specific CD8 T cell response (Thimme et al., 2003).

In contrast, in chronic hepatitis B virus infection the HBV-specific T cells are scarce and functionally impaired. CD8 T cells lose their effector function (potential to secrete of cytokines), express exhaustion markers such as PD-1 on their surface and are prone to apoptosis (A. Tan et al., 2015). Furthermore, regulatory CD4 Foxp3+ T cells can be hyper-activated, which secrete IL-10 leading to further suppression of virus specific CD8 T cells (Manigold & Racanelli, 2007). As a reason, various factors can be named, but of high importance is the persistent exposure to high doses of HBV antigens (Carlo Ferrari, 2015).

1.2.3 B-cell mediated adaptive immunity

Besides the cellular component, adaptive immunity also consists of a humoral response, which is formed by B cells that carry a B cell receptor (BCR) on their surface or secrete antigen-specific antibodies.

The BCR is the membrane bound version of an antibody and is capable of recognizing antigens of various origins. Each BCR consists of six protein chains in total: two identical immunoglobulin (Ig) light and heavy chains, responsible for antigen binding, and an Igα and an Igβ chain that are crucial for intracellular signaling (Figure 3 A). Ig heavy and light chain are connected with each other via disulfide bonds and are generated by V(D)J-gene rearrangements contributing to the various specificities (Murphy & Weaver, 2017).

The BCR is formed during B-cell development in the bone marrow and each new B cell expresses BCRs of the Ig isotype IgM. These B cells are functionally immature and have to complete their maturation in secondary lymphoid tissues, leading to differentiation and expression of surface IgD (Seifert & Kuppers, 2016). Thereafter, mature, naïve B cells are capable of recognizing foreign antigens and circulate between secondary lymphoid tissues and in the blood.

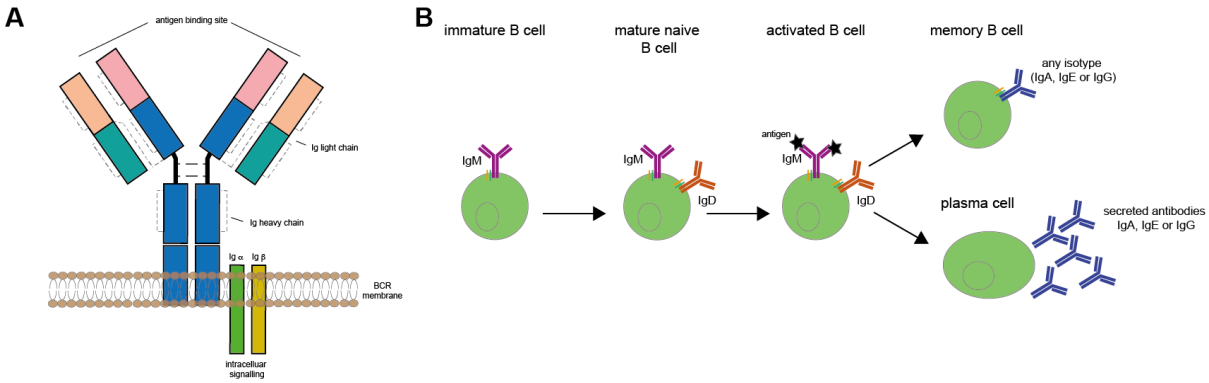

Figure 3. Schematic representation of the B cell receptor and B-cell development.
(A) B cell receptor (BCR) structure with immunoglobulin (Ig) heavy and light chain and the antigen binding site as well as Ig α and β chain for signal transduction up on antigen encounter. Blue – Ig constant heavy chain, pink – Ig variable heavy chain, turquoise – Ig constant light chain, orange – Ig variable light chain, green and yellow – Igα and β chain for signaling, dashed lines indicate disulfide bonds. (B) B-cell development with isotype switch upon antigen recognition. Scheme modified from (Murphy & Weaver, 2017).

Naïve B cells that encounter antigens require CD4 T-cell help to become fully activated. Upon activation, two ways of differentiation can be taken: First, B cells can differentiate into short-living plasma cells that downregulate the BCR expression, but in exchange secrete high amounts of antibodies. These antibodies have low antigen affinity, as plasma cells have not undergone somatic hypermutation. Instead they provide a fast first response to the antigen. Second, so-called germinal centers (GCs) can be established in the secondary lymphoid organs. Inside GCs B cells undergo several rounds of affinity maturation and proliferation (Kurosaki et al., 2015). As a result, a B-cell pool with highest antigen affinities is established. Furthermore, B cells can undergo class switching during germinal center reaction. This leads to the expression of IgG, IgA or IgE (Figure 3 B). Class switched, affinity matured B cells then leave the GCs either as memory B cells with high affinity BCRs or as long living plasma cells that secrete high amounts of high affinity antibodies (Murphy & Weaver, 2017). Memory B cells survive for a long period of time and promote

protection also after antigen re-exposure as they are able to rapidly differentiate into plasma cells (Kurosaki et al., 2015; Seifert & Kuppers, 2016).

The released antibodies recognize antigens in the circulation or on the surface of infected cells. Depending on the type of antigen, several ways of antibody dependent antigen elimination exist: For instance, antibodies can directly recognize viruses, leading to virus neutralization. Antibodies and antigens can form immune complexes, which can be noticed by the complement system. Complement activation thus induces lysis of the respective cell or antigen. In addition, antibodies in immune complexes can also be recognized by Fc receptors on Kupffer cells and macrophages. These cells phagocytose and degrade the antigen in a process called antibody dependent cellular phagocytosis (ADCP). Similarly, Fc receptors on NK cells can bind to antibodies attached to antigens on infected cells, leading to NK-cell activation and target cell lysis. This process is called antibody dependent cellular cytotoxicity (ADCC) (Nimmerjahn & Ravetch, 2008; E. John Wherry & Masopust, 2016).

1.2.3.1 B-cell response in HBV infection

The role of HBV-specific B cells and antibodies in the outcome of HBV infection is not fully understood so far. What is known is that envelope specific (anti-HBs) antibodies secreted from B cells, induced upon vaccination, efficiently protect from infection. Anti-HBs antibodies in HBIg preparations are capable of preventing vertical transmission or reinfection after liver transplantation (Neumann-Haefelin & Thimme, 2018). In addition, the treatment with B cell depleting drugs, such as rituximab can induce HBV reactivation in patients that previously controlled the virus. This points at the importance of a properly functioning B-cell response for virus control (Loomba & Liang, 2017).

Similar to the T-cell response, the B-cell response differs with regard to the status of HBV infection. Upon viral clearance, serum HBsAg is lost and functional HBsAg-specific B cells secrete high amounts of virus neutralizing antibodies (Ma et al., 2019; Neumann-Haefelin & Thimme, 2018). On the contrary, in chronically infected (CHB) patients, HBsAg-specific B cells have an altered phenotype and seem to be functionally impaired, although they are present with similar frequencies as in acute or resolved HBV infection. The phenotype is defined as atypical memory B cells that express low levels of memory B-cell marker CD27, but high levels of

inhibitory molecules such as PD-1 or Fc receptor-like protein 5 (FcRL5). Furthermore, these B cells mainly express IgM and are unable to mature into antibody secreting cells after *in vitro* stimulation (Burton et al., 2018; Le Bert et al., 2019; Poonia et al., 2018; Salimzadeh et al., 2018). As for T cells, the high load of circulating HBsAg is believed to impede the HBV-specific B-cell response by complexing the available antibodies and by steady stimulation of the BCRs (Corti et al., 2018). Fortunately, functional impairment seems to be reversible and was be partially restored *in vitro*, by blocking PD-1 and stimulation with interleukin 2 (IL-2), interleukin 4 (IL-4) and CD40 Ligand (CD40L) mimicking CD4 T-cell help (Salimzadeh et al., 2018).

Besides the envelope specific B cells and antibodies, antibodies directed against HBV nucleocapsid (HBc) and HBeAg exist. The presence of anti-HBe antibodies in HBeAg positive CHB patients was associated with low levels of HBV replication and favorable disease outcome (Ma et al., 2019). In contrast, anti-HBc antibodies have been shown to be enriched in CHB patients and were correlated with HBV-induced liver disease and inflammation (Le Bert et al., 2019). Furthermore, regulatory B cells (Bregs) were enriched in patients with chronic HBV infection. Bregs secreted the inhibitory cytokine IL-10, which suppressed the activation of HBV-specific cytotoxic CD8 T cells and enhanced the function of CD4 regulatory T cells (Das et al., 2012; Liu et al., 2016).

In summary, not only the T-cell response is impaired during chronic HBV infection, but also B cells are dysfunctional. Therefore, new therapeutic approaches that support functional cure of HBV, should aim at restoring the HBV-specific B- and T-cell response.

1.3 Novel therapeutic options for the treatment of chronic HBV infection

As described earlier, current treatment options for chronic HBV infection with Peg-IFNα and NUCs are limited with regard to cure or control of infection. Novel therapies are under development, but so-far no clinical approval has been achieved. Several of the present investigations focus on the restoration of the impaired immune response against HBV, while others aim at directly interfering with the virus life cycle in order to promote functional cure or complete killing of infected hepatocytes.

1.3.1 Antibody-based therapy

1.3.1.1 HBsAg-specific polyclonal antibodies

The use of antibodies as therapeutics has a long history, since 1890 when *Emil von Behring* developed the first serum therapy against diphtheria infection (Behring, 1890). Nevertheless, only after the structural discovery of antibodies and the possibility to isolate and culture B cells, antibody-based immunotherapies were developed (Kohler & Milstein, 1975). Nowadays antibodies are broadly used either for passive immunization or for targeted immunotherapeutic approaches of several types of cancer, autoimmune diseases and against infectious diseases.

While polyclonal antibodies are secreted from different B cells with varying specificities, monoclonal antibodies (mAbs) are derived from a single B cell clone with a distinct specificity. Polyclonals are usually prepared from pooled plasma or serum of animals or humans and are mainly used for disease prophylaxis, passive immunization or for the treatment of antibody deficiencies (Robbins et al., 1996).

With regard to HBV infection, polyclonal antibodies have already been used for passive immunization for a long time. As described in section 1.1.3.1, HBIg is given as post-exposure prophylaxis to prevent mother-child transmission or re-infection after liver transplantation (Beasley et al., 1983). The preparations contain anti-HBs antibodies directed against HBV envelope proteins. Most of those antibodies target the S-domain and prevent from infection by virus neutralization and blocking of HBV attachment to HSPG on hepatocytes (Corti et al., 2018).

HBV infected cells secrete a vast excess of subviral particles, besides infectious virions. They are believed to be responsible for distracting the host immune response in chronic HBV patients (C. Ferrari, 2015). Therefore, HBIg preparations were also investigated in CHB patients in order to clear HBsAg from the circulation. Two studies showed a temporary reduction of HBsAg and HBV DNA, but long-term clearance of HBsAg was not observed after high dose of HBIg injections (Reed et al., 1973; van Nunen et al., 2002). Furthermore, HBIg is a product derived from serum of humans with high anti-HBs titers, which renders the preparation expensive and batch-to-batch variations frequent. Due to additional concerns with regard to biosafety, as it is a blood product, a number of recombinant monoclonal antibodies (mAbs) against HBsAg were developed with different techniques and from different species. Their efficacy was so far mainly investigated pre-clinically.

1.3.1.2 HBsAg-specific monoclonal antibodies

After the first generation of monoclonal antibodies by *Kohler* and *Milstein*, mAbs directed against several targets were developed. In 1986, the FDA approved the first monoclonal antibody Moromonab-CD3 (also named OKT-3) directed against CD3 on T cells. It induced T-cell apoptosis and was used for the treatment of organ transplant recipients, who became resistant to steroid treatment (S. L. Smith, 1996). Today, 75 FDA-approved mAbs are used against various diseases and several more are under clinical and preclinical investigation, especially for the treatment of viral infections e.g. with Ebola virus, human immunodeficiency virus (HIV) or dengue virus (Caskey et al., 2019; Rijal et al., 2019; Salazar et al., 2017).

Naturally, during viral infections antibodies have a dual role: On the one hand, they capture viruses and thereby interfere with the viral life cycle, for instance by blocking the entry into the host cell. On the other hand, antibodies can communicate the presence of infectious particles to effector cells via their Fc region, thus inducing a robust immune response against the virus. However, some viral infections persist and even if combinations of drugs are applied immune control is hardly achieved. This is due to strategies of the pathogens to evade the host immune response (Caskey et al., 2019). Therefore, the administration of monoclonal antibodies targeting specific features of the virus life cycle may help to promote virus control.

The most prominent field of antibody application for persistent viral infection is HIV. In 2018, the FDA approved the first monoclonal for the treatment of HIV-infection. Ibalizumab does not target the virus itself, but recognizes a conformational epitope on CD4, which blocks virus entry (Beccari et al., 2019). In addition, mAbs directly targeting the virus are under early clinical investigation. Results are promising, but the difficulty to find a robust epitope that is not affected by the high mutation rate of HIV remains problematic (Caskey et al., 2019).

For the treatment of persistent HBV infection mAbs offer great potential as they may fulfill several functions in order to promote the restoration of the impaired HBV-specific immune response: First, they can neutralize virions and subviral particles and remove them from the circulation. This lowers the overall antigen load and may help to reverse T- and B-cell exhaustion. Second, mAbs can block the viral attachment to the hepatocyte and thereby prevent from (re-) infection. Third, antibodies may induce Fc-mediated immune effector cell activation, which can lead

to phagocytosis or hepatocyte lysis. This will reduce the pool of HBV cccDNA that serves as viral replication template. Fourth, antibodies that capture antigens can form immune complexes that may lead to the activation of HBV-specific T cells (Corti et al., 2018).

Currently several mAbs are under preclinical investigation and few have already been used in small pilot studies in CHB patients with varying success. Monoclonal antibodies against HBV usually target HBV envelope proteins, as there are several accessible epitopes on the large, middle and small protein version (Figure 4).

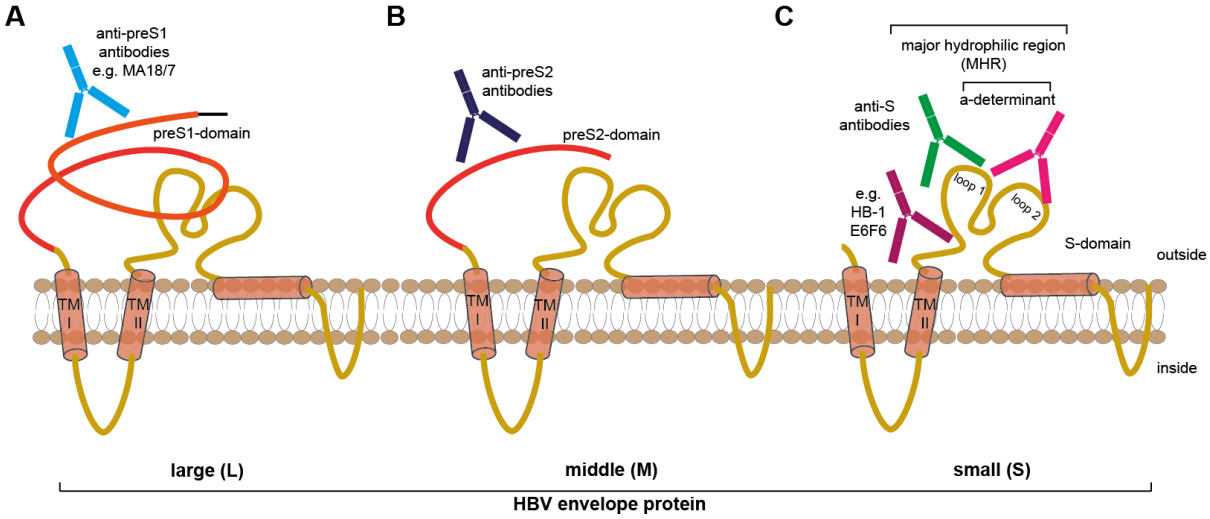

Figure 4. Illustration of HBV envelope protein membrane assembly and localization of potential epitopes for monoclonal antibodies.
(A) Large envelope protein with mAbs binding in the preS1 domain. (B) Middle HBV envelope protein with antibodies recognizing the preS2 domain. (C) Small envelope protein with antibodies recognizing epitopes within the a-determinant (loop1 or loop2) and the major hydrophilic region. yellow – S-domain, red – preS2-domain, orange – preS1-domain. Scheme modified from (Gao et al., 2017).

Most antibody epitopes are either located within the preS1 domain of the large or at the S-domain of the small HBV Env protein. Only very few antibodies target the preS2 domain. These have been shown to be restricted to some HBV genotypes (Gao et al., 2017). The preS1 domain is a 107 amino acids long polypeptide, exposed to the outside of the viral particles. It contains the receptor-binding domain of HBV. Anti-PreS1 antibodies such as 2H5-A14, MA18/7 or 4D11 have been shown to efficiently block the engagement of preS1 with the cellular receptor NTCP and neutralize HBV infection with high potency *in vitro* (Bremer et al., 2011; Gao et al., 2017; Li et al., 2017). Furthermore, therapeutic efficacy by inducing antibody-Fc-dependent effector functions was shown in a mouse model for 2H5-A14

and resulted in reduced levels of circulating HBsAg and intrahepatic HBV DNA. The proposed mode of action was ADCC and ADCP upon recognition of antibody Fc region by Fc receptors on macrophages and NK cells (Li et al., 2017).

The vast majority of recombinant mAbs, but also antibodies that result from clearance of natural infection or vaccination are directed against the S-domain of the small HBV Env protein (Figure 4 C) (Gao et al., 2017). The actual structure of the S-domain is unknown, but it is assumed that the protein consists of several transmembrane domains defining extra- and intracellular regions of the protein. Antibody epitopes are located in the extracellular region, the major hydrophilic region (MHR), which has a distinct conformation and is stabilized by several disulfide bridges (Bruss, 2004; Suffner et al., 2018). Within the MHR the so-called “a-determinant” is located with a proposed two-loop structure (Figure 4 C). Many mAbs recognize conformation-dependent epitopes within the a-determinant and are, similar to the anti-PreS1 mAbs, very potent neutralizing antibodies (Cerino et al., 2015; Golsaz Shirazi et al., 2014; W. Wang et al., 2016). They prevent from the initial interaction of the virion with the hepatocyte surface via heparin sulfate proteoglycans (HSPG) (Tajiri et al., 2010). Another group of S-domain specific mAbs recognize a linear epitope located in the MHR, but outside the a-determinant at position $S^{119\text{-}125}$. This region is conserved within different HBV geno- and subtypes. mAbs HB-1 and E6F6 belong to this group and have been shown to efficiently neutralize HBV infection of different genotypes and HBV immune escape mutants (Kucinskaite-Kodze et al., 2016; Zhang et al., 2016). In addition, E6F6 was investigated for its therapeutic potential in different mouse models. After single dose of E6F6, HBsAg and HBV DNA levels were suppressed for several weeks and viral spread was reduced in human-liver chimeric mice. Furthermore, it seemed that E6F6 was capable of restoring the HBV-specific CD8 T-cell response induced by the Fc receptor dependent phagocytosis of antibody-antigen immune complexes (Zhang et al., 2016).

Besides the preclinical investigation of anti-HBs mAbs, very few have been evaluated in a clinical setting with patients chronically infected with HBV: Tuvirumab, a human mAb directed against the a-determinant of the S-domain, was shown to reduce the level of HBsAg in CHB patients by at least 50%. Furthermore, in three patients, who received tuvirumab in combination with interferon alpha, circulating

HBsAg was undetectable. However, this effect only lasted for a few weeks (van Nunen et al., 2001). In another study, HBV-AB^{XTL}, a combination of two mAbs targeting two different epitopes on the a-determinant, showed suppression of HBV DNA and HBsAg after single and multiple doses, but a long-term clearance of HBsAg was neither observed (Galun et al., 2002). Therefore, the studies were put on hold. Currently, the therapeutic efficacy of mAb GC1102/HB-C7A is investigated in a phase-2 study in CHB patients with low levels of HBsAg, but results are not available at this point (Corti et al., 2018).

Based on the few clinical studies with CHB patients, the application of anti-HBs mAbs may have a potential to treat patients, as circulating HBsAg can be lowered, but new molecules with more efficient binding and effector functions such as E6F6 need to be developed. One concern of many currently developing mAbs is their murine origin. For the application in humans, chimerization or humanization is needed, but this harbors the risk of reducing the antibody efficacy, which has only recently been shown for E6F6 (Kang et al., 2018). Therefore, potent fully human recombinant monoclonal antibodies need to be developed.

1.3.1.3 Checkpoint inhibitors

Cancer cells as well as persistent viral infections can activate immune-inhibitory pathways. Antibodies that target immune checkpoints are capable of blocking these and can thereby trigger anti-tumor or anti-viral immune responses. The immune checkpoints include PD-L1 and PD-1 or cytotoxic T-lymphocyte associated protein-4 (CTLA-4). While CTLA-4 is exclusively expressed on T cells, PD-1 expression can be found on T as well as B cells. CTLA-4 attenuates the T-cell activation and suppresses T-cell function. As a consequence, T-cell mediated anti-tumor or anti-virus immunity is dampened. Blocking the inhibitory effect of CTLA-4 has been shown to improve the immune response towards tumor cells and therefore led to the development of mAbs targeting CTLA-4 (Leach et al., 1996). Ipilimumab, the first CTLA-4 mAb was approved in 2011 for metastatic melanoma and prolongs the overall survival of patients (Lipson & Drake, 2011).

Similar effects were seen in cancer patients when PD-1 was blocked with mAbs. The first PD-1 mAb nivolumab was approved in 2014 for advanced stage melanoma (Robert et al., 2015). Further anti-PD-1 antibodies followed in 2015 and 2018 for the treatment of various types of cancer (Kwok et al., 2016; Markham & Duggan, 2018).

PD-1 recognizes its ligand PD-L1 that is expressed on antigen presenting cells or on tumor cells. Malignant cells that express PD-L1 can induce T-cell suppression. Therefore mAbs targeting PD-L1 were developed and have been shown to be very efficient. The first PD-L1 antibody was approved in 2016, atezolizumab, and is now used for the treatment of urothelial carcinoma, metastatic non-small cell lung cancer and triple negative breast cancer (Heimes & Schmidt, 2019; Markham, 2016; Socinski et al., 2018).

Chronic HBV infection is characterized by exhaustion of T and B cells, which express high levels of PD-1 (Boni et al., 2007; Burton et al., 2018). Furthermore, malignant HCC cells express PD-L1 (Calderaro et al., 2016). In order to improve the impaired immunity against HBV and target malignant cells in HCC, antibodies directed against these checkpoint inhibitors have been investigated. *In vitro* studies with PD-1/PD-L1 blockade indicated improvements in the T- and B-cell response (Bengsch et al., 2014; Salimzadeh et al., 2018). However, in a woodchuck model of HBV infection, as well as in a small clinical trail, an effect of PD-1 antibody nivolumab was only observed in a minority of animals and patients (Balsitis et al., 2018; Gane et al., 2017). In contrast, HCC patients treated with PD-1-/PD-L1-mAbs indicated high response rates, but further studies have to be conducted to fully evidence this (El Dika et al., 2019).

1.3.1.4 New antibody constructs

Besides the classical full-length IgG monoclonal antibodies several new formats have been developed. Among those are antibody drug conjugates (ADCs), antibody fragments such as $F(ab)_2$- and Fab-fragments, glyco-engineered antibodies or bi-specific antibodies (bsAbs). ADCs and bi-specific antibodies have already been approved for the treatment of cancer. While standard antibodies have two binding sites for the same antigen, bi-specifics harbor binding sites for different antigens. This allows for other modes of action, such as engaging immune cells to tumor cells or blocking cell signaling (Suurs et al., 2019). The first bi-specific antibody, catumaxomab, was approved by the EMA (European Medicines Agency) in 2009 for the treatment of malignant ascites recognizing CD3 and epithelial cell adhesion molecule (EpCAM) (Seimetz et al., 2010). In 2014/15 blinatumomab was approved for Philadelphia Chromosome negative B cell acute lymphoblastic leukemia (ALL)

with binding site for CD3 and CD19 (Przepiorka et al., 2015). Both bsAbs belong to the group of so-called bispecific T-cell engager antibodies (BiTEs). They bind to CD3 of the TCR on the one side and on the other side to a tumor antigen. When both, the T-cell and the tumor cell are bound, a cytolytic synapse is formed and T cells are activated. This induces the release of cytotoxic modulators such as perforin and granzyme and leads to tumor cell killing (Offner et al., 2006). Furthermore, not only T-cell engagement to tumor cells can be achieved, but also other effector or immune cells can be connected with tumor cells. For instance, NK cells can be linked via CD16 to CD30 expressing Hodgkin's lymphoma cells (Rothe et al., 2015). Currently, 36 BiTEs are in clinical trials, but also other bsAbs constructs are investigated. Here, the antigen binding sites target multiple epitopes on one antigen leading to co-localization on cancer cells (Suurs et al., 2019).

For treating HBV infection, T-cell redirection with bsAbs has been studied intensively *in vitro* in HBsAg-expressing cells. In this laboratory, bsAbs with binding sites for CD3 or CD28 on T cells and HBsAg on hepatocytes were developed. The application of those bsAbs in combination with peripheral blood mononuclear cells (PBMC) to hepatoma cell lines, infected with HBV, efficiently induced T-cell re-direction and target cell killing (Bohne et al., 2015; Quitt, 2020). Furthermore, *Kruse* and collaborators showed promising results in a mouse model after the application of HBsAg/CD3 bi-specific antibodies (Kruse et al., 2017).
Another bi-specific antibody, recognizing two different epitopes on HBsAg was developed by *Tan et al.*. C4D2-BsAb demonstrated a strong neutralization capacity for HBV, which was superior compared with the combination of both parental antibodies. Additionally, C4D2-BsAb was able to inhibit the secretion of HBsAg after internalization into hepatocytes (W. Tan et al., 2013).

1.3.2 Adoptive T-cell therapy

Similar to BiTEs, the aim of adoptive T-cell therapy is to redirect patients' immune cells towards a certain target. T cells are *ex vivo* expanded, genetically engineered and subsequently re-infused into patients. Engineering of T cells can lead to the expression of natural T-cell receptors or so-called chimeric antigen receptors (CARs) that recognize the target of interest. Upon antigen recognition, the T cell is activated, cytokines are released and target cell lysis is induced.

CAR-T cells recognize antigens expressed on the surface of a target cell. Their specificity originates from an antibody single chain variable fragment (scFv), liked to a spacer domain, a transmembrane domain and a signaling domain to induce T-cell activation upon antigen encounter. It is independent of the peptide-MHC-complex (Borrie & Maleki Vareki, 2018). First CAR T-cell therapies were approved in 2017 in the US for the treatment of relapsed or refractory B-cell acute lymphoblastic leukemia (ALL) and relapsed or refractory large B-cell lymphoma. Those CAR T-cells target CD19 on B cells and obtained great response to this type of therapy (Leahy et al., 2018; Neelapu et al., 2017).
T-cells grafted with natural TCRs recognize a specific peptide presented on the respective MHC molecule. The first clinical trial with TCR-engineered T cells was for the treatment of metastatic melanoma targeting MART-1 and showed tumor regression in some patients (Morgan et al., 2006).

For the treatment of chronic HBV infection, CAR T-cells as well as TCR-engineered T cells have been investigated intensively *in vitro* and *in vivo* to restore the HBV-specific immune response. CAR T-cells developed in our laboratory recognize HBV envelope proteins (S-CAR) on the surface of infected hepatocytes. Upon activation, cytokine secretion and target cell killing was induced (Bohne et al., 2008). Furthermore, in a HBV transgenic mouse model, S-CAR-redirected T cells could control HBV replication and the viral load was decreased (Krebs et al., 2013).
In addition, T cells with TCRs redirected towards HBV have been generated and indicate a sustained antiviral effect in cell culture and in mouse models (Gehring et al., 2011; Kah et al., 2017; Wisskirchen et al., 2017). Transfer of T cells grafted with HBV-specific TCRs into HBV-infected humanized mice controlled the HBV infection and viral markers were under the limit of detection (Wisskirchen et al., 2019). Additionally, the application of HBV-specific TCR-engineered T cells in a patient with HBV-associated HCC induced a substantial reduction of HBsAg levels in the serum (Qasim et al., 2015).

1.3.3 Therapeutic Vaccination

In contrast to prophylactic vaccines that aim for disease prevention, therapeutic vaccination is used to treat after a disease occurred. It relies on the principle of inducing or enhancing the patient's own immune response towards a disease and to

eventually control the disease. Most therapeutic vaccines were developed against viral infections or cancer and either initiate cytotoxic T cells or antibody secretion of B cells. The first therapeutic vaccine with FDA-approval in 2010 was sipuleucel-T against metastatic prostate cancer. It showed a prolonged survival of patients after vaccination (Cheever & Higano, 2011).

For chronic HBV infection, the aim of therapeutic vaccination is to overcome HBV-specific immune tolerance and to induce HBV-specific cytotoxic T-cells that can efficiently kill infected hepatocytes (Dembek et al., 2018). In order to treat chronic HBV infection, several vaccine strategies and formulations have been tested and are still under investigation. A first therapeutic vaccine approach was based on the prophylactic vaccine containing recombinant HBsAg. This lowered the viral load in CHB patients for some time, but a sustained virus control was not observed, indicating the need for more potent vaccine strategies (Pol et al., 2001).
In our laboratory, the *TherVacB* approach is currently under development, which includes adjuvant and particulated HBsAg and HBcAg allowing the induction of neutralizing antibodies as well as priming of both CD4 and CD8 T cells. With an additional MVA (Modified-Vaccinia-Ankara) vector boost, T-cell responses are expanded. This strategy has been shown to induce both anti-HBs seroconversion as well as HBsAg- and HBcAg-specific CD8 T-cells responses in HBV transgenic mice and was able to overcome HBV-induced immune tolerance in mice with low and intermediate antigen levels (Backes et al., 2016). Furthermore, immune tolerance was also resolved in mice with higher antigen load, after the vaccine strategy was adjusted with CpG-application (Kosinska et al., 2019). Lowering the antigen load by shRNA or siRNA allowed *TherVacB* to even break immune tolerance in high-titer HBV replicating mice (Michler et al., 2020). This points at the great potential of therapeutic vaccination in chronic HBV infection. Other vaccine strategies were also investigated and either use other routes of administration such as NASVAC, a nasal vaccine candidate, which seems to reduce HBV DNA in CHB patients or other ways to deliver the antigens such as the DNA based vaccine GX-100 that showed viral suppression in some patients (Al-Mahtab et al., 2013; S. H. Yang et al., 2006).

1.4 Strategies for the generation of monoclonal antibodies

1.4.1 Development of the antibody repertoire

A potent adaptive immune response particularly relies on the generation of a diverse repertoire of antibodies, which can either be secreted from a B cell or act as membrane-bound B cell receptor (BCRs). BCRs are assembled from a large pool of immunoglobulin gene segments during a process called somatic recombination that takes place during early B-cell development. During this process, a diverse antibody repertoire is formed. It is estimated in humans with at least 10^{11} variants. However, the number of specificities is limited to the total number of B cells present at a specific time point in a person (Murphy & Weaver, 2017).

Antibodies are proteins composed of two types of polypeptide chains, known as heavy and light chains, which are associated via disulfide bonds. Five different heavy chain isotypes (α, β, γ, δ, μ) are known in humans defining the antibody class. For the light chain, two types kappa (κ) and lambda (λ) exist. Each heavy and light chain has a variable (V) domain, composed of approximately 110 amino acids and a constant (C) domain with various lengths. Each light chain is usually made up of one constant (C_L) and one variable domain (V_L) (Figure 5). The heavy chain contains one variable domain (V_H) and either three constant domains (C_H1, C_H2, C_H3) with a hinge region in case of antibody classes α, γ and δ or four constant domains (C_H1, C_H2, C_H3 and C_H4) in the case of ε and μ (Murphy & Weaver, 2017).

Antigen binding takes place at the heavy and light chain variable domains. They are generated by recombination of a set of randomly arranged variable (V), diversity (D) and joining (J) germline gene segments. Notably, D segments can only be found in the V_H locus and are not needed in the recombination of the light chain. In the genome, the chromosomal region of the different genes is diverse (Murphy & Weaver, 2017). While heavy chain gene segments are located on chromosome 14, kappa and lambda light chain gene loci are found on chromosome 22 and 2. The immunoglobulin (Ig) heavy chain locus contains 123-129 variables (IGHV), 27 diversity (IGHD) and nine joining (IGHJ) gene segments, in addition to eleven constant genes (IGHC). In contrast, kappa and lambda light chain loci comprise of only 37 (IGKV) or 31 (IGLV) variable and five (IGKJ) or six (IGLJ) joining gene segments (Lefranc, 2007).

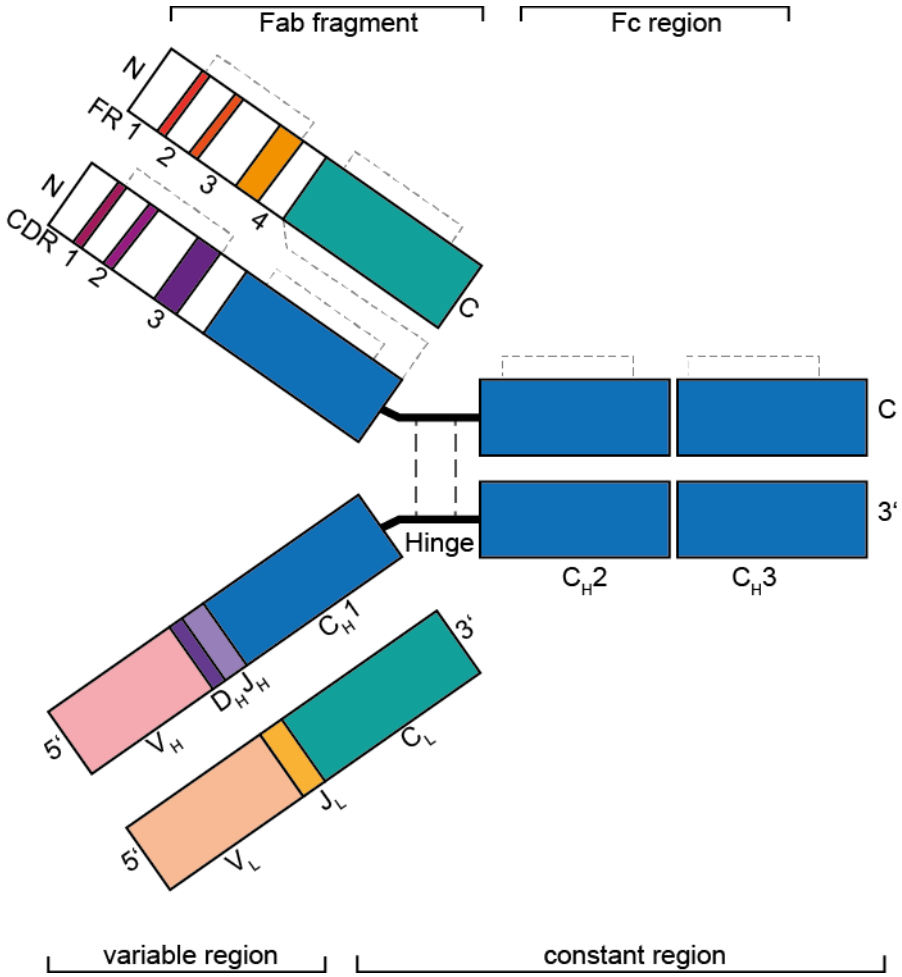

Figure 5. Schematic structure of an IgG molecule.
The bottom chains represent domains encoded from germline V, (D), and J gene segments, indicating the variable and constant region of an IgG antibody. The top chains represent the framework regions (FR) 1-4 and the complementarity determining regions (CDR) 1-3. The Fab fragment contains the antigen-binding site, whereas the Fc region is responsible for mediating effector function. Dashed lines indicate disulfide bonds. Scheme modified from (Georgiou et al., 2014).

During the process of V(D)J-recombination different V-, (D)- and J-gene segments are randomly ligated to a complex exon and are subsequently connected to the upstream located leader region and constant region during mRNA splicing. Once a functional combination of V(D)J-genes was selected the others cannot be expressed anymore. As a consequence, one B cell can only express one specific chain (Brady et al., 2010). Productive Ig heavy and Ig light chains are expressed and the complete antibody is assembled first as a membrane-bound immunoglobulin M (IgM) on the surface of an immature B cell (Georgiou et al., 2014). These B cells then undergo a selection for self-tolerance outside the bone marrow. B cells that survive in the periphery differentiate further to mature, naïve B cells additionally express surface IgD. Mature IgM+IgD+ B cells form the naïve B-cell repertoire (Figure 3 B) (Murphy &

Weaver, 2017). Antigen specificity of antibodies from different B-cell clones varies strongly. However, variable gene sequences between different antibodies mainly differ in the three so-called complementarity-determining regions (CDRs), which mostly dictate the antigen-specificity. More conserved regions, the framework regions (FR) surround the CDRs. CDR3 is the most diverse region, caused by added or deleted nucleotides at the junction between ligated V-, (D-) and J-gene segments during V(D)J-recombination (Figure 5) (Georgiou et al., 2014).

B cells that are activated upon antigen recognition proliferate in the germinal centers (GCs) in the secondary lymphoid organs. A process called somatic hypermutation, which introduces point mutations in the variable regions of the heavy and the light chain, accompanies this clonal expansion. On the one hand, some mutations can modify the amino acid sequence in the conserved framework region. This may lead to destruction of the antibody structure and thus to B-cell deactivation. On the other hand, mutations that occur in one of the CDRs may increase the affinity of the antibody for an antigen. Consequently, B cells with lower affinities are out-competed. High affinity B cells are then selected to differentiate further into antibody secreting plasma cells or long-living memory B cells. Additionally, the isotype of an antibody can be switched during clonal expansion. This is dependent on the course of immune response and is for instance stimulated via cytokines secreted from T cells (Murphy & Weaver, 2017). IgM+IgD+ B cells can switch to IgG+, IgA+ or IgE+ B cells, with each Ig class harboring different effector functions. IgG type antibodies make up the majority of serum antibodies against various pathogens and possess several effector functions such as opsonization, complement activation, neutralization and antibody dependent cell phagocytosis (ADCP) or antibody-dependent cytotoxicity (ADCC) as explained earlier (Vidarsson et al., 2014).

1.4.2 Generation of monoclonal antibodies

In 1975 *Kohler* and *Milstein* first described and generated monoclonal antibodies (mAbs) after fusing splenic cells from a mouse, immunized against an antigen, with a mouse myeloma cell line (Kohler & Milstein, 1975). This technique was called hybridoma technology and is used frequently until today to generate mAbs against almost any antigen. However, the use of those mAbs is often limited to research or diagnostic applications, since murine antibodies applied to humans can cause

severe immune responses against the murine protein. Furthermore, the effector function of mouse antibodies in humans is restricted (Tiller, 2011). To circumvent the limitations, murine mAbs have to be engineered by chimerization or humanization, which is often associated with loss of efficacy (Kaluza et al., 1992). Another way of bypassing is the use of human hybridoma technology. This is based on the recovery of B-cell lines from transgenic mice that harbor a partial or the complete human immunoglobulin repertoire. Nevertheless, one big drawback remains: B-cell development and antigen processing differ between mice and human. Therefore, mice are unable to completely mimic the human immune repertoire. Another obstacle of human hybridoma is the difficulty to expand the cells to a sufficient population of antigen-specific B cells to be used for antibody production (Lonberg, 2005; S. A. Smith & Crowe, 2015).

Several new technologies that completely rely on human protein sequences have been developed to overcome those issues. These methods include combinatorial display technologies, like phage, yeast or mammalian cell display, immortalization of human B cells with Epstein-Barr Virus (EBV) or single B cell antibody approaches (Tiller, 2011).

1.4.2.1 Immortalization of human B cells by transformation

One way of generating human monoclonal antibodies is the immortalization of human B cells with Epstein-Barr virus (EBV) (Michael Steinitz et al., 1977). EBV infects B cells via the entry receptor CD21, leading to the outgrowth of permanent lymphoblastoid cell lines (LCLs) (Nemerow et al., 1985). After transformation, B cells grow rapidly in suspension, but keep the characteristic of the initially infected cell, for example the expression and secretion of immunoglobulins. With the addition of specific stimuli somatic hypermutation and isotype class switching also take place. However, the resulting antibodies often have lower affinities compared to *in vivo* mutated B cells. The resulting LCLs can then be evaluated for the secretion of antigen-specific antibodies (M. Steinitz, 2014).

Transformation can easily by carried out from PBMC, but it takes at least two weeks until the outgrowth of immortal lines is achieved. In addition, the immortalization efficiency is generally low and EBV immortalized B cells often secrete only low amounts of antibodies. With the addition of CpG oligonucleotide, a toll-like receptor-9 (TLR9) agonist, during B-cell immortalization antibody secretion can partially be

improved (Traggiai et al., 2004). Furthermore, cultures need to be supplemented with cyclosporine A to prevent EBV-specific T cells from killing transformed B cells (Wallace et al., 1987). EBV transformed B cells often die during culture as they have chromosomal instability (S. A. Smith & Crowe, 2015).
Once stable B-cell cultures are achieved and antigen-specificity was confirmed as positive, the respective clones are selected for individual cell outgrowth to obtain single B-cell clones secreting antibodies with only a single specificity. Antigen-specific B cells are expanded until a sufficient number of cells is achieved to amplify immunoglobulin variable chain genes with reverse transcriptase polymerase chain reaction (RT-PCR) (Traggiai et al., 2004).

An alternative way to generate mAbs from culturing peripheral blood B cells is based on the *in vitro* activation and proliferation of B cells by triggering the surface receptor CD40 in the presence of interleukin-4 (IL-4). This combination mimics B-cell activation via CD4 T-helper cells and leads to the differentiation of memory B cells or plasma cells that secrete antibodies (Banchereau et al., 1991; Wiesner et al., 2008). After approximately ten days of culture, supernatants can be analyzed for the presence of antigen-specific antibodies. Similar to EBV transformed B cells, antigen-specific cells are then selected for limited dilution cloning to achieve single B-cells clones that secrete monoclonal antibodies.
CD40 stimulation can be induced via the addition of soluble anti-CD40 antibodies, or upon culturing of B cells on a feeder cell layer that express CD40 ligand (CD40L), which is recognized by CD40. MAb 89 and G28-5 were the first anti-CD40 antibodies that induced strong B-cell proliferation in combination with recombinant IL-4 (Clark & Ledbetter, 1986; Valle et al., 1989). Later, fibroblasts transfected with CD40L were generated and induced the differentiation of B cells mainly into memory cells (Armitage et al., 1992; Arpin et al., 1995).

The biggest advantage of both methods, compared for instance with display technologies, is that native antibodies are isolated and the natural pairing of V_H and V_L chains is preserved (Tiller, 2011). However, due to the very low frequency of antigen-specific B cells in peripheral blood, many clones have to be screened until high affinity antibodies are detected (Crotty et al., 2004; M. J. Smith et al., 2017).

This makes both strategies labor-intensive and indicates the need to combine it with B-cell pre-selection.

1.4.2.2 Single B cell antibody technology

A more straightforward possibility to generate mAbs was developed in 1996 by *Babcook* and co-workers. They used molecular cloning and immunoglobulin variable region complementary DNAs (cDNAs) of single rabbit or murine lymphocytes for the production of specific antibodies (Babcook et al., 1996). This method was refined and then allowed the direct amplification of human variable immunoglobulin heavy and light chain genes from single human B cells with subsequent expression of recombinant human mAbs in cell cultures (Meijer et al., 2006; K. Smith et al., 2009; Tiller et al., 2008).

Similar to the culture methods, the single B cell antibody approach allows the identification of the original pairing of variable heavy and light chain, as it exists in human B cells. Moreover, a great advantage of this method is the isolation of functional mAbs reactive against conformational epitopes that predominantly occur *in vivo*. However, the method also harbors a few drawbacks, which mainly lay in the need to find adequate human donors and highly selective molecular baits that will be recognized only by specific BCRs (Tiller, 2011).

The generation of mAbs with single B cell antibody technology requires several successive steps, which are depicted in Figure 6: The first step is the isolation of single B cells. Depending on the study aim single B cells can be isolated randomly or in an antigen-specific manner. A suitable B cell source is either peripheral blood or lymphoid tissue, but the latter is more difficult to obtain from humans (Tiller, 2011). Irrespective whether random or antigen-specific B cells are isolated, the most frequently used method is fluorescence-activated cell sorting (FACS). Using FACS, cells can clearly be sorted in terms of their stage of development or differentiation based on the expression of certain cell surface markers. In addition, it can be combined with pre-selection of B cells with coated magnetic beads, yielding in very pure (antigen-specific) B cells (Kodituwakku et al., 2003). The most important groups of B cells are class-switched memory B cells and antibody secreting plasma cells, as they have undergone somatic hypermutation and bear BCRs with high antigen affinities (Tiller, 2011).

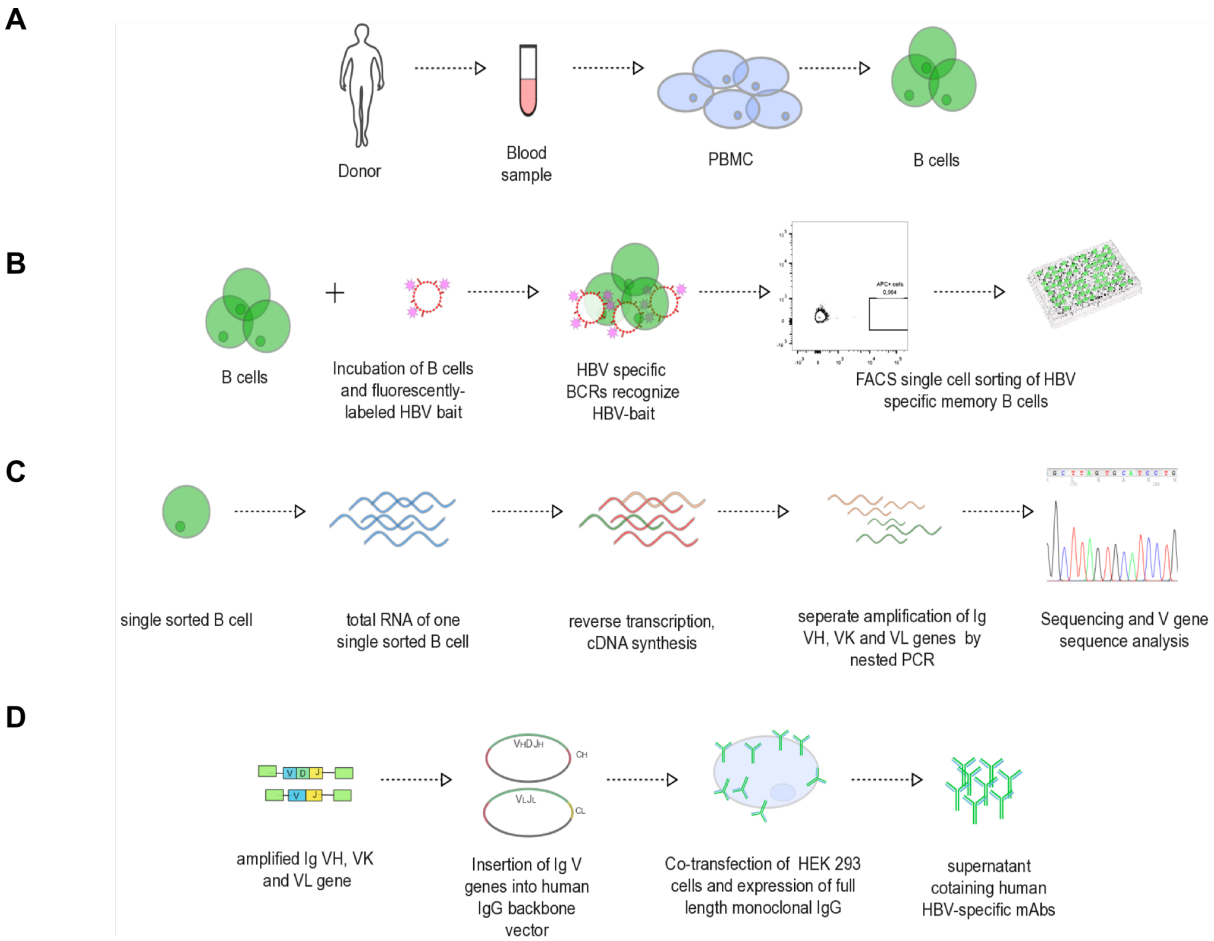

Figure 6. Sequential steps of single B-cell antibody technology.
(A and B) Identification and isolation of single antigen-specific memory B cells with flow cytometry after enrichment of human peripheral blood B cells and incubation with fluorescently labeled HBV baits. (C) Amplification and sequence analysis of immunoglobulin variable chain gene segments from single B cells. (D) Cloning and expression specific recombinant antibodies from corresponding heavy and light chain genes.

With regard to the isolation of antigen-specific B cells, the selection of a highly specific molecular bait that is recognized only by specific BCRs is crucial. Peptides or proteins, whole virions or virus-like particles and B-cell tetramers that present linear B-cell epitopes can be used as B-cell antigen (Cox et al., 2016; Franz et al., 2011). Regardless of the type of antigen that is used, it needs to be labeled either with biotin, a fluorochrome or any other detection reagent to be visualized with a flow cytometer (Moody & Haynes, 2008). Moreover, appropriate donors are fundamental. These have to have an immune response against the pathogen or a vaccine of interest (K. Smith et al., 2009). Once the B cells of interest are identified, single cells are isolated and immediately frozen on dry ice, leading to cell lysis (Tiller et al., 2008).

The second step focuses on the construction of complementary DNA (cDNA) and the amplification of immunoglobulin variable heavy and light chain genes expressed in each single B cell. In order keep rare B-cell mRNA and prevent cross-contamination, cDNA is usually synthesized in the original plate that was used for cell sorting (Tiller, 2011). Reverse transcription is directly followed by nested PCR to amplify Ig gene transcripts. In the first round, PCR forward primer mixes, complementary to specific V-gene leader sequences, and a single reverse primer, specific for the constant region, are used to amplify the respective Ig heavy and light chain genes. For the second PCR run, nested primer and primer mixes are used that are complementary to specific V-gene segments and the constant region (Marks et al., 1991; Tiller et al., 2008). The second PCR is conducted to amplify the DNA in sufficient amounts to obtain sequences of variable heavy and light chain genes and to increase sensitivity and specificity (K. Smith et al., 2009). Additionally, restriction sites for later cloning can be introduced. However, two limitations have to be considered: First, different B-cell types contain different amounts of mRNA transcripts, which may result in difficulties to synthesize cDNA (Franz et al., 2011; Tajiri et al., 2010). Second, the primer set used for amplification limits the number of variable genes that can be amplified (Scheid et al., 2011; Tiller, 2011).
After amplification, single cell Ig gene transcripts are sequenced and rearranged V(D)J-gene segments can be identified using databases such as IgBlast (https://www.ncbi.nlm.nih.gov/igblast/; 19.12.2019) or IMGT V-quest (http://www.imgt.org/IMGT_ vquest/input; 19.12.2019). Sequences can be analyzed for the presence of deletions, mutations and insertions, but also CDR and FR can be identified. In addition, B-cell antibody repertoires can be investigated (Tiller, 2011).

The last step of monoclonal antibody generation from single B cells is used for antibody expression and specificity testing. The amplified corresponding variable heavy and light chain genes are cloned into Ig expression vectors of choice. Various antibody formats can then be expressed in different organisms (K. Smith et al., 2009). Ig genes are usually expressed as antigen-binding Fab-fragments in bacteria, whereas transient or stable expression in mammalian cells such as Human embryonic kidney cells 293 (HEK293 cells) or Chinese hamster ovary cells (CHO cells) often results in full length IgG formats (Tiller, 2011). Upon production of sufficient amounts of proteins, the new antibodies can be evaluated for specificity with various assays for instance with enzyme-linked immunosorbant assay (ELISA).

Specific mAbs can then be produced, purified and further characterized structurally and functionally.

While the single B cell antibody technology offers several distinct advantages and has successfully been used to generate broadly neutralizing human monoclonal antibodies against HIV, it has been selected to generate human antibodies against HBV (Klein et al., 2012; Scheid, Mouquet, Feldhahn, Seaman, et al., 2009).

1.5 Aims of the work

Chronic HBV infection is still a major health problem, especially because current treatment options are limited and rarely achieve cure. The immune response plays a crucial role in the outcome of HBV infection and is impaired in chronically infected patients. Currently, several antiviral immunotherapeutic approaches are under investigation. Antibodies are one option and are already efficiently used for the prevention of HBV infection. Furthermore, upon HBV clearance, antibodies directed against the viral envelope proteins (anti-HBs antibodies) maintain long-term virus control. In order to support the defective B-cell response in chronic HBV patients, immunotherapies with anti-HBs antibodies have been carried out, but were not followed up due to high production efforts for polyclonal sera and the limited availability of potent binders. Therefore, the overall aim of this study was to generate novel recombinant human monoclonal antibodies directed against HBV envelope proteins that could be used for immunotherapeutic applications.

As a first step, the frequency of HBV-specific memory B cells in the blood of vaccinated individuals was determined. Blood memory B cells are easily accessible and have high antigen affinities. Analysis of the number of antigen-specific B cells in blood gave insight whether it was at all feasible to isolate those cells for antibody generation.

In a next step, suitable antigenic baits were prepared for the identification and isolation of HBV-specific memory B cells with flow cytometry. It was investigated whether these antigens are selectively recognized by HBV-specific B cell receptors.

Using those baits, two different methods for the generation of HBV-specific monoclonal antibodies were explored and antibodies were generated upon B-cell isolation. In order to determine the success of the B-cell isolation method, antibody specificities were evaluated.

Finally, upon successful specificity testing, the most potent candidates were selected for structural and functional characterization studies. The new anti-HBs monoclonal antibodies were explored by determining the antigen affinity, the epitope, the neutralizing capacity, and the immune effector function.

2 Results

2.1 Generation of HBV-specific monoclonal antibodies

New therapeutic treatments for chronic HBV infection are urgently needed. One option could be an immunotherapeutic approach with antibodies. Since the viral antigens are expressed on the surface of HBV infected hepatocytes they can serve as potent targets for antibodies. Furthermore, antibodies can capture circulating HBsAg and thereby help to restore the host immune response, as high loads of viral antigens are believed to be the main trigger for immune exhaustion (Cerino et al., 2019). The efficacy of antibody-based therapy in chronic HBV patients has already been evaluated in a few studies, but further progress is so far restricted due to the limited availability of high affinity fully human binders. Therefore, the following sections will focus on the identification and isolation of HBV-specific human B cells from peripheral blood of healthy volunteers. This will provide the basis for the generation of new human immunoglobulins using B-cell immortalization and single B cell antibody technology.

2.1.1 Identification of HBV-specific memory B cells with ELISpot

Several different ways for the generation of human monoclonal antibodies from peripheral blood exist. All of them rely on the frequency of circulating antigen-specific B-lymphocytes. This frequency is generally very low and highly dependent on the immune status of a person for instance after vaccination or infection. In order to estimate the number of HBV-specific B cells in peripheral blood of different individuals and to select optimal donors for the following B-cell isolation we first performed a B-cell ELISpot with PBMC isolated from different healthy volunteers. Two donors (donor 16 and 20) received HBV-booster vaccination seven days prior to blood donation, as this time point correlates with the peak of anti-HBs antibodies in the serum (Salimzadeh et al., 2018). Donor 01 resolved an acute HBV infection and donor 09 was HBV naïve, with no detectable anti-HBs antibodies in the quantitative diagnostic anti-HBs test (Architect platform).

After isolation, PBMC were either stimulated *in vitro* with R848 and IL-2 for five days or cultured for five days in medium only. After incubation, the supernatant was used for ELISA analysis and the cells were plated onto ELISpot plates. Beforehand, the plates were coated with anti-human IgG, to estimate the frequency of total IgG

secreting cells or with HBsAg, to capture antigen-specific antibodies from antibody secreting plasma cells (ASCs). Stimulation induced the differentiation of memory B cells into ASCs indicated by the detection of IgG+ spots. B cells without stimulation were not able to secrete detectable IgG (Figure 7 A). Due to the limited number of PBMC only two replicates of donor 09 were plated. The number of IgG+ spots was slightly different between the different donors, ranging from 100 to 350 spots per well. This corresponded to a frequency of IgG+ memory B cells of 4-8% of total PBMC and was within the expected range of up to 10% of IgG+ memory B cells in peripheral blood (Figure 7 C).

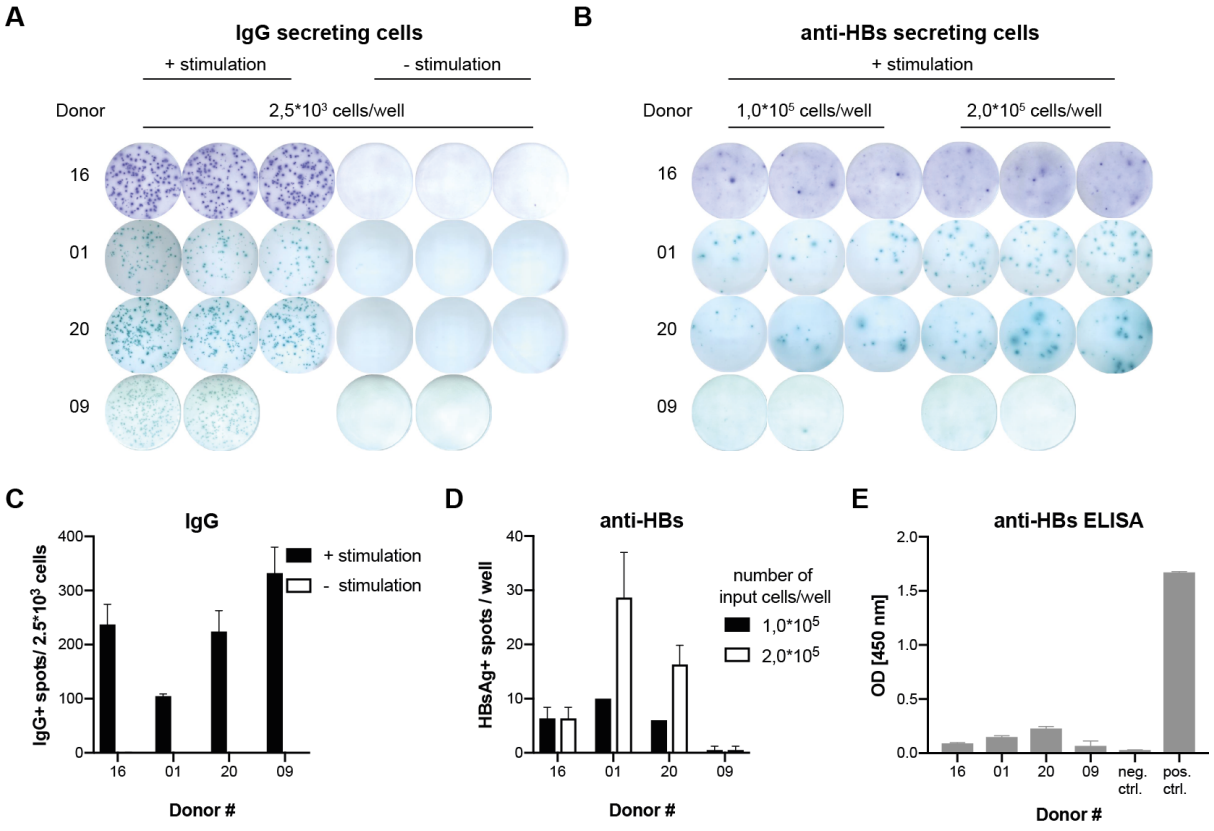

Figure 7. Identification of IgG+ and HBsAg-specific B cells in peripheral blood of healthy donors with ELISpot
(A and B) Representative ELISpot well image of antibodies secreted from antibody secreting cells (ASCs) from two HBV-vaccinated donors 16 and 20, one HBV-resolved donor 01 and one HBV naïve donor 09. (A) Human IgG ELISpot and (B) ELISpot detecting HBsAg-specific antibodies (C) Quantification of IgG+ spots secreted from 2.5*10^3 input PBMC per well. (D) Quantification of HBsAg+ spots comparing two input cell numbers. (E) Detection of HBsAg-specific antibodies with ELISA in cell culture supernatant of stimulated PBMC. Supernatant from unstimulated cells was used as negative control (neg. ctrl.) and supernatant containing an anti-HBs antibody was used as positive control (pos. ctrl.). Mean and SD are shown.

Antigen-specific antibodies were identified on HBsAg coated ELISpot plates. Anti-HBs antibodies were secreted from cells isolated from donors 01, 16 and 20, but not from the HBV naïve donor 09 (Figure 7 B). The number of anti-HBs+ spots increased with rising number of input cells for donor 01 and 20. For donor 16, the number of positive spots remained constant, although the input cell number increased (Figure 7 D). Overall, based on the number of anti-HBs spots detected, the frequency of HBsAg-specific memory B cells in PBMC was estimated with 0.01%. This was low, but within an expected range.

Additionally, the presence of anti-HBs antibodies in cell culture supernatant after five days of stimulation was analyzed with ELISA. For this, ELISA plates were coated with HBsAg and cell culture supernatant was applied. Captured anti-HBs antibodies were detected with polyclonal goat anti-human IgG HRP antibodies. Generally, the signal intensity was low. Strongest signal was measured with supernatant from cells of donor 20. Supernatant from the naïve donor was negative for anti-HBs antibodies (Figure 7 E). However, ELISpot and ELISA results were not directly comparable, which may be due to different assay sensitivities.

In summary, upon stimulation, antigen-specific memory B cells secreted anti-HBs antibodies that could both be detected with ELISpot and ELISA. The frequency of specific B cells was estimated with 0.01% of total PBMC in healthy HBV vaccinated or resolved individuals. For HBV naïve donors, no HBsAg-specific B cells were seen. As consequence, following B-cell isolation experiments were performed only with B cells isolated from HBV-booster vaccinated donors or the one donor with resolved acute infection.

2.1.2 Evaluation of HBV-specific baits to identify antigen-specific B cells in PBMC with FACS

With an estimated frequency of 0.01% of HBsAg-specific memory B cells in PBMC, we next aimed at isolating these cells, as their immunoglobulin genes can be used for recombinant monoclonal antibody generation. For this, three fluorescently labeled variants of HBV subviral particles (SVPs) were prepared. These were used as baits to selectively bind to the B-cell receptors of HBV-specific IgG+ CD19+ memory B cells. Before cell isolation, each variant was evaluated for specificity.

2.1.2.1 Detection of HBV-specific memory B cells with Alexa647-SVPs

The first bait consisted of HBV subviral particles (SVPs), purified from supernatant of HBV producing cell line HepAD38. SVPs were chemically labeled with Alexa Fluor 647 (Alexa647) dye via NHS-coupling. Jochen Wettengel kindly performed purification and labeling of the particles. HBV SVPs have the advantage to contain the three HBV envelope proteins small, middle and large, instead of only the small protein as recombinant e.g. yeast-derived HBsAg. This allows the identification of a broad repertoire of memory B cells for antibody generation.

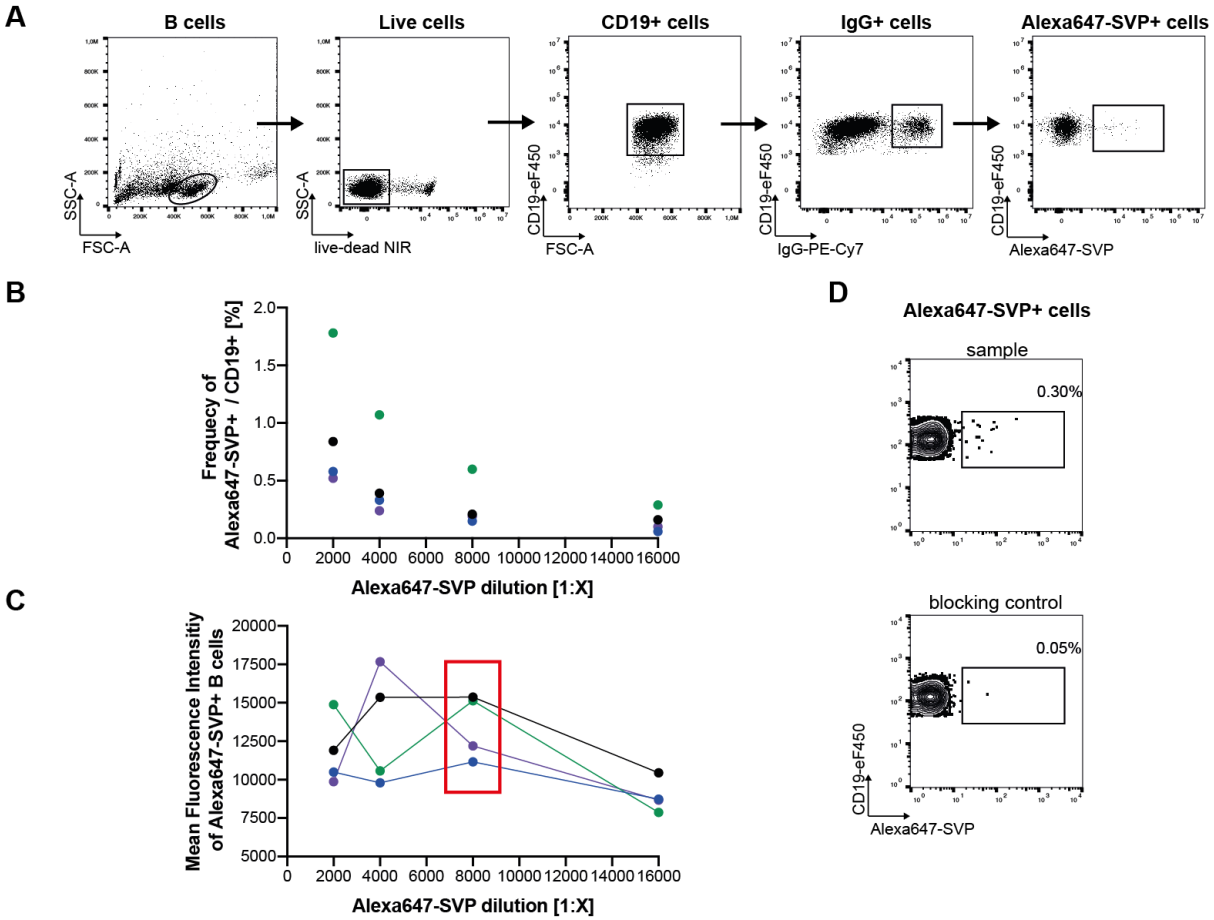

Figure 8. Evaluation of Alexa647-labeled SVPs for the identification of HBV-specific memory B cells with FACS.
(A) Representative gating strategy to identify Alexa647+ memory B cells with Alexa647-SVPs. (B) Correlation of Alexa647-SVPs dilution and frequency of Alexa647+ B cells of CD19+ B cells from 4 donors (indicated by different colored dots). (C) Mean fluorescence intensity (MFI) of Alexa647+ cells plotted against Alexa647-SVP dilution to determine optimal staining concentration. Optimal condition marked in red (D) Analysis of bait specificity after blocking with non-labeled SVPs. Plots show the frequency of Alexa647-SVP+ cells of CD19+ B cells.

To evaluate the specificity and the optimal bait concentration, pre-enriched human B cells from four HBV-vaccinated volunteers were incubated with serial dilutions of Alexa647-SVPs and analyzed with flow cytometry. Antigen-binding memory B cells were identified with a five-step gating strategy, gating for live, CD19+ IgG+ and Alexa647+ memory B cells (Figure 8 A). A correlation between the concentration of Alexa647-SVP used for staining and the frequency of Alexa647-binding cells was observed. More labeled-SVPs resulted in a higher frequency of positive cells for all donors, ranging from 1.7% to 0.01% of CD19+ cells (Figure 8 B). Since frequencies of >1% are very likely to be unspecific (M. J. Smith et al., 2017), we next determined the optimal bait concentration to identify HBV-specific memory B cells, by calculating the mean fluorescence intensity (MFI) of Alexa647-SVP+ cells. The MFI correlates with number of SVPs recognized by the BCR. Consequently, highest MFI is an indicator for receptor saturation. The maximum MFI was reached with a dilution of 1:8000 for B cells from three of four donors. B cells from one donor (purple line) indicated highest MFI with a dilution of 1:4000, but at 1:8000 the MFI was still within the range of the other donors (Figure 8 C). As a result, following cell isolation experiments were performed with a dilution of 1:8000. Additionally, the specificity of Alexa647-SVPs was investigated upon blocking BCRs with 100-fold excess of non-labeled SVPs before adding Alexa647-labeled ones. With this the signal was blocked by 80% (Figure 8 D) pointing at a specific recognition of Alexa647-SVPs through the B cell receptor.

2.1.2.2 Detection of HBV-specific memory B cells with HBsAg-Alexa594

The next strategy involved the use of HBsAg purified from serum of HBV carriers, which was kindly provided by Roche Diagnostics GmbH (Penzberg, Germany). HBsAg was labeled in-house with Alexa Fluor 594 (Alexa594) dye with the same chemical method as Alexa647-SVPs. As performed before, pre-enriched B cells from different HBV vaccinated donors were incubated with serial dilutions of labeled HBsAg and analyzed on a cytometer gating for live, CD19+ IgG+ and Alexa594+ memory B cells. With escalating concentrations more HBsAg binding CD19+ memory B cells were detected. Frequencies ranged from 0.05% to 0.7% of CD19+ B cells. A linear correlation was observed among all donors indicating a specific recognition of HBsAg-Alexa594 through the BCR, but no saturation (Figure 9 A and B). The MFI of Alexa594+ cells was used to determine the ideal concentration

for the detection of antigen-specific memory B cells. Different MFI level were observed between donors with high and low anti-HBs serum titer, indicating that the serum antibody titer should be considered for donor selection (Figure 9 C). The MFI peaked at an HBsAg-Alexa594 concentration of 1.25 µg/mL when B cells from two high titer donors were used. For a third high titer donor (pink line), the maximum MFI was determined with a concentration 0.63 µg/mL (Figure 9 C), but the frequency of HBsAg+ B cells was lower compared to the other donors (Figure 9 B). As a consequence, we decided to use HBsAg-Alexa594 with a concentration of 1.25 µg/mL for the isolation of HBV-specific memory B cells in the following experiments.

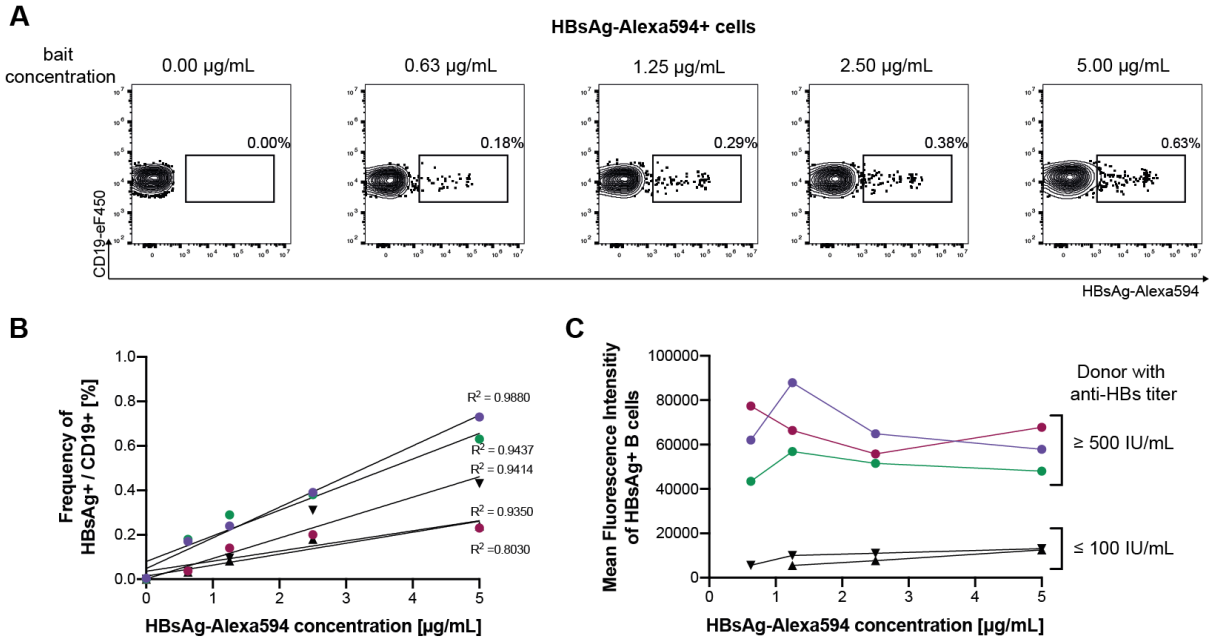

Figure 9. Evaluation of HBsAg-Alexa594 as bait for the identification of HBV-specific memory B cells with FACS.
(A) Representative flow cytometry plot of Alexa594+ cells after incubation with serial dilution of HBsAg-Alexa594 bait. Frequencies of Alexa594+ cells of CD19+ cells are shown and cells were pre-gated for live, CD19+ IgG+ cells. (B) Correlation analysis of the concentration of HBsAg-Alexa594 and the frequency of HBsAg+ cells of five donors. R^2 was calculated with linear regression. (C) Mean fluorescence intensity (MFI) of HBsAg+ cells in dependency of HBsAg-Alexa594 concentration used for staining.

2.1.2.3 Identification of HBV-specific memory B cells with HBsAg-biotin

To test a third bait, serum purified HBsAg was labeled with biotin via NHS-coupling instead of a fluorescent dye. The molecular weight of biotin is less, compared with Alexa Fluor 647 or 594 and therefore, the risk of shielding potential epitopes via the fluorophore is decreased. Furthermore, the combination of biotin with streptavidin for

detection allows signal amplification and thereby a better differentiation between binding and non-binding cells (M. J. Smith et al., 2017). As for the other baits, B cells of two donors, one HBV naïve donor and one with resolved acute infection, were incubated with increasing concentrations of HBsAg-biotin followed by addition of allophycocyanin (APC)-labeled Streptavidin. Most HBsAg+ cells were detected with lowest HBsAg-biotin dilution (1:10) when B cells from the donor with resolved acute HBV infection were used. The frequency ranged from 0.015% to 0.032% of CD19+ memory B cells. In contrast, the frequency of positive cells remained constant and low (0.01% of CD19+ cells), when B cells isolated from the HBV naïve donor were incubated with different bait dilutions (Figure 10 A). Overall, the frequency of positive cells was lower compared to that determined with the other baits. The ideal bait dilution for B-cell isolation experiments was determined by comparing the MFI of Streptavidin-APC+ cells between the two donors. The maximum MFI was reached at a dilution of 1:25 when B cells from the donor with resolved infection were stained. Furthermore, this dilution obtained the biggest difference between the MFIs of the two donors (Figure 10 B). As a consequence, the 1:25 dilution of HBsAg-biotin was selected for following B-cell isolation experiments.

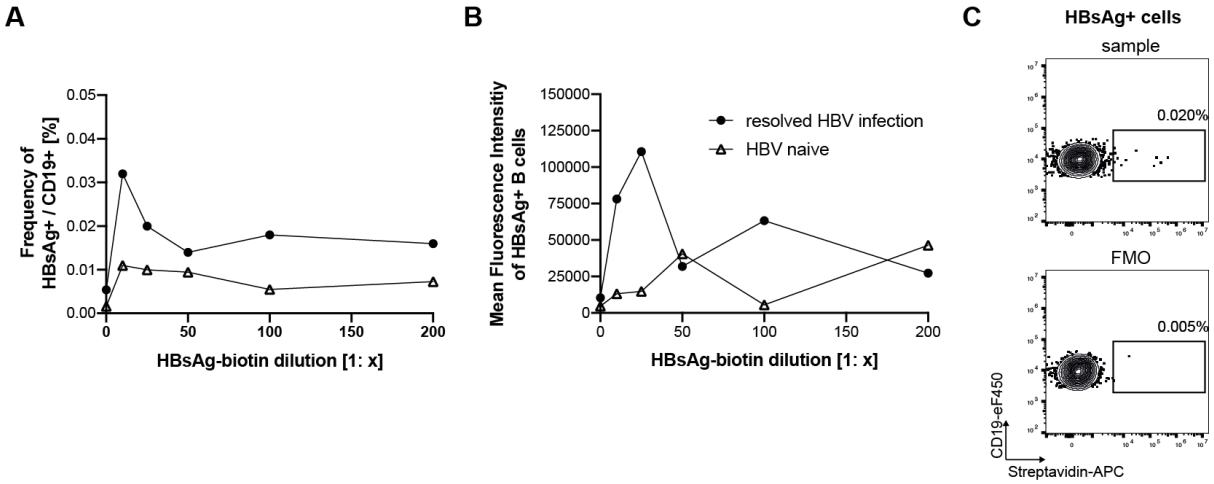

Figure 10. Evaluation of HBsAg-biotin as bait for the identification of HBV-specific memory B cells with FACS.
(A) Frequency of HBsAg+ cells of CD19+ cells and (B) Mean Fluorescence Intensity of HBsAg+ cells of two donors upon staining with serial dilution of HBsAg-biotin. (C) Comparison of HBsAg+ cells of CD19+ B cells in sample and fluorescence minus one (FMO) control to differentiate between background and specific binding of HBsAg-biotin bait and Streptavidin-APC.

In addition, a fluorescence minus one control (FMO) was included during cell analysis to exclude non-specific streptavidin binding to cell surface receptors. This

obtained only little background, 0.005% due to non-specific Streptavidin binding (Figure 10 C).

In summary, all baits were capable of binding to HBV-specific B cell receptors selectively on the surface of CD19+ IgG+ memory B cells. The frequency of detecting antigen-specific memory B cells at optimal bait concentrations ranged from 0.3% with Alexa647-SVPs and HBsAg-A594 to 0.02% with HBsAg-biotin and Streptavidin-APC. Although the frequency of positive cells varied, each bait could be used to isolate HBV-specific memory B cells in the following experiments.

2.1.3 Isolation of HBV-specific memory B cells for antibody cloning

Two strategies were followed in order to extract the genetic information of immunoglobulin variable chain genes from memory B cells for antibody generation. The first strategy relied on the transformation and outgrowth of B cells after cell sorting followed by limiting dilution cloning. In the first approach, B cells were either immortalized with Epstein-Barr virus (EBV) or transformed by the continuous stimulation with CD40L-expressing cells and IL-4. The second approach used single B cell antibody technology (Tiller et al., 2008; Wardemann et al., 2003). Antigen-specific memory B cells were identified using the fluorescently labeled baits (see section 2.1.2), isolated by single cell sorting. Immunoglobulin variable genes of each cell were subsequently amplified without further cultivation. With regard to antibody cloning, the advantage of both strategies compared with others for instance phage display is the preservation of the natural pairing of immunoglobulin heavy and light chain.

2.1.3.1 Transformation of antigen-specific B cells

EBV immortalization to generate HBsAg-specific B-cell lines

B-cell transformation with EBV is a frequently used method for antibody generation. After transformation, B cells grow rapidly in suspension, but keep the characteristic of the initially infected B cell such as expression and secretion of immunoglobulins (M. Steinitz, 2014). This can be used to enrich antigen-specific B cells for antibody cloning.

Initially, in order to efficiently transform human B cells with EBV, EBV-containing medium was produced from marmoset B95-8 cells. Its capability to transform B cells was investigated with PBMC from a donor with resolved acute HBV infection. For transformation, cells were cultured in the presence of cyclosporine A and EBV-containing media for two weeks. The supernatant of two individual cultures was collected and analyzed for the presence of human IgG and HBsAg-specific antibodies by ELISA. Human IgG was already detectable in the supernatant after one week and remained constant until week two. PBMC cultured without EBV also secreted small quantities of IgG (Figure 11 A). Additionally, cell clustering was observed under the microscope, after two weeks (Data not shown), indicating that B-cell proliferation was induced and EBV media was capable of transforming B cells.

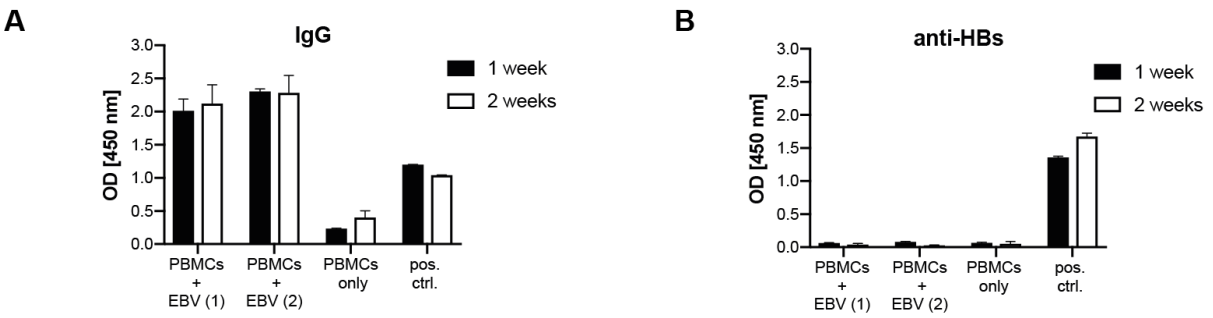

Figure 11. Antibody secretion of B cells after PBMC stimulation with EBV medium
ELISA analysis for the presence of human IgG (A) and anti-HBs antibodies (B) in cell culture supernatant of PBMC transformed with EBV one week and two weeks after start of culture. Positive control (pos. ctrl.) refers to supernatant from anti-HBs secreting cell line. Mean and SD are shown.

For the detection of HBsAg-specific antibodies an anti-HBs ELISA was performed with the supernatant. Unfortunately, no HBsAg-specific antibodies were detected, although PBMCs originated from a donor with recent HBV booster vaccination and high anti-HBs serum titer (≥1000 IU/mL) (Figure 11 B). In conclusion, B-cell transformation with EBV starting from full PBMC did not yield in the detection of HBsAg-specific antibodies.

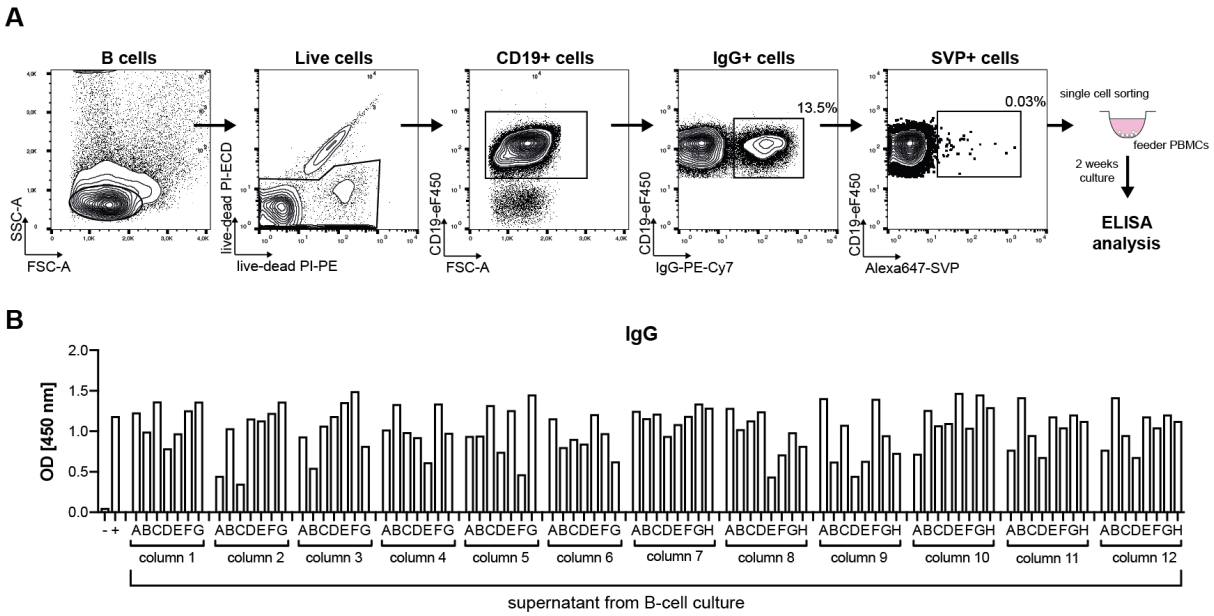

Figure 12. Transformation of single sorted Alexa647-SVP+ memory B cells with EBV. (A) Representative gating strategy for the isolation of single Alexa647-SVP+ memory B cells followed by B-cell culture in the presence of allogeneic, irradiated feeder PBMC and EBV medium. (B) ELISA analysis for the secretion of human IgG after two weeks of B-cell culture. "+" Positive control (medium supplemented with human anti-HBs IgG). "-" Negative control (cell culture supernatant with feeder cells only).

In order to increase the probability to transform antigen-specific B cells with EBV, B cells from a donor with resolved acute HBV infection were first enriched from PBMC, and then incubated with Alexa647-SVP bait. Alexa647-SVP+ memory B cells were identified and finally individually sorted into 96-well U-bottom plates containing EBV medium as well as irradiated, allogeneic feeder PBMC, CpG and IL-2 (Figure 12 A). After two weeks of incubation, the supernatant was screened for the presence of human IgG and HBV-specific antibodies with ELISA. All wells were positive for the secretion of human IgG (Figure 12 B). However, ELISA analysis for anti-HBs specific antibodies remained negative, indicating that single B cells can be cultured in the presence of feeder PBMC and EBV, but enrichment of antigen-specific B cells with Alexa647-SVPs was not successful. In conclusion, using this approach immortalization of antigen-specific B cells with EBV was not successful and consequently we were unable to establish HBV-specific lymphoblastoid cell lines for the generation of monoclonal antibodies.

CD40 stimulation of human B cells

Besides the transformation with EBV, stable antibody secreting B cells can be established from memory B cells with continuous stimulation of CD40 on the B-cell surface. Triggering of CD40 via its ligand CD40L and supplementation with IL-4 mimics B-cell activation by T helper cells and thereby leading to cell differentiation, proliferation and antibody secretion (Wiesner, 2008). CD40L-expressing L929 feeder cells were kindly provided by Andreas Moosmann from DZIF Research Group Host Control of Viral Latency and Reactivation (Helmholtz Center Munich, Germany).

Initially CD19+ B cells from PBMC of two HBV-vaccinated donors were isolated in a bulk with fluorescently activated cell sorting (FACS). Sorted cells were then seeded into 96-well F-plates on irradiated CD40L-expressing feeder cells in the presence of IL-4. In contrast to the previous experiments, where single cells were seeded, the seeding density was increased to 400 cells per well. Six plates of two donors were prepared in total. Figure 13 A shows a schematic overview of the gating strategy and cell culture procedure. The supernatant was analyzed for the secretion of IgG with ELISA, after two weeks of incubation. IgG was detected in most wells from both donors (data now shown), but OD values differed from well to well. Wells with high IgG reactivity (OD_{450nm} >1.0) suggested reasonable proliferation and were therefore selected for further culture. These cells were re-seeded on freshly irradiated feeder cells and further cultivated for two weeks before retesting. This procedure of IgG analysis and re-seeding was repeated twice until week six. After six weeks, not only IgG secretion was investigated, but also anti-HBs reactivity. All wells were positive for IgG, except for well H10 (Figure 13 B upper panel). However, only one well of each donor F12 (Donor 01) and F10 (Donor 05) indicated slight reactivity against the coated HBsAg (Figure 13 B lower panel). These cells were once more re-seeded to show anti-HBs reactivity. The supernatant was then tested for specificity two weeks later. Final ELISA analysis indicated the secretion of HBsAg-specific IgG antibodies in both wells, suggesting successful activation of antigen-specific B cells through the continuous stimulation of CD40 (Figure 13 C). In order to achieve monoclonal outgrowth for later Ig gene amplification, the cells were re-seeded again on freshly irradiated L929 feeder cells but with a density of 0.3 cells per well for limiting dilution cloning. Unfortunately, all cells died during this process and consequently the genetic information about the HBV-specific BCR could not be obtained.

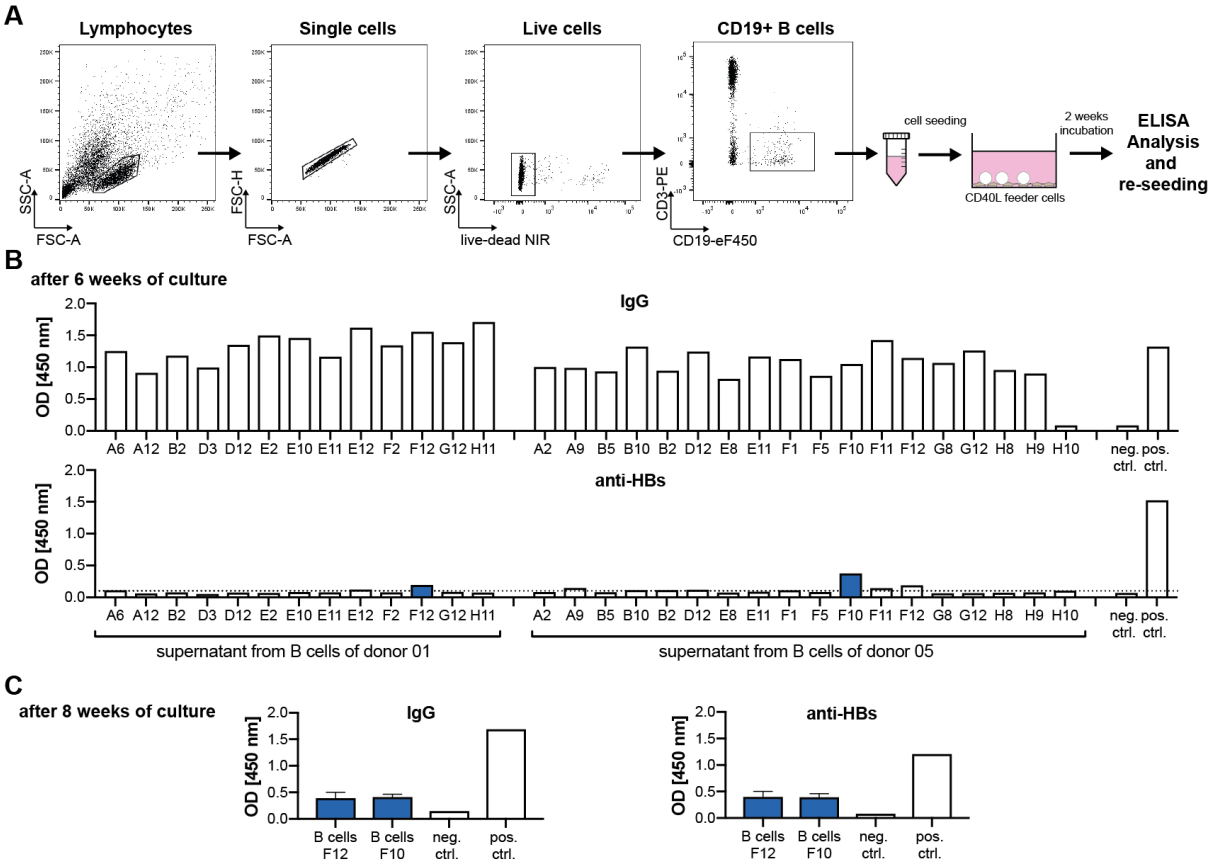

Figure 13. Continuous CD40L stimulation of CD19+ B cells for the enrichment anti-HBs secreting B cells.
(A) Representative gating strategy for the isolation of CD19+ B cells with FACS followed by cell seeding in 96-well plates on irradiated CD40L-expressing feeder cells in the presence of IL-4. Every two weeks cells were re-seeded after positive ELISA for IgG secretion. (B) Representative ELISA analysis of CD40L-stimulated B cells of two donors for the secretion of IgG and anti-HBs specificity after 6 weeks. (C) Final ELISA results after 8 weeks of culture and re-seeding of two wells F12 (donor 01) and F10 (donor 05).

After detecting anti-HBs antibodies only in two wells out of six 96-well plates, we next aimed at increasing the yield of antigen-specific cells obtained from B cell cultures. Therefore, B cell sorting with HBV-baits (HBsAg-Alexa594 and HBsAg-biotin) was performed (see 2.1.2 for bait evaluation). On the one hand, B cells from an HBV-booster vaccinated donor were incubated with 1.25 µg/mL HBsAg-Alexa594 and 234 live, CD19+ IgG+ HBsAg-Alexa594+ B cells were sorted into a tube. These cells were then seeded in two wells of a 96-well plate in the presence of freshly irradiated CD40L-feeder cells and IL-4 (Figure 14 A). As before, cells were re-seeded on fresh feeder cells every two weeks. ELISA analysis six weeks after cell sorting indicated IgG secretion in both wells. However, only one well was slightly positive for anti-HBs antibodies (Figure 14 B). On the other hand, cell sorting with HBsAg-biotin bait and B-cell culture was carried out in parallel in the same way.

95 HBsAg-biotin+ IgG+ CD19+ memory B cells of one donor and 80 positive cells of another HBV vaccinated donor were bulk sorted and seeded in two wells each in the presence of feeder cells and IL-4. ELISA analysis four weeks later indicated IgG secretion, but only little reactivity against HBsAg in one well (well 2, donor 01) (Figure 14 C). Due to the little success, the cells were not cultured further.

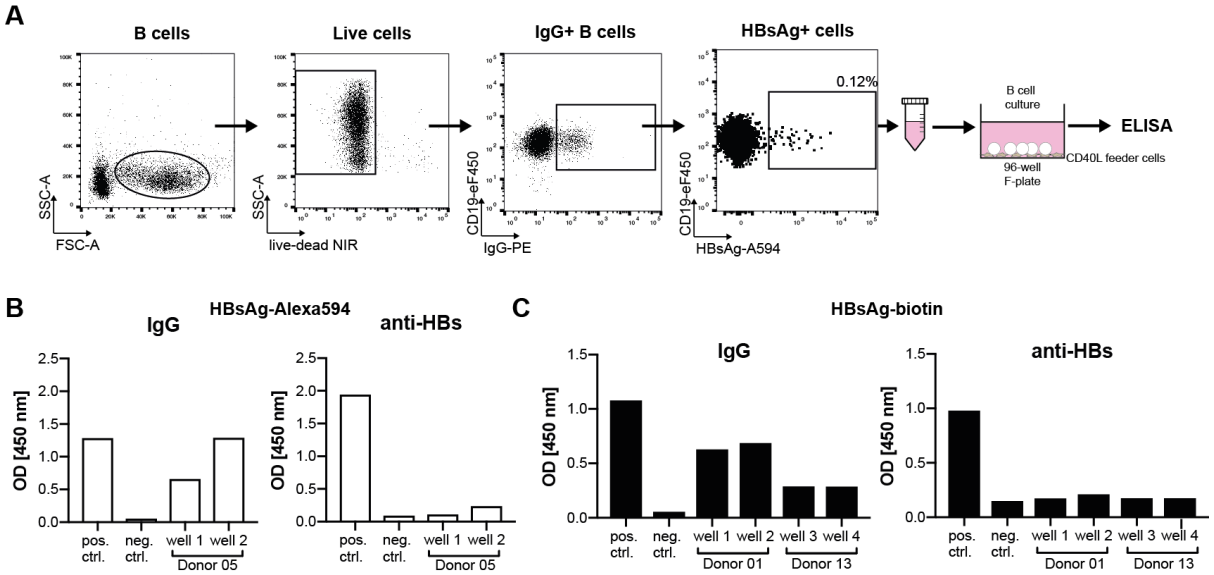

Figure 14. CD40L-stimulation of pre-enriched HBsAg-specific memory B cells
(A) Representative gating strategy to isolate HBsAg-specific memory B cells with HBsAg-Alexa594 as bait, followed by B cell culture on CD40L-feeder cells. (B) Determination of IgG secretion and anti-HBs specificity with ELISA after B-cell culture for six weeks. (C) ELISA analysis for the secretion of IgG and anti-HBs antibodies in supernatant of B-cell cultures after cell sorting with HBsAg-biotin.

Overall, continuous stimulation of sorted B cells with CD40L, expressed on L929 feeder cells, induced the differentiation of memory B cells into antibody secreting cells indicated by the detection of human IgG in cell culture supernatant. However, the detection of anti-HBs antibodies remained low, although antigen-specific B cells were enriched with cell sorting before culture. As a result, continuous CD40L-stimulation of B cells did not prove to be useful for monoclonal antibody generation.

2.1.3.2 Single B cell antibody technology

Neither the stimulation of B cells with CD40L nor the transformation of B cells with EBV resulted in stable antigen-specific B-cell lines that could be used to recover immunoglobulin variable genes for antibody cloning. As a consequence, we then

performed single cell sorting of HBV-specific B cells with subsequent immunoglobulin variable chain gene amplification without further cultivation.

For this, B cells were first pre-enriched from PBMC from healthy volunteers and then incubated either with Alexa647-SVPs, HBsAg-Alexa594 or HBsAg-biotin to isolate HBV-specific memory B cells. For each preparation the optimal bait concentration, determined in section 2.1.2, was used in order to achieve maximum yield of antigen-specific B cells. A single gating strategy for all baits was used to identify live, CD19+ IgG+ and HBV+ B cells (Figure 15 A, Alexa647-SVPs (B); HBsAg-Alexa594 (C); HBsAg-biotin (D)). Positive cells were sorted individually into 96-well PCR plates and immediately frozen on dry ice.

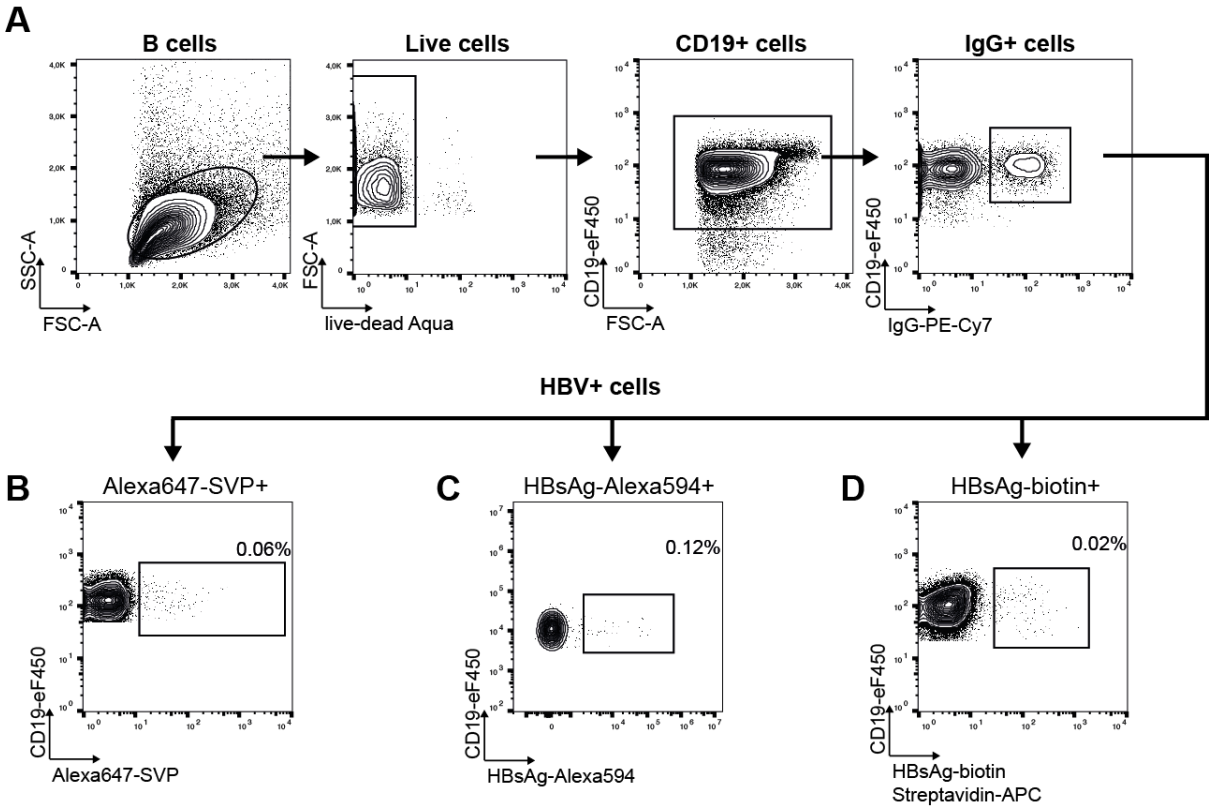

Figure 15. Representative gating strategy for the isolation of single HBV-specific memory B cells with various HBV-baits.
(A) Pre-enriched B cells were first incubated with the different HBV baits and HBV-specific cells were identified with gating for live, CD19+ IgG+ Alexa647-SVP+ (B), HBsAg-Alexa594+ (C) or HBsAg-biotin+ (D) cells. Positive cells were sorted individually into 96-well PCR plates. Frequencies of CD19+ B cells are indicated.

15 independent rounds of single cell sorting with the different baits were carried out in total. B cells originated from six donors. Five received HBV booster vaccination seven days prior blood donation and one donor resolved an acute HBV infection

earlier in life (Table 1). A summary of all sorts performed is shown in Table 1. With the Alexa647-SVPs 384 antigen-specific cells were captured in two rounds of single cell sorting. This correlated with a frequency of 0.04% - 0.06% of CD19+ B cells (Table 1, Sorting A and B). After incubation with HBsAg-Alexa594 for one round of single cell sorting, the frequency of antigen-specific B cells slightly increase. However, only 40 positive cells were sorted (Table 1; Sorting 1).

Table 1. Frequencies of HBV-specific B cells sorted with different HBV-baits in independent single B cells sorting approaches

Sorting	Bait	Further marker	Donor	# of HBV+ B cells sorted	# of B cells analyzed	Frequency of CD19+B cells [%]
A	Alexa647-SVP		Resolved acute infection	257	1,710,000	0.04
B	Alexa647-SVP		Resolved acute infection	127	425,000	0.06
1	HBsAg-Alexa594		HBV booster vaccination	40	240,000	0.12
2	HBsAg-biotin Streptavidin-APC		Resolved acute infection	60	550,000	0.07
3	HBsAg-biotin Streptavidin-APC		Resolved acute infection	16	160,000	0.04
4	HBsAg-biotin Streptavidin-APC		Resolved acute infection	62	831,000	0.01
5	HBsAg-biotin Streptavidin-APC		Resolved acute infection	83	345,000	0.04
6	HBsAg-biotin Streptavidin-PE		Resolved acute infection	87	1,260,000	0.04
7	HBsAg-biotin Streptavidin-PE		HBV booster vaccination	84	1,500,000	0.02
8	HBsAg-biotin Streptavidin-APC		Resolved acute infection	33	664,000	0.02
9	HBsAg-biotin Streptavidin-APC		HBV booster vaccination	34	942,000	0.04
10	HBsAg-biotin Streptavidin-Alexa647	CD27	Resolved acute infection	56	1,220,000	0.04
11	HBsAg-biotin Streptavidin-Alexa647	CD27	Resolved acute infection	28	81,000	0.13
12	HBsAg-biotin Streptavidin-Alexa647	CD27	HBV booster vaccination	44	1,010,000	0.08
13	HBsAg-Alexa594	CD27	HBV booster vaccination	44	900,000	0.06

HBsAg-biotin in combination with Streptavidin-APC was used in six rounds of single cell sorting (Table 1, Sorting 3, 4, 5, 8 and 9). On average HBsAg-biotin+ memory B cells were isolated with a frequency of 0.04% (0.01% - 0.07%) of CD19+ B cells (Table 1). Overall, the frequency of sorted cells was lower compared with previous bait evaluation experiments (see section 2.1.2). As a consequence, the single cell sorting strategies used were optimized in order to increase assay specificity and B-cell yield. First, Streptavidin-APC was replaced by phycoerytrin (PE)-labeled Streptavidin, which has the highest brightness index of all fluorophores and therefore improves the detection of low expressed surface markers such as antigen-specific BCRs. However, the frequency of isolated HBV-specific memory B cells could not be increased (Sorting 6 and 7, Table 1). In the next step, the protein-label of Streptavidin was exchanged against Alexa Fluor 647 dye, as it is much smaller compared to PE and APC. Due to their size, the use of APC and PE can lead to epitope shielding and thereby interfere with the detection of rare antigen-specific B cells (M. J. Smith et al., 2017). Additionally, the memory B cell marker CD27 was included into the staining panel as the expression of CD27 correlates with somatic hypermutation of the BCR (Wu et al., 2011) and we aimed at isolating high affinity maturated B cells. With this optimization the frequency of HBsAg-biotin+ memory B cells isolated from CD19+ cells increased to 0.08% (Sorting 10, 11 and 12, Table 1). Not only HBsAg-biotin was combined with CD27, but also HBsAg-Alexa594 to further increase the selection for memory B cells. Here, 44 HBsAg-Alexa594 positive cells were isolated, which corresponded to a frequency of 0.06% of CD19+ cells (Sorting 13, Table 1). Overall, 1059 single memory B cells were sorted and the frequency of isolated HBV-specific memory B cells was comparable among the different baits ranging from 0.01% to 0.12%. However, even with the few optimizations the frequency remained lower in comparison with previous bait-evaluation experiments (section 2.1.2). This might be a consequence of cell sorter properties and settings.

2.1.4 Cloning of monoclonal antibodies from single cell mRNA

In contrast to the previously performed B-cell cultures, HBV-specificity of sorted and frozen memory B cells can only be determined after recombinant antibody cloning. Therefore, the following section will focus on the amplification of immunoglobulin variable chain genes from mRNA of each individual cell, sequence analysis, antibody

cloning and evaluation of mAb specificity. Each step was performed separately for every round of single cell sorting. However, to obtain a better overview, the results are presented as a summary.

2.1.4.1 Amplification of Ig variable genes

Each BCR consists of two antigen-binding sites. These are made up of immunoglobulin (Ig) heavy and light chains, which are translated from separate mRNAs. To recover Ig variable heavy (H) and light chain genes by PCR for recombinant antibody cloning, cDNA was reverse transcribed from mRNA of each single sorted cell. B cells isolated during sorting A (in total three PCR plates, Table 1) were sent to Cologne and Ig variable genes were kindly amplified and analyzed in collaboration with Florian Klein's laboratory by Christoph Kreer (Institute of Virology, University of Cologne, Germany). In total he retrieved 173 PCR products for heavy or light chain genes. The recovery rate for any heavy, kappa light or lambda light chain gene varied between 20-24%. Among these, 37 pairs of heavy and corresponding light chain were amplified (Table 2). In addition, 4% of the wells obtained a heavy chain and both, kappa and lambda light chains (data not shown), indicating that most likely two B cells were sorted into one well of a PCR plate.

B cells isolated during the other rounds of single cell sorting were amplified in-house following Ig variable gene amplification protocol established by *Tiller et al.* (Tiller et al., 2008). Variable heavy, kappa light (K) and lambda light (L) chain genes were amplified separately with three sets of primers by nested PCR. The amplification of human immunoglobulin variable heavy chain genes yielded in 187 PCR products that corresponded to an average frequency of 18% (Table 2). Dependent on the sorting, the recovery rate for variable heavy chain genes ranged from 1.7% to 83% (Table 2). For the two light chain variants, kappa and lambda, PCR products were obtained in 183 and 148 wells respectively. This corresponded to an average recovery rate of 19% (3.4% - 61%) for the amplification of variable kappa light genes and 12% (1.3% - 29%) for the amplification of lambda light chain genes (Table 2).

Table 2. Frequency of Ig variable genes amplified from single sorted HBV-specific B cells by nested PCR.

Sorting	# of B cells sorted	frequency of Ig variable genes amplified [%]			# of heavy + light chain couples	# of total products
		heavy	kappa light	lambda light		
A	257	22.6	20.2	24.1	37	173
B	127	25.2	26.8	26.0	18	99
1	40	5.0	5.0	5.0	2	6
2	60	1.7	0.0	0.0	0	1
3	16	Not amplified				
4	62	22.6	24.2	9.7	12	35
5	83	6.0	0.0	0.0	0	5
6	87	6.9	3.4	2.3	3	11
7	84	11.9	11.9	11.9	10	30
8	33	33.3	21.2	18.2	6	24
9	34	2.9	8.8	2.9	1	5
10	56	1.8	5.4	1.8	1	5
11	28	Not amplified				
12	48	83.3	56.3	25.0	22	79
13	44	13.6	61.4	29.5	6	46
Total	1059	18% (187)	19% (183)	12% (148)	118 (12%)	472 (23%)

For antibody cloning it is most important to retrieve the corresponding couple of heavy and light chain from one B cell. This was achieved in 118 wells, leading to an amplification efficiency of 12% (Table 2). In about 3%, IgH chains were amplified together with both Ig kappa and Ig lambda light chain (data not shown). This was similar to the amplification done in Cologne, again suggesting the deposit of two B cells in one well during cell sorting. In summary, the recovery rate to obtain any Ig variable gene was low (23%), but comparable between the two sites. Nevertheless, most rounds of single cell sorting obtained at least one couple of corresponding heavy and light chain gene, which could be used for antibody cloning after sequence analysis.

2.1.4.2 Immunoglobulin variable chain gene analysis

Before recovered Ig variable genes were used for cloning, all PCR products were purified and sent for sequencing. To enable the cloning of functional antibodies, sequences were first analyzed with regard to a complete open reading frame (ORF)

and the complementary determining region 3 (CDR3). Furthermore, the germline V(D)J-genes segments with highest identity were identified using the IMGT information system (Lefranc et al., 2015). This allowed gaining information about the clonality of the sorted B-cell population and the identification of V- and J-gene segment specific primers for cloning PCRs.

Among all PCR products sequenced, most were classified as productive and re-arranged Ig entities. Sequences with frame-shift mutations or incomplete ORFs were excluded from further analysis and from antibody cloning, as these would prevent functional protein expression. Based on identical CDR3 sequences and identical use of V- and J-gene segments 13 B-cell clones were identified (Table 3 and Figure 16 A). Some clones were identified from different B-cell donors (e.g. clone 6 and clone 8-12) suggesting that those B cells captured a specific antigen e.g. HBsAg that was used for single cell sorting (Table 3). Beside the B-cell clones, several unique couples of heavy and light chains genes were identified (Table 4). These sequences could not be clustered and made up 67.9% of all 277 sequences analyzed (Figure 16 A). The distribution of heavy and kappa light chain couples compared to heavy and lambda light chain couples was 60% to 37%, which reflects the 2:1 ratio of kappa vs. lambda light chains in healthy individuals. Furthermore, the collaboration with Florian Klein's laboratory obtained 7 clones and 30 unique couples of heavy and light chain genes from sorting A. However, sequence alignment with our sequences did not show overlapping clones.

Table 3. B-cell clones identified from single sorted B cells of different HBV booster vaccinated or acute resolved HBV donors.

Clones were clustered on the basis of identical CDR3 sequences and same Ig V- and J-gene segment usage.

		Heavy chain					Light chain							
Clone	Clonal group	VH	DH	JH	CDR3-IgH(aa)	CDR3 length	IgL	V-kappa	J-kappa	CDR3-IgK(aa)	CDR3 length	V-lambda	J-lambda	CDR3-IgL(aa)	CDR3 length
12D10	1	IGHV1-18*01	IGHD3-22*01	IGHJ4*02	CARERRTYFYDTGGQFDYW	19	K	no seq							
12D11	1	IGHV1-18*01	IGHD3-22*01	IGHJ4*02	CARERRTYFYDTGGQFDYW	19									
12D12	1	IGHV1-18*01	IGHD3-22*01	IGHJ4*02	CARERRTYFYDTGGQFDYW	19									
4D10	2	IGHV1-3*01	IGHD2-2*01	IGHJ4*02	CARDQRVGSSWFLPQPIDNW	20	K	IGKV4-1*01	IGKJ2*01/02	CQQYYGTPTF	10				
5C12	2	IGHV1-3*01	IGHD2-2*01	IGHJ4*02	CARDQRVGSSWFLPQPIDNW	20									
5E09	2	IGHV1-3*01	IGHD2-2*01	IGHJ4*02	CARDQRVGSSWFLPQPIDNW	20									
5F09	2	IGHV1-3*01	IGHD2-2*01	IGHJ4*02	CARDQRVGSSWFLPQPIDNW	20									
5G05	2	IGHV1-3*01	IGHD2-2*01	IGHJ4*02	CARDQRVGSSWFVPQPIDNW	20									
8B10	3	IGHV3-30*01/18	IGHD2-15*01	IGHJ4*02	CARGIGGSAYTGGDYW	16	K	IGKV4-1*01	IGKJ3*01	CQQYYATPTF	11				
4D07	3	IGHV3-30*01/18	IGHD2-16*01	IGHJ5*01	CARGIGGSAYTGGDYW	16	K	IGKV4-1*01	IGKJ3*01	CQQYYATPFTF	11				
6A03	4	IGHV4-34*01/12	IGHD3-3*01	IGHJ6*02	CAREMYYNFWGSFNYYHYGMDVW	23	L					IGLV1-51*02	IGLJ1*01	CGTWDNSLSARVF	13
8A11	4	IGHV4-34*01/12	IGHD3-3*01	IGHJ6*02	CAREMYYNFWGSFNYYHYGMDVW	23	L					IGLV1-51*02	IGLJ1*01	CGTWDNSLSARVF	13
4B03	4	IGHV4-34*01/12	IGHD3-3*01	IGHJ6*02	CAREMYYNFWGSFNYYHYGMDVW	23	L					IGLV1-51*02	IGLJ1*01	CGTWDNSLSARVF	13
4D04	4	IGHV4-34*01/12	IGHD3-3*01	IGHJ6*02	CAREMYYNFWGSFNYYHYGMDVW	23	L					IGLV1-51*02	IGLJ1*01	CGTWDNSLSARVF	13
4A10	4	IGHV4-34*01/12	IGHD3-3*01	IGHJ6*02	CAREMYYNFWGSFNYYHYGMDVW	23									
4C02	5	IGHV4-61*08	IGHD6-19*03	IGHJ6*03	CARDFLYSSGWGWFYYYMDVW	21	K	IGKV1-39*01	IGKJ1*01	CQQSYSTPRTF	11				
8A09	5	IGHV4-61*08	IGHD6-19*01	IGHJ6*03	CARDFLYSSGWGWFYYYMDVW	21									
4D05	6	IGHV3-21*01	IGHD4-23*01	IGHJ6*02	CTRDTVEAHLYYYYGMDVW	19	K	IGKV3-11*01	IGKJ4*01	CQQRSNWPLTF	11				
13C02	6						K	IGKV3-11*01	IGKJ4*01	CQQRSNWPLTF	11				
B1G01	7						K	IGKV1-39*01,	IGKJ1*01	CQQSYSTPWT	10				
B1A06	7						K	IGKV1-39*01	IGKJ1*01	CQQSYSTPWT	10				
13B04	8						K/L	IGKV3-15*01	IGKJ1*01	CQQYNNWPWTF	11	no seq result			
13C05	8						K/L	IGKV3-15*01	IGKJ1*01	CQQYNNWPWTF	11	no seq result			
7D05	9	IGHV3-30-3*01	IGHD3-9*01	IGHJ4*02	CASGQGPGERYFDYYGSDYW	20	K	IGKV1-5*03	IGKJ1*01	CQQYNSYPWTF	11				
13A09	9						K	IGKV1-5*03	IGKJ1*01	CQQYNSYPWTF	11				
8A03	10						K	IGKV4-1*01	IGKJ4*01	CQQYYSIPVTF	11				
12A12	10						K	IGKV4-1*01	IGKJ4*01	CQQYYSNPLTF	11				
4B09	11						L					IGLV1-44*01	IGLJ2*01	CAAWDDSLNGPVF	13
13D04	11	IGHV4-34*01/02/04	IGHD3-10*01	IGHJ6*03	CARERGLGYYGSGAYYYYYMDVW	23	L					IGLV1-44*01	IGLJ3*02	CAAWDDSLNGRVF	13
13D02	12	IGHV4-34*01	IGHD1-26*01	IGHJ4*02	CARFGSYW	8	L					IGLV2-14*01	IGLJ1*01	CSSYTSTNTRVF	12
13C11	12						L					IGLV2-14*01	IGLJ1*01	CSSYTSTNTRVF	12
B1F01	13						L					IGLV1-44*01	IGLJ3*02	CTAWEDSLNGPVF	13
B1G01	13						L					IGLV1-44*01	IGLJ3*02	CTAWEDSLNGPVF	13
A2A03	14	IGHV1-2*04	IGHD1-26*01	IGHJ3*02	CATIVGVITADAFDI	15	L					IGLV2-11*01	IGLJ2*01	CCSYAGRYRV	10
A3B12	15	IGHV3-23D*02	IGHD3-10*02	IGHJ4*02	CARRRAFVSGSYMGMTFDY	19	L					IGLV2-14*01	IGLJ3*02	CSSYTNTITG	10
A2B12	16	IGHV3-23*01	IGHD6-19*01	IGHJ4*02	CAKRPPCCSGGSFYKFEY	17	L					IGLV2-14*01	IGLJ2*01	CSSYTSSSILV	11
A2B04	17	IGHV3-72*01	IGHD3-3*02	IGHJ3*02	CTRVNYFDPNGYSKNTFDI	19	L					IGLV1-51*01	IGLJ2*01	CGTWDLSLNHVV	12
A3A08	18	IGHV3-74*01	IGHD4-11*01	IGHJ4*02	CVRGSYSGGWAEAY	14	L					IGLV8-61*01	IGLJ3*02	CVLFMGRGIWV	11
A2C08	19	IGHV4-61*01	IGHD2-8*01	IGHJ5*02	CARALVGSCRNGACYTRWFDL	21	K	IGKV4-1*01	IGKJ1*01	CQQYYSTPPT	10				
A2B02	20	IGHV4-61*01	IGHD2-8*01	IGHJ5*02	CARALVGSCSNGACYTRWFDL	21	K	IGKV4-1*01	IGKJ1*01	CQQYYYTPPT	10				

Table 4. Unique couples of immunoglobulin variable heavy and light chain genes identified from single memory B cells of different HBV booster vaccinated or acute resolved HBV donors.

		Heavy chain					Light chain							
Clone	**Clonal group**	**VH**	**DH**	**JH**	**CDR3-IgH(aa)**	**CDR3 length**	**IgL**	**V-kappa**	**J-kappa**	**CDR3-IgK(aa)**	**CDR3 length**	**V-lambda**	**J-lambda**	**CDR3-IgL(aa)**	**CDR3 length**
10C07		IGHV4-59*02	IGHD5-18*0	IGHJ4*02	CAKDRIHYGSADW	13	K/L	IGKV1-9*01	IGKJ5*01	CQQLNSYPLTF	11	IGLV2-8*01	IGLJ2*01	CSSYAGSNNLIF	12
12A02		IGHV3-53*02	IGHD6-19*01	IGHJ4*02	CASFVPINRNGWYYYDYW	18	K/L	IGKV1-39*01	IGKJ1*01	CQQSYSTPWTF	11	IGLV2-14*01	IGLJ1*01	CSSYRRTNTFVF	12
12A03		IGHV3-7*03	IGHD3-3*01	IGHJ4*02	CARHYNTYFDYW	12	K/L	IGKV1-39*01	IGKJ1*01	CQQSYSTPWTF	11	IGLV2-14*01	IGLJ1*01	CSSYRRTNTFVF	12
12A06		IGHV4-59*01	IGHD3-16*01	IGHJ4*02	CARGVKFDSW	10	K/L	IGKV1-39*01	IGKJ1*01	CQQSYSTPWTF	11	IGLV1-40*01	IGLJ3*02	CQSYDSRLSAWVF	13
12A07		IGHV3-7*03	IGHD5-18*01	IGHJ4*02	CVRYGYGYGLPFDYW	15	K	IGKV4-1*01	IGKJ5*01	CQQYYSTPGTF	11				
12A08		IGHV3-23*04	IGHD2-15*01	IGHJ6*02	CAIEGCSGGSCYDYYYYGMDVW	22	K/L	IGKV4-1*01	IGKJ5*01	CQQYYSTPGTF	11	IGLV2-11*01	IGLJ3*02	CCSYTSSYTWVF	12
12A09		IGHV4-38-2*01	IGHD3-22*01	IGHJ5*02	CARSYYYDSSDYYPNLNWFDPW	22	L					IGLV2-11*01	IGLJ3*02	CCSYTSSYTWVF	12
12B02		IGHV1-8*01	IGHD3-22*01	IGHJ5*02	CARGLYYNTTNYYWFDPW	19	K	IGKV4-1*01	IGKJ5*01	CQQYYNSPPITF	11				
12B03		IGHV1-8*01	IGHD3-22*01	IGHJ5*02	CARGLYYYNTTNYYWFDPW	19	K	IGKV2-30*01	IGKJ2*01	CMQGKFWPNTF	11				
12B04		IGHV1-8*01	IGHD3-22*01	IGHJ5*02	CARGLYYYNTTNYYWFDPW	19	K/L	IGKV1-5*03	IGKJ2*01	CQQYNSYSYTF	11	IGLV2-8*01	IGLJ3*02	CSSYAGSNNLEF	12
12B06		IGHV3-30-3*01	IGHD2-15*01	IGHJ3*01	CARDRFTVAATRYALDVW	18	K	IGKV3-11*01	IGKJ2*01	CQQRSNWPPYTF	11				
12B09		IGHV3-20*01	IGHD3-10*01	IGHJ6*02	CVRISGSRFHRYYYGLDVW	19	K	IGKV1-5*03	IGKJ1*01	CQQYHNFPWTF	11				
12C01		IGHV4-38-2*01	IGHD3-10*01	IGHJ4*02	CARDTYYYGPGSPKSGDFW	19	K	IGKV1-39*01	IGKJ3*01	CQQSYIMVTF	11				
12C02		IGHV3-7*03	IGHD3-16*01	IGHJ4*02	CARVQFSSETSQYRPLQYW	19	K	IGKV1-39*01	IGKJ3*01	CQQSYIMVTF	11				
12C03		IGHV3-7*01	IGHD2-2*01	IGHJ5*02	CARKLYYYDAIYGWFDPW	18	K	IGKV1-39*01	IGKJ3*01	CQQSYIMVTF	11				
12C04		IGHV3-74*01	IGHD2-21*01	IGHJ4*02	CARTPAYKEGDFYRPFDYW	19	K	IGKV2-30*01	IGKJ2*01	CVQGTQW*#YTF	11				
12C07		IGHV1-3*01	IGHD3-10*01	IGHJ4*02	CARGEGFYDSCGYW	14	K	IGKV1-9*01	IGKJ1*01	CQQLNSYPRTF	11				
12C08		IGHV1-8*01	IGHD3-22*01	IGHJ5*02	CARGLYYYNTTNYYWFDPW	19	K	IGKV1-39*01	IGKJ3*01	CQQSYIMVTF	11				
12C08		IGHV1-8*01	IGHD3-22*01	IGHJ5*02	CARGLYYYNTTNYYWFDPW	19	K	IGKV1-39*01	IGKJ3*01	CQQSYIMVTF	11				
12C11		IGHV4-4*02	IGHD6-13*01	IGHJ6*02	CARRGSTWNHYYYGMDVW	18	K	IGKV4-1*01	IGKJ4*01	CQQYYGTLLTF	11				
12D01		IGHV1-18*01	IGHD3-22*01	IGHJ4*02	CARERRTYFYDTGGQFDYW	19	K	IGKV4-1*01	IGKJ1*01	CQQYYNIATF	11				
12D02		IGHV3-20*01	IGHD3-22*01	IGHJ4*02	CARDLSYDSSGLPYYFDYW	19	K/L					IGLV2-8*01	IGLJ3*02	CSSYAGSNNFVF	12
12D03		IGHV3-21*01	IGHD1-7*01	IGHJ6*02	CARSPRYNWNFGAEDDYYYGMDVW	24	K	IGKV1-39*01	IGKJ5*01	CQQSHSTPITF	11				
12D04		IGHV4-59*01	IGHD6-13*01	IGHJ2*01	CARGAYSSSWSFQGWYFDLW	20	L					IGLV1-47*01	IGLJ3*02	CVAWDDSLSVWVF	13
12D05		IGHV3-33*03	IGHD1-1*01	IGHJ5*01	CARDRDYWTPINWFDPW	17	K/L	IGKV1-39*01	IGKJ3*01	CQQSYIMVTF	11	IGLV1-44*01	IGLJ1*01	CASWDDSLKGHVF	13
12D06		IGHV4-59*01	IGHD3-16*01	IGHJ5*02	CARDVDWGSHWFDPW	16	K	IGKV4-1*01	IGKJ2*01	CQQYYSSPQTF	11				
12D07		IGHV1-8*01	IGHD3-9*01	IGHJ5*02	CARGIYYYNTGNYKWL#DPW	20	K	IGKV1-39*01	IGKJ3*01	CQQSYIMVTF	11				
12D08		IGHV1-18*01	IGHD3-22*01	IGHJ4*02	CARERRTYFYDTGGQFDYW	19	K	IGKV3D-20*01	IGKJ4*01	CQQYGSS#ALTF	11				
12D10		IGHV1-18*01	IGHD3-22*01	IGHJ4*02	CARERRTYFYDTGGQFDYW	19	K	no seq							
12D11		IGHV1-18*01	IGHD3-22*01	IGHJ4*02	CARERRTYFYDTGGQFDYW	19									
13D01		IGHV1-3*01	IGHD3-16*01	IGHJ4*02	CARGVPGSTTYW	12	K	IGKV1-16*02	IGKJ5*01	CQQYNSYPPTF	11				
13D06		IGHV4-59*02	IGHD1-26*01	IGHJ4*02	CARAWGGKEVGAKPFDYW	18	K/L	No seq result				IGLV7-46*01	IGLJ2*01	CLLSYSGAQVVF	12
13D08		IGHV7-4-1*02	IGHD3-3*01	IGHJ6*02	CARPLKYDLWTGFGNPREYYYHYYGFDVW	29	K	IGKV3-20*01	IGKJ5*01	CQQYGGSPPITF	11				
1A11_A594		IGHV5-51*01	IGHD3-9*01	IGHJ3*02	CARRDYDVLTGYFSDAFDIW	20	K	IGKV4-1*01	IGKJ2*01	CQQYYSTPYTF	11				
4B04		IGHV3-64D*06	IGHD4-23*01	IGHJ4*02	CAKDGGPTVVTYDCW	15	K	IGKV3-20*01	IGKJ1*01	CQQYNNSPRTF	11				
4D03		IGHV3-15*07	IGHD5-18*01	IGHJ4*02	CTTEGLRGLSYGFDYW	16	L					IGLV1-47*01	IGLJ3*02	CAGWDGSLSGWVF	13
4D06		IGHV3-49*04	IGHD2-21*02	IGHJ4*02	CSRAAGGYFAAPFDNW	16	K	IGKV1-5*03	IGKJ4*01	CQQYNEYSLTF	11				
4D08		IGHV3-48*03	IGHD3-3*01	IGHJ2*01	CARDDLLWSWYFDLW	15	L					IGLV2-23*02	IGLJ1*01	CCSYSRISTYVL	13
4D12		IGHV4-4*02	IGHD2-21*01	IGHJ4*02	CARDSYCGGDCYSYWSSW	18	K	IGKV1-5*03	IGKJ2*01	CQQYKSYSEYTF	12				
6A09		IGHV3-7*01	IGHD2-2*01	IGHJ5*02	CARSPYSTRYNWFGPW	16	K	IGKV1-33*01	IGKJ2*01	CQQYDNLPYTF	11				
6B05		IGHV3-15*07	IGHD2-21*02	IGHJ4*02	CITDPGHCGGDICAYW	16	K/L	IGKV1-39*01	IGKJ2*01	CQQSYSTP#TF	11	IGLV2-14*01	IGLJ2*01	CSSYTSSSTLSSVVF	15
7A08		IGHV3-30*03	IGHD3-3*01	IGHJ6*02	CAKDVARAIFGVVISSYYGMDVW	23	K	IGKV1-33*01	IGKJ2*01	CQQYANLPLTF	11				
7C04		IGHV3-11*01	IGHD2-2*01	IGHJ6*02	CAREAYCNSTSFSNYYYNGMGVW	23	K	IGKV2-28*01	IGKJ1*01	CMQALQARTF	10				
7E09		IGHV4-31*03	IGHD2-2*02	IGHJ3*02	CARDQRLLGYCSSTSCYSHAFDIW	24	K/L	IGKV1-39*01	IGKJ4*01	CQQSYSTSLTF	11	IGLV2-8*01	IGLJ2*01	CSSYAGSNNLVLF	13

7E12		IGHV3-11*06	IGHD2-15*01	IGHJ3*02	CVGGGWLDDGFDIW	14	**K/L**	IGKV1-27*01	IGKJ1*01	CQKYNSAPRTF	11	IGLV2-23*01	IGLJ1*01	CCSYAGSPYIF	11
7F04		IGHV4-59*08	IGHD2-8*02	IGHJ3*02	CARLYPWGPREGNSFDIW	18	**K**	IGKV1-39*01	IGKJ2*01	CQQSYTTPHTF	11				
7F05		IGHV3-7*03	IGHD2-15*01	IGHJ4*02	CAREGFCSDGSCPGTNYFDNW	21	**L**					IGLV2-14*01	IGLJ2*01	CSSYTSSRLLYVVF	14
7F06		IGHV3-7*01	IGHD2-2*01	IGHJ5*02	CARNFFYAFDPW	12	**L**					IGLV2-14*01	IGLJ1*01	CNSYTSSSTPVVF	13
7F07		IGHV3-21*01	IGHD1-26*01	IGHJ5*01	CARERGVGAPGNWLDSW	17	**K/L**	IGKV1-9*01	IGKJ3*01	CQQRNSCPPXTF	12	IGLV2-14*01	IGLJ1*01	CSSIRSSSTLVF	12
7G06		IGHV1-3*01	IGHD5-12*01	IGHJ3*02	CARQYSSHDMFDHLDMW	17	**K**	IGKV1-5*03	IGKJ2*02	CQQYNSYXQFTF	12				
8A01		IGHV4-38-2*01	IGHD5-12*01	IGHJ5*01	CARGASRNPRDSGYYFNWFDFW	22	**K**	IGKV4-1*01	IGKJ4*01	CQQYYSIPLTF	11				
8A12		IGHV3-7*03	IGHD2-15*01	IGHJ5*02	CARDRYCSGGGCFWRWFDPW	20	K	IGKV4-1*01	IGKJ1*01	CQQYYGTPLTF	11				
8B06		IGHV4-34*01	IGHD3-3*01	IGHJ6*02	CAREMYYNFWGSFNYYHYGMDVW	23	L					IGLV2-11*01	IGLJ1*01	CCSYAGSYTYVF	12
8B12		IGHV3-30*03	IGHD2-2*01	IGHJ4*02	CAKVRYCSSANCYGAYYFDYW	21	**L**					IGLV2-18*02	IGLJ1*01	CSSYTSSSTLXF	12
9C04		IGHV3-33*03	IGHD1-20*01	IGHJ4*02	CARGPFNWNNPVGNSPVVGYYFDLW	25	**K**	IGKV4-1*01	IGKJ4*01	CQQYYSSPPTF	11				
A2C10		IGHV5-51*01	IGHD4-17*01	IGHJ5*02	CARRLGDYYPNWFDP	15	**L**					IGLV3-21*02	IGLJ2*01	CQVWDSTSDHHVV	13
A2D06		IGHV3-23*01	IGHD2-15*01	IGHJ5*02	CVKPPLRXNVIDS	13	**K**	IGKV1-12*01	IGKJ4*01	CQQGFDFPLT	10				
A3G01		IGHV4-38-2*01	IGHD2-2*02	IGHJ3*02	CARDGGWNIVVRNGFEI	17	**K**	IGKV4-1*01	IGKJ1*01	CQQYYSTPWT	10				
B1A08		IGHV3-21*01	IGHD3-9*01	IGHJ4*02	CARDHYDILVGYYNF	15	**K**	IGKV3-11*01	IGKJ5*01	CQQRSNWPIX	10				
B1B08		IGHV3-74*01	IGHD5-18*01	IGHJ4*02	CVRGSYSGGWAEAY	14	**L**					IGLV2-23*02	IGLJ3*02	CCSHGGTYWVF	11
B1C07		IGHV3-23*04	IGHD2-21*01	IGHJ4*02	CARRRAFVSGIFTGMTFDH	19	**L**					IGLV1-40*01	IGLJ3*02	CQSYDRSLSASVF	13
B1E09		IGHV3-23*04	IGHD3-10*01	IGHJ4*02	CAKLMVRGVWFFDY	14	**K**	IGKV3-20*01	IGKJ5*0	CQHYDTSPSVT	11				
B1G06		IGHV4-59*08	IGHD1-14*01	IGHJ4*02	CASPPKGTPEAFFDX	15	**K**	IGKV3-15*01	IGKJ1*01	CQQYIYWPPWT	11				
B2C04		IGHV3-53*02	IGHD1-14*01	IGHJ6*02	CAKAPTRDGMDVW	13	**K**	IGKV3-11*01	IGKJ1*01	CHHRNGWPWTF	11				
B2C06		IGHV3-74*0	IGHD1-7*01	IGHJ4*02	CTKESNGNSHFW	12	**L**					IGLV1-51*02	IGLJ3*02	CGTWDSSLSAEVF	13
B2D10		IGHV3-33*01	IGHD3-22*01	IGHJ6*02	CARAINYYDSSGYYLHYYGMDVW	23	**L**					IGLV1-44*01	IGLJ2*01	CAAWDYSLGVVF	12
B2E05		IGHV3-7*03	IGHD2-15*01	IGHJ3*02	CARDPSSSAFDIW	13	**K**	IGKV2-30*02	IGKJ3*01	CMQGTRGVTF	10				
B2E08		IGHV1-3*01	IGHD3-10*01	IGHJ4*02	CARDKGLVILHAPDYW	16	**K**	IGKV1-8*01	IGKJ1*01	CQQYYSYPRTF	11				
B2E11		IGHV4-59*08	IGHD1-1*01	IGHJ3*02	CASRTGIELHYAFDSW	16	**L**					IGLV2-23*01	IGLJ3*02	CCSYAGSSAWVF	12
B2G09		IGHV5-51*01	IGHD3-16*01	IGHJ5*01	CARHWGSSSPVQGWFDSW	18	**L**					IGLV1-51*01	IGLJ3*02	CATWDTRLNTWVF	13
B2G12		IGHV4-31*06	IGHD2-15*01	IGHJ4*02	CARWGQLVLGYFDFW	15	**L**					IGLV2-8*01	IGLJ1*01	CSSFAGSSTYVF	12

In addition, we analyzed the distribution of CDR3 length of all heavy chain genes. Short CDR3 regions are an indicator for affinity matured, antigen-experienced memory B cells and could give a hint, whether HBV-specific memory B cells were isolated. Throughout our analysis most CDR3 regions contained 19 amino acids, followed by 20 and 15 amino acids, but a clear distribution towards one length was not observed (Figure 16 B). Another indicator for the isolation of antigen-specific B cells is the enrichment of a certain V- and J-gene segment. Therefore, we compared the V- (IGHV) and J-gene (IGHJ) segments of all heavy chain genes sequenced. Most immunoglobulin variable heavy chain genes that were isolated used IGHV3-7 V-gene segment, followed by IGHV1-3, IGHV4-34 and IGHV4-59 (Figure 16 C). The analysis of J-gene segment usage obtained a clear preference for IGHJ4 indicating the enrichment of specific B cells (Figure 16 D).

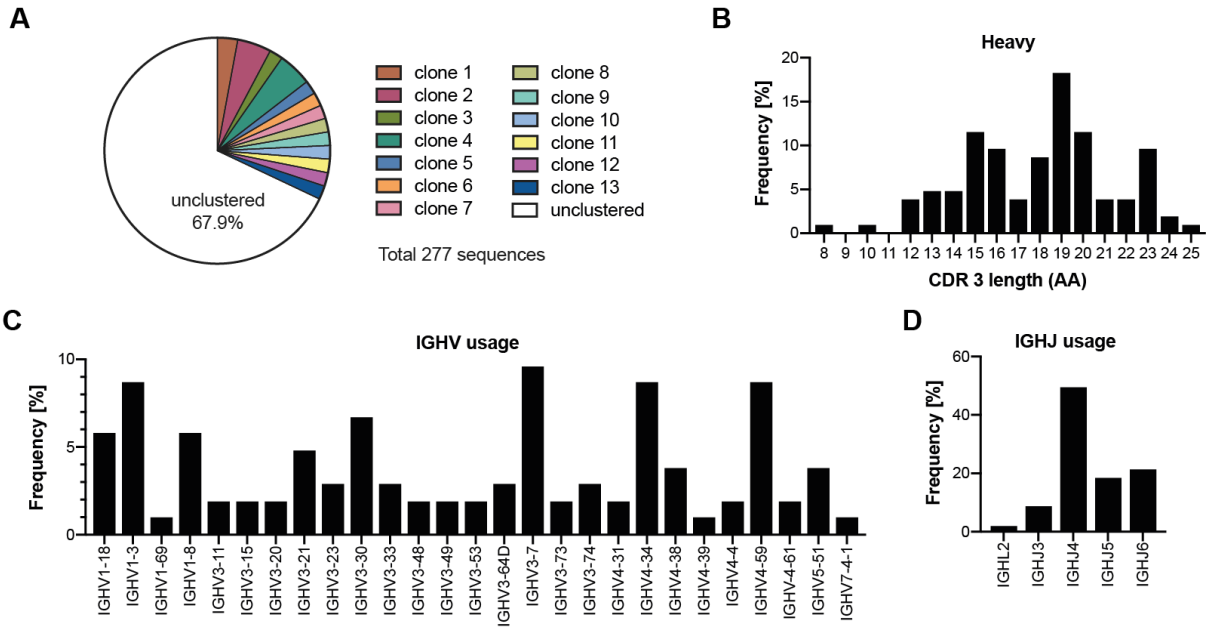

Figure 16. Sequence analysis of immunoglobulin variable chain genes from single sorted memory B cells.
(A) Sequence cluster analysis of 277 heavy and light chain sequences identified 13 clones (colored segments). White segment indicates the frequency of unique, unclustered sequences. (B) Analysis of CDR3 length among all heavy chain genes sequenced. (C and D) Frequency of IGHV and IGHJ gene segment usage within all heavy chain sequences analyzed.

In summary, 20 clones and several unique couples of heavy and light chain genes were identified from single memory B cells of different donors at different sites. Heavy chain gene repertoire analysis obtained an increased CDR3 length of 19 amino acids, a preference for V-gene segments IGHV3-7 followed by IGHV1-3,

IGHV4-34 and IGHV4-59 was well as J-gene segment IGHJ4, suggesting the enrichment of antigen-specific memory B cells.

2.1.4.3 Specificity testing of new recombinant monoclonal antibodies

In order to finally proof whether the isolated memory B cells were HBV-specific, recombinant IgG class 1 monoclonal antibodies (mAbs) were cloned. For this, not only sequences derived from B-cell clones, but also most unique couples of heavy and light chain genes were selected. In a first step, restriction sites were introduced with an additional PCR using the appropriate V-gene specific forward and J-gene specific reverse primers, identified during sequence analysis. All PCR products were cloned in frame with the respective constant region genes (IgG1, Igk1 or Igl2) encoded by eukaryotic expression vectors. Corresponding heavy and light chain plasmids were transiently co-transfected in HEK293 cells to allow antibody expression and secretion. Supernatant was collected at day three after transfection and IgG expression was evaluated with ELISA on anti-human IgG coated plates. Most transfections resulted in the detection of IgG with ELISA, but signal intensities varied (Figure 17 A). For 60 antibodies a mean OD_{450nm}>1.0 was observed, suggesting high protein concentration in the supernatant. In contrast 4 of 76 mAbs cloned did not result in detectable IgG (Table 5) pointing at a failure of protein expression. The anti-HBs ELISA was performed to explore whether the newly generated mAbs were specific for HBsAg that was used for single B cell sorting in the beginning. Unfortunately, only two antibodies, 4D06 and 4D08, of 76 mAbs tested, indicated strong antigen-specificity (Figure 17 B and Table 5). The remaining 74 did not recognize plate bound HBsAg, suggesting that neither of the single cell sorting approaches and HBV-baits were able to efficiently isolate high affinity HBV-specific memory B cells. In order to further validate this result, an additional ELISA was performed. Therefore, we used Protein G coated ELISA plates to selectively capture mAbs in the cell culture supernatant first and then we determined antigen-specificity upon addition of HBsAg-biotin and Avidin-HRP. With this ELISA seven additional mAbs indicated reactivity against HBsAg, but with lower signal intensity (Figure 17 C and Table 5).

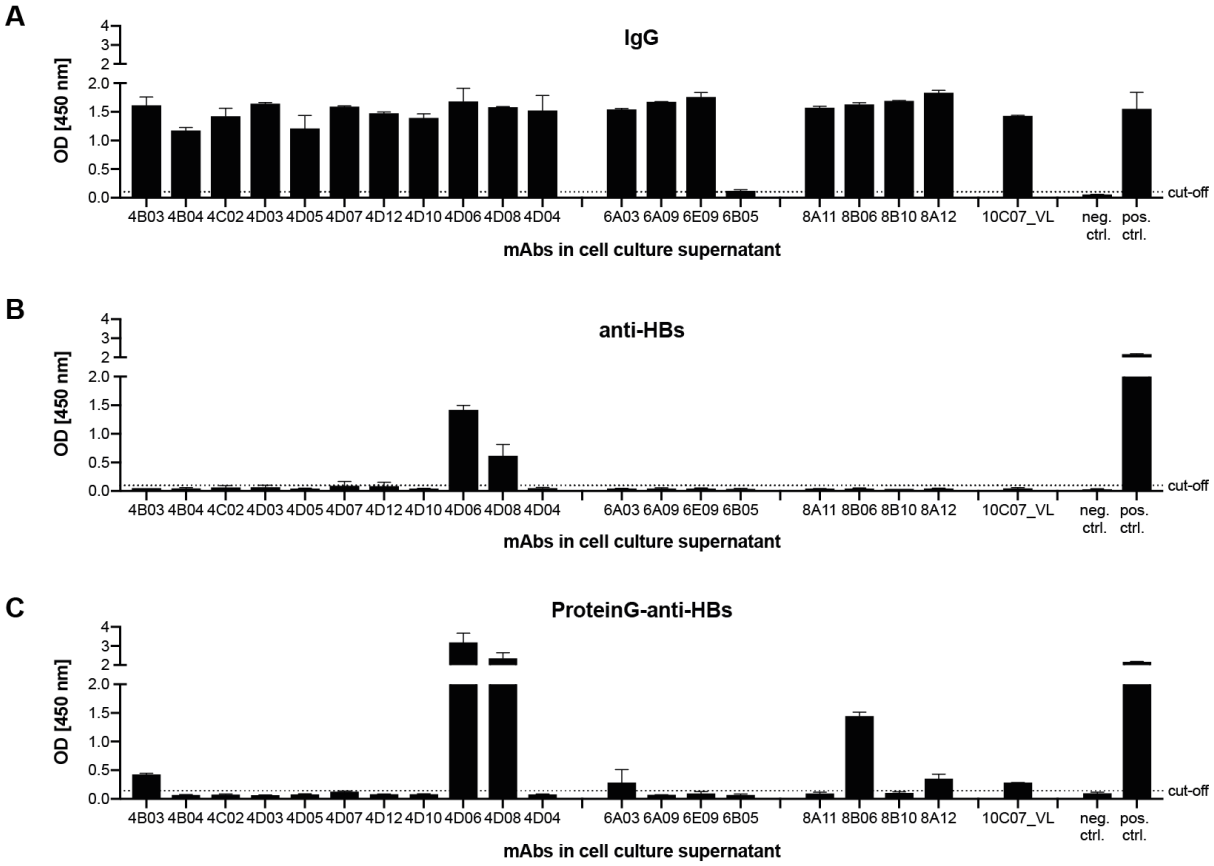

Figure 17. IgG expression and HBsAg-specificity of mAbs generated from mRNA of single memory B cells.
(A) Representative ELISA analysis for the expression of human IgG after transient co-transfection of corresponding antibody heavy and light chain expression vectors. (B) Representative anti-HBs ELISA, detecting mAbs in cell culture supernatant with specificity for plate bound HBsAg. (C) ELISA analysis of the interaction of HBsAg and mAbs after IgG immobilization with Protein G. Mean and SD are shown.

In summary, single B cell antibody technology allowed the generation of monoclonal antibodies from mRNA of single memory B cells without previous B-cell cultivation. However, pre-selection of antigen-specific B cells with different HBV-specific antigen baits and single cell sorting only resulted in the generation two highly reactive mAbs and six antibodies with limited HBsAg-specificity. Nevertheless, the two strong binders 4D06 and 4D08 were selected for further characterization studies.

Table 5. Overview of IgG expression and HBsAg-specificity of mAbs generated from single memory B cells. ++ OD_{450nm} >1.0; + OD_{450nm} > cut-off; - OD_{450nm} < cut-off; cut-off: mean OD_{450nm} of negative control plus 3 x SD; n.d. not determined; blue: mAbs reactive in both anti-HBs ELISA; grey: mAbs reactive only in ProteinG anti-HBs ELISA

Sorting	mAb	IgG	anti-HBs	ProteinG anti-HBs
A	A2A03	++	+	n.d.
	A2B12	++	-	n.d.
	A2B04	++	-	n.d.
	A3A08	++	-	n.d.
	A2C08	++	-	n.d.
	A2B02	++	-	n.d.
	A2D06	++	-	n.d.
	A3G01	++	-	n.d.
	A2C10	++	-	n.d.
1	1A11	++	+	n.d.
4	4B03	++	-	+
	4D04	++	-	-
	4D05	++	-	-
	4D06	++	++	++
	4D08	++	++	++
	4D10	++	-	-
	4D03	++	-	-
	4C02	+	-	-
	4D12	+	-	-
	4B04	+	-	-
	4D07	++	-	-
	4D03	++	-	-
6	6A03	++	-	+
	6A09	++	-	-
	6E09	++	-	-
7	7A08	++	-	n.d.
	7C04	++	-	-
	7G06	+	-	-
	7F07_VK	+	-	n.d.
	7F07_VL	++	-	n.d.
	7F06	++	-	-
	7D05	++	-	n.d.
	7E12_VK	-	-	n.d.
	7F05	++	-	n.d.
	7E09_VK	++	-	-
	7E09_VL	++	-	-
	7F04	++	-	-
B	B1A08	++	-	n.d.
	B1E09	++	-	n.d.
8	8B06	+	-	+
	8A01	++	-	n.d.
	8B12	++	-	-
	8B10	++	-	-
	8A11	++	-	-
	8A12	+	-	+
9	9C04	-	-	n.d.
10	10C07_VK	+	-	-
	10C07_VL	+	-	+
12	12A02_VK	++	-	-
	12A02_VL	++	-	-
	12A03_VK	++	-	-
	12A03_VL	++	-	-
	12A04	+	-	-
	12A06_VK	++	-	-
	12A06_VL	++	-	-
	12A07	++	-	-
	12A08_VK	++	-	-
	12A08_VL	++	-	-
	12A09	++	-	-
	12B01	++	-	-
	12B02	++	-	-
	12B03	++	-	-
	12B04_VK	++	-	-
	12B04_VL	++	-	-
	12B06	++	-	-
	12B09	++	-	-
	12C01	+	-	-
	12C02	++	-	-
	12C03	++	-	-
	12C07	+	-	-
	12C11	++	-	-
	12D01	++	-	-
	12D04	+	-	-
	12D06	+	-	-
13	13D02	++	-	+
	13D04	++	-	+
	13D01	++	-	-
	13D08	+	-	-

2.2 *In vitro* characterization of new HBsAg-specific monoclonal antibodies

In order to use monoclonal antibodies as therapeutic agents against chronic hepatitis B virus infection antibody characteristics need to be evaluated carefully. Among all antibodies cloned from single human memory B cells, only mAbs 4D06 and 4D08 indicated high HBsAg-specificity. Therefore, the two were selected for further characterization studies with regard to antigen affinity, neutralization capacity or effector cell activation. This will be explored in the following sections.

2.2.1 Antibody production and purification

For the evaluation of antibody function highly pure proteins are of particular importance. Therefore, a small-scale production was established. Antibodies 4D06 and 4D08 were expressed in HEK293 cells after transient co-transfection with the respective expression vectors. Antibody-containing supernatant was collected at day three, five and seven post transfection. In order to avoid unspecific interactions from medium supplements during the following experiments, mAbs were purified with Protein G column affinity chromatography. The cell culture supernatant was loaded on a column and Protein G coupled beads selectively captured IgG via the fragment crystallizable (Fc) region. After washing mAbs were eluted with low pH elution buffer. The flow through (FL) during equilibration and washing steps as well as the elution fractions (EL) were collected and analyzed with anti-HBs ELISA to determine antibody-containing fractions. Purification profiles of 4D06 and 4D08 differed, but elution fractions EL 2-6 indicated a positive signal for both mAbs after ELISA development. The flow through FL 1-3 collected during column equilibration, washing and sample loading was negative, indicating the selective binding of mAbs to Protein G beads. FL 4 of 4D06 purification, collected after elution, contained some remaining antibody, suggesting an incomplete elution from the column (Figure 18 A and B). After purification antibody-containing fractions (EL 2-6) were pooled and proteins were concentrated by filtration to achieve reasonable working concentrations. Antibody concentration was determined with Bradford Assay. On average 0.8 mg of each antibody was purified from 75 mL cell culture supernatant. The concentration ranged from 0.5 mg/mL to 1.8 mg/mL.

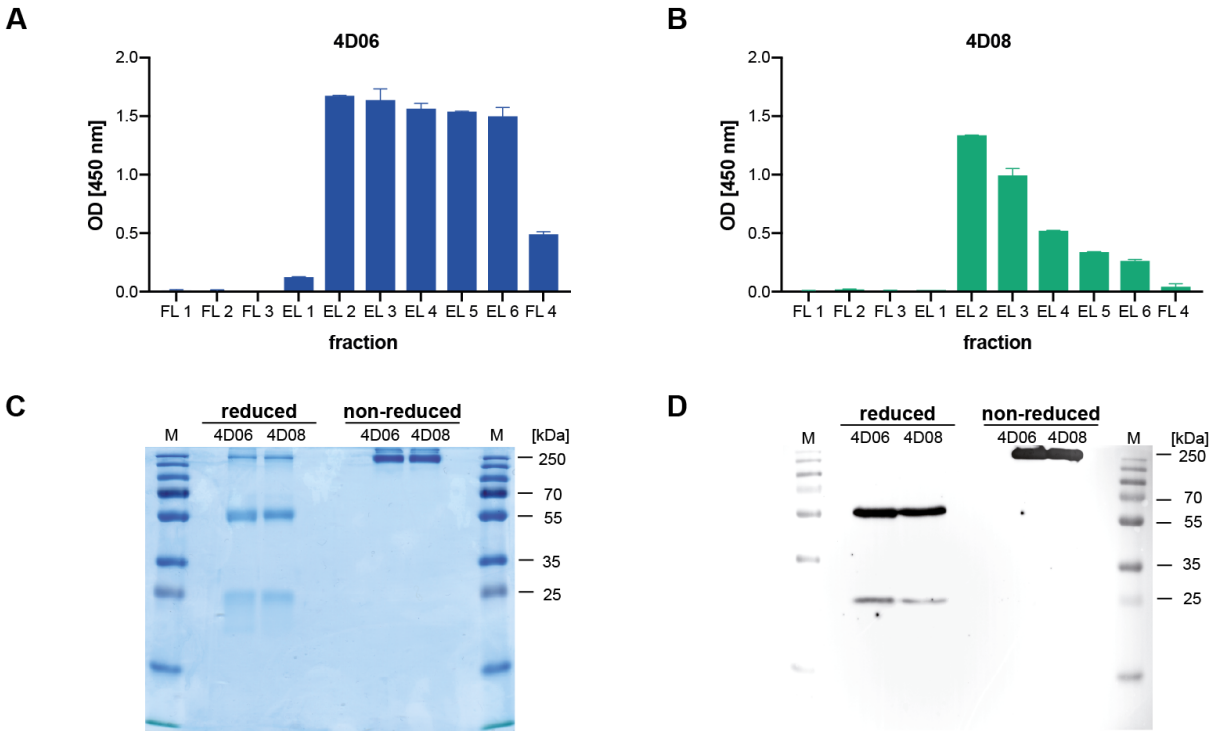

Figure 18. Purification of 4D06 and 4D08 with Protein G affinity chromatography. Elution profile of 4D06 (A) and 4D08 (B) determined with anti-HBs ELISA. Purity assessment of 4D06 and 4D08 with PAGE under reducing and non-reducing conditions. (C) Total protein stain with Coomassie. (D) Western Blot and staining with polyclonal goat-anti human IgG HPR.

In a next step antibody purity was assessed with polyacrylamide gel electrophoresis (PAGE) under reducing and non-reducing conditions either with total protein staining with Coomassie or with Western blot and anti-human IgG staining. Under non-reducing conditions only a single band was detected for both constructs at the size of approximately 140 kDa, indicating the full-length IgG molecule. In contrast, two protein bands were visible under reducing conditions. The molecular weight of 50 kDa and 25 kDa corresponded to the antibody heavy and light chains. Additionally, a third, higher molecular weight band was determined with Coomassie staining under reduced conditions. This was identified as non-reduced full-length IgG due to incomplete protein reduction.

In summary, mAbs 4D06 and 4D08 were successfully expressed in HEK293 cells after transient transfection. Protein G column purification yielded on average in 0.8 mg highly pure antibody, which were used for *in vitro* characterization studies.

2.2.2 Structural characterization of 4D06 and 4D08

2.2.2.1 Epitope mapping

Type and location of the epitope recognized by anti-HBV antibodies seem to influence therapeutic efficacy and neutralizing capacity. Furthermore, antibodies recognizing a certain linear epitope on the small HBV envelope protein are known to be very potent against escape mutations (Gao et al., 2017). First, in order to evaluate whether 4D06 and 4D08 recognize a linear or a conformational epitope on HBV envelope (HBV Env) proteins, a Dot blot was performed. HBV Env proteins were dotted on a membrane either under non-reducing conditions, keeping the native three-dimensional structure of HBsAg or under reducing conditions, leading to linearization of the proteins. mAbs 4D06, 4D08 and HB-1 were used as primary antibodies for detection. The HB-1 antibody was kindly provided by Dieter Glebe (Justus-Liebig University, Giessen, Germany) and served as a positive control, recognizing a known linear epitope in the small HBV Env protein at position $S^{119\text{-}125}$ in the antigenic loop (a-determinant) of HBsAg (Kucinskaite-Kodze et al., 2016). All mAbs recognized the antigen under native conditions. However, the reactivity was lost for 4D06 under reducing conditions, indicating the recognition of a conformational epitope. For HB-1 and 4D08 dots were detected under reducing conditions suggesting a linear epitope (Figure 19 A). This was further verified with a Western blot. For this, HBsAg was denatured by cooking at 95°C for 20 minutes in Dot blot buffer and resulting HBV Env proteins were separated by SDS-PAGE. HBV envelope proteins were detected as described before with 4D06, 4D08 and HB-1, hence confirming previous findings. The blot was empty for 4D06 indicating a denaturation sensitive epitope. In contrast, two bands at a size of 27 kDa and 24 kDa were detected with 4D08 pointing at the recognition of a linear epitope. Additionally, one band with higher molecular weight was detected at approximately 50 kDa, representing a dimer of small HBV Env protein (Figure 19 B) and pointing at insufficient protein linearization (Suffner et al., 2018).

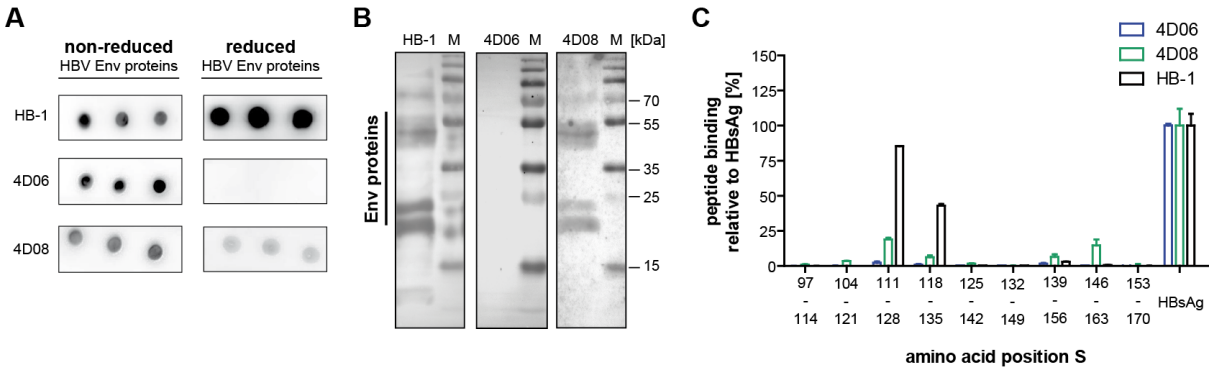

Figure 19. Classification and localization of 4D06 and 4D08 epitope.
(A) Dot Blot and (B) Western Blot detecting HBV envelope proteins under non-reduced and reduced conditions with HB-1, 4D06 and 4D06 as primary antibodies and HRP-coupled polyclonal IgG as secondary antibody. (C) Peptide ELISA with 18mer overlapping peptides to localize epitope position on HBsAg. Peptide binding was normalized to full-length protein binding. Mean and SD are shown.

To further localize the epitope on the small HBV Env protein recognized by 4D06 and 4D08, an ELISA with 18mer overlapping peptides spanning the main antigenic region of HBsAg between amino acid position S^{97} and S^{170} was performed. The control antibody HB-1 was reactive against two peptides $S^{111\text{-}128}$ and $S^{118\text{-}135}$ containing its known linear epitope at positions $S^{119\text{-}125}$. 4D06 did not recognize any peptide, confirming the recognition of a conformational epitope that was not present in the selected peptides. However, antibody 4D08 did not react with a specific peptide. Four peptides with different locations in the protein were recognized (Figure 19 C). This was in contrast to previous results and pointed towards the recognition of a conformational rather than a linear epitope for 4D08. Unfortunately, we were unable to further define the epitope locations of both mAbs.

2.2.2.2 Antibody affinity

The most critical feature of an antibody is its antigen affinity. Therefore, EC_{50} values, as estimate for affinity, were determined for 4D06 and 4D08 with anti-HBs ELISA. Similarly, as for specificity determination, serum purified HBsAg was adsorbed to an ELISA plate and serial dilutions of purified 4D06 and 4D08 were added. After ELISA development, EC_{50} values were calculated with non-linear regression. Both antibodies obtained EC_{50} values in the nanomolar range. 4D06 indicated higher affinity with 18.5 nM than 4D08 with 158 nM (Figure 20 A and B), but both can be classified as high affinity human monoclonal antibodies.

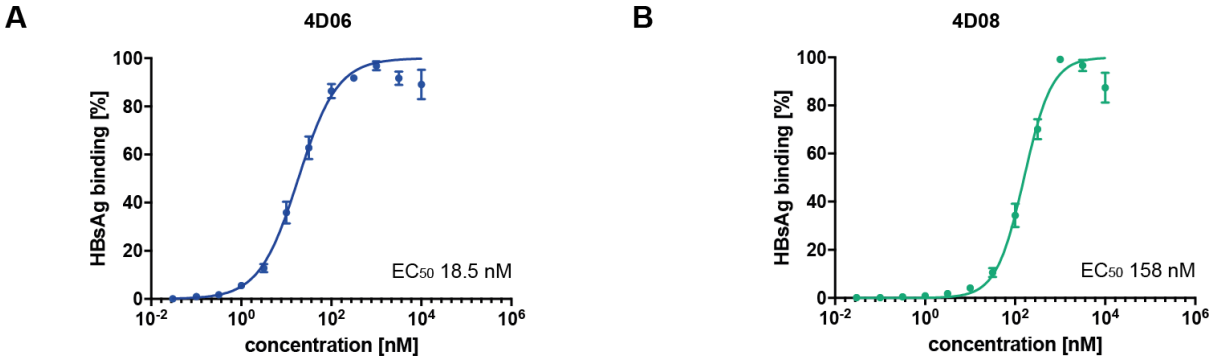

Figure 20. Affinity determination of 4D06 and 4D08 with ELISA.
Anti-HBs ELISA analysis of the interaction between 4D06 (A) or 4D08 (B) and HBsAg to obtain EC_{50} values. EC_{50} values were calculated by nonlinear regression analysis. Measurements of three independent experiments were normalized. Mean and SD are shown.

2.2.3 Functional characterization of 4D06 and 4D08

2.2.3.1 HBV-uptake inhibition and virus neutralization capacity

In order to target HBV infection, not only structural characteristics, but especially antibody function such as virus neutralization are of great importance. Therefore, we first investigated the capacity of 4D06 and 4D08 to prevent virus uptake: Differentiated HepG2 NTCP cells susceptible to HBV were used as target cells. First, cell culture derived and purified HBV (genotype D) was pre-incubated with mAbs at a concentration of 100 nM. This solution was added to the cells at 4°C, allowing virus attachment. A subsequent shift back to 37°C induced synchronized HBV uptake. At indicated time-points (three, six and 24 hours) the cells were lysed and intracellular HBV rcDNA as well as HBV cccDNA content was determined by qPCR as markers for infection. Intracellular HBV rcDNA increased in a time-dependent manner, when cells were infected with HBV only (Figure 21 A). Furthermore, cccDNA was detectable 24 hours after infection (Figure 21 B). Pre-treatment with mAb 4D08 allowed HBV uptake within the analyzed timeframe of three, six and 24 hours indicated by the detection of intracellular rcDNA (Figure 21 A), but cccDNA was not detectable 24 hours after inoculation. In contrast, neither rcDNA nor cccDNA was detected in cell lysates after pre-incubation with 4D06 or the controls (HBIg (hepatitis B immunoglobulin preparation) and Hep (Heparin)), indicating that virus uptake was completely blocked (Figure 21 A and B). Although rcDNA was detected in cell lysates after pre-incubation of HBV and 4D08, both antibodies seem to be capable of preventing early steps of HBV infection as no cccDNA was formed. However, the underlying mechanism is currently unknown.

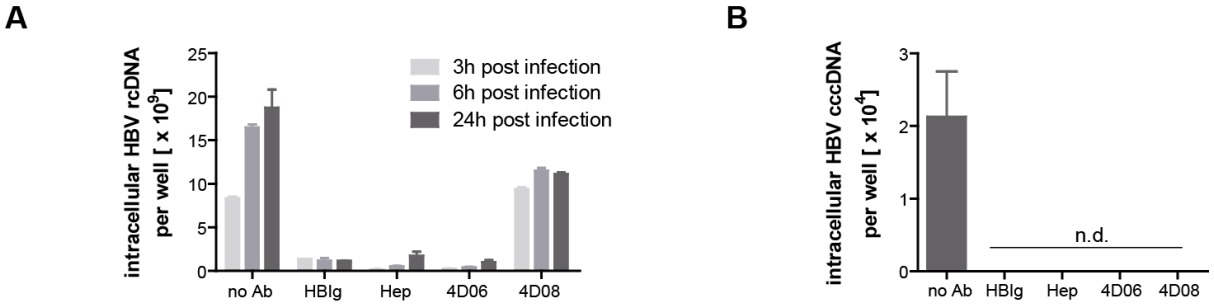

Figure 21. 4D06 and 4D08 prevent HBV uptake in HepG2 NTCP cells.
(A) Analysis of intracellular HBV rcDNA in HepG2 NTCP cell lysate 3h, 6h, and 24h post infection after pre-incubation of HBV and mAbs. (B) Analysis of intracellular cccDNA in cell lysate 24h post infection. HBIg (Hepatitis B immunoglobulin preparation) and Hep (Heparin) served as positive controls known to block HBV uptake. Mean and SD are shown.

A neutralization assay was established to further investigate the potential of 4D06 and 4D08 to prevent infection in a longer timeframe. Differentiated HepG2 NTCP cells were infected with HBV after pre-incubation with different antibody concentrations. In order to enhance infection and virus spread polyethylene glycol (PEG) was added shortly before infection (Michailidis et al., 2017). After incubation for 18 hours the virus-containing medium was removed and fresh medium was added. The medium was exchanged on day four and eight post-infection. The establishment of HBV infection was evaluated by measuring HBeAg secreted into the supernatant and cccDNA concentration in cell lysates. This assay was not only used for the evaluation of neutralization capacity of mAbs 4D06 and 4D08, but was also applied to characterize additional HBV-specific antibodies such as 4G4 (Golsaz-Shirazi et al., 2017).

A concentration dependent decrease of HBeAg was observed at day four and eight post-infection. Complete virus neutralization was achieved with 4D06 at a concentration of 100 nM, whereas 1000 nM of 4D08 had to be used to reach a comparable result (Figure 22 A and B). Quantification of intracellular cccDNA in cell lysates eight days post infection obtained a similar trend, with 4D06 being more potent in neutralizing than 4D08. Furthermore, cccDNA levels detected by qPCR were used to calculate IC_{50} values in order to estimate the therapeutic potency of mAbs 4D06 and 4D08 *in vitro*. Both antibodies indicated high potency, as nanomolar concentrations were sufficient to achieve 50% virus neutralization (Figure 22 C and D).

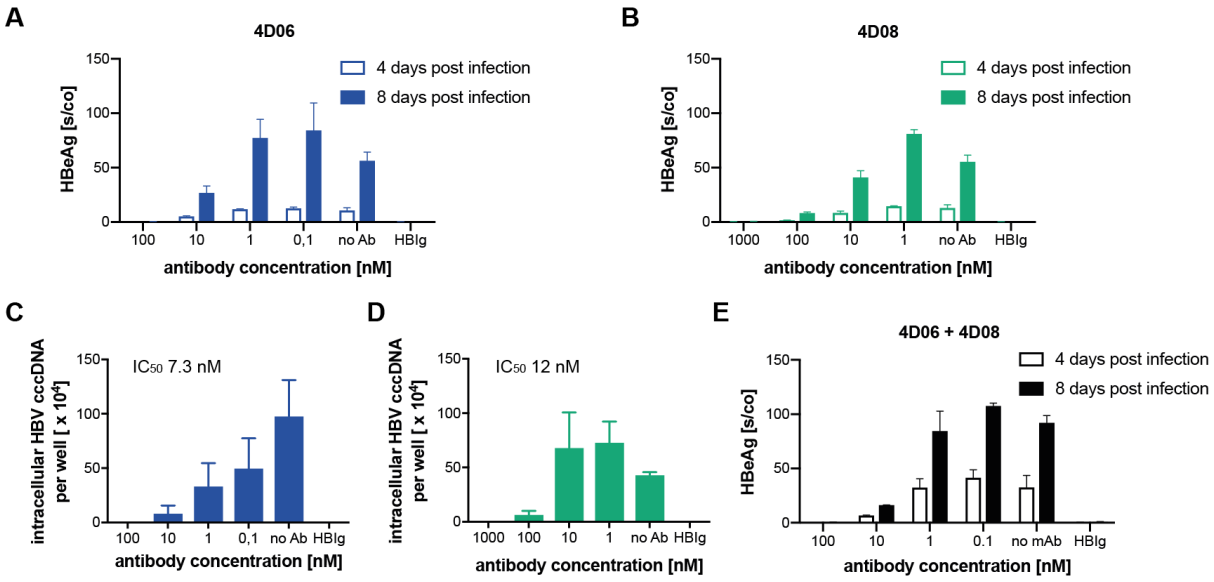

Figure 22. 4D06 and 4D08 are capable of neutralizing HBV infection dose-dependently. ELISA analysis of HBeAg secreted from HBV infected HepG2 NTCP cells after pre-incubation of HBV with serial dilutions of 4D06 (A) and 4D08 (B). Quantitative analysis of HBV cccDNA by qPCR in cell lysate eight days post-infection after pre-incubation with 4D06 (C) and 4D08 (D). (E) ELISA analysis of HBeAg in supernatant after combinatorial pre-incubation of 4D06 and 4D08 and HBV. HBIg (Hepatitis B Immunoglobulin preparation) Mean and SD are shown.

In order to explore whether the neutralization capacity of 4D06 and 4D08 can be enhanced by combinatorial application, the neutralization assay was repeated. For this, both mAbs were pre-incubated in a 1:1 ratio at various concentrations together with HBV before differentiated HepG2 NTCP cells were infected. At day four and eight post infection, the medium was exchanged and the HBeAg level was determined in the supernatant. However, it did not decline further compared to the single application of 4D06, suggesting that 4D06 and 4D08 do not act synergistically (Figure 22 A and E).

In conclusion, both mAbs can prevent HBV uptake and are capable of neutralizing HBV infection with genotype D in a concentration dependent manner. 4D06 seems to be superior to 4D08 and the combined application of 4D06 and 4D08 does not enhance their potency.

2.2.3.2 Effect of 4D06 and 4D08 on established HBV infection

With regard to a potential therapeutic application against chronic hepatitis B virus infection not only the prophylactic effect of 4D06 and 4D08, but also the effect on an already established HBV infection needs to be explored. This was investigated with differentiated and infected HepG2 NTCP cells. Nine days after infection, antibodies

were applied at a concentration of 100 nM for five days every 24 hours. The approved nucleoside analogue entecavir (ETV) was used as a control, known to suppress viral replication and spread, but having no impact on the secretion of HBsAg. Viral parameters such as HBsAg and HBeAg were determined before and after treatment in cell culture supernatant and intracellular HBV cccDNA was quantified by qPCR from cell lysates on day five. The HBsAg concentration decreased in the supernatant after application of 4D06 or 4D08 for five days, whereas the treatment with entecavir indicated no effect on HBsAg concentration. However, the combination of all (4D06, 4D08 and ETV), showed a further decline of HBsAg compared to the single antibodies (Figure 23 A). This combinatorial effect was in contrast to the previous observations from neutralization assay, indicating that 4D06 and 4D08 do not have a synergistic effect on prevention of HBV infection (see section 2.2.3.1).

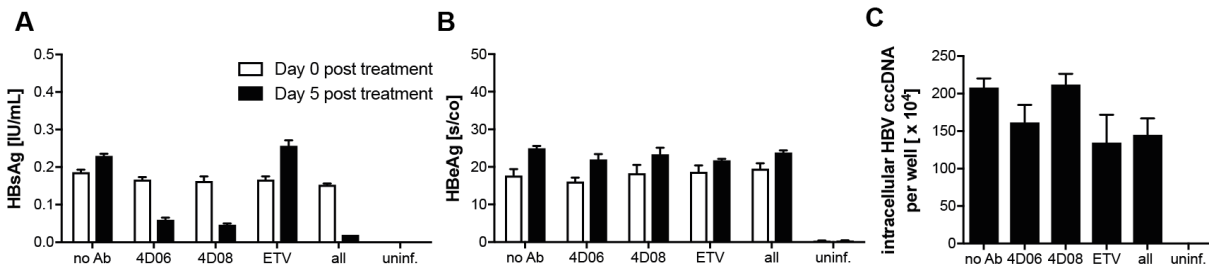

Figure 23. Therapeutic effect of 4D06 and 4D08 on HBV-infected HepG2 NTCP cells. Analysis of HBsAg (A) and HBeAg (B) level in cell culture supernatant before and after treatment of HBV-infected HepG2 NTCP cells with mAbs or ETV. (C) Quantitative analysis of cccDNA concentration in cell lysates of HBV-infected cells five days post antibody treatment. (ETV, Entecavir; all, combination of 4D06, 4D08 and ETV; uninf., non-infected HepG2 NTCP cells). Mean and SD are shown.

For HBeAg, none of the treatments indicated any change (Figure 23 B) and only a moderate effect on intracellular HBV cccDNA was observed upon treatment either with 4D06 or ETV or when the combination of all was applied (Figure 23 C). These findings suggest that both mAbs were able to capture soluble HBsAg secreted from HBV infected cells, but hardly any further antiviral effect was observed. Merely the continuous application of 4D06 seemed to be capable of preventing HBV spread as cccDNA concentrations of ETV and 4D06 treated cells were comparable.

2.2.3.3 Broadly neutralizing capacity of 4D06 and 4D08

Both, 4D06 and 4D08 were capable of neutralizing infection of HepG2 NTCP cells with HBV genotype D in a concentration dependent manner (see section 2.2.3.1). However, currently not only one but nine HBV genotypes (A-I) can be classified, from which five (A-E) seem to be responsible for causing 96% of chronic HBV infections worldwide (Velkov et al., 2018). Therefore, the reactivity of 4D06 and 4D08 against further genotypes was then investigated: First an indirect ELISA with HBsAg from several HBV geno- and subtypes (HBV genotype reference panel for HBsAg assay, Paul-Ehrlich Institute, Langen, Germany) was performed. HBsAg-specific monoclonal antibodies from Murex ELISA Kit (Murex HBsAg Version3, DiaSorin, Saluggia, Italy) were used to capture the different antigens on an ELISA plate. Afterwards, biotinylated 4D06 or 4D08 were added and mAbs were detected with HRP-coupled Avidin. 4D06 revealed a strong reactivity against all tested geno- and subtypes, with strongest binding to HBsAg from genotype A and weakest binding to genotypes B and H (Figure 24 A). In contrast, monoclonal antibody 4D08 seemed to have a strong preference for HBsAg from HBV genotype E, whereas A and D resulted in a weaker signal. Genotypes F and H indicated lowest reactivity (Figure 24 B).

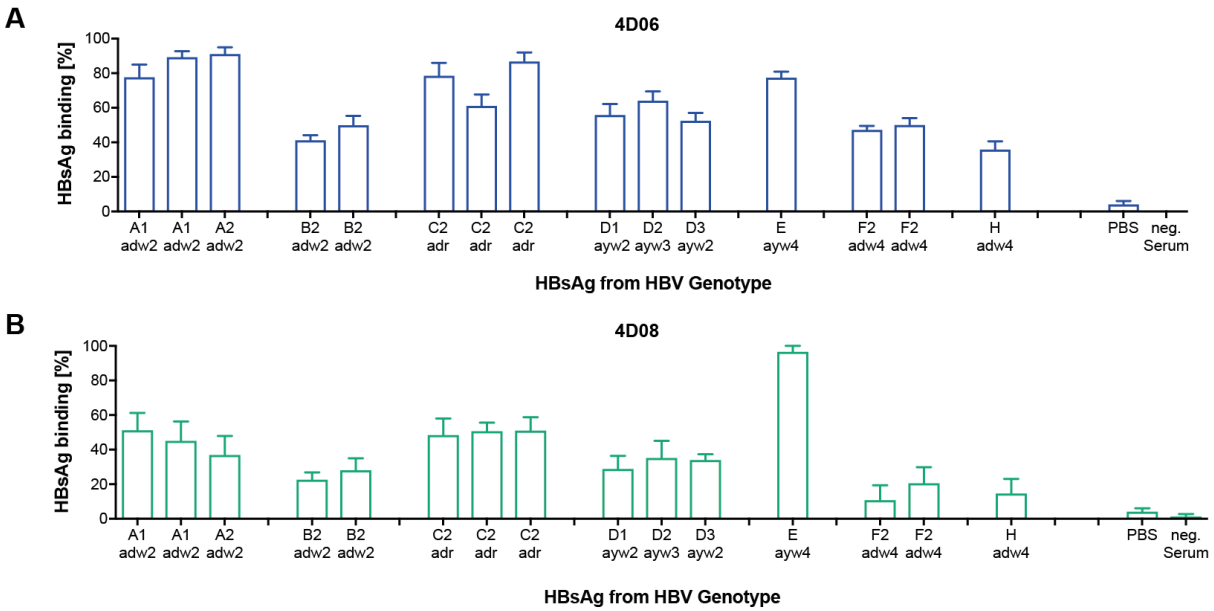

Figure 24. 4D06 and 4D08 recognize HBsAg from various HBV Genotypes.
ELISA analysis of the interaction of mAbs 4D06 (A) or 4D08 (B) and HBsAg from several HBV geno- and subtypes. Binding was normalized among three independent experiments. Mean and SD are shown.

In a next step, immunofluorescence staining on Huh7 cells, transiently transfected with HBV genotypes A-D, was performed. Staining with monoclonal antibodies 4D06 and 4D08 was positive for all genotypes, whereas non-transfected mock cells did not indicate unspecific antibody binding (Figure 25).

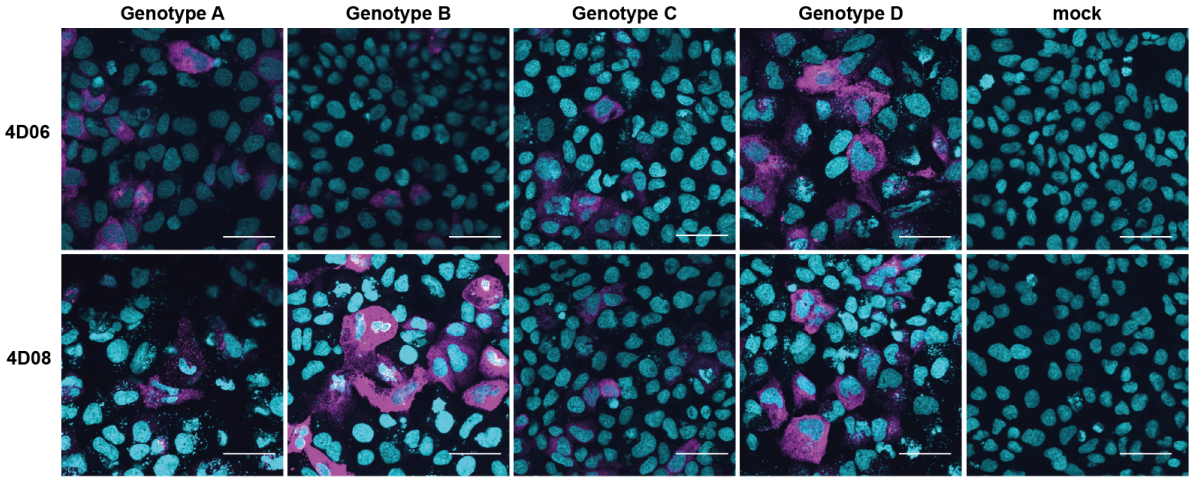

Figure 25. 4D06 and 4D08 recognize HBsAg in Huh7 cells from four most relevant HBV genotypes A, B, C, and D.
Huh7 cells seeded on cover slips were transfected with plasmids encoding four different HBV genotypes A-D. Four days post-transfection, cells were fixed, permeabilized and immunostained with 4D06 or 4D08 as primary antibody. For the mAbs detection, polyclonal goat anti-human IgG Alexa Flour 647 (pink) was used. Slides were mounted with DAPI (cyan) mounting solution. Mock cells were not transfected, but stained in the same way. Scale bars represent 50 µm.

In the last step, the broad neutralization capacity of 4D06 and 4D08 against HBV genotypes A-H was evaluated. In order to circumvent HBV purification and to avoid antibody binding to HBV SVPs, hepatitis delta virus (HDV) enveloped with HBsAg from HBV genotypes A-H was used. Delta virus was produced upon co-transfection of Huh7 cells with plasmids encoding HDV genome and HBV envelope proteins A-H. This resulted in HDV enveloped with HBV envelope proteins derived from all HBV genotypes. Virus-containing supernatant was collected at day ten to 14 post transfection (Figure 26 A). Similarly, as for the previous neutralization assays with genotype D, serial dilutions of mAbs 4D06 and 4D08 were pre-incubated with HDV-containing supernatant. Next, Huh7 cells stably expressing NTCP were infected. Seven days post inoculation, hepatitis delta antigen (HDAg) was stained via immunofluorescence staining and HDAg-positive cells were quantified with automated image acquisition. This experiment was performed in Stephan Urban's Lab (Molecular Virology, Universitätsklinikum Heidelberg, Germany) by Wenshi

Wang. As a result both mAbs had neutralizing activity against all HBV genotypes (A-H) on pseudo-typed HDV particles. In accordance with the previous data (see section 2.2.3), 4D06 was more efficient (10-fold stronger neutralization) compared with 4D08 (Figure 26 B and C). However, the neutralization capacity varied within the different genotypes. Strongest neutralization activity was observed for both mAbs against genotype A and least against genotype B. Intermediate neutralization capacity was observed against genotype C and G (Figure 26 B and C). These results were comparable with previous ELISA data, except for genotype E. In this case, the ELISA indicated a strong preference of 4D08 for genotype E, which was not observed during neutralization assay. This change in preference might be a consequence of assay sensitivity.

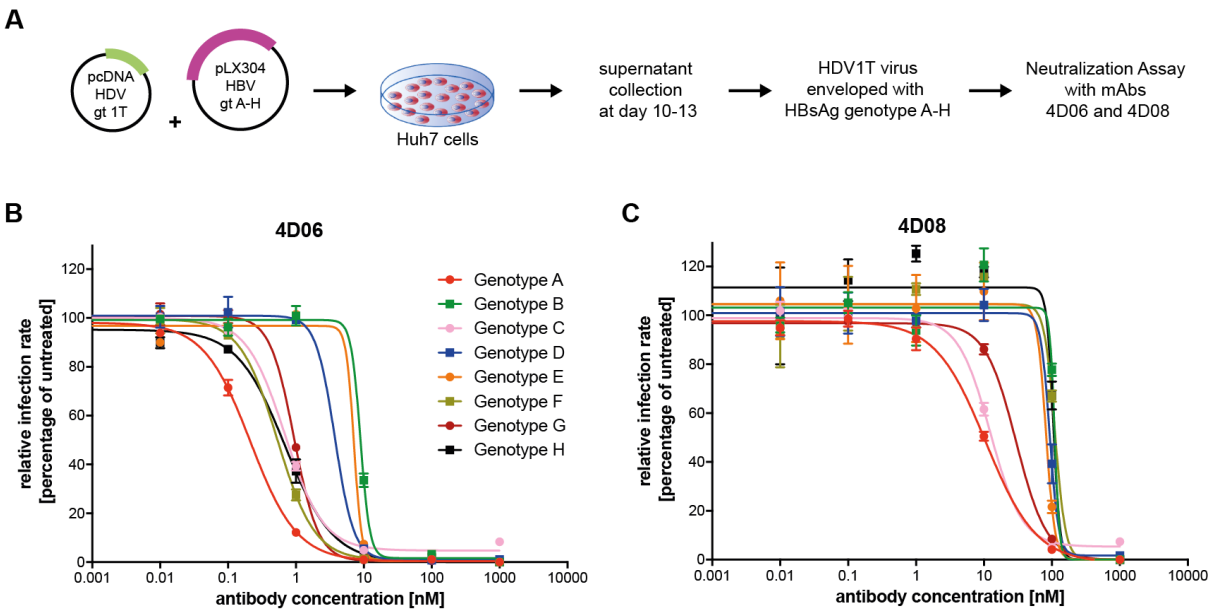

Figure 26. 4D06 and 4D08 have broadly neutralizing capacity.
(A) Schematic overview of the production of HDV virus enveloped with HBsAg from various HBV genotypes followed by neutralization assay. Relative quantification of HDAg in Huh7 NTCP cells after pre-incubation with hepatitis delta virus enveloped with HBV genotypes A-H and serial dilutions of mAbs 4D06 (B) or 4D08 (C).

In conclusion, monoclonal antibodies 4D06 and 4D08 were capable of recognizing HBsAg from several HBV geno- and subtypes with ELISA as well as in HBV expression cells. Furthermore, they can efficiently neutralize infection with HBV genotypes A-H in the setting of hepatitis delta virus envelopment with HBV envelope proteins. Therefore, both mAbs can be classified as broadly neutralizing antibodies.

2.2.4 Antibody effector function

Antibodies are bi-functional molecules. Besides their capability to recognize surface expressed antigens at the antigen-binding site, they have the potential to activate immune effector cells via the Fc region. This region can be recognized by Fc receptors (FcRs) on immune effector cells. Upon activation they can induce target cell killing via antibody dependent cell-mediated cytotoxicity (ADCC) or antibody dependent cell-mediated phagocytosis (ADCP). Effector cell activation through IgG1 is mainly mediated by three FcγRs, namely CD16 (FcγRIII), CD32a (FcγRIIa) and CD64 (FcγRI) (Bruhns, 2012).

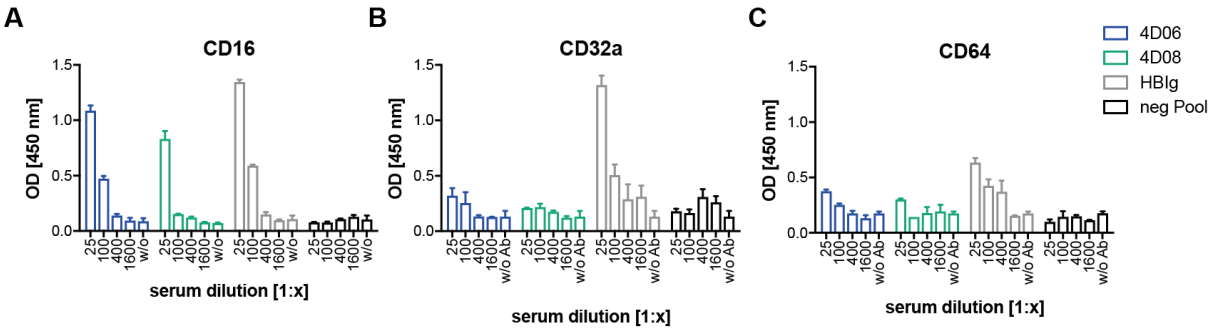

Figure 27. mAbs induce effector cell activation upon recognition of CD16 and plate-bound HBsAg.
Analysis of IL-2 secretion from (A) CD16-, (B) CD32a- and (C) CD64-expressing mouse thymoma cells upon activation through clustering of antibodies 4D06 and 4D08 recognizing plate-bound HBsAg.

An activation assay was performed to determine whether IgG1 monoclonal antibodies 4D06 and 4D08 were capable of activating Fc-receptor expressing cells upon antigen recognition. This assay was carried out in collaboration with Valeria Falcone (Department of Virology, Freiburg University, Freiburg, Germany). Serial dilutions of 4D06 and 4D08 were incubated on plate-bound HBsAg before mouse reporter cells, stably expressing human CD16, CD32a or CD64 were added. Upon Fc recognition the reporter cells released IL-2, which was determined with ELISA. The release of IL-2 was measured in CD16-expressing cells after recognition of both antibodies as well as HBIg control (Figure 27 A). Cells expressing Fc gamma receptor CD32a or CD64, showed no activation when 4D06 and 4D08 were present (Figure 27 B and C) indicating that the Fc domains of the two antibodies are preferentially recognized by FcγRIII (CD16).

CD16 is mainly expressed on NK cells, macrophages and monocytes (Bournazos et al., 2017). We performed an NK-cell activation assay to further investigate if natural CD16-expressing human NK cells can recognize antibodies 4D06 and 4D08. For this PBMC were isolated and incubated with 100 nM 4D06 or 4D08 on plate bound HBsAg for six hours. Flow cytometry was used to identify the frequency of CD16 expressing NK cells and their activation status (Figure 28 A). The frequency of CD3- CD56+ NK cells decreased in the presence of 4D06 or 4D08 and HBsAg (Figure 28 B). Additionally, less CD16+ NK cells were detected after incubation of PBMC, mAbs and plate-bound HBsAg indicating that 4D06 and 4D08 were recognized by CD16 on NK cells. The reduction was slightly pronounced after application of 4D06 (Figure 28 B).

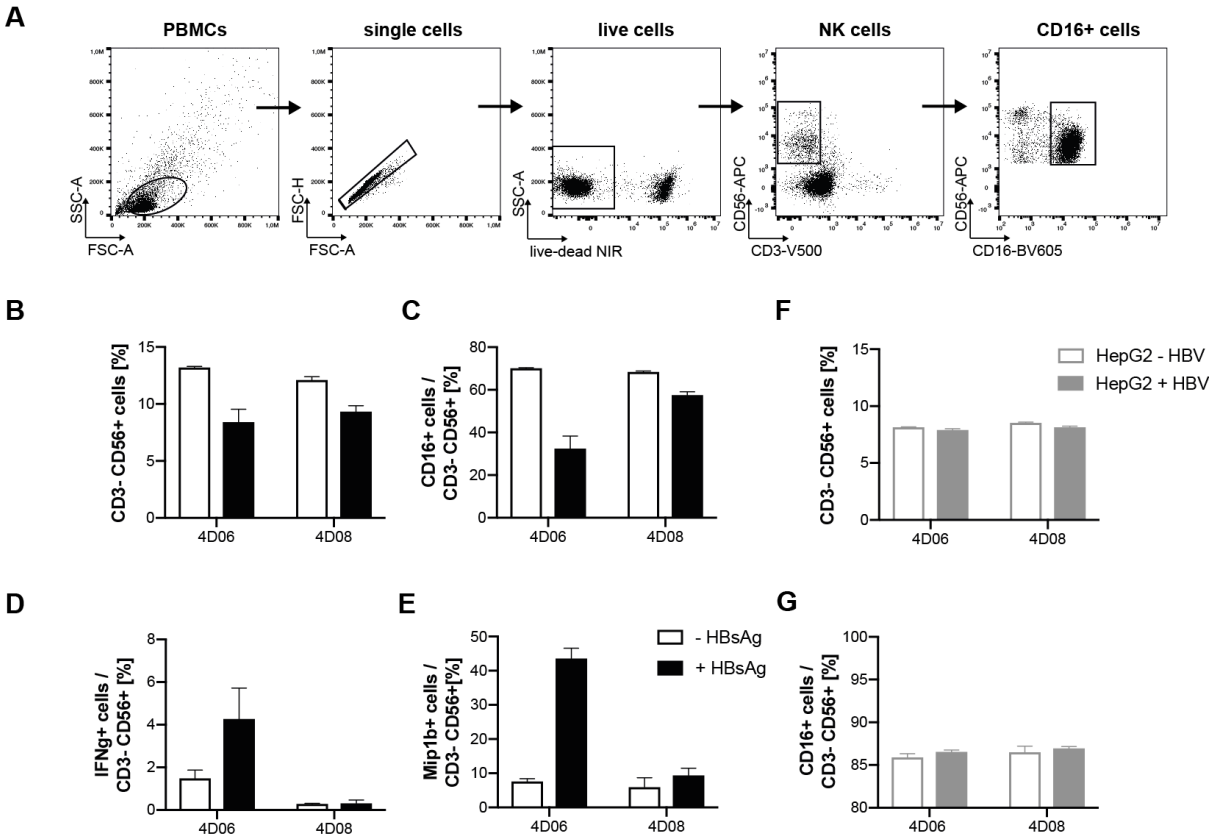

Figure 28. NK cells activation after recognition of 4D06 or 4D08 and HBsAg.
(A) Representative gating strategy to identify human CD16+ CD3- CD56+ NK cells. (B) Frequency of CD3- CD56+ NK cells, (C) frequency of CD16+ cells (C) frequency of IFNg+ cells and frequency of Mip1b+ cells (E) of CD3- CD56+ NK cells after stimulation with mAb 4D06 or 4D08 and plate bound HBsAg for six hours. Frequency of CD3- CD56+ NK cells (F) and CD16+ cells (G) after incubation of PBMC and mAbs for six hours in the presence of HBV-infected HepG2 NTCP cells.

In addition to the analysis of CD16+ NK cells upon staining for interferon gamma (IFNg) and Mip1b, NK-cell activation was investigated. The frequency of IFNg+ and Mip1b+ NK cells was increased in the presence of 4D06, but not with 4D08 (Figure 28 D and E), suggesting that the recognition of antibody with antigen did not fully induce NK-cell activation. Furthermore, this did not occur, when HBV-infected HepG2 NTCP cells were used as target cells instead of plate bound HBsAg (Figure 28 F and G).

In summary, the Fc region of both mAbs was recognized by Fcγ receptor CD16 expressed on the surface of mouse reporter cells. Additionally, human peripheral blood NK cells seem to recognize 4D06 and 4D08 in the presence of immobilized HBsAg, but NK cells were only partially activated.

3 Discussion

A curative treatment for chronic hepatitis B virus (HBV) infection is currently missing. Several new antiviral immunotherapeutic approaches are under investigation, but so far none has reached clinical approval. Immunotherapies with anti-HBs antibodies have been carried out, to support the defective B-cell immune response in chronic hepatitis B patients, but were not followed further due to the limited availability of suitable binders or high production costs of polyclonal human serum preparations. In this thesis, methods for the generation of novel recombinant fully human HBV-specific monoclonal antibodies were explored and several antibodies were generated. Among all, two anti-HBs mAbs were investigated more carefully. These obtained high antigen affinity, broad neutralization capacity and the potential to activate immune effector cells. Their potential as immunotherapeutic agents will be discussed in the following sections.

3.1 Generation of HBV-specific human monoclonal antibodies

Human monoclonal antibodies have successfully been generated for the treatment of several diseases, especially for the therapy of cancer and autoimmune disease. In the field of chronic infectious disease, therapeutic applications with mAbs are under investigation and promising results are seen in HIV treatment studies (Caskey et al., 2019). In regards to HBV infection, antibodies are already used for prophylaxis, but for the treatment of persistent infection their efficacy still has to be analyzed. Beside the high costs for production of hepatitis B immunoglobulin preparations, most currently available recombinant HBV-specific monoclonal antibodies were isolated from mouse hybridoma. This has distinct disadvantages concerning the application in humans: Mouse protein sequences can cause severe side effects and as a consequence mAbs need chimerization or humanization. However, this can result in loss of efficacy (Kaluza et al., 1992). Furthermore, the mouse immunoglobulin repertoire does not exactly display the specificities of antibodies evolved in humans, which is of special importance in the background of HBV since mice are no natural hosts of the virus (Hwang & Park, 2018; Tiller, 2011). In order to overcome this hurdle we investigated three approaches for the generation of fully human monoclonal antibodies against hepatitis B virus (HBV) on the basis of selected, antigen-specific peripheral blood memory B cells, which will be discussed below.

3.1.1 Low frequency of HBV-specific memory B cells in peripheral blood

Before B-cell isolation was performed the frequency of circulating HBV-specific B cells was determined. Generally, the frequency of antigen-specific B cells in peripheral blood is very low ranging from 0.005% to 0.05% and is highly dependent on the current immune status of a person (Crotty et al., 2004; M. J. Smith et al., 2017). Vaccination can increase the pool of antigen-specific B cells as it selectively triggers their development. Memory B cells are of special interest as they persist for a long time in the blood after vaccination or infection, have undergone affinity maturation and can rapidly proliferate and differentiate into plasma cells when they re-encounter a known antigen (Seifert & Kuppers, 2016).

In order to generate HBV-specific monoclonal antibodies from blood memory B cells, we established an anti-HBs B-cell ELISpot to first estimate their number in healthy volunteers. For this estimation, B cells from a donor with resolved acute HBV infection or from donors who had received HBV booster vaccination seven days prior blood donation were compared with B cells isolated from an HBV naïve individual. Blood donation at day seven after booster vaccination was chosen, since this time point has been shown to correlate with the peak of anti-HBs-specific B cells in blood and should therefore allow a more frequent identification of the respective cells (Galson et al., 2015; Salimzadeh et al., 2018; Tian et al., 2018).

In vitro stimulation induced the differentiation of memory B cells into IgG-secreting cells, without significant differences between the different donors (Figure 7). This was in accordance with previous reports (Jahnmatz et al., 2013; Pinna et al., 2009; Walsh et al., 2013), showing that the stimulation with TLR agonist R848 and IL-2 can efficiently induce the differentiation of memory B cells into IgG-secreting cells. Furthermore, a few B cells isolated from donors with booster vaccination or resolved acute HBV infection were HBsAg-specific, whereas no anti-HBs antibody secreting cells (ASCs) were detected in the HBV naïve subject (Figure 7). The frequency of anti-HBs secreting cells (approximately 0.01%) was within the range of previously published data, although B cells from only four individuals were analyzed. Other groups obtained about 100 HBsAg-specific B cells within one million PBMC, if a donor was challenged with HBsAg before (Tian et al., 2018; Tuaillon et al., 2006; Valats et al., 2010). In addition, the numbers of anti-HBs+ spots were comparable

between the donor who recovered from HBV infection and the two vaccinated individuals, suggesting that vaccination and immunization by infection may be of similar efficacy concerning on the generation of HBsAg-specific antibodies. However, to proof this hypothesis a bigger cohort would be needed. With regard to the HBV-naïve volunteer, in our study no anti-HBs secreting cells were detected with ELISpot. This was in accordance with results from other investigators and pointed at the extremely low frequency of antigen-specific B cells in the blood, without prior induction by vaccination or infection (Tuaillon et al., 2006; Ward et al., 2008).

Furthermore, the secretion of anti-HBs antibodies in supernatants from B-cell cultures was analyzed with ELISA. Signal intensities were low and not clearly different from the HBV naïve donor (Figure 7), although HBV positive donors had serum anti-HBs titers >1000 IU/mL at the day of blood donation. As a reason, anti-HBs antibodies detected with by ELISA mainly resulted from *in vitro* stimulated memory B cells that secrete low amounts of antibodies. In contrast, serum anti-HBs antibodies determined after blood donation are most likely secreted from short-living plasma cells, that release high amounts of antibodies. These cells were already induced by the booster vaccination before blood donation.

In addition, the ELISpot indicated a higher frequency of anti-HBs secreting B cells as more antigen-specific antibodies were determined in contrast to ELISA. This can be explained by a higher sensitivity of the ELISpot assay. While secreted antibodies are directly captured on a membrane during ELISpot, antibodies are diluted in cell culture supernatant before ELISA detection (Tuaillon et al., 2006).

In conclusion, HBV-specific blood memory B cells can be identified with ELISpot upon *in vitro* stimulation despite the low frequency of 0.01% of PBMC. With regard to antibody generation, donor selection is needed as anti-HBs antibodies were only detected among donors with booster vaccination or resolved infection. B cells from naïve individuals can be used as controls, as no HBsAg-specific B cells were detected.

3.1.2 Human memory B cells seem to capture HBV-baits

With an estimated frequency of 0.01% of HBsAg-specific memory B cells in PBMC, we aimed at isolating those cells for antibody generation. ELISpot assay does not allow downstream application of cells. Therefore, flow cytometry coupled to cell

sorting was selected to identify and isolate HBV-specific memory B cells from blood. This has two advantages: First, antigen-specific memory B cells can be identified *ex vivo* without previous stimulation, resulting in a more precise, but potentially lower frequency than ELISpot. Second, downstream analysis of cells, in combination with cell sorting is possible. However, to capture low frequent HBV-specific B cells, a highly selective fluorescently labeled antigen is indispensable. For this we created three versions of HBV-baits that were recognized by B-cell receptors expressed on the surface of HBV-specific memory B cells (Figure 8, Figure 9, Figure 10). In contrast to previous studies that used recombinant small HBsAg derived from yeast, CHO or HEK cells (Burton et al., 2018; Salimzadeh et al., 2018; Ward et al., 2008), we focused on HBV subviral particles (SVPs) purified from cell culture of HBV-producing cell line HepAD38 and HBsAg purified from human serum of HBV carriers. The main advantage for later antibody cloning was that both antigens contained the three HBV envelope proteins small (S), middle (M) and large (L) and thereby increased the potential to isolate additional M- and/or L-specific B cell receptors (BCRs). For all baits the optimal staining concentration was determined by antigen titration and calculation of mean fluorescence intensities (Figure 8, Figure 9, Figure 10). This is a standard procedure to obtain optimal antibody dilution for staining cell surface molecules, but it can be transferred for the identification of antigen-specific B-cell receptors. The maximum MFI then correlated with B-cell receptor saturation (Cox et al., 2016).

In addition to the selective antigen, the type of fluorescent label was carefully chosen. Two baits were directly chemically labeled with Alexa Fluor 647 or 594 dyes. Alexa Fluor dyes have a low molecular weight and a high brightness index, supporting the detection of rare antigen-specific cells. For the third B-cell antigen biotinylation was performed. Biotin is even smaller than Alexa Fluor dyes and the probability of shielding potential epitopes is further decreased. Moreover, the combination of biotin with streptavidin leads to signal amplification, which is important for the detection of rare specificities (M. J. Smith et al., 2017). These labeling strategies have already been used by others and successfully led to the generation of antigen-specific monoclonal antibodies on the basis of antigen-specific single cell sorting (Cox et al., 2016; W. Tan et al., 2013; Woda & Mathew, 2015). Nevertheless, their use has to be carefully evaluated with regard to specificity. *Woda*

and Methew for instance indicated in their study isolating dengue virus specific memory B cells that a few B cells were specific for the Alexa Fluor dye itself, which suggested that some BCRs bind to non-relevant epitopes. To overcome this, they introduced a non-specific antigen labeled with Alexa Fluor dye (Woda & Mathew, 2015). Unfortunately, we cannot rule out this issue completely, as we neither labeled an unspecific antigen with the respective dyes to determine background staining, nor tested Alexa647-SVPs or HBsAg-Alexa594 with B cells from an HBV naïve donor. Instead, the degree of labeling of our antigens was carefully evaluated in order to avoid an excess of dye molecules on the surface of our antigens that could shield potential epitopes. In addition, a blocking control with non-labeled antigen was included, which indicated 80% reduction of the positive signal and pointed at a specific detection (Figure 8). This was comparable with previously published results using similar methods, showing signal inhibition between 50-85%, when B cells were pre-incubated in excess of a non-labeled antigen (Cox et al., 2016; M. J. Smith et al., 2017; Woda & Mathew, 2015). Furthermore, we evaluated the degree of unspecific binding of HBsAg-biotin and streptavidin. B cells isolated from the HBV naïve donor were incubated with HBsAg-biotin. It indicated a slight background signal of 0.01% at low fluorescence intensity (Figure 10). The gating strategy was optimized and the respective gate was set stricter towards high fluorescence intensities to avoid this background. However, this increased the risk of loosing some of the few antigen-specific B cells. Furthermore, similar to *Smith et al.* (M. J. Smith et al., 2017), an FMO control was introduced to estimate the background originating from non-specific streptavidin binding (Figure 10). It showed few streptavidin reactive B cells. However, *Moody* and colleagues pointed out that this can hardly be avoided as the natural antibody repertoire of B cells is to a very small extent reactive against streptavidin (Moody & Haynes, 2008).

Apart from the selection of highly specific antigens coupled to bright fluorophores, a reasonable gating strategy is of high importance for the identification of rare antigen-specific cells. In order to compare the three baits a single gating strategy was developed, including magnetic B-cell enrichment prior cell analysis and the use of IgG as memory B cell marker, detecting class switched and affinity matured B cells only. The enrichment step prior analysis was performed to avoid as many

unspecific cells as possible in order decrease assay background and thereby increase the detection of rare cells (M. J. Smith et al., 2017).

We selected IgG as memory B cell marker. On the one hand, due to reasonable identification of the respective B cell population with flow cytometry. 15-20% of peripheral blood B cells are IgG+ memory B cells (Seifert & Kuppers, 2016). On the other hand, IgG+ B cells are known for their high affinity maturation status and the selection of IgG+ B cells has already successfully led to the generation of potent monoclonal antibodies (Cox et al., 2016; Scheid, Mouquet, Feldhahn, Walker, et al., 2009; W. Tan et al., 2013). However, this was in contrast to many other studies using flow cytometry for the identification of HBV-specific memory B cells. Most frequently surface marker CD27 was used. It is classified as the memory B cell marker, enabling the identification of several classes of memory B cells including IgG, IgA, IgM and IgD and bypassing the selection of one isotype-switched B-cell class (Burton et al., 2018; Cox et al., 2016; Ward et al., 2008). Other investigators used CD27 and negative selection with IgM or a combination of IgM, IgD and IgA, as it is believed that direct IgG staining could lead to B cell activation followed by B-cell death (Franz et al., 2011; Woda & Mathew, 2015). However, not all mutated and isotype switched memory B cells are CD27+ and *Cox* and colleagues demonstrated that neither the inclusion of CD27 nor negative selection with IgM, IgD and IgA had any influence on the number of IgG secreting cells in their assay (Cox et al., 2016; Seifert & Kuppers, 2016; Wu et al., 2011).

For specificity-evaluation of our HBV-baits we additionally compared the frequencies of HBsAg-specific memory B cells with previous publications and with our ELISpot data. HBV-specific memory B cells were identified with a frequency of 0.02-0.3% of CD19+ B cells at optimal staining conditions with few donor-to-donor variations (Figure 8, Figure 9, Figure 10). This was comparable with observations from several other groups, although the fluorescently labeled antigens and gating strategies were different. The frequency of HBsAg-specific B cells in blood of vaccinated individuals was estimated with 0.18-0.4% of CD19+ B cells (Burton et al., 2018; Salimzadeh et al., 2018; Ward et al., 2008). Furthermore, frequencies obtained with flow cytometry matched with the numbers of HBsAg-specific cells obtained by ELISpot, if taking into account that B cells make up approximately 10% of PBMC (Figure 7).

3.1.3 Evaluation of methods for the isolation of HBV-specific B cells for antibody cloning

Several approaches for the generation of monoclonal antibodies exist. The most frequently used methods are hybridoma technology, where splenic B cells are fused with myeloma cells, and antibody generation from phage display libraries. However, both methods have disadvantages: The introduction of protein sequences of non-human origin (e.g. mouse) can cause unwanted immune responses in patients and random pairing of variable heavy and light chains genes that do not occur naturally in B cells can lead to ineffective antibodies (Tiller, 2011). New procedures, such as single B-cell technologies have been developed to avoid this, and have been successfully applied to generate fully human monoclonal antibodies directed against different pathogens (Cox et al., 2016; Gaebler et al., 2013; Traggiai et al., 2004). As described in the results section, two strategies for the isolation of antigen-specific memory B cells for human antibody generation against HBV were investigated in parallel. Both used antigen-specific B-cell sorting, allowing the recovery of naturally occurring heavy and light chain pairs and will be discussed below.

3.1.3.1 Culturing of sorted memory B cells for antibody generation

First, we combined cell sorting of HBV-specific memory B cells with B-cell transformation, followed by B-cell culture and specificity testing. This procedure is straightforward, as antibody specificities are determined before labor-intensive antibody cloning. On the one hand, antigen-specific IgG+ memory B cells were identified with Alexa647-SVPs. Single cells were then cultured in the presence of EBV (Figure 12). B-cell immortalization with EBV is a frequently used method for the generation of monoclonal antibodies, but the transformation can be very inefficient (M. Steinitz, 2014). On the other hand, CD19+ B cells or HBV-specific IgG+ memory B cells, enriched with HBsAg-Alexa594 or HBsAg-biotin bait, were continuously stimulated with CD40L expressed on feeder cells. CD40L in addition with IL-4 is able to mimic T-cell help and thereby activates B cells and induces the proliferation of memory B cells (Wiesner et al., 2008). Antigen-specific memory B cells were sorted with a frequency of 0.03% to 0.12% of CD19+ B cells. This was lower compared with frequencies obtained during bait evaluation (Figure 8 and Figure 9) and in contrast to

previous publications using a similar strategy for HBsAg-specific B-cell sorting (Burton et al., 2018; Salimzadeh et al., 2018; Ward et al., 2008). This could be due to too little HBV-bait used for staining, leading to the isolation of only few HBV+ memory B cells. Despite that, upon stimulation, most B cells proliferated and secreted IgG antibodies in the cell culture supernatants (Figure 12).

Only a few CD40L-stimulated B cells secreted anti-HBs antibodies (Figure 13 and Figure 14), indicating that antigen-specific B-cell sorting with the HBV-baits failed to efficiently select B cells with HBV-specific B cell receptors. Furthermore, the few HBsAg-specific cells that were detected upon CD40-stimulation died during limiting dilution cloning (Figure 13). This prevented the isolation of B cell receptor mRNA for antibody cloning. B-cell death during B-cell culture was already observed by others and could be a consequence of long-term (more than ten weeks) CD40L stimulation and less genetic stability (Wiesner et al., 2008).

3.1.3.2 Single B cell antibody technology

Besides culturing sorted B cells with EBV medium or CD40L-expressing feeder cells, the isolation of single antigen-specific memory B cells followed by direct cloning of recombinant antibodies from single B cell mRNA without further cultivation was investigated. With this, the long process of culturing B cells was avoided, but it also comprised the drawback that a remarkable amount of work went into monoclonal antibody making first, before knowing their specificity (Cox et al., 2016). For single cell sorting the three HBV-baits Alexa647-SVPs, HBsAg-Alexa594 and HBsAg-biotin were used and single HBV-specific cells were isolated with a frequency of 0.01-0.12% of CD19+ B cells (Table 1). As for B-cell cultures, the frequencies of HBV-specific B cells were lower compared with frequencies obtained by others using HBsAg labeled with fluorescent dyes as B-cell bait (Burton et al., 2018; Salimzadeh et al., 2018; Ward et al., 2008). This may be a result of too little antigen used for staining. Consequently, less antigen binding to the BCR occurred and only few antigen-specific B cells could be detected (M. J. Smith et al., 2017).

Immunoglobulin variable gene amplification efficiency is low

In contrast to B-cell cultures, specificities of sorted and frozen memory B cells can only be determined after antibody cloning. This relies on the amplification of

immunoglobulin (Ig) chain genes from mRNA of single B cells. Nested PCR was used to amplify Ig variable chain genes based on the method described by *Tiller et al.* (Tiller et al., 2008). The amplification efficiency was 20-24% for any immunoglobulin variable heavy, kappa light or lambda light chain gene. Corresponding couples of heavy and light chains were only obtained in 12% of the wells (Table 2). In comparison with the original publication that indicated an efficiency of 30-60% for amplification of heavy and light chain gene pairs, our results were markedly lower (Tiller et al., 2008). This could be a consequence of incorrect placement of positive cells into the well during cell sorting, but it could also be a result of the very low mRNA content in IgG+ memory B cells, that makes amplification very inefficient (Franz et al., 2011; Tajiri et al., 2010).

Furthermore, the amplification efficiency is generally highly variable between independent rounds of sorting and can depend on the status of somatic mutations in the immunoglobulin variable chain genes. In addition, sequences with high numbers of mutations may not be amplified as PCR primers fail to recognize the corresponding sequence (Scheid et al., 2011). For HBsAg-specific memory B cells, the mutation rate is known to be high, but whether this was the reason for low amplification rates is not known (Galson et al., 2015). Nevertheless, to improve the efficiency of single cell PCR, it might be beneficial to pre-amplify the mRNA via the addition of a single stranded T7 RNA polymerase promoter sequence. This has been shown to increase the yield to 80% to obtain PCR products from single cells (Franz et al., 2011). Furthermore, another set of PCR primers could be used to avoid loss of primer binding when high mutations rates are expected in the variable chain genes (Galson et al., 2015; Scheid et al., 2011).

HBV-specific B-cell repertoire seems to be very diverse.

PCR products were sequenced for antibody cloning and to gain some information about the HBV-related B-cell repertoire. Based on identical CDR3 sequences and V- and J-gene segment usage, 20 B-cell clones were identified among all blood donors (Table 3 and Figure 16). The identification of B-cell clones suggested a specific recognition of the fluorescently labeled HBsAg via B-cell receptors (Gaebler et al., 2013). Some clones were identified within different individuals. This can be a hint for B-cell specificity to a common stimulus (HBsAg by vaccination or infection) and

might be an indication for selection pressure on the B-cell repertoire (Galson et al., 2015). However, besides the B-cell clones, far more unique couples of heavy and light chains were identified (Table 4), which more likely points at a random recognition of our HBV-baits rather than a specific selection of certain B cells.

In addition, we analyzed the distribution of CDR3 length and the usage of V- and J-gene segments among all immunoglobulin variable heavy chain gene sequences. CDR3-shortage is believed to be an indicator for affinity maturation of antigen-experienced memory B cells (Chaudhary & Wesemann, 2018). Repertoire analysis of HBsAg+ B cells by *Galson et al.* showed a decrease in CDR3 length after HBV-booster vaccination reaching a minimum of 16 amino acids at day seven (Galson et al., 2016; Galson et al., 2015). In contrast, most CDR3 in our samples isolated at day seven post vaccination consisted of 19 amino acid residues (Figure 16) pointing towards the isolation of less mutated and less specific B cells (Galson et al., 2016; Galson et al., 2015). However, when we analyzed the use of certain immunoglobulin heavy chain V- and J-gene segments, we found similarities among our sequences and the previous data (Galson et al., 2016). *Galson et al.* obtained a strong increase in the usage of V-gene segment IGHV3-7 in HBV vaccine-specific clusters. This V-gene segment was also enriched in our sequences (Figure 16) assuming its importance in HBV-specific B-cell repertoire development. Furthermore, sequencing data of another study, isolating HBsAg-specific mAbs from vaccinated individuals with a cell-microarray indicated the enrichment of various IGHV3 gene segments, indicating that IGHV3 segments might be important in the HBV-specific B cell repertoire (Tajiri et al., 2010). On the contrary, *Wang et al.* identified 21 unique clones from phage display libraries screening for human anti-HBs mAbs of which the majority consisted of IGHV1 V-gene segments (W. Wang et al., 2016). Although all studies used cells isolated from healthy volunteers with booster vaccination, the vaccines were from different producers. This may lead to a different B-cell response and indicates the broad spectrum of affinities that plays a role in prophylaxis of HBV-infection with HBsAg-vaccines.

Novel monoclonal antibodies recognize HBsAg

In order to finally proof antigen-specificity of the selected memory B cells, heavy and light chain expression vectors were constructed and 76 monoclonal antibodies were

expressed in HEK293 cells. Among all, nine monoclonals indicated specificity for HBsAg with ELISA. Seven of these were originally captured with HBsAg-biotin as B-cell bait and two of them, 4D06 and 4D08, indicated strong reactivity (Table 5 and Figure 17). Both mAbs were isolated from unique B cells and used IGHV3 V-gene segments (Table 4). This was similar to most anti-HBs mAbs isolated by *Tajiri* and co-workers and pointed at a potential importance of IGHV3 for the HBV-specific B-cell repertoire (Tajiri et al., 2010). However, the majority of mAbs were not reactive against HBsAg. This is in accordance with our previous observations from culturing HBV-bait-sorted B cells in the presence of EBV or CD40L-expressing feeder cells. It indicated that our HBV-baits were not stringent enough to be exclusively captured by specific B-cell receptors, although they were carefully evaluated regarding background staining and unspecific binding before. In comparison, *Gaebler et al.* similarly cloned 37 mAbs against HIV-1 envelope from sorted HIV-1 reactive memory B cells. Of those only 15 were reactive. Furthermore, they reported of capturing non-HIV-1 specific B cells with their bait and identified two B-cell clones that were detected in a control sort as well as in the original experiment (Gaebler et al., 2013). This suggested that some B cells seem to be cross-reactive and are able to also capture unrelated antigens. According to *Galson et al.*, these polyreactive B cells seem to be a major part to the normal B-cell repertoire (Galson et al., 2016).

Another reason for the high number of unspecific mAbs and B cells could be the capturing of mostly low affinity B-cell receptors during cell sorting. The very low frequency of HBV-bait positive B cells (Table 1), close to the limit of detection, already indicated this (M. J. Smith et al., 2017; Townsend et al., 2001). Furthermore, capturing of low affinity B cells might also be due to the amine-reactive chemical labeling of our antigens. This can disrupt important epitopes and thereby prevent specific antigen recognition (Franz et al., 2011; Moody & Haynes, 2008; Woda & Mathew, 2015). In contrast, it has been shown that chemically labeled HBsAg can successfully be used for the isolation of HBsAg-specific memory B cells not only in blood of HBV-vaccinated healthy individuals, but also in blood of patients with chronic HBV infection (Burton et al., 2018; Le Bert et al., 2019; Salimzadeh et al., 2018). However, the amount of labeled HBsAg used for those assays was 16-fold higher compared to e.g. HBsAg-Alexa594 that was used in this study. Capturing of low affinity B cells might also be a consequence of the time point of blood donation, seven days after booster vaccination. Circulating memory B cells get quickly

activated after vaccination and terminally differentiate into plasma cells. These cells secrete high amounts of antibodies, which can be detected in the serum and lead to high anti-HBs titers. On the contrary, plasma cells downregulate the expression of B cell receptors and thus are difficult to detect (Moody & Haynes, 2008). At the same time, the high affinity memory B cells may still develop in germinal centers and will therefore be detected at later time-points after vaccination, for instance at day 14 to 21 after vaccination (Galson et al., 2016). Moreover, with the selection of only IgG+ memory B cells during cell sorting, we may have missed several specificities. Although IgG+ memory B cells are thought to be the ones with highest levels of affinity maturation, in the background of HBV it has been shown that the pool of anti-HBs specific memory B cells additionally consists of IgM and IgA isotypes (Le Bert et al., 2019; Tuaillon et al., 2006).

In summary, only single B cell antibody technology, which combines the single cell sorting approach with subsequent amplification of immunoglobulin variable chain genes allowed the generation of HBsAg-specific monoclonal antibodies. Among 1059 single memory B cells sorted, nine anti-HBs mAbs were detected and two (4D06 and 4D08) showed high reactivity. B-cell cultures with CD40L-expressing feeder cells also obtained HBV-specific B cells, but it was not possible to isolate those cells and gain immunoglobulin sequence information. In our hands the different approaches turned out to be very inefficient. Antigen-selection seems to be the most crucial step to determine high affinity antibodies. With regard to HBV, this is especially difficult, since HBV envelope proteins are only available as subviral particles harboring several potential, but also many non-relevant B-cell epitopes. Although different antigens and labeling strategies were investigated, it seems that additional steps for a more precise selection are needed. One promising option is the use of double staining. The same antigen will be labeled with a second dye and during analysis only B cells stained positive for both colors will be selected. This has been already successfully used to isolate antigen-specific B cells by different researchers (Moody & Haynes, 2008; Salimzadeh et al., 2018; Woda & Mathew, 2015). In order to increase the pool of potentially specific memory B cells staining of only CD27 instead of a selected Ig isotype might be an option (Crotty et al., 2004; Ward et al., 2008). Furthermore, antigen-specific plasma cells might be used instead of memory B cells. Plasma cells are present in larger quantities shortly after booster

vaccination and have already undergone a couple of rounds of affinity maturation. As they do not express surface BCRs one could make use of an immunoglobulin-capture assay recently developed by *Pinder et al.* that cross-links secreted antibodies with the responsible plasma cell (Pinder et al., 2017).
In conclusion, different approaches for the generation of HBV-specific human monoclonal antibodies from blood memory B cells were performed, but only one method resulted in the development of two highly specific binders.

3.2 Characterization of HBV-specific monoclonal antibodies

Antibody-based therapy is widely used for the treatment of cancer or autoimmune disease. In the background of HBV infection, antibodies are already used for passive immunization. Polyclonal hepatitis B immunoglobulin preparations (HBIg) are given prophylactically, to prevent mother to child transmission or re-infection after liver transplantation (Terrault et al., 2018). With regard to chronic HBV infection, preliminary studies in chronic patients have shown that antibody-based therapy can positively impact on viremia but long-term effects are so far limited (Ma et al., 2019). *In vitro* and *in vivo* studies with recombinant monoclonal antibodies have indicated several modes of action and could also show prolonged viral suppression (W. Wang et al., 2016; Zhang et al., 2016). Therefore, we have characterized our newly generated anti-HBs monoclonals 4D06 and 4D08 with regard to structural properties and prophylactic and therapeutic potential. The results of structural and functional characterization will be discussed below.

3.2.1 Structural characterization

The two monoclonal antibodies 4D06 and 4D08 were generated from single memory B cells. Both obtained high affinity for HBsAg, with 4D06 indicating slightly lower EC_{50} value than 4D08 (Figure 20). Although EC_{50} values are only an estimate for affinity, the obtained nanomolar concentrations for 4D06 (15.8 nM) and 4D08 (158 nM) were comparable with affinity constants determined for other HBsAg-reactive monoclonal antibodies, ranging from 500 nM to 1.2 pM (Golsaz Shirazi et al., 2014; Kucinskaite-Kodze et al., 2016; W. Tan et al., 2013).
The detection of particular epitopes seems to be very important regarding the potential of monoclonal antibodies to neutralize HBV infection (Gao et al., 2017).

Most published HBsAg-specific antibodies recognize linear or conformational epitopes in the a-determinant of HBsAg. It is the most important antigenic determinant in the S-domain of the envelope proteins (Kucinskaite-Kodze et al., 2016; W. Tan et al., 2013; Zhang et al., 2016). Epitope characteristics of 4D06 and 4D08 differed: 4D06 failed to detect reduced small HBV envelope proteins in Western Blot and Dot Blot, but was able to recognize the native protein (Figure 19). This suggested a conformational epitope formed from different amino acid residues across the protein. HBsAg mutants with site-directed mutations covering the extracellular domains of the small envelope protein will be required to exactly map the 4D06-epitope. In contrast, 4D08 was capable of recognizing both, the native and the reduced form of small HBV envelope proteins (Figure 19), pointing at a linear rather than a conformational epitope. In order to further localize the epitope of 4D08, 18mer overlapping peptides spanning the major hydrophilic region (MHR) of the HBV Env protein S-domain were used. The MHR is exposed to the outside of the SVP and many neutralizing antibodies recognize epitopes in this immunogenic area (Kucinskaite-Kodze et al., 2016; Tajiri et al., 2010). A continuous stretch of amino acids involved in the binding of 4D08 could not observed but the assay indicated two regions potentially important for the recognition (Figure 19). One region is located in the first loop (AA 124-137) of the a-determinant of HBsAg and another shortly before the beginning of a proposed amphipathic helix (AA 156-169) (Suffner et al., 2018). This is contradictory to the previous Dot blot and Western blot results, which pointed at the recognition of a linear epitope. For the determination of the exact epitope of 4D08 either a peptide-epitope spot assay will be needed to identify the linear epitope or similar as for 4D06 an assay with HBsAg mutants with site directed mutations will be needed to obtain a conformational epitope. So far, the current results point at a “partially linear” epitope for 4D08 and a conformational epitope for 4D06.

3.2.2 Functional characterization

Besides structural features of antibodies, knowledge about their mode of action is most important. Antibodies targeting HBV should not only have prophylactic function to prevent from infection by virus neutralization, but should also be capable of at least lowering circulating HBsAg concentration. Optimal function of a monoclonal antibody concerning the treatment of chronic HBV infection would be a combined

effect of capturing circulating HBsAg and the recognition of HBV envelope proteins on the surface of infected cells that triggers the activation of immune effector cells to induce killing of infected hepatocytes. Thereby the disease outcome may be improved. Whether 4D06 and 4D08 fulfill these criteria will be discussed below.

3.2.2.1 4D06 and 4D08 have broadly neutralizing capacity

Virus neutralization has been shown to efficiently prevent from HBV infection. 4D06 and 4D08 were evaluated for HBV-uptake inhibition and neutralization capacity in cell culture. Both mAbs prevented HBV-uptake in HepG2 NTCP cells. HBV cccDNA establishment was not observed after pre-incubation with both mAbs, but HBV rcDNA was detected in cell lysates after pre-incubation of virus and 4D08 (Figure 21). This difference in rcDNA detection could be a hint towards diverse mechanisms of uptake inhibition. While 4D06 may prevent HBV uptake by directly blocking the first attachment of virions to heparan sulfate proteoglycans (HSPG) on the hepatocyte surface, 4D08 may function intracellularly. Hepatocytes express neonatal Fc receptors, which can bind IgG in endosomes. Thereby antibody uptake into the cell can be promoted (Blumberg et al., 1995). 4D08 and virus may be taken up by endocytosis explaining the detection of rcDNA. Following lysosomal degradation of the virus may then prevent cccDNA formation. In accordance with this hypothesis it has been shown that HBsAg-specific antibodies present in Hepatitis B immunoglobulin preparations can be endocytosed by hepatocyte-derived cell lines. Furthermore, two monoclonal anti-HBs antibodies were capable of blocking HBsAg secretion after cellular uptake (Neumann et al., 2010; Schilling et al., 2003). However, to proof whether endosomal uptake and lysosomal degradation is one mechanism of virus neutralization of 4D08, further assays need to be developed. For instance, live cell imaging with fluorescently tagged virus and antibody can be used, to localize HBV and antibody in the cell.

Besides uptake inhibition, 4D06 and 4D08 were capable of HBV neutralization (genotype D) in a concentration dependent manner. 4D06 was superior to 4D08, indicated by a 10-fold lower mAb concentration of 4D06 that was necessary to obtain complete neutralization (Figure 22). Additionally, IC_{50} values were calculated as an indicator for antibody potency. IC_{50} values for both were in the low nanomolar range and were comparable with IC_{50} values obtained for other anti-HBs mAbs (Gao et al., 2017; Golsaz-Shirazi et al., 2017; Kucinskaite-Kodze et al., 2016). However, it is

complicated to properly compare the different results due to the use of different cell lines for infection (e.g. HepG2 or HepaRG cells), different multiplicities of infection and different methods for neutralization (Golsaz-Shirazi et al., 2017; W. Tan et al., 2013; W. Wang et al., 2016).
The combination of two monoclonals directed against HBsAg can have a synergistic neutralization effect (Neumann et al., 2010; W. Tan et al., 2013). This was also investigated for 4D06 in combination with 4D08. However, the application of both mAbs in combination did not show improved neutralization capacity, compared to 4D06 alone (Figure 22). One possible explanation for the nearly antagonistic effect could be that their epitopes are in close proximity and the combinatorial application causes steric hindrance. As a consequence no further reduction of HBeAg in cell culture supernatant was observed during neutralization assay when both mAbs were incubated together.

Furthermore, the neutralization potential against various HBV geno- and subtypes was investigated. A broad neutralization capacity is very important, as broadly neutralizing antibodies can be used to treat infections independent of the HBV genotype that causes the infection. Approximately 96% of chronic HBV infections worldwide are caused by five different genotypes A-E and among those genotype C is the most frequent (Velkov et al., 2018). Furthermore, broadly neutralizing antibodies recognize epitopes in conserved regions of HBsAg, which are less effected by amino acid substitutions introduced upon virus mutation (Kucinskaite-Kodze et al., 2016; W. Wang et al., 2016). Both mAbs had the capability to recognize and neutralize eight different HBV genotypes (A-H) with a similar preference for genotype A and C (Figure 24 to Figure 26). Thus, 4D06 and 4D08 were classified as broadly neutralizing antibodies.

3.2.2.2 mAbs capture HBsAg secreted from HBV infected cells

Current standard therapy for chronic HBV infection is based on immune modulation with pegylated interferon or on nucleos(t)ide analogues (NUCs) such as tenofovir or entecavir (Fanning et al., 2019). NUCs target the reverse transcription of HBV and can reduce viral titers to undetectable levels, but they have no effect on the transcription and translation of viral mRNAs. Thus, the secretion of viral proteins such as HBsAg and HBeAg is not affected. In contrast, antibodies targeting HBsAg

can reduce this level by forming immune complexes, which can be cleared from the circulation (Corti et al., 2018). Therefore, beside the neutralizing effect of 4D06 and 4D08, their potential to capture subviral particles secreted from HBV infected cells was investigated. As expected, both mAbs were able to recognize secreted HBsAg in cell culture supernatant of HBV-infected HepG2 NTCP cells. The effect was slightly pronounced, when mAbs were applied in combination with the approved nucleoside analogue entecavir, which had no impact on HBsAg secretion alone. Moreover, 4D06 seemed to be capable of preventing from (re-) infection similar to ETV as cccDNA levels were comparable (Figure 23). This observation could be due a synergistic effect of the nucleoside analogue and the antibody. While ETV inhibits the formation of new virions and thereby lowers the total number of infectious particles in the supernatant, mAbs capture secreted particles and inhibit the infection of healthy cells. A similar effect has already been shown in a small pilot study with chronic HBV patients indicating that the combinatorial application of lamivudine and antibodies is beneficial for the outcome of chronic HBV infection (van Nunen et al., 2002). However, to conclude such a substantial therapeutic effect of 4D06 and 4D08 further evaluation is needed, especially *in vivo*.

3.2.2.3 4D06 and 4D08 harbor CD16-dependent effector function

The therapeutic effect of antibodies does not only originate from antigen recognition and immune complex formation but is also mediated through the activation of immune effector cells upon antibody recognition (Nimmerjahn & Ravetch, 2008). Antibodies can be recognized via their Fc region by Fc receptors (FcRs) expressed on the surface of various immune cells. Triggering of activating Fc receptors can induce several effector functions, such as phagocytosis by macrophages, degranulation and cytokine release by neutrophils or NK cells or complement activation and will result in target cell death (Lu et al., 2018; Nimmerjahn & Ravetch, 2008). For each antibody isotype corresponding FcRs exist. IgG molecules are recognized by Fc gamma receptors (FcγRs), of which three classes are known FcγRI (CD64), FcγRIIa (CD32a) and FcγRIII (CD16) (Nimmerjahn & Ravetch, 2008).

With regard to HBV infection, antibody dependent cell-mediated cytotoxicity (ADCC) induced by NK cells is assumed to be one very important mechanism in the control of acute infection (Bertoletti & Le Bert, 2018; Cerino et al., 2019; Fisicaro et al.,

2019). To investigate whether monoclonals 4D06 and 4D08 were capable of inducing such an immune effector function, first human FcγR expressing mouse reporter cells were incubated in the presence of mAbs and immobilized HBsAg. CD16-expressing cells were activated upon recognition of antibody-antigen complexes, but not CD32a- and CD64-expressing reporter cells, indicating that the Fc region of both, 4D06 and 4D08, are preferentially recognized by FcγRIII (Figure 27). Furthermore, human peripheral NK cells, one of the main cell types expressing CD16, recognized 4D06 and 4D08 in the presence of plate-bound HBsAg and were partially activated (Figure 28). However, when HBV-infected HepG2 NTCP cells were used as target cells neither NK-cell binding nor activation was observed (Figure 28). NK-cell activation is tightly regulated and highly dependent on the crosslinking of FcγRs upon binding to antibody Fc regions. Plate-bound HBsAg seems to be capable to induce such clustering of 4D06 and 4D08 with NK cells, whereas the amount of surface expressed envelope protein on infected HepG2 cells seems to be too little to promote NK cell recognition and FcγR clustering. Besides NK cells, also macrophages, eosinophils and neutrophils express CD16 (Nimmerjahn & Ravetch, 2008). These cells are additional potent effector cells and seem to be important for the antibody-induced killing of infected hepatocytes. Zhang and co-workers could show that FcγR-mediated phagocytosis is responsible for anti-HBs antibody mediated HBV clearance (Zhang et al., 2016). With regard to 4D06 and 4D08, effector function via phagocytosis could also be a mode of action. This would be beneficial for chronic HBV therapy as macrophages are present in relatively high quantities in the liver (Li et al., 2017). However, if that is the case for 4D06 and 4D08 needs to be determined with further activation assays.

Furthermore, it seems that 4D06 and 4D08 are only partially recognized by CD16 expressed on human NK cells. In order to improve the affinity, Fc engineering could be considered. Here, amino acid residues at distinct positions in the Fc region are substituted. Such substitutions have been shown to enhance the binding with FcγRIII or FcγRII and resulted in stronger ADCC or antibody dependent cell-mediated phagocytosis (ADCP) (X. Wang et al., 2018).

3.3 Antibody-based therapy in comparison with other therapeutic approaches targeting chronic HBV infection

Current therapeutic options for the treatment of chronic HBV infection rely on pegylated Interferon alpha (Peg-IFN) or nucleos(t)ide analogues (NUCs). However, these only induce disease remission but mostly fail in a complete eradication of the virus (Fanning et al., 2019). So-called functional cure, a sustained control of the viral replication, defined by the loss of serum HBsAg, undetectable HBV DNA and the development of anti-HBs antibodies, is only achieved in less than 10% of the cases (Bertoletti & Le Bert, 2018; Revill et al., 2019). As a reason, NUCs only suppress the viral replication by targeting HBV DNA synthesis, but they are inactive in eradicating the cccDNA of HBV in infected hepatocytes. Furthermore, NUCs have no impact on the viral protein translation. Thus, a high level of HBsAg secretion is maintained. This is believed to play a major role in HBV-related suppression of B- and T-cell responses (Bengsch et al., 2014; Burton et al., 2018; Salimzadeh et al., 2018). At this point, antibodies such as newly generated mAbs 4D06 or 4D08 or polyclonal HBIg preparations could come into play. Several mAbs have been shown to be capable of lowering the amount of circulating HBsAg. Additionally, they can prevent from *de novo* infection by blocking HBV uptake (Golsaz-Shirazi et al., 2017; Neumann et al., 2010; Tajiri et al., 2010; van Nunen et al., 2001; W. Wang et al., 2016). Furthermore, two *in vitro* studies with monoclonals indicated that antibodies are additionally able to trigger immune effector functions via their Fc regions. The investigators showed that NK cells and Kupffer cells were activated to eliminate infected hepatocytes via ADCC or ADCP (Li et al., 2017; Zhang et al., 2016). Taken together these results are promising. Whether antibodies alone can achieve long-term virus control due to the reduction of soluble HBsAg and the eradication of HBV-infected cells still needs to be investigated.

However, a combination of immunotherapy with antibodies and other therapeutic approaches seems to be feasible. Antibodies could lower the level of circulating HBsAg and prevent from (re-) infection by neutralization, while for instance NUCs suppress the viral replication and thereby the secretion of new infectious viral particles. First investigations towards this direction have been made upon a monthly injection of HBIg in patients chronically infected with the hepatitis B virus, who had

received long-term NUC treatment before. As a result, the HBsAg titer was reduced and two patients achieved a sustained loss of HBsAg so that antiviral therapy was discontinued (Tsuge et al., 2016). Similarly, the application of monoclonal antibodies and interferon alpha indicated a transient decrease of serum HBsAg to background levels and three of six patients exhibited a loss of HBV DNA and HBsAg that was maintained until the end follow-up (van Nunen et al., 2001).

Therapeutic vaccination aims at inducing a robust HBV-specific T- and B-cell response, with T-cells that are capable of recognizing and eradicating HBV-infected hepatocytes (Dembek et al., 2018). Several vaccine strategies have already been tested in different trials and animal models (Bertoletti & Le Bert, 2018). The success varied but it seems, at least in animal models, that HBV tolerance can be broken after therapeutic vaccination with specific strategies (Kosinska et al., 2019). However, the main principle of therapeutic vaccination relies on the activation of already rare, exhausted and metabolically altered HBV-specific T and B cells (Bengsch et al., 2014; Boni et al., 2007; Burton et al., 2018; Le Bert et al., 2019; Salimzadeh et al., 2018). Thus, the application of antibodies in combination with therapeutic vaccination may be beneficial. Antibodies may first decrease circulating HBsAg and thereby counteract its immunosuppressive function. Therapeutic vaccination may then induce HBV-specific T-cell responses to control the infection by killing infected hepatocytes. Moreover, therapeutic vaccination with mammalian cell-derived hepatitis B envelope proteins has been shown to induce high levels anti-HBs antibodies that could then help to control the suppression of the viral replication (Hoa et al., 2009).

Similarly, to antibodies several siRNA molecules are currently under investigation that target different HBV transcripts including HBV envelope protein mRNA. These were able to reduce HBsAg in patients and in an animal model it has been shown that the combined application of therapeutic vaccination and siRNA treatment induced a prolonged control of HBV replication (Michler et al., 2020; Yuen et al., 2019). However, the application of siRNAs in comparison to antibodies has a disadvantage, which is the molecule delivery. While for antibodies the routes of administration are already well investigated, for siRNAs it has been shown that the way of delivery can be problematic (Setten et al., 2019). Furthermore, broadly

neutralizing antibodies are capable of targeting HBsAg from various HBV genotypes with similar efficacy while success of siRNA molecules is highly dependent on sequence similarities at the target site. This can vary in different geno- and subtypes of HBV.

With regard to lowering the level of circulating HBsAg, so-called nucleic acid polymers (NAPs) have been investigated. These have been shown to block viral entry of different viruses including HBV and were also potent in inhibiting the release of HBsAg from infected hepatocytes (Vaillant, 2019). Their function seems to be similar to HBIg preparations and two monoclonal antibodies (HepeX-B), which inhibited the secretion of HBsAg from cells upon antibody endocytosis (Neumann et al., 2010; Schilling et al., 2003). However, in contrast to those mAbs, the exact mode of action of NAPs is largely unknown. This may have a negative impact on future drug approval.

As functional HBV-specific T cells are missing in chronic HBV patients, therapeutic approaches with adoptive T-cell transfer have been developed (Bertoletti & Le Bert, 2018; A. T. Tan & Schreiber; Wisskirchen et al., 2019). Here, T cells are *ex vivo* equipped with HBV-specific T-cell receptors or antibody-based chimeric antigen receptors that recognize HBV-infected cells. These T cells are able to induce hepatocyte killing and thereby promote virus control (Krebs et al., 2013; Wisskirchen et al., 2019). This strategy seems to be very effective as especially CD8 effector T scells are grafted with HBV-specific TCRs. However, big drawbacks are the need of genetic modification of T cells and the high risk of developing severe side effects such as a cytokine release syndrome (Bertoletti & Le Bert, 2018; Hay, 2018). The application of antibodies also harbors the potential of promoting side effects, but in patient studies, HBIg as well as recombinant mAbs were so far well tolerated (Tsuge et al., 2016; van Nunen et al., 2001). Furthermore, T cells need to be modified specifically for each patient. This is labor-intensive. In contrast, monoclonal antibodies can be applied to every donor without modification. Although antibodies itself do not directly influence the HBV-specific T-cell response, it may be that the formation of immune complexes with HBsAg and monoclonal antibodies promotes antigen presentation and thereby induces the stimulation of virus-specific T-cell responses (Corti et al., 2018). A hint towards such a mechanism has been given by

work of *Zhang* and co-workers. They could show, that the frequency of HBsAg-specific CD8+ T cells increased in HBV-infected mice treated with monoclonal antibody E6F6 (Zhang et al., 2016).

3.4 Conclusion

The present thesis shows that HBV-specific human monoclonal antibodies can be generated from immunoglobulin variable chain genes of single HBsAg-specific memory B cells of healthy HBV-vaccinated volunteers. *In vitro* characterization of two new recombinant monoclonals, 4D06 and 4D08, obtained high antigen affinity, broad neutralization capacity and the potential to induce Fc-mediated CD16-related immune effector cell activation. Whether these two molecules are capable of both decreasing HBsAg in the circulation as well as inducing Fc-dependent hepatocyte killing *in vivo* has to be determined in future studies.

In general, monoclonal antibodies directed against HBsAg have the potential to impact on several features of chronic hepatitis B virus infection. Therefore, it is worthwhile to further investigate their potency especially in a combined therapeutic application with other currently developing treatment strategies.

4 Material and Methods

4.1 Materials

4.1.1 Devices

Product	Supplier
PCR Cycler TOptical Gradient 96	Biometra
Architect™ platform	Abbot Laboratories
BEP III platform	Siemens Healthcare
Centrifuge 5920R	Eppendorf
CTL ImmunoSpot® S6 Ultra-V Analyzer	Cellular Technology Limited (CTL) Europe
CytoFLEX S	Beckmann Coulter
MoFlo Astrios EQ cell sorter	Beckmann Coulter
ELISA-Reader infinite F200	Tecan
Flow Cytometer FACS Canto II™	BD Bioscience
Freezing device	Nalgene / Biocision Coolcell
Fusion Fx7	PeqLab
Agarose Gel Chambers	PeqLab
Incubator Heracell 150	Heraeus Holding GmbH
Light Cycler® 480 II	Roche Diagnostics
InvitrogenTM Dynal DynaMagTM-15	Thermo Fisher Scientific
Multi-channel Pipettes	Ergo One
NanoDrop One	Thermo Fisher Scientific
Nanophotometer OD 600	IMPLEN GmbH
Neubauer improved hemocytometer	Brand
NucleoCounter NC250	Chemometic
Pipette ‘Accu-jet pro’	Brand
Pipettes	Eppendorf
Shaker and incubator for bacteria	INFORS AG; Heraeus Holding GmbH
Sterile Hood HERA Safe	Thermo Fisher Scientific
T professional Trio Thermocycler	Analytik Jena
Table-top centrifuge 5417R	Eppendorf

Thermo Mixer F1.5	Eppendorf
BD FACS Aria Cell Sorted	BD Biosciences
Peristaltic Pump MasterFlex L/S	Cole Parmer
Intas Chemostar M6	Intas Science imaging
Confocal Microscope	Carl Zeiss AG
Mini Trans-Blot ® cell	Bio-Rad

4.1.2 Consumables

Product	**Supplier**
96 well plates for qPCR, Frame Star 480/96	4titude
96-well plates for PCR, semi-skirted	PeqLab
Amicon Ultra Centrifugal Filters, 30K, 2 mL	Merck
Butterfly cannula	Sarstedt
Cell culture flasks, dishes, plates	TTP
Cell strainer, 100 µm	Falcon
Cover slips	VWR
Cryo vials	Grainer Bio One
Cuvette	Implen
ELISA 96-well plates Nunc MaxiSorb	Thermo Fisher Scientific
FACS plate 96-well, V-bottom	Roth
Falcon tubes 15 mL/50 mL	Grainer Bio One
Filcons, sterile 20 µm	SLG
Filter tips	Greiner Bio One
HiTrab Protein G HP column, 1mL	GE Life sciences
Immobilon-P, PVDF membrane, 0.45 µm	Merck
MasterFlex Tubing, L/S 16	Cole Parmer
Multiscreen$_{HTS}$ IP Filter 96-well plate, 8-stripes, ELISpot plate	Merck
Needles	Braun
Adhesive foil for microplates and PCR	PeqLab
PCR Tubes	Thermo Fisher Scientific
Pierce^{TM} ProteinG coated Plates,	Thermo Fisher Scientific

8-well stripes, Clear	
Pipette Tips 10 µL – 1 mL	Biozym / Greiner Bio One / Gilson
Pipettes (disposable) 2 mL, 5 mL, 10 mL, 50 mL	Greiner Bio One
Protein Lo Bind Tubes 1.5 mL	Eppendorf
Reaction Tubes 1.5 mL, 2 mL	Greiner Bio One, Eppendorf
Reagent reservoirs, sterile	Corning
Sterile Filters, 0.45 µm, 0.2 µm	Sarstedt
Surgical Disposable Scalpels	Braun
Syringes	Braun
Zeba™ Spin desalting columns, 7K MWCO, 5ml	Invitrogen

4.1.3 Chemicals and reagents

Products	**Supplier**
2-Phenoxyethanol	Roth
Acetic acid	Roth
Agarose	PeqLab
Ammonium persulfate (APS)	Roth
Ampicillin	Roth
Acrylamide/Bisacrylamide, Rotiphorese Gel 40	Roth
Biocoll separating solution (density 1.077 g/mL)	Biochrom
Blasticidin S HCl 50 mg	Invitrogen
Bovine Gamma Globulin Standard	Pierce
Bovine serum albumin (BSA)	Roth
Bradford Reagent	Thermo Fisher Scientific
Brefeldin A (BFA)	Sigma
Collagen R	Serva
Coomassie Brilliant blue G-250	Roth
CpG ODN 10103 (10 mg/mL)	Invivogen

Cyclosporine A (1 µg/mL)	Invivogen
Dapi Fluorochrome G	Southern Biotech
Dimethyl sulfoxide (DMSO)	Sigma
Disodium phosphate (Na_2HPO_4)	Roth
Smart Ladder, 200 bp - 10kb	Eurogentech
Dulbecco's Modified Eagle's Medium (DMEM)	Gibco
ECL solution	GE Healthcare Amersham
EDTA disodium salt (Na_2EDTA)	Roth
Fetal calf serum (FCS)	Gibco
Fugene® HD Transfection reagent	Promega
Glycine	Roth
Glycine-HCl	Roth
Heparin-Natrium 25000	Ratiopharm
HEPES 1M	Gibco
human IL-2 Proleucin	Novartis
human recombinant IL-4	R&D systems
Hydrochloric acid (HCl)	Roth
Isopropanol	Roth
L-Glutamine, 200 mM	Gibco
Laemmli-Buffer (4X)	Bio-Rad
Live/Dead™ fixable Aqua dead cell stain	Invitrogen
Live/Dead™ fixable Near-IR dead cell stain	Invitrogen
Magnesium chloride (MgCl2)	Sigma
Powdered Milk (milk)	Roth
Non-essential amino acids (NEAA), 100X	Gibco
LDS Sample buffer, non-reducing	Pierce
OptiMEM	Gibco
PageRuler™ plus pre-stained protein ladder 10 – 250 kDa	Thermo Fisher Scientific
Paraformaldehyde (PFA), 4%	ChemCruz
PEG6000	Merck
Penicillin Streptomycin, 10,000 U/mL (100X)	Gibco

Phorbol 12-myristate 13-acetate (PMA)	Sigma
Phosphate-buffered saline (PBS) 10X	Gibco
Polyethylenimne (PEI)	Polyscience
Potassium chloride (KCl)	Roth
Potassium hydrogen carbonate ($KHCO_3$)	Roth
Propidium iodide (PI)	Roth
RNAsin (RNAse Inhibitor), 40 U/µL	Promega
Roti®-Safe Gel Stain	Roth
RPMI 1640	Gibco
Sodium bicarbonate ($NaHCO_3$)	Roth
Sodium carbonate (Na_2CO_3)	Roth
Sodium dihydrogen phosphate (NaH_2PO_4)	Roth
Sodium hydroxide (NaOH)	Roth
Sodium pyruvate, 100 mM	Gibco
Sulfuric acid, (H_2SO_4), 2N	Roth
TEMED, N,N,N',N'-Tetramethyl ethylenediamine	Roth
TMB substrate for ELISpot	MabTech
TMB, stabilized chromagen (for ELISA)	Invitrogen
Tris Base	Roth
Trypan blue	Gibco
Trypsin-EDTA	Gibco
Tryptone	Roth
Tween 20	Roth
Yeast extract	Roth
β-Mercaptoethanol, 50 mM	Gibco

4.1.4 Buffers and solutions

Buffer	Ingredients
B cell buffer	0.1% (w/w) BSA 0.6% (w/w) Sodium citrate 2 mM EDTA in PBS
B cell isolation buffer	0.1% (w/w) BSA 2mM EDTA in PBS
Binding buffer	0.02 M sodium phosphate in MilliQ H_2O, pH 7.0
Blocking and assay buffer for Western blot and Dot blot	5% (w/w) milk in TBS-T buffer
Carbonate buffer (0.1M)	5.76 g Sodium bicarbonate 3.31 g Sodium carbonate in 1L H_2O, pH 9.6
Coomassie destain solution	10% (v/v) Acetic acid 50% (v/v) Methanol 40% (v/v) H_2O
Dot Blot buffer	0.125 M Tris base, pH 6.8 4% (w/w) SDS 25% (v/v) glycerol 10% (v/v) β-Mercaptoethanol in H_2O
ELISA blocking solution	5% BSA in PBS
ELISA wash	0.05% Tween-20 in PBS
Elution buffer	0.1 M Glycine-HCl in MilliQ H_2O, pH 2.7
FACS buffer	0.1% BSA in PBS
Lower buffer (SDS-PAGE)	0.5 M Tris-HCl 10% SDS (w/w) in H_2O, pH 6.8
Lysis buffer	RNAsin 12U DTT 10 mM PBS 0.5X in RNAse-free H_2O
Neutralization buffer	1 M Tris-HCl in MilliQ H_2O, pH 9.0

SDS-Running buffer (10X)	30 g Tris Base 144 g Glycine 10 g SDS in 1L H2O, pH 8.3
TAE Buffer (50X)	2M Tris Base 2M Acetic acid 50 mM EDTA 50 mM in H_2O, pH 8.0
TBS-T buffer (10X)	24 g Tris base 88 g NaCl 0.1% Tween-20 in 1L H_2O, pH 7.6
Transfer buffer (10X)	30.8 g Tris base 144.1 g glycine in 1L H_2O
Transfer buffer working solution (1X)	100 mL Transfer buffer (10X) 200 mL Methanol 700 mL H_2O
Upper buffer (SDS-PAGE)	1.5 M Tris-HCl 10% SDS (w/w) in H_2O, pH 8.8

4.1.5 Kits

Product	**Supplier**
Alexa Fluor™ 594 Microscale Protein Labeling Kit	Invitrogen
ARCHITECT anti-HBsAg Reagent Kit	Abbott
ARCHITECT HBsAg Reagent Kit	Abbott
Dynabeads™ Untouched™ Human B cell Kit	Invitrogen
Enzygnost HBeAg test	Siemens Healthcare Diagnostics
EZ-Link™ Micro Sulfo-NHS-Biotinylation Kit	Thermo Fisher Scientific
Fixation/Permeabilization Solution Kit	BD Biosciences
GeneJet Gel extraction Kit	Thermo Fisher Scientific
GeneJet Plasmid Miniprep Kit	Thermo Fisher Scientific

High pure PCR Purification Kit	Roche
HotStarTaq DNA polymerase (1000 U)	Qiagen
Human IgG ELISpot^{BASIC} (HPR)	MabTech
LightCycler 480 SYBR green master mix	Roche
Murex HBsAg Version 3	DiaSorin
NuceloBond ® Xtra Midi	Macherey-Nagel
NucleoSpin Tissue DNA Kit	Macherey-Nagel
SuperScript^{TM} III First Strand Synthesis Kit	Invitrogen

4.1.6 Enzymes

Enzyme	Supplier
FastAP	Thermo Fisher Scientific
FastDigest restriction enzymes including FastDigest Green Buffer (10X)	Thermo Fisher Scientific
Phusion Hot Start Flex 2x Master Mix	New England Biolabs
T4 DNA Ligase including T4 Ligase buffer	Thermo Fisher Scientific
T5 Exonuclease including NEB 4 buffer	New England Biolabs

4.1.7 Primers

Primers were purchased from Microsynth AG or Invitrogen.

Primer name	Sequence	Application
5' L-VH 1	ACAGGTGCCCACTCCCAGGTGCAG	Ig PCR1
5' L-VH 3	AAGGTGTCCAGTGTGARGTGCAG	Ig PCR1
5' L-VH 4/6	CCCAGATGGGTCCTGTCCCAGGTGCAG	Ig PCR1
5' L-VH 5	CAAGGAGTCTGTTCCGAGGTGCAG	Ig PCR1
5' L-VK 1/2	ATGAGGSTCCCYGCTCAGCTGCTGG	Ig PCR1
5' L-VK 3	CTCTTCCTCCTGCTACTCTGGCTCCCAG	Ig PCR1
5' L-VK 4	ATTTCTCTGTTGCTCTGGATCTCTG	Ig PCR1
5' Pan VK	ATGACCCAGWCTCCABYCWCCCTG	Ig PCR2
5' L-VL 1	GGTCCTGGGCCCAGTCTGTGCTG	Ig PCR1
5' L-VL 2	GGTCCTGGGCCCAGTCTGCCCTG	Ig PCR1

5’ L-VL 3	GCTCTGTGACCTCCTATGAGCTG	Ig PCR1
5’ L-VL 4/5	GGTCTCTCTCSCAGCYTGTGCTG	Ig PCR1
5’ L-VL 6	GTTCTTGGGCCAATTTTATGCTG	Ig PCR1
5’ L-VL 7	GGTCCAATTCYCAGGCTGTGGTG	Ig PCR1
5’ L-VL 8	GAGTGGATTCTCAGACTGTGGTG	Ig PCR1
5’ Kpn2I VH 1	CTGCATCCGGAGTACATTCCCAGGTGCAG CTGGTGCAG	Ig PCR2
5’ Kpn2I VH 1/5	CTGCATCCGGAGTACATTCCGAGGTGCAG CTGGTGCAG	Ig PCR2
5’ Kpn2I VH 3	CTGCATCCGGAGTACATTCTGAGGTGCAG CTGGTGGAG	Ig PCR2
5’ Kpn2I VH3-23	CTGCATCCGGAGTACATTCTGAGGTGCAG CTGTTGGAG	Ig PCR2
5’ Kpn2I VH 4	CTGCATCCGGAGTACATTCCCAGGTGCAG CTGCAGGAG	Ig PCR2
5’ Kpn2I VH 4-34	CTGCATCCGGAGTACATTCCCAGGTGCAG CTACAGCAGTG	Ig PCR2
5’ Kpn2I VH 1-18	CTGCATCCGGAGTACATTCCCAGGTTCAG CTGGTGCAG	Ig PCR2
5’ Kpn2I VH 1-24	CTGCATCCGGAGTACATTCCCAGGTCCAG CTGGTACAG	Ig PCR2
5’ Kpn2I VH 3-33	CTGCATCCGGAGTACATTCTCAGGTGCAG CTGGTGGAG	Ig PCR2
5’ Kpn2I VH 3-9	CTGCATCCGGAGTACATTCTGAAGTGCAG CTGGTGGAG	Ig PCR2
5’ Kpn2I VH 4-39	CTGCATCCGGAGTACATTCCCAGCTGCAG CTGCAGGAG	Ig PCR2
5’ Kpn2I VH 6-1	CTGCATCCGGAGTACATTCCCAGGTACAG CTGCAGCAG	Ig PCR2
5’ Kpn2I VK 1-5	CTGCATCCGGAGTACATTCTGACATCCAG ATGACCCAGTC	Ig PCR2
5’ Kpn2I VK 1-9	TTGTGCTGCATCCGGAGTACATTCAGACA TCCAGTTGACCCAGTCT	Ig PCR2
5’ Kpn2I VK1D-43	CTGCATCCGGAGTACATTGTGCCATCCGG ATGACCCAGTC	Ig PCR2
5’ Kpn2I VK 2-24	CTGCATCCGGAGTACATGGGGATATTGTG	Ig PCR2

	ATGACCCAGAC	
5’ Kpn2I VK 2-28	CTGCATCCGGAGTACATGGGGATATTGTG ATGACTCAGTC	Ig PCR2
5’ Kpn2I VK 2-30	CTGCATCCGGAGTACATGGGGATGTTGTG ATGACTCAGTC	Ig PCR2
5’ Kpn2I VK 3-11	TTGTGCTGCATCCGGAGTACATTCAGAAA TTGTGTTGACACAGTC	Ig PCR2
5’ Kpn2I VK 3-15	TTGTGCTGCATCCGGAGTACATTCAGAAA TTGTGTTGACACAGTC	Ig PCR2
5’ Kpn2I VK 3-20	TTGTGCTGCATCCGGAGTACATTCAGAAA TTGTGTTGACGCAGTCT	Ig PCR2
5’ Kpn2I VK 4-1	CTGCATCCGGAGTACATTCGGACATCGTG ATGACCCAGTC	Ig PCR2
5’ AgeI VL 1	CTGCTACCGGTTCCTGGGCCCAGTCTGTG CTGACKCAG	Ig PCR2
5’ AgeI VL 2	CTGCTACCGGTTCCTGGGCCCAGTCTGCC CTGACTCAG	Ig PCR2
5’ AgeI VL 3	CTGCTACCGGTTCTGTGACCTCCTATGAG CTGACWCAG	Ig PCR2
5’ AgeI VL 4/5	CTGCTACCGGTTCTCTCTCSCAGCYTGTG CTGACTCA	Ig PCR2
5’ AgeI VL 6	CTGCTACCGGTTCTTGGGCCAATTTTATG CTGACTCAG	Ig PCR2
5’ AgeI VL 7/8	CTGCTACCGGTTCCAATTCYCAGRCTGTG GTGACYCAG	Ig PCR2
3’ Cγ CH1	GGAAGGTGTGCACGCCGCTGGTC	Ig PCR1
3’ IgG (internal)	GTTCGGGGAAGTAGTCCTTGAC	Ig PCR2 + sequencing
3’ ApaI JH 1/2/4/5	TGCGAAGGGCCCGCTGAGGAGACGGTGAC CAG	Ig PCR2
3’ ApaI JH 3	TGCGAAGGGCCCGCTGAAGAGACGGTGAC CATTG	Ig PCR2
3’ ApaI JH 6	TGCGAAGGGCCCGCTGAGGAGACGGTGAC CGTG	Ig PCR2
3’ Ck543	GTTTCTCGTAGTCTGCTTTGCTCA	Ig PCR2
3’ Ck494	GTGCTGTCCTTGCTGTCCTGCT	Ig PCR2 + sequencing
3’ RsrII JK 1/4	GCCACCGGTCCGTTTGATYTCCACCTTGG	Ig PCR2

	TC	
3’ RsrII JK 2	GCCACCGGTCCGTTTGATCTCCAGCTTGG TC	Ig PCR2
3’ RsrII JK 3	GCCACCGGTCCGTTTGATATCCACTTTGG TC	Ig PCR2
3’ RsrII JK5	GCCACCGGTCCGTTTAATCTCCAGTCGTG TC	Ig PCR2
3’ CL	CACCAGTGTGGCCTTGTTGGCTTG	Ig PCR1
3’ XhoI CL	CTCCTCACTCGAGGGYGGGAACAGAGTG	Ig PCR2 + sequencing
PrP fw	TGCTGGGAAGTGCCATGAG	qPCR, normalization
KC_leader_fwd	GATCAAGCTTGCCACCATGGATTTTGAGG TGCAGATTTTCAGCTTCCTGCTAATCAGT GCCTCAGTCTCCGGAATGGAGACACAT	cloning pB1k1A
HC_leader_fwd	GATCAAGCTTGCCACCATGGATTTTGAGG TGCAGATTTTCAGCTTCCTGCTAATCAGT GCCTCAGTCTCCGGAATGAACTTAGGG	cloning pA1k3A
WA610_rev	CAGCCACGGTCCGTTTTATTTCCAGCTTG GTCCCCCCTCCGAAC	cloning pB1k1A
WA614_rev	ACGCTTGGGCCCTTGGTGCTGGCTGAGGA GACTGTGAGAGTGGTGCCTTG	cloning pA1k3A
WA579_CH1	GGCTGCCTGGTGAAGGACTACTTC	sequencing pA1k3A
WA469_polyA	GAAAGGACAGTGGGAGTGGCACCTTC	sequencing pA1, pB1
PrP rev	CGGTGCATGTTTTCACGATAGTA	qPCR, normalization
cccDNA 2251+	AGCTGAGGCGGTATCTA	qPCR, HBV cccDNA
cccDNA 92-	GCCTATTGATTGGAAAGTATGT	qPCR, HBV cccDNA
HBV 1745	GGAGGGATACATAGAGGTTCCTTGA	qPCR, HBV rcDNA
HBV 1844	GTTGCCCGTTTGTCCTCTAATTC	qPCR, HBV rcDNA

4.1.8 Plasmids

Plasmid name	Transgene	Source
pA1k3A (plasmid bank #1255)	human IgG1 heavy chain constant, including cloning site for Ig variable region and human leader sequence	L. Wolff
pB1k1A (plasmid bank #1254)	human Ig kappa light chain constant, including cloning site for Ig kappa variable region and human leader sequence	L. Wolff
mAb_pIgL (plasmid bank #1256)	human Ig lambda light chain constant, including cloning site for Ig lambda variable region	F. Klein
mAb_pIgH (gamma1) (plasmid bank #1257)	human IgG1 heavy chain constant, including cloning site for Ig variable region	F. Klein
pRVHBV1.5_A	1.5 over-length wt HBV genome, genotype A	V. Bruss
pZDonor_N4214_ Genotype B_1.5 (plasmid bank # 768)	1.5 over-length wt HBV genome, genotype B	D. Glebe
pZDonor_N3825_C1_1.5 (plasmid bank #769)	1.5 over-length wt HBV genome, genotype C	D. Glebe
pRR_NeoK_XA_wtHBV1.3_ genotype D (plasmid bank # 911)	1.3 over-length wt HBV genome, genotype D	J. Wettengel
pA1-huIgG-scFvC8 (plasmid bank #277)	single chain fragment variable C8 (antibody binding site for HBsAg)	F. Pinci
p84-mCherry-S-Zeo (plasmid bank #578)	small HBV envelope protein fused with mCherry fluorescent protein	J. Wettengel
pJC126	HDV genotype 1 John Taylor	S. Urban
pLX304-HB2.7 (gt A-H)	HBV env proteins genotype A-H	S. Urban

4.1.9 Cell lines, bacterial strains and virus

Cell line / Bacterial strain	Description	Supplier
B95-8 cells	Epstein-Barr Virus (EBV) producing Marmoset B-Lymphoblastoid cell line	AG Protzer
BW5147 thymoma cells	Mouse thymoma cell line, stably expressing FcγR-CD3ζ (either human FcγRIIIA, FcγRIIA or FcγRI)	H. Hengel, Universitätsklinikum Freiburg
LL8-CD40L feeder cells	L929 mouse fibroblast cell line stably transfected with CD40L	A. Moosmann, Helmholtz Center Munich
HEK 293	Human embryonic kidney cell line; transformed with fragments of adenovirus type 5 DNA	AG Protzer
HepG2	Human hepatoblastoma derived cell line	AG Protzer
HepG2 NTCP	HepG2 cells expressing NTCP, Clone K7; enabling infection of HBV	generated by D. Stadler
Huh7	Human hepatoma cell line	AG Protzer
E. coli *STBL3*	Chemical competent *Escherichia coli* cells	Invitrogen
E. coli *TOP10*	Chemical competent *Escherichia coli* cells	Invitrogen
HBV (genotype D, *adw*)	Virus purified from stable transfected HepAD38 cell culture supernatant	AG Protzer, generated and purified by J. Wettengel

4.1.10 Media

Medium	Ingredients	
RPMI wash medium	RPMI 1640	500 mL
	Pen/Strep, 10,000 U/ml	5.5 mL
RPMI complete medium	RPMI 1640	500 mL
	Pen/Strep, 10,000 U/mL	5.5 mL
	FCS	50 mL
	L-Glutamine, 200 mM	5.5 mL
	NEAA, 100X	5.5 mL
	Sodium pyruvate, 100 mM	5.5 mL
	HEPES, 1 M	12.5 mL
RPMI plus medium	RPMI 1640	500 mL
	Pen/Strep, 10,000 U/mL	5.5 mL
	FCS	50 mL
	L-Glutamine, 200 mM	5.5 mL
	Sodium pyruvate, 100 mM	5.5 mL
DMEM complete medium	DMEM	500 mL
	Pen/Strep, 10,000 U/mL	5.5 mL
	FCS	50 mL
	L-Glutamine, 200 mM	5.5 mL
	NEAA, 100X	5.5 mL
	Sodium pyruvate, 100 mM	5.5 mL
Differentiation medium	DMEM	500 mL
	Pen/Strep, 10,000 U/mL	5.5 mL
	FCS	50 mL
	L-Glutamine, 200 mM	5.5 mL
	NEAA, 100X	5.5 mL
	Sodium pyruvate, 100 mM	5.5 mL
	DMSO	10.5 mL
Freezing medium	FCS	90% (v/v)
	DMSO	10% (v/v)

LB medium	Tryptone	10 g
(for 1 L, pH 7.0)	Yeast extract	5 g
	NaCl	10 g

4.1.11 Proteins and Peptides

Proteins

Protein	Application	Supplier
HBsAg, (ad), serum purified	FACS, ELISA, ELISpot	Roche
HBV subviral particles (non-labeled SVPs)	FACS	AG Protzer, J. Wettengel, purified from HepAD38 cell culture supernatant (sucrose gradient, fraction 4)
HBV subviral particles labeled with Alexa Fluor 647 dye (Alexa647-SVPs)	FACS	AG Protzer, J. Wettengel, labeled with Alexa Fluor 647 dye via NHS kit
1st WHO International Reference Panel for HBV Genotypes for HBsAg Assays	ELISA	Paul-Ehrlich-Institute

Peptides

Peptides were used for epitope peptide ELISA and were provided by Martin Feuerherd (Virology, Immune Monitoring Group) and were purchased from Genaxxon.

Peptide	Sequence
S^{97-114}	LLDYQGMLPVCPLIPGSS
$S^{104-121}$	LPVCPLIPGSSTTSTGPC
$S^{111-128}$	PGSSTTSTGPCRTCTTPA
$S^{118-135}$	TGPCRTCTTPAQGTSMYP
$S^{125-142}$	TTPAQGTSMYPSCCCTKP
$S^{132-149}$	SMYPSCCCTKPSDGNCTC
$S^{139-156}$	CTKPSDGNCTCIPIPSSW
$S^{146-163}$	NCTCIPIPSSWAFGKFLW
$S^{153-170}$	PSSWAFGKFLWEWASARF

4.1.12 Antibodies

Antibody	Dilution	Article number	Supplier
Avidin HRP	1:500	18-4100-51	eBioscience
CD16-BV605	1:100	302039	Biolegend
CD19-eF450	1:40	48-0199-42	eBioscience
CD19-V500	1:40	561125	BD Biosciences
CD27-PE-Cy7		560609	BD Biosciences
CD27 BV421		562513	BD Biosciences
CD3-PE	1:20	12-0039-42	BD Biosciences
CD3-V500	1:100	560770	BD Bioscience
CD56-APC	1:50	IM2474	Beckman Coulter
goat anti-human IgG (H+L)	1:500	A18807	Invitrogen
goat anti-human IgG Alexa Fluor 647	1:1000	A21445	Invitrogen
goat anti-human IgG HRP	1:1000 1:10,000	A8667	Sigma

goat anti-mouse IgG HRP	1:1000 1:10,000	A21235	Sigma
HB-1 monoclonal antibody	0.5µg/mL		Dieter Glebe
HBIg			Kedrion Biopharma
Hepatect CP ®			Biotest
human BD Fc Block	2.5 µg/well	564219	BD Biosciences
IFNγ-FTIC	1:40	554700	BD Biosciences
IgG-PE-Cy7	1:20	561298	BD Biosciences
IgG-PE	1:20	555787	BD Biosciences
IgG-FITC	1:20	560962	BD Biosciences
IgG-BV605	1:20	563246	BD Biosciences
JES6-5H4	1:500		BD Pharmigen
JES6-1A12	1:500		BD Pharmigen
Mip1β-PE	1:200	550078	BD Pharmigen
Nabi-HB			Nabi Biopharmaceuticals
Streptavidin-AlexaFluor647	1.5 µg/mL	532357	Invitrogen
Streptavidin-APC	1:200	17-4317-82	eBioscience
Streptavidin-PE	1:250	12-4317-87	eBioscience
Streptavidin-HRP	1:1000		Dianova

4.1.13 Software

Software	Supplier
FlowJo 10.4	BD Biosciences
CytExpert	Beckman Coulter
FACS Diva	Becton Dickinson
Graph Pad Prism 8	Graph Pad Software Inc.
i-control™ software	Tecan Group
Lightcycler 480 Software	Roche
Serial Cloner	Serial Basics
Windows 7/8/10, MS Office	Windows
Summit Cell Sorting Software	Beckman Coulter

4.2 Methods

4.2.1 Molecular biology methods

4.2.1.1 Polymerase chain reaction (PCR)

Polymerase chain reactions (PCRs) were used for molecular cloning of plasmids pA1k3A (#1255) and pB1k1A (#1254) using Phusion Hot Start Flex Master Mix according to the manufacturer's protocol. Each reaction was performed in a total volume of 50 µL. For this, 1.5 µL of each primer (stock 20 µM), 1-10 ng plasmid DNA, 25 µL 2X Phusion Master Mix and water were mixed. The amplification was performed as following: First denaturation at 99°C for 30 s, followed by 36 cycles with 99°C for 30 s, 72°C for 60 s, 72°C for 5 minutes and final cooling at 4°C.

4.2.1.2 Single cell RT-PCR

For cDNA synthesis from total RNA of single sorted antigen-specific memory B cells the Invitrogen™ first strand cDNA synthesis kit was used and the protocol described by *Tiller et al.* (Tiller et al., 2008) was followed. Briefly, PCR plates with single sorted cells were thawed on ice and cDNA synthesis was performed in a total volume of 14 µL/well in the original sorting plate. The preparation was carried out on ice and in a PCR cabinet. A reaction mix containing nuclease-free water, 150 ng random hexamer primer, 0.5 µL of 25 mM each nucleotide dNTP mix was prepared. 6 µL of that mixture were added to each well of the sorting plate. After mixing and incubation for 10 minutes at 42°C, the plate was chilled on ice for at least two minutes. Following that, a cDNA synthesis mix was prepared containing 1X RT buffer, 2 µL of 25 mM $MgCl_2$, 1 µL 0.1 M DTT, 0.5% (v/v) Igepal CA-630, 20 U RNAse out, 4 U RNAsin and 50 U Superscript III reverse transcriptase. The mixture was added to the pre-incubated dNTP, primer, RNA mix and carefully suspended. Reverse transcription was carried out at 25°C for 10 minutes, 50°C for 60 minutes and 94°C for 5 minutes. Finally, cDNA was stored at -20°C.

4.2.1.3 Immunoglobulin (Ig) gene amplification by nested PCR

The amplification of Ig heavy, Ig kappa and Ig lambda variable genes was carried out independently by nested PCR. All PCR reactions were performed in 96-well plates in a total volume of 40 µL/well. A master mix containing 200 mM each primer or primer mix (Table 6), 300 µM each dNTP, 1X PCR buffer and 1.2 U HotStarTaq DNA

polymerase was prepared with nuclease-free water. For all 1st PCR reactions primer mixes and 3.5 µL cDNA as template was used. The nested PCR reactions (2nd PCR) were performed with gene-specific primers or primer mixes and with 3.5 µL of unpurified first PCR product. Each PCR run consisted of 50 cycles at 94°C for 30 s, 58°C for 30 s, 72°C for 55s (1st PCR) or 45s (2nd PCR). Each program started with an initial activation step at 95°C for 10 minutes. Proper amplification was evaluated with an agarose gel electrophoresis (1% agarose) and analyzed using Fusion Fx7 gel-documentation device. Upon successful amplification, PCR products were purified with High pure PCR purification kit, an aliquot was sent for sequencing and the remaining PCR product was stored at -20°C.

In order to ligate the obtained Ig variable chain genes into the respective expression vectors, a third PCR run was performed to introduce restriction sites. For this, specific V-gene forward and J-gene specific reverse primers that were identified during sequence analysis were used and unpurified first PCR product served as template. The cycler program for 2nd PCR was used.

Table 6. Primer and primer mix used for nested Ig PCRs

1st PCR	**Forward primer mix**	**Reverse primer**
variable heavy (VH)	**L-VH$_{mix}$** (5' L-VH 1, 5' L-VH3, 5' L-VH4/6, 5' L-VH 5)	3' Cγ CH1
variable kappa light (VK)	**L-VK$_{mix}$** (5' L-VK 1/2, 5' L-VK3, 5' L-Vk4)	3' Ck543
variable lambda light (VL)	**L-VL$_{mix}$** (5' L-VL 1, 5' L-VL 2, 5' L-VL 3, 5' L-VL 4/5, 5' L-VL 6, 5' L-VL 7, 5' L-VL 8)	3' CL

2nd PCR	Forward primer (mix)	Reverse primer
variable heavy (VH)	**Kpn2I VH_{mix}** (5' Kpn2I VH 1, 5' Kpn2I VH 1/5, 5' Kpn2I VH 3, 5' Kpn2I VH 3-23, 5' Kpn2I VH 4, 5' Kpn2I VH4-34, 5' Kpn2I VH1-18, 5' Kpn2I 1-24, 5' Kpn2I VH 3-33, 5' Kpn2I VH 3-9, 5' Kpn2I VH 4-39, 5' Kpn2I VH 6-1)	3' IgG internal
variable kappa light (VK)	5' Pan Vk	3' Ck494
variable lambda light (VL)	**5' AgeI VL_{mix}** (5' AgeI VL 1, 5' AgeI VL 2, 5' AgeI VL 3, 5' AgeI VL 4/5, 5' AgeI VL 6, AgeI VL 7/8)	3' CL

4.2.1.4 Immunoglobulin sequence analysis

Purified 2nd PCR Ig variable gene products were sent for sequencing with the respective primers (3' IgG internal, 3' Ck494 and 3' CL; see section 4.1.7). For sequence analysis, nucleotide sequences were first *in silico* translated into the respective amino acid sequence using serial cloner 2.6.1. The amino acid sequences were then analyzed with regard to a complete open reading frame (ORF). Complementarity determining regions (CDRs) 1-3 were identified with *abYsis antibody database* (http://www.abysis.org/; 13.12.2019). Sequences with complete ORFs were further examined by comparison against the nucleotide sequence database of human immunoglobulins IMGT (http://www.imgt.org/IMGT_vquest/input; 13.12.2019) to identify germline V(D)J-gene segments with highest identity.

4.2.1.5 Restriction enzyme digestion

To obtain gene fragments for molecular cloning, restriction enzymes were used to digest PCR products and plasmids. In addition, digestion control was carried out after plasmid DNA isolation. Each reaction was performed in a total volume of 10 µL, with 500 ng PCR product or 1 µg plasmid DNA, 1 µL FastDigest Green Buffer (10X), 1 µL of the appropriate FastDigest restriction enzyme and water. The mix was

incubated for 20-60 minutes at 37°C. Per reaction, 1 µL FastAP for 5' and 3' dephosphorylation was added, if plasmids were digested to prevent self ligation without insert.

4.2.1.6 Agarose gel electrophoresis and gel extraction

Plasmid DNA or PCR products were examined on a 1% agarose gel prepared with 1X TAE buffer and 10 µL RotiSafe gel stain per 50 mL gel. To estimate the size of the DNA fragment, a DNA ladder was run in parallel to the samples. The gel was run at 120-150 V until sufficient separation of the fragments was reached. Products were analyzed with Fusion Fx7 gel documentation device.

DNA fragments that were needed for molecular cloning were cut out of the gel with a scalpel and DNA was extracted with GeneJet gel extraction kit according to the manufacturer's instructions.

4.2.1.7 Ligation

For ligation, 100 ng of the linearize plasmid DNA were ligated in a 3:1 (insert: backbone) ratio with the desired insert DNA fragment. DNA, 1 µL T4 Ligase, 1 µL T4 Ligase Buffer and water to achieve a total volume of 10 µL were mixed and incubated for at least 20 minutes at room temperature. If not used immediately, the ligation reaction was stored at -20°C.

4.2.1.8 Transformation of E.coli

For the amplification of plasmid DNA, *E.coli STBL3* or *TOP10* were transformed. First, bacteria (50 µL aliquots) were thawed on ice. Then, 5 µL of the ligation reaction was added and incubated for 5-20 minutes on ice. After that, a heat shock was performed for 45 s at 42°C in a water bath and bacteria were chilled on ice for at least two minutes. Bacteria were then spread on ampicillin-containing LB-plates and incubated overnight at 37°C.

4.2.1.9 Isolation of plasmid DNA

Transformed *E.coli* were amplified in 5 to 100 mL overnight cultures with LB-medium containing 100 µg/mL ampicillin at 37°C and 185 rpm. Bacteria were harvested with centrifugation at 3200 xg for 15 minutes at 4°C, after cultures reached an absorbance (OD_{600nm}) of maximum 1.5. Plasmid DNA was isolated according to the

manufacturer's instructions either with GeneJet Plasmid Miniprep kit for cultures up to 5 mL or with NucleoBond Xtra plasmid midi prep kit for cultures up to 100 mL.

4.2.1.10 Sequencing

For sequencing, samples were diluted to a concentration of 20-100 ng/µL in a volume of 20 µL. 20 µL of the respective primer (10 µM) was as well prepared and both were sent to the external sequencing provider GATC Eurofins Genomics (Ebersberg, Germany). Sequencing results were downloaded and analyzed with Serial Cloner 2.6.1.

4.2.1.11 Determination of DNA concentration

Plasmid and genomic DNA concentrations were determined with NanoDrop one spectral photometer using the appropriate buffer solution as blank and DNA determination settings.

4.2.1.12 DNA isolation from cell culture

Cellular DNA was extracted from cell cultures upon cell lysis with Nucleo Spin Tissue kit according to manufacturer's instructions. DNA content was determined and isolated DNA was frozen at -20°C until use in different assays.

4.2.1.13 quantitative PCR (qPCR)

Quantitative PCR (qPCR) was performed to determine total intracellular HBV rcDNA or intracellular HBV cccDNA. For cccDNA quantification, the extracted cellular DNA was first digested with T5 exonuclease to remove linear DNA, rcDNA or nicked DNA from the sample and to increase the selectivity for cccDNA as described by (Xia et al., 2017). For each reaction, 8.5 µL extracted DNA were mixed with 1 µL NEB buffer 4 and 0.5 µL T5 exonuclease. The mix was incubated for 30 minutes at 37°C followed by a subsequent heat inactivation at 99°C for 5 minutes. Thereafter, the samples were diluted 1:4 with molecular grade water.

For each qPCR reaction, 4 µL sample DNA, 5 µL LightCycler 480 SYBR green master mix, 0.5 µL forward primer and 0.5 µL reversed primer (stock 20 µM) were mixed. The respective primers for cccDNA or rcDNA quantification are listed in section 4.1.7. qPCR was performed with a LightCycler 480 Real-time PCR system and data was either analyzed quantitatively with an external plasmid standard or by

advanced relative quantification and normalization to the single copy prion protein (PrP) gene.

For intracellular rcDNA the following qPCR program was used:

	T [°C]	t [s]	Ramp [°C/s]	Acquisition mode	Cycles
Denaturation	95	300	4.4		1
Amplification	95	15	4.4	single	45
	60	10	2.2		
	72	25	4.4		
Melting	95	10	4.4	continuous 5/°C	1
	65	60	2.2		
	95		0.11		
Cooling	40	1	2.2		1

The qPCR program for cccDNA was the following:

	T [°C]	t [s]	Ramp [°C/s]	Acquisition mode	Cycles
Denaturation	95	600	4.4		1
Amplification	95	15	4.4	single	50
	60	5	2.2		
	72	45	4.4		
	88	2	4.4		
Melting	95	1	4.4	continuous 5/°C	1
	65	15	2.2		
	95		0.11		
Cooling	40	30	2.2		1

4.2.1.14 Protein labeling

Alexa Fluor 594 labeling of HBsAg

In order to identify and isolate HBsAg-specific memory B cells, HBsAg purified from human serum was labeled with Alexa Fluor 594 dye. For this purpose, the Alexa Fluor™ 594 microscale labeling kit was used and the manufacturer's instructions

were followed. 100 µg HBsAg (1 µg/mL) was used as starting material. After conjugation, the degree of labeling (DOL) and the protein concentration was determined with Nanodrop One spectral photometer, according to the protocol. A DOL of 1.72 was calculated for HBsAg-Alexa594, indicating that approximately 1.7 dye molecules were coupled to one molecule of HBsAg.

Biotinylation of HBsAg and monoclonal antibodies 4D06 and 4D08

For the identification of HBsAg-specific memory B cells with flow cytometry, human serum purified HBsAg was labeled with biotin. 1 mL of HBsAg (1 mg/mL) was conjugated with biotin with the EZ-Link™ Micro Sulfo-NHS-Biotinylation kit according to the manufacturer's protocol. Labeled HBsAg-biotin was purified from remaining unbound biotin with Zeba-spin columns and centrifugation at 1000 xg for 2 minutes.

For Murex ELISA, to investigate whether mAbs 4D06 and 4D08 recognize HBsAg of different HBV genotypes, both mAbs were biotinylated. Here, 0.5 mg purified antibody was conjugated with biotin with EZ-Link™ Micro Sulfo-NHS-Biotinylation kit according to the manufacturer's protocol. As described before, labeled mAbs were purified from remaining free biotin with Zeba-spin columns and centrifugation at 1000 xg for 2 minutes.

4.2.1.15 Sodium dodecyl sulfate polyacrylamide gel electrophoresis

To examine antibody purity after purification or estimate antibody epitopes, a sodium dodecyl sulfate polyacrylamide gel electrophoresis (SDS-PAGE) was executed. For this, a 12.5% separating gel was prepared by mixing 2.5 mL water, 1.9 mL lower buffer, 3.25 mL acrylamide, before 12,5 µl TEMED and 24 µL APS were added for polymerization. The solution was transferred to the gel-casting chamber. In order to achieve an even running front, the liquid gel was overlayed with isopropanol. After polymerization, the isopropanol was discarded and the stacking gel was prepared. Here, 1.2 mL water, 0.5 mL upper buffer, 0.35 mL acrylamide were mixed with 3.25 µL TEMED and 21 µL APS for polymerization. This solution was added on top of the separating gel to the gel-casting chamber. A 10-well comb was added to create sample pockets. After polymerization, SDS-gel was removed from the casting chamber and placed into the running chamber, which was subsequently filled with

1X SDS-running buffer. Protein samples were prepared either in reducing buffer or non-reducing buffer: 0.1-5.0 µg protein, 5 µL buffer (4X) and PBS (1X) filled up to a total volume of 20 µL were mixed. Samples with reducing buffer were additionally incubated for 10-20 minutes at 95°C before sample loading. In order to apply the samples, the comb was removed, samples and a protein marker were loaded and the gel was run at 85 V (≈ 200 mA) until desired protein separation was achieved.

4.2.1.16 Total protein stain with Coomassie after SDS-PAGE

After running the SDS-PAGE, the gel was removed from the chamber and carefully transferred into Coomassie staining solution to stain total protein. The gel was incubated overnight shaking. The next day, de-staining solution was prepared and the gel was transferred to remove excess of Coomassie stain. De-staining lasted for at least one day, while the de-staining solution was exchanged three times. Finally, after sufficient de-staining, the gel was scanned with Epson Scanner for analysis.

4.2.1.17 Western Blot

For Western blot analysis, proteins were separated with SDS-PAGE as described before. After running, the gel was removed from the chamber and proteins were transferred to a PVDF membrane via wet blotting. For this, the membrane was first activated with methanol for 3 minutes and then calibrated in 1X transfer buffer. Additionally, Whatman paper was soaked for at least 5 minutes in 1X transfer buffer. Membrane and Whatman paper were assembled in the blotting cassette according to the manufacturer's instructions. Then, the cassette was placed into the blotting chamber, which was filled up with transfer buffer and a frozen cooling pack. Blotting was performed on ice, to avoid overheating and proteins were transferred at 200-300 mA for 1.5 hours. Following protein transfer, the membrane was blocked with 5% milk in TBS-T buffer for one hour at room temperature. The membrane was then incubated overnight at 4°C with primary antibodies diluted 1:1000-1:10,000 in blocking solution. The next day, after washing the membrane three times for 10 minutes with TBS-T buffer incubation with secondary antibodies (1:10,000 in blocking solution) followed for 2 hours at room temperature. Membrane development was performed with ECL detection solution according to the manufacturer's protocol using the Intas Chemostar M6, after washing the membrane three times for 10 minutes with TBS-T buffer.

4.2.1.18 Dot Blot

Antibodies can recognize linear or conformational epitopes. In order to determine the type of antibody epitope a Dot blot was performed. First, a PVDF membrane was activated with pure methanol for a few seconds, followed by repeated rinsing of the membrane in PBS for equilibration. HBsAg (1 µg/mL), purified from human serum was used as sample. For native protein conformation, HBsAg was diluted in PBS. For protein linearization, samples were diluted in dot blot buffer and incubated at 95°C for 10 minutes to achieve complete protein reduction. The activated membrane was cut into pieces of 1 cm x 3 cm and on each piece three drops of 2 µL of reduced or non-reduced antigen were dropped. The drops were dried completely, before the membrane pieces were blocked with blocking solution for one hour at room temperature. Primary antibodies 4D06, 4D08 and HB-1 were diluted in blocking solution (10 µg/mL) and membranes were transferred to the respective antibody solution. After incubation for two hours at room temperature, all pieces were washed three times for 10 minutes with TBS-T buffer and then incubated for 1 hour at room temperature with secondary antibodies (polyclonal goat anti-human IgG conjugated with HRP or goat anti-mouse IgG conjugated with HRP, 1:10,000 diluted in blocking solution). Finally, membranes were washed for three times again in TBS-T buffer and ECL detection solution was added according to the manufacturer's instructions. Membranes were analyzed with Intas Chemostar M6.

4.2.2 General cell culture methods

All cell lines and primary cells were cultured under sterile conditions and were only handled under a laminar airflow clean hood. Incubation took place at 37°C, 5% CO_2 and 95% humidity.

4.2.2.1 Maintenance of cell lines

Adherent cells were sub-cultured in DMEM complete medium or in RPMI complete medium and were passaged 1:3 to 1:20 every three to four days depending on confluency. LL8-CD40L feeder cells, HepG2, HepG2 NTCP and Huh7 cell lines were detached upon treatment with trypsin for 5-10 minutes at 37°C and vigorous re-suspension to obtain a single cell suspension. HEK293 cells were harvested with very short (max. 2 minutes at 37°C) trypsin-treatment and re-suspension. For

HepG2-derived cells, culture flasks and plates were pre-treated with collagen R (1:10 in H_2O) and washed twice with PBS, before cell seeding.

Semi-adherent B95-8 cells were kept in RPMI complete medium and harvested by vigorously re-suspension. Every three to four days the cells were passaged in a 1:10 ratio.

4.2.2.2 Counting of cells

After harvesting or isolation, cells were re-suspended carefully to obtain a single cell suspension. Counting was performed manually. Therefore, 10 µL of cell suspension was mixed with 10 µL of trypan blue to stain dead cells. Cells were counted in a Neubauer Improved hemocytometer under a light microscope. Automated cell counting was performed with the NucleoCounter NC-250. For this, 20 µL cell suspension were mixed with 1 µL Solution 18 and added to the counting plate.

4.2.2.3 Freezing and thawing of cells

In order to freeze cells, cells were harvested and centrifuged at 350 xg for 5 minutes. The pelleted cells were resuspended in 500 µL freezing medium per cryo vial. The vials were subsequently transferred to a cell freezing device and immediately stored at –80°C. Temperature decline was approximately 1°C per minute. After at least one day, cryo tubes were transferred to an -80°C box or in liquid nitrogen for storage.
To thaw cells, 1 mL pre-warmed medium was added to frozen cells and carefully resuspended until cells were thawed. Then, the cell suspension was transferred to a 50 mL falcon tube containing 20 mL pre-warmed medium. Upon centrifugation at 350 xg for 5 minutes, cells were resuspended in the respective cell culture medium and seeded in an appropriate cell culture flask.

4.2.2.4 Isolation of human PBMC

Human PBMC were isolated from whole blood of healthy donors. Blood was mixed with heparin to avoid coagulation and was diluted 1:1 in RPMI wash medium. 25 mL of diluted blood was overlayed onto 12.5 mL Biocoll separating solution and centrifuged at 1,200 xg for 20 minutes without break. The lymphocyte ring was collected and transferred to a fresh 50 mL falcon tube. Two lymphocyte rings were pooled into one new falcon. Each tube was filled up with RPMI wash medium and

centrifuged for 10 minutes at 700 xg. The supernatant was discarded; cells were resuspended in 30 mL wash medium and centrifuged at 70 xg for 20 minutes with break 5. Next, the cells were washed two times with medium (350 xg, 5 minutes). Finally the supernatant was discarded and PBMC were resuspended in an appropriate volume of RPMI complete medium. Cells were counted and either frozen, rested overnight at 37°C or further processed for B-cell isolation.

4.2.2.5 B-cell enrichment with Dynabeads

For the detection of antigen-specific B cells with flow cytometry, B cells were enriched from PBMC with Dynabeads™ Untouched™ human B cell kit. For this, PBMC were thawed and counted and 50 x 10^6 PBMC were centrifuged at 350 xg for 5 minutes. Then, the supernatant was discarded and cells were resuspended in 10 mL B-cell buffer. After transfer to a fresh 15 mL falcon tube, PBMC were centrifuged again at 350 xg for 5 minutes. Then, PBMC were resuspended with 10 mL B-cell isolation buffer and after another centrifugation the manufacturer's protocol was followed. Finally, enriched B cells were centrifuged, resuspended in 2 mL RPMI complete medium and counted. Freshly enriched B cells were rested overnight in the incubator with a density of 2 x 10^6 cells/mL before use.

4.2.2.6 Production of Epstein-Barr virus containing medium

B cells were immortalized after transformation with Epstein-Barr virus (EBV). Therefore, EBV-containing medium was prepared. Marmoset B95-8 cells were seeded in T_{75} flasks with a density of 1.0 x10^6 cells/mL and incubated for 1h at 37°C in the presence of 20 ng/mL PMA. Then, cells were transferred to a 50 mL falcon tube and washed three times with RPMI complete medium by centrifugation (350 xg, 5 minutes, room temperature). Afterwards, the cells were resuspended in 10 mL RPMI complete medium and incubated for three days. To finally harvest EBV-containing medium, the supernatant was collected, transferred to a falcon tube and centrifuged at 300 xg for 10 minutes at 4°C, before filtering through a 0.45 µm sterile filter and storage at -80°C.

4.2.2.7 Irradiation of cells

In order to culture single isolated B cells, a feeder cell layer is needed to provide stimuli for proliferation and differentiation. For this purpose, either LL8-CD40L feeder

cells or allogeneic PBMC were irradiated with 180 Gy or 35 Gy. Irradiated LL8 cells were seeded in 96-well F-bottom plates with a density of 1.0 x 10^6 cells/well. PBMC were seeded with a density of 4.0 x 10^5 cells/well in 96-well U-bottom plates. LL8 cells were incubated for at least two days before use and could be kept for two weeks after irradiation. PBMC were used immediately after irradiation.

4.2.2.8 B-cell transformation

Transformation of PBMCs with EBV

For EBV transformation, 1.0 x 10^6 overnight rested PBMC were incubated with 1 mL EBV-containing medium for 2 hours at 37°C in a 50 mL falcon tube. Afterwards, 2 mL RPMI complete medium and 2 µL cyclosporine A were added and cells were seeded in a 6-well plate. PBMC were incubated for two weeks. Transformation was evaluated by visual examination for cell clusters under a light microscope, as well as by ELISA for IgG detection.

Transformation of Alexa647-SVP-specific B cells with EBV

Single sorted Alexa647-SVP+ memory B cells were incubated in the presence of allogeneic feeder PBMC (40,000 cells/well), CpG ODN 10103 (2.5 µg/mL), human recombinant IL-2 (2 ng/mL) and EBV-containing medium (30% v/v) in RPMI complete medium. After incubation for two weeks, cell culture supernatant was analyzed for the presence of IgG and anti-HBs antibodies with ELISA.

CD40L stimulation of B cells

Sorted B cells were seeded in RPMI complete medium at a density of up to 400 cells/well on irradiated LL8-CD40L feeder cells in the presence of human recombinant IL-4 (2 ng/mL) in a volume of 200 µL/well. Once per weeks B cells were re-seeded. For this, 100 µL/well of cell culture supernatant was removed and stored at 4°C for IgG and anti-HBs ELISA. Then, 100 µL/well fresh RPMI complete medium supplemented with IL-4 was added, B cells were resuspended by pipetting up and down and transferred to a new plate with fresh feeder cells.

4.2.2.9 Transfection of cells

In order to express a protein of interest HEK293 cells or Huh7 cells were transfected with plasmid DNA. For this, cells were seeded in a 6-well plate to obtain approximately 80% confluence at the day of transfection. 5000 ng plasmid DNA was diluted in 300 µL OptiMEM medium. Carefully 15 µL Fugene® HD transfection reagent was added and the mix was incubated for 10 minutes at room temperature. In the meantime, a medium change was performed. Thereafter, the DNA/Fugene mix was added to the cells drop-by-drop and incubated for two to three days, before 2-4 mL fresh medium was added or cells were used for other assays.

4.2.2.10 HBV infection

HepG2 NTCP cells were seeded on collagen coated plates with densities of 3 x 10^5 to 1.0 x 10^6 cells/well and differentiated for two days DMEM differentiation medium supplemented with 2.5% DMSO. Cells were infected with HBV (MOI 100-500, genotype D) in the presence of 4% (v/v) PEG6000 for 18 hours. Purified HBV was kindly provided by Jochen Wettengel. After incubation, the inoculum was removed, cells were washed three times with PBS and replaced in the incubator with fresh DMEM differentiation medium. Every four days, the supernatant was collected for HBeAg determination to monitor infection and cells were provided with fresh medium.

4.2.2.11 HBV Uptake assay

In order to evaluate the potential of monoclonal antibodies to prevent HBV uptake *in vitro* the HBV uptake assay was performed. Anindita Chakraborty established this assay. HepG2 NTCP cells were seeded with a density of 3 x 10^5 cells/well on collagen-coated 24-well plates and differentiated for two days with 2.5% DMSO in DMEM differentiation medium. HBV inoculum was prepared by mixing viral particles (MOI 100, genotype D) with 100 nM antibody and incubation for 30 minutes at 37°C. Cells were pre-chilled on ice for 15 min and HBV containing inoculum was added to cells for 1 hour on ice enabling the virus to bind to the cell surface. Medium was changed and cells were subsequently shifted to 37 °C for 3 to 24 hours. Cells were washed two times with PBS, shortly trypsinized for 3 minutes, and either replaced in the incubator with differentiation medium for later cccDNA or HBeAg measurements or lysed and collected for total intracellular HBV rcDNA determination.

4.2.2.12 Neutralization assay

The neutralization assay was performed to evaluate the antibody capacity to neutralize HBV infection. For this, HepG2 NTCP cells were seeded with a density of 3 x10^5 cells/well on collagen-coated 24-well plates and differentiated for two days with 2.5% DMSO in DMEM differentiation medium. HBV inoculum was prepared by mixing viral particles (MOI 100, genotype D) with serial dilution of antibodies (0.01-1000 nM) and incubation for 3 hours at 37°C. After incubation, PEG 6000 was added to achieve a final concentration of 4% (v/v). The final solution was mixed carefully and cells were subsequently inoculated. After an incubation of 18 hours, the inoculum was removed, cells were washed three times with PBS and replaced with DMEM differentiation medium. The supernatant was collected at day 4 and 8 for HBeAg measurement. On day 8 post-infection, cells were lysed and collected for cccDNA and total intracellular HBV rcDNA determination.

4.2.2.13 Antibody treatment assay

To evaluate the effect of anti-HBs antibodies on established HBV infection, HepG2 NTCP cells were seeded and differentiated as described in section 4.2.2.10. In addition to HBeAg, HBsAg was determined in the supernatant on day eight post-infection. From day nine to 14, cells were treated with antibodies 4D06 or 4D08 and/or entecavir every 24 hours. For this purpose, the differentiation medium was supplemented with antibodies at a concentration of 100 nM or entecavir (2 nM) and the supernatant was collected for HBeAg and HBsAg determination. On day 14, all cells were lysed and collected for intracellular cccDNA measurements.

4.2.2.14 Testing anti-HBs antibodies in HDV background for neutralization

The following experiment was kindly performed by Wenshi Wang in Heidelberg in Stephan Urban's Lab.

Virus production

HDV enveloped with different genotypes of HBV envelope protein (genotype A-H) was produced by co-transfection of Huh7 cells with pJC126 (HDV genotype 1, kindly provided by John Taylor) and the corresponding plasmids pLX304-HB2.7 gtA-H (8 plasmids encoding HBV genotype A-H envelope proteins, respectively). The cell

culture supernatant containing HDV virus was harvested from day 10 to 13 post transfection.

Infection and neutralization assay

Huh7-NTCP cells were seeded in 96-well plates one day before infection (2.5×10^4 cells/well). On the day of infection, antibodies were serially diluted in DMEM complete medium and mixed with HDV-containing medium. The virus/antibody mixtures were incubated for 60 minutes at 37°C. After incubation, the mixture was 1:2 diluted with DMEM complete containing 8% PEG6000 and used as inoculum for Huh7-NTCP cells. The final concentration of antibodies in the inoculum ranged from 0.01 nM to 1000 nM. One day after infection, the inoculum was removed, the cells were washed with PBS and further cultivated. Medium was changed every three days. At day 6 or 7 post infection, cells were fixed and analyzed by immunofluorescence assay.

Immunofluorescence assay

At the end of the infection experiment, treated cells were fixed in 4% PFA for 30 minutes, followed by 30 minutes incubation in permeabilization buffer (PBS, 0.25% Triton X 100). After 30 minutes incubation in blocking buffer (PBS, 0.05% Tween-20, 3% BSA), cells were incubated for 1 hour with anti-HDAg antibody diluted in blocking buffer. After washing for three times, secondary antibodies goat anti-rabbit IgG Alexa Fluor 555 were added for 1 hour. Finally, the cells were imaged and analyzed by an automated immunofluorescence microscopy.

4.2.3 B-cell Enzyme-Linked ImmunoSpot assay (ELISpot)

To estimate the number of IgG-secreting B cells and HBsAg-specific B cells at a single cell level, a B-cell Enzyme-Linked ImmunoSpot assay (ELISpot) was performed. For this purpose, PBMC were thawed, resuspended in RPMI complete medium and counted. 2×10^6 cells/mL were either incubated with R848 (1µg/mL, Mabtech) and human recombinant IL-2 (10ng/mL, Mabtech) or without for five days in a 6-well plate. On day four, ELISpot plates were activated under sterile conditions according to the manufacturer's instructions and coated with the respective antigen. For total IgG ELISpot, anti-human IgG (15 µg/mL, MabTech) was coated with 100µL/well in PBS. For HBsAg-specific ELISpot, sterile HBsAg (10 µg/mL, Roche,

serum purified) was used. Plates were incubated overnight at 4°C. The next day, the plates were washed five times with sterile PBS and blocked with RPMI complete medium for 2h at room temperature. In the meantime, stimulated PBMCs were carefully resuspended from the 6-well plate and centrifuged (350 xg, 5 minutes). The supernatant was collected for anti-HBs ELISA and cells were counted, after re-suspension in 2 mL RPMI complete. For total IgG ELISpot 2.5 x 10^3 cells/well were transferred to the plate (triplicates), for HBsAg ELISpot 1.0 - 2.0 x 10^5 cells/well were added and incubate for 18 h at 37°C. The further assay was performed according to the manufacturer's instructions using HRP-coupled detection antibodies. Spot quantification was performed with a CTL-ImmunoSpot® S6 Ultra-V Analyzer.

4.2.4 Enzyme-Linked Immunosorbant Assay (ELISA)

4.2.4.1 anti-HBs ELISA

To determine the specificity of monoclonal antibodies for HBsAg and enzyme-linked immunosorbant assay (ELISA) was performed. For this, 96-well MaxiSorb ELISA plates were coated with HBsAg (Roche, serum purified, 1 µg/mL in PBS; 50 µl/well) at 37°C for 30 minutes. Plates were washed five times with ELISA wash and blocked with ELISA blocking solution (200 µL/well) for 1 hour at room temperature, shaking at 300 rpm. After another washing step, antibody-containing samples ((B)-cell culture supernatant (undiluted), supernatant from B-cell ELISpot (undiluted) or purified monoclonal antibodies (1:50 dilution in PBS)) were added and incubated for 2 hours at room temperature, shaking. The detection antibody, polyclonal goat anti-human IgG coupled with HRP (diluted 1:1000 in PBS) was added and incubated for 1 hour at room temperature, shaking, after washing. The assay was developed with the addition of TMB substrate and the reaction was stopped with 2N H_2SO_4. Conversion of the substrate was determined by measurement of OD_{450nm} subtracted by OD_{560nm} on an ELISA Reader infinite F200.

4.2.4.2 IgG ELISA

To determine human IgG secreted from B cells or antibody transfected cells, an IgG ELISA was performed. For this 96-well MaxiSorb ELISA plates were coated with polyclonal goat anti-human IgG (H+L) (diluted 1:500 in PBS) for 30 minutes at 37°C.

The further experiment was carried out in the same way, as described in section 4.2.4.1 (anti-HBs ELISA).

4.2.4.3 Protein G-anti-HBs ELISA

Protein G-anti-HBs ELISA was performed to determine HBsAg-specific monoclonal antibodies in the supernatant of transfected cells. Here, pre-coated protein G plates were activated upon rinsing each well three times with ELISA wash. After that, antibody-containing supernatant was added in a volume of 100 µL/well and followed by incubation for 1 hour at room temperature. Antibodies were captured with Protein G via their Fc region. Then, the plates were washed four times with ELISA wash, to remove free antibodies, before HBsAg-biotin (1:200 in PBS; 100 µl/well) was added and incubated for one hour at 37°C. For detection, Avidin-HRP (1:500 in PBS, 100 µL/well) was incubated for an additional hour at 37°C, after washing. The ELISA was developed, upon addition of TMB substrate. The reaction was stopped with 2N H_2SO_4 after substrate conversion and analyzed with an ELISA reader infinite F200 by measuring OD_{450nm} subtracted by OD_{560nm}.

4.2.4.4 Epitope peptide ELISA

To localized the epitope of 4D06 and 4D08 on HBV envelope protein, an epitope peptide ELISA was performed. Here, 10 µM of each 18mer peptide (see section 4.1.11) was immobilized on a 96-well MaxiSorb ELISA plate in carbonate buffer in a volume of 100 µL/well overnight at 4°C. The plate was blocked with ELISA blocking buffer for two hours at room temperature, after washing with ELISA wash for four times. Antibodies 4D06, 4D08 and HB-1 were added (1 µg/ml in PBS) and incubated for two hours at room temperature. The plate was washed for four times with ELISA wash, before polyclonal goat anti-human IgG or goat anti-mouse IgG conjugated with HRP (1:1000 in PBS) was incubated for 1 hour at room temperature. Finally, the plate was washed again and TMB substrate was added for development. The reaction was stopped after substrate conversion with 2N H_2SO_4. Substrate conversion was determined as described before.

4.2.4.5 Antibody affinity determination (EC_{50}) with ELISA

In order to estimate the antibody affinity the anti-HBs ELISA was performed, with minor changes regarding sample preparation and development: Purified monoclonal

antibodies were used as samples serially diluted from 10,000 nM to 0.03 nM in PBS in triplicates. Antibody dilutions were incubated for one hour at room temperature. Assay development was stopped exactly 1 minute after adding TMB substrate. EC_{50} values were calculated with non-linear regression using Graph Pad Prism 8.0.

4.2.4.6 Murex ELISA for HBsAg genotype reactivity

To determine whether 4D06 and 4D08 recognize HBsAg from various HBV geno- and subtypes the Murex ELISA was performed. For this, the Murex HBsAg Version 3 Kit was used with some modifications: First, the number of wells required for the test were activated by addition of 25 µL/well assay diluent. Next, 5 IU/well HBsAg from each HBV genotype (PEI HBsAg reference panel) as well as controls were added and incubated for 1 hour at 37°C (75 µL/well). After incubation of 25 µL/well of biotinylated primary antibodies (4D06-biotin or 4D08-biotin, 0.5µg/ml in PBS) for 30 minutes at 37°C, 25 µL/well Avidin-HRP (1:500 in PBS) was added and further incubated for 30 minutes at 37°C. Only now, all wells were washed for four times with ELISA wash, before 100 µL/well TMB substrate was added and incubated for 15 minute at 37°C for assay development. The reaction was stopped by adding 50 µL/well 2N H_2SO_4 and substrate conversion was analyzed by measuring OD_{450nm} subtracted from OD_{560nm} with an ELISA reader infinite F200.

4.2.4.7 HBV parameters

In order to determine the success of infection and viremia *in vitro*, HBeAg as well as HBsAg in the cell culture supernatant were determined. This was done with Enzygnost HBeAg Kit on the BEP III platform or with quantitative HBsAg test on the ARCHITECT™ platform.

4.2.5 Identification of antigen-specific cells with HBV-baits and flow cytometry (FACS)

4.2.5.1 Alexa647-SVP B-cell staining

Up to 3.0 x 10^5 overnight rested pre-enriched B cells were transferred to a 96-well V-bottom plate and washed once with FACS buffer (350 xg, 5 min, 4°C) before the first staining step. Cells were stained with different dilutions of Alexa647-SVPs (1:2000 -1:16,000) in a volume of 50 µL/well in FACS buffer. After incubation on ice

for 30 minutes in the dark, cell were washed two times with FACS buffer. For the blocking control, B cells were first stained with non-labeled SVPs (1:4) on ice for 30 minutes and then with Alexa647-SVPs (1:8000) on ice for 30 minutes in the dark. Subsequently, the cells were stained for surface markers with the respective antibodies, IgG-PE-Cy7 and CD19-eF450, diluted in live/dead™ fixable Near-IR dead cell stain (1:1000) and FACS buffer in a volume of 50 µL/well. Cells were washed three times after an incubation of 30 minutes in the dark, on ice. Finally the cells were resuspended in 200 µl FACS buffer and analyzed on a FACS Canto II or a Cytoflex S flow cytometer. Data analysis was performed with FlowJo.

4.2.5.2 HBsAg-Alexa594 B-cell staining

Pre-enriched, rested B cells were transferred to a 96-well V-bottom plate with a density of up to 3.0 x 10^5 cells/well. Cells were washed once with FACS buffer (350 xg, 5 min, 4°C) and incubated with different concentrations of HBsAg-Alexa594 (0.63 µg/mL - 5 µg/ml) for 30 minutes on ice, in the dark, in a volume of 50 µL/well. After two washing steps, surface markers were stained with the respective antibodies (CD19-eF450 and IgG-PE-Cy7) in a volume of 50 µL/well in live/dead™ fixable Aqua dead cell stain (1:1000) and FACS buffer. After an incubation of 30 minutes on ice, in the dark cells were washed three times with FACS buffer and finally resuspended in 200 µL buffer for acquisition. B cells were analyzed on a Cytoflex S flow cytometer and data analysis was performed with FlowJo.

4.2.5.3 B-cell staining with HBsAg-biotin

Overnight rested B cells were transferred to a 96-well V-bottom plate for staining with a density of up to 3.0 x 10^5 cells/well and washed once with FACS buffer (350 xg, 5 min, 4°C). HBsAg-biotin was added in serial dilution (1:25 - 1:200) in a volume of 50 µl/well in FACS buffer. For the fluorescence minus one (FMO) control, one well did not receive HBsAg. After an incubation for 30 minutes on ice, in the dark, two washing steps with FACS buffer followed. Then, cells were stained with surface marker-specific antibodies (CD19-eF450 and IgG-PE-Cy7), Streptavidin-APC, Streptavidin-PE or Steptavidin-Alexa647 in live/dead fixable™ Aqua dead cell stain (1:1000) in FACS buffer. Cells were incubated for 30 minutes on ice in the dark. Before acquisition on a Cytoflex S flow cytometer, cells were washed three times

with FACS buffer and resuspended in 200 µL buffer. Data analysis was performed with FlowJo.

4.2.6 Isolation of B cells with FACS sorting

4.2.6.1 Cell sorting of antigen-specific memory B cells

To isolated HBsAg-specific memory B cells, 2.5 x 10^6 pre-enriched B cells were transferred to a 96-well V-bottom plate. For controls, only up to 2.0 x 10^5 B cells were used. B cells were washed once with FACS buffer (350 xg, 5 min, 4°C) and human Fc Block (0.5 µg/well) diluted in FACS buffer was incubated for 10 minutes at room temperature. Subsequently, the HBV-bait was added with the respective concentration (Alexa647-SVP 1:8000, HBsAg-Alexa594 1.25 µg/mL or HBsAg-biotin 1:25) and incubated for 30 minutes in the dark, on ice. Cells were washed two times with FACS buffer, before incubation with antibodies for surface and live/dead staining (CD19-eF450; IgG-PE-Cy7; Streptavidin-APC). After incubation for 30 minutes in the dark on ice, B cells were washed three times and finally resuspended in 1 mL FACS buffer. Before acquisition, cells were filtered through sterile filcons in order to obtain single cell suspension. Cells were analyzed, cell duplets were excluded and antigen-specific B cells were isolated either as bulk population or as individual cells with MoFlo Astrios or MoFloII cell sorter. Data was analyzed with FlowJo.

For B-cell cultures, cells were deposited in cold RPMI complete medium under aseptic conditions. Single B cells were directly sorted into a 96-well cell culture plates containing 100 µL/well medium. Cells sorted as a bulk were collected in falcon tubes and afterwards seeded in 96-well plates with an appropriate density ranging from 50 to 400 cells/well. B cells that were single sorted for subsequent immunoglobulin gene amplification were deposited in 96-well PCR plates containing 4µL/well ice-cold lysis buffer. After sorting, plates were sealed, immediately frozen on dry ice and stored at -80°C until used.

4.2.6.2 CD19+ B cell sorting for B-cell culture

Overnight rested PBMC were transferred to a 96-well V-bottom plate and washed once with FACS buffer. Subsequently, PBMC were stained with CD19-eF450, CD3-PE and live/dead fixable Near-IR dead cell dye (1:1000) for 30 minutes in the

dark, on ice. After two washing steps with FACS buffer, PBMC were resuspended in 1 mL buffer and filtered through sterile filcons in order to achieve a single cell suspension. Finally, CD19+ B cells were bulk sorted on BD FACS Aria cell sorted into falcon tubes containing cold RPMI complete medium. Data was analyzed with FlowJo.

4.2.7 Antibody production and purification

4.2.7.1 Antibody production

For antibody production, HEK 293 cells were seeded in T_{150} cell culture flasks to obtain 80% confluency at the day of transfection. 1 ml OptiMEM was mixed with 25 µg of antibody heavy chain plasmid DNA and 25 µg corresponding light chain plasmid DNA. After adding 150 µL Fugene® HD transfection reagent the solution was incubated for 10 minutes at room temperature. Meanwhile, 25 mL fresh DMEM complete medium was added to the cells. After the transfection solution was added carefully, cells were incubated for in total 9 days. Every three days the antibody containing supernatant was collected, filtered though 0.45 µm sterile filter and stored at 4°C. At the end of culture, cells were discarded and the collected supernatant was analyzed for antibody concentration with ELISA (IgG and anti-HBs).

4.2.7.2 Antibody purification and concentration determination

After confirming the presence of monoclonal antibodies in collected cell culture supernatant, mAb were purified with protein G column affinity chromatography. The purification procedure was carried out with a peristaltic pump and a protein G column connected to a 1.6 mm tube. All reagents were brought to room temperature first, before the column wash washed with 5 column volumes (CVs) water and 5 CVs binding buffer at a flow rate of 1 mL/minute. After column equilibration, the antibody-containing supernatant was loaded with a flow rate of 1.5 mL/minute. Next, the column was washed with 10 CV of binding buffer. Before elution, Protein loBind reaction tubes were prepared with 75 µL/tube of neutralization buffer. Antibodies were eluted with a flow rate of 1 mL/minute and 12 CVs, in 1mL fractions. Following elution, the column was re-equilibrated with 10 CVs binding buffer and stored in 20% ethanol at 4°C. Flow through (FL) and elution fractions (EL) were stored at 4°C until further processing.

After purification, all fractions were examined with anti-HBs ELISA. Antibody-containing fractions were pooled and concentrated with Amicon Ultra centrifugal filters to obtain reasonable working concentrations. For this, Amicon filters were wetted with 1X PBS via centrifugation at 3,200 xg for 2 minutes at room temperature. Pooled antibody-containing fractions were added and concentrated to a final volume of 1 mL by centrifugation at 3,200 xg for 20 minutes at room temperature. Protein concentration was followed by buffer exchange. Here, PBS was added twice to the concentrate and Amicon filters were centrifuged until 1 mL antibody solution remained. Sample recovery was achieved according to manufacturer's instructions.

To finally determine the antibody concentration a Bradford assay was performed in 96-well plate format. Concentrated antibodies were diluted 1:2 to 1:20 in PBS. For quantification, bovine gamma globulin protein standard was prepared in serial 1:2 dilutions from 2 mg/mL to 0 mg/mL. The assay was carried out according to the manufacturer's protocol and protein concentration was determined by measuring absorbance at 595 nm with Tecan reader infinite F 200. Antibody concentration was calculated with linear regression.

4.2.8 Immunofluorescence staining

In order to determine the antibody specificity for HBsAg of different HBV genotypes an immunofluorescence staining was performed. For this, Huh7 cells seeded on cover slips in 24-well plates were transiently transfected with plasmids (pRVHBV1.5; pZDonor_N3825_C1:1.5; pZDonor_N4214_B:1.5; pRR_wtHBV_1.3) encoding HBV genotypes A, B, C and D. 72 hours after transfection, the supernatant was collected for HBeAg measurement to evaluated HBV expression. Subsequently, cells were fixed with 4% PFA for 10 minutes at room temperature. Next, cells were washed once with PBS and permeabilzed with 0.5% (v/v) saponin in PBS for 10 minutes at room temperature. After blocking for two hours at room temperature in PBS supplemented with 0.1% saponin and 10% goat serum, primary antibodies 4D06 or 4D08 (1:400 in blocking solution) were incubated overnight at 4°C. The next day, cells were washed three times for 10 minutes in PBS plus 0.1% saponin, before the secondary antibodies, goat anti-human IgG Alexa Fluor647 (1:1000) were incubated

for two hours at room temperature in the dark in PBS with 0.1% saponin, 2% goat serum. Three washing steps with PBS plus 0.1% saponin were followed by one time washing with PBS, before cover slips were mounted with Dapi-mounting solution on microscopic slides. Finally, slides were analyzed with a confocal microscope.

4.2.9 Assessment of IgG-dependent activation of FcγRs

The assay used for testing IgG-dependent activation of FcγRs has been previously described by (Corrales-Aguilar et al., 2013) and was kindly performed by Valeria Falcone. It is based on co-cultivation of viral antigen with BW5147 mouse reporter cells stably expressing FcγR-ζ chain receptor, which stimulate IL-2 production in the presence of IgG that is able to activate FcγRs upon antigen-opsonization.

Briefly, 4-fold serial dilutions of human anti-HBs mAbs 4D06 and 4D08 were incubated with surface-immobilized HBsAg for 30 minutes at 37°C in an atmosphere of 5% CO_2. As negative and positive controls, anti-HBs negative human serum and commercially available hepatitis B virus immunoglobulins (HBIg; Kedrion Biopharma) were used, respectively. To remove unbound IgG, the plates were washed three times with DMEM containing 10% FCS before addition of BW:FcγRIII-ζ reporter cells for 16h at 37°C in a 5% CO_2 atmosphere. To release intracellular IL-2, BW:FcγRIII-ζ reporter cells were thoroughly resuspended with 100 µl/well of ELISA sample buffer (PBS with 10% FCS and 0,1% Tween-20). Mouse IL-2 was released in the supernatant and was measured by ELISA using the capture antibody JES6-1A12 (1:500 in sample buffer) and the biotinylated detection antibody JES6-5H4 (1:500 in sample buffer). Streptavidin-HRP (1:1000 in sample buffer) was added and incubated for 30 minutes at room temperature. Subsequently, the plates were washed with sample buffer (PBS 10% FCS/ 0,1% Tween-20) before addition of TMB substrate. The reaction was stopped with 1 M H_2SO_4 and the absorbance was measured at 450 nm.

4.2.10 NK-cell activation assay

To investigate the FcγR-dependent NK-cell activation potential of mAbs 4D06 and 4D08, PBMC were incubated in the presence of both antibodies and target antigen. One day prior analysis, a 96-well F-plate was coated with HBsAg purified from human serum (2.5 µg/mL in PBS, 100 µL/well) overnight at 37°C or HBV-infected

HepG2 cells were seeded in a 96-well plate with a density of 4.0 x 10^4 cells/well. The following day, the respective plate was washed three times with PBS and mAbs (100 nM, 100 µL/well) were incubated for 2 hours at 4°C. Next, the plate was washed again and overnight rested PBMC containing NK effector cells were added with a density of 1.0-2.0 x 10^5 cells/well and incubated for 6 hours at 37°C. After one hour, Brefeldin A (BFA, 1:1000) was added to block the secretion of cytokines and chemokines.

For NK-cell activation analysis, PBMCs were carefully resuspended and transferred to a 96-well V-bottom plate. Cells were washed once with cold FACS buffer by centrifugation (350 xg, 5 minutes, 4°C), before staining with surface markers (CD3, CD56, CD16) and live/dead fixable™ Near-IR dead cell stain (1:1000) for 30 minutes on ice in the dark in a total volume of 50 µl/well. Cells were washed two times with FACS buffer, before cytofix/cytoperm solution (100 µL/well) was added and incubated for 20 minutes on ice in the dark. Following two washing steps with perm/wash buffer, antibodies for intracellular cytokine staining (IFNg and Mip1b) were incubated for 30 minutes in perm/wash buffer on ice in the dark. Thereafter, cells were washed two times with perm/wash and were finally, resuspended in 200 µL/well FACS buffer. Analysis was performed with a Cytoflex S cytometer and with FlowJo.

List of figures

List of tables

Bibliography

Al-Mahtab, M., Akbar, S. M., Aguilar, J. C., Uddin, M. H., Khan, M. S., & Rahman, S. (2013). Therapeutic potential of a combined hepatitis B virus surface and core antigen vaccine in patients with chronic hepatitis B. *Hepatol Int, 7*(4), 981-989. doi:10.1007/s12072-013-9486-4

An, P., Xu, J., Yu, Y., & Winkler, C. A. (2018). Host and Viral Genetic Variation in HBV-Related Hepatocellular Carcinoma. *Front Genet, 9*, 261. doi:10.3389/fgene.2018.00261

Armitage, R. J., Fanslow, W. C., Strockbine, L., Sato, T. A., Clifford, K. N., Macduff, B. M., . . . et al. (1992). Molecular and biological characterization of a murine ligand for CD40. *Nature, 357*(6373), 80-82. doi:10.1038/357080a0

Arpin, C., Dechanet, J., Van Kooten, C., Merville, P., Grouard, G., Briere, F., . . . Liu, Y. J. (1995). Generation of memory B cells and plasma cells in vitro. *Science, 268*(5211), 720-722. doi:10.1126/science.7537388

Babcook, J. S., Leslie, K. B., Olsen, O. A., Salmon, R. A., & Schrader, J. W. (1996). A novel strategy for generating monoclonal antibodies from single, isolated lymphocytes producing antibodies of defined specificities. *Proc Natl Acad Sci U S A, 93*(15), 7843-7848. doi:10.1073/pnas.93.15.7843

Backes, S., Jager, C., Dembek, C. J., Kosinska, A. D., Bauer, T., Stephan, A. S., . . . Protzer, U. (2016). Protein-prime/modified vaccinia virus Ankara vector-boost vaccination overcomes tolerance in high-antigenemic HBV-transgenic mice. *Vaccine, 34*(7), 923-932. doi:10.1016/j.vaccine.2015.12.060

Balsitis, S., Gali, V., Mason, P. J., Chaniewski, S., Levine, S. M., Wichroski, M. J., . . . Tenney, D. J. (2018). Safety and efficacy of anti-PD-L1 therapy in the woodchuck model of HBV infection. *PLoS One, 13*(2), e0190058. doi:10.1371/journal.pone.0190058

Banchereau, J., de Paoli, P., Valle, A., Garcia, E., & Rousset, F. (1991). Long-term human B cell lines dependent on interleukin-4 and antibody to CD40. *Science, 251*(4989), 70-72. doi:10.1126/science.1702555

Beasley, R. P., Hwang, L. Y., Stevens, C. E., Lin, C. C., Hsieh, F. J., Wang, K. Y., . . . Szmuness, W. (1983). Efficacy of hepatitis B immune globulin for prevention of perinatal transmission of the hepatitis B virus carrier state: final report of a randomized double-blind, placebo-controlled trial. *Hepatology, 3*(2), 135-141.

Beccari, M. V., Mogle, B. T., Sidman, E. F., Mastro, K. A., Asiago-Reddy, E., & Kufel, W. D. (2019). Ibalizumab, a Novel Monoclonal Antibody for the Management of Multidrug-Resistant HIV-1 Infection. *Antimicrob Agents Chemother, 63*(6). doi:10.1128/AAC.00110-19

Behring, E. v., Kitasato, S. . (1890). Ueber das Zustande kommen der Diphtherie-Immunität und der Tetanus-Immunität bei Thieren. *Deutsche Medizinische Wochenschrift, 49*. doi:https://doi.org/10.17192/eb2013.0164

Bengsch, B., Martin, B., & Thimme, R. (2014). Restoration of HBV-specific CD8+ T cell function by PD-1 blockade in inactive carrier patients is linked to T cell differentiation. *J Hepatol, 61*(6), 1212-1219. doi:10.1016/j.jhep.2014.07.005

Bertoletti, A., & Le Bert, N. (2018). Immunotherapy for Chronic Hepatitis B Virus Infection. *Gut Liver, 12*(5), 497-507. doi:10.5009/gnl17233

Biron, C. A. (2016). Chapter 4 - Innate Immunity: Recognizing and Responding to Foreign Invaders—No Training Needed. In M. G. Katze, M. J. Korth, G. L. Law, & N. Nathanson (Eds.), *Viral Pathogenesis (Third Edition)* (pp. 41-55). Boston: Academic Press.

Blumberg, R. S., Koss, T., Story, C. M., Barisani, D., Polischuk, J., Lipin, A., . . . Simister, N. E. (1995). A major histocompatibility complex class I-related Fc receptor for IgG on rat hepatocytes. *J Clin Invest, 95*(5), 2397-2402. doi:10.1172/JCI117934

Bohne, F., Chmielewski, M., Ebert, G., Wiegmann, K., Kurschner, T., Schulze, A., . . . Protzer, U. (2008). T cells redirected against hepatitis B virus surface proteins eliminate infected hepatocytes. *Gastroenterology, 134*(1), 239-247. doi:10.1053/j.gastro.2007.11.002

Bohne, F., Hasreiter, J., Quitt, O., Bruss, V., Moldenhauer, G., Momburg, F., & Protzer, U. (2015). Bispecific antibody constructs mediate immunotherapeutic retargeting of effector cells towards HBV infected target cells. *Z Gastroenterol, 53*(01), A5_10. doi:10.1055/s-0034-1397214

Boni, C., Fisicaro, P., Valdatta, C., Amadei, B., Di Vincenzo, P., Giuberti, T., . . . Ferrari, C. (2007). Characterization of hepatitis B virus (HBV)-specific T-cell dysfunction in chronic HBV infection. *J Virol, 81*(8), 4215-4225. doi:10.1128/JVI.02844-06

Borrie, A. E., & Maleki Vareki, S. (2018). Chapter Five - T Lymphocyte–Based Cancer Immunotherapeutics. In L. Galluzzi & N.-P. Rudqvist (Eds.), *International Review of Cell and Molecular Biology* (Vol. 341, pp. 201-276): Academic Press.

Bournazos, S., Wang, T. T., Dahan, R., Maamary, J., & Ravetch, J. V. (2017). Signaling by Antibodies: Recent Progress. *Annual Review of Immunology, 35*(1), 285-311. doi:10.1146/annurev-immunol-051116-052433

Brady, B. L., Steinel, N. C., & Bassing, C. H. (2010). Antigen receptor allelic exclusion: an update and reappraisal. *J Immunol, 185*(7), 3801-3808. doi:10.4049/jimmunol.1001158

Bremer, C. M., Sominskaya, I., Skrastina, D., Pumpens, P., El Wahed, A. A., Beutling, U., . . . Glebe, D. (2011). N-terminal myristoylation-dependent masking of neutralizing epitopes in the preS1 attachment site of hepatitis B virus. *J Hepatol, 55*(1), 29-37. doi:10.1016/j.jhep.2010.10.019

Bruhns, P. (2012). Properties of mouse and human IgG receptors and their contribution to disease models. *Blood, 119*(24), 5640-5649. doi:10.1182/blood-2012-01-380121

Bruss, V. (2004). Envelopment of the hepatitis B virus nucleocapsid. *Virus Res, 106*(2), 199-209. doi:10.1016/j.virusres.2004.08.016

Burton, A. R., Pallett, L. J., McCoy, L. E., Suveizdyte, K., Amin, O. E., Swadling, L., . . . Maini, M. K. (2018). Circulating and intrahepatic antiviral B cells are defective in hepatitis B. *J Clin Invest, 128*(10), 4588-4603. doi:10.1172/JCI121960

Calderaro, J., Rousseau, B., Amaddeo, G., Mercey, M., Charpy, C., Costentin, C., . . . Pawlotsky, J. M. (2016). Programmed death ligand 1 expression in hepatocellular carcinoma: Relationship With clinical and pathological features. *Hepatology, 64*(6), 2038-2046. doi:10.1002/hep.28710

Cao, J., Zhang, J., Lu, Y., Luo, S., Zhang, J., & Zhu, P. (2019). Cryo-EM structure of native spherical subviral particles isolated from HBV carriers. *Virus Res, 259*, 90-96. doi:10.1016/j.virusres.2018.10.015

Caskey, M., Klein, F., & Nussenzweig, M. C. (2019). Broadly neutralizing anti-HIV-1 monoclonal antibodies in the clinic. *Nature Medicine, 25*(4), 547-553. doi:10.1038/s41591-019-0412-8

Cerino, A., Bremer, C. M., Glebe, D., & Mondelli, M. U. (2015). A Human Monoclonal Antibody against Hepatitis B Surface Antigen with Potent Neutralizing Activity. *PLoS One, 10*(4), e0125704. doi:10.1371/journal.pone.0125704

Cerino, A., Mantovani, S., Mele, D., Oliviero, B., Varchetta, S., & Mondelli, M. U. (2019). Human Monoclonal Antibodies as Adjuvant Treatment of Chronic Hepatitis B Virus Infection. *Front Immunol, 10*, 2290. doi:10.3389/fimmu.2019.02290

Chaudhary, N., & Wesemann, D. R. (2018). Analyzing Immunoglobulin Repertoires. *Front Immunol, 9*, 462. doi:10.3389/fimmu.2018.00462

Cheever, M. A., & Higano, C. S. (2011). PROVENGE (Sipuleucel-T) in prostate cancer: the first FDA-approved therapeutic cancer vaccine. *Clin Cancer Res, 17*(11), 3520-3526. doi:10.1158/1078-0432.CCR-10-3126

Chisari, F. V., Isogawa, M., & Wieland, S. F. (2010). Pathogenesis of hepatitis B virus infection. *Pathol Biol (Paris), 58*(4), 258-266. doi:10.1016/j.patbio.2009.11.001

Clark, E. A., & Ledbetter, J. A. (1986). Activation of human B cells mediated through two distinct cell surface differentiation antigens, Bp35 and Bp50. *Proc Natl Acad Sci U S A, 83*(12), 4494-4498. doi:10.1073/pnas.83.12.4494

Cornberg, M., Protzer, U., Petersen, J., Wedemeyer, H., Berg, T., Jilg, W., . . . Awmf. (2011). [Prophylaxis, diagnosis and therapy of hepatitis B virus infection - the German guideline]. *Z Gastroenterol, 49*(7), 871-930. doi:10.1055/s-0031-1273462

Corrales-Aguilar, E., Trilling, M., Reinhard, H., Merce-Maldonado, E., Widera, M., Schaal, H., . . . Hengel, H. (2013). A novel assay for detecting virus-specific antibodies triggering activation of Fcgamma receptors. *J Immunol Methods, 387*(1-2), 21-35. doi:10.1016/j.jim.2012.09.006

Corti, D., Benigni, F., & Shouval, D. (2018). Viral envelope-specific antibodies in chronic hepatitis B virus infection. *Curr Opin Virol, 30*, 48-57. doi:10.1016/j.coviro.2018.04.002

Cox, K. S., Tang, A., Chen, Z., Horton, M. S., Yan, H., Wang, X. M., . . . Vora, K. A. (2016). Rapid isolation of dengue-neutralizing antibodies from single cell-sorted human antigen-specific memory B-cell cultures. *MAbs, 8*(1), 129-140. doi:10.1080/19420862.2015.1109757

Crotty, S., Aubert, R. D., Glidewell, J., & Ahmed, R. (2004). Tracking human antigen-specific memory B cells: a sensitive and generalized ELISPOT system. *J Immunol Methods, 286*(1-2), 111-122. doi:10.1016/j.jim.2003.12.015

Dane, D. S., Cameron, C. H., & Briggs, M. (1970). Virus-like particles in serum of patients with Australia-antigen-associated hepatitis. *Lancet, 1*(7649), 695-698. Retrieved from http://www.ncbi.nlm.nih.gov/pubmed/4190997

Das, A., Ellis, G., Pallant, C., Lopes, A. R., Khanna, P., Peppa, D., . . . Maini, M. K. (2012). IL-10-producing regulatory B cells in the pathogenesis of chronic hepatitis B virus infection. *J Immunol, 189*(8), 3925-3935. doi:10.4049/jimmunol.1103139

Dembek, C., Protzer, U., & Roggendorf, M. (2018). Overcoming immune tolerance in chronic hepatitis B by therapeutic vaccination. *Curr Opin Virol, 30*, 58-67. doi:10.1016/j.coviro.2018.04.003

El Dika, I., Khalil, D. N., & Abou-Alfa, G. K. (2019). Immune checkpoint inhibitors for hepatocellular carcinoma. *Cancer, 125*(19), 3312-3319. doi:10.1002/cncr.32076

European Association for the Study of the Liver. Electronic address, e. e. e., & European Association for the Study of the, L. (2017). EASL 2017 Clinical Practice Guidelines on the management of hepatitis B virus infection. *J Hepatol, 67*(2), 370-398. doi:10.1016/j.jhep.2017.03.021

Fanning, G. C., Zoulim, F., Hou, J., & Bertoletti, A. (2019). Therapeutic strategies for hepatitis B virus infection: towards a cure. *Nat Rev Drug Discov, 18*(11), 827-844. doi:10.1038/s41573-019-0037-0

Ferrari, C. (2015). HBV and the immune response. *Liver International, 35*(s1), 121-128. doi:10.1111/liv.12749

Ferrari, C. (2015). HBV and the immune response. *Liver Int, 35 Suppl 1*, 121-128. doi:10.1111/liv.12749

Fisicaro, P., Rossi, M., Vecchi, A., Acerbi, G., Barili, V., Laccabue, D., . . . Boni, C. (2019). The Good and the Bad of Natural Killer Cells in Virus Control: Perspective for Anti-HBV Therapy. *Int J Mol Sci, 20*(20). doi:10.3390/ijms20205080

Franz, B., May, K. F., Jr., Dranoff, G., & Wucherpfennig, K. (2011). Ex vivo characterization and isolation of rare memory B cells with antigen tetramers. *Blood, 118*(2), 348-357. doi:10.1182/blood-2011-03-341917

Gaebler, C., Gruell, H., Velinzon, K., Scheid, J. F., Nussenzweig, M. C., & Klein, F. (2013). Isolation of HIV-1-reactive antibodies using cell surface-expressed gp160Deltac(BaL.). *J Immunol Methods, 397*(1-2), 47-54. doi:10.1016/j.jim.2013.09.003

Galson, J. D., Truck, J., Clutterbuck, E. A., Fowler, A., Cerundolo, V., Pollard, A. J., . . . Kelly, D. F. (2016). B-cell repertoire dynamics after sequential hepatitis B vaccination and evidence for cross-reactive B-cell activation. *Genome Med, 8*(1), 68. doi:10.1186/s13073-016-0322-z

Galson, J. D., Truck, J., Fowler, A., Clutterbuck, E. A., Munz, M., Cerundolo, V., . . . Kelly, D. F. (2015). Analysis of B Cell Repertoire Dynamics Following Hepatitis B Vaccination in Humans, and Enrichment of Vaccine-specific Antibody Sequences. *EBioMedicine, 2*(12), 2070-2079. doi:10.1016/j.ebiom.2015.11.034

Galun, E., Eren, R., Safadi, R., Ashour, Y., Terrault, N., Keeffe, E. B., . . . Dagan, S. (2002). Clinical evaluation (phase I) of a combination of two human monoclonal antibodies to HBV: safety and antiviral properties. *Hepatology, 35*(3), 673-679. doi:10.1053/jhep.2002.31867

Gane, E., Gaggar, A., Nguyen, A. H., Subramanian, G. M., McHutchison, J. G., Schwabe, C., & Dunbar, R. (2017). A phase1 study evaluating anti-PD-1 treatment with or without GS-4774 in HBeAg negative chronic hepatitis B patients. *Journal of Hepatology, 66*(1), S26-S27. doi:10.1016/S0168-8278(17)30315-X

Gao, Y., Zhang, T. Y., Yuan, Q., & Xia, N. S. (2017). Antibody-mediated immunotherapy against chronic hepatitis B virus infection. *Hum Vaccin Immunother, 13*(8), 1768-1773. doi:10.1080/21645515.2017.1319021

Gehring, A. J., Xue, S. A., Ho, Z. Z., Teoh, D., Ruedl, C., Chia, A., . . . Bertoletti, A. (2011). Engineering virus-specific T cells that target HBV infected hepatocytes and hepatocellular carcinoma cell lines. *J Hepatol, 55*(1), 103-110. doi:10.1016/j.jhep.2010.10.025

Georgiou, G., Ippolito, G. C., Beausang, J., Busse, C. E., Wardemann, H., & Quake, S. R. (2014). The promise and challenge of high-throughput sequencing of the antibody repertoire. *Nat Biotechnol, 32*(2), 158-168. doi:10.1038/nbt.2782

Golsaz Shirazi, F., Mohammadi, H., Amiri, M. M., Singethan, K., Xia, Y., Bayat, A. A., . . . Shokri, F. (2014). Monoclonal antibodies to various epitopes of hepatitis B surface antigen inhibit hepatitis B virus infection. *J Gastroenterol Hepatol, 29*(5), 1083-1091. doi:10.1111/jgh.12483

Golsaz-Shirazi, F., Amiri, M. M., Farid, S., Bahadori, M., Bohne, F., Altstetter, S., . . . Shokri, F. (2017). Construction of a hepatitis B virus neutralizing chimeric monoclonal antibody recognizing escape mutants of the viral surface antigen (HBsAg). *Antiviral Res, 144*, 153-163. doi:10.1016/j.antiviral.2017.06.013

Guidotti, L. G., & Chisari, F. V. (2006). Immunobiology and pathogenesis of viral hepatitis. *Annu Rev Pathol, 1*, 23-61. doi:10.1146/annurev.pathol.1.110304.100230

Guidotti, L. G., Rochford, R., Chung, J., Shapiro, M., Purcell, R., & Chisari, F. V. (1999). Viral clearance without destruction of infected cells during acute HBV infection. *Science, 284*(5415), 825-829. doi:10.1126/science.284.5415.825

Hay, K. A. (2018). Cytokine release syndrome and neurotoxicity after CD19 chimeric antigen receptor-modified (CAR-) T cell therapy. *Br J Haematol, 183*(3), 364-374. doi:10.1111/bjh.15644

Heimes, A. S., & Schmidt, M. (2019). Atezolizumab for the treatment of triple-negative breast cancer. *Expert Opin Investig Drugs, 28*(1), 1-5. doi:10.1080/13543784.2019.1552255

Hoa, P. T., Huy, N. T., Thu le, T., Nga, C. N., Nakao, K., Eguchi, K., . . . Hirayama, K. (2009). Randomized controlled study investigating viral suppression and serological response following pre-S1/pre-S2/S vaccine therapy combined with lamivudine treatment in HBeAg-positive patients with chronic hepatitis B. *Antimicrob Agents Chemother, 53*(12), 5134-5140. doi:10.1128/AAC.00276-09

Hwang, J. R., & Park, S. G. (2018). Mouse models for hepatitis B virus research. *Lab Anim Res, 34*(3), 85-91. doi:10.5625/lar.2018.34.3.85

Jahnmatz, M., Kesa, G., Netterlid, E., Buisman, A. M., Thorstensson, R., & Ahlborg, N. (2013). Optimization of a human IgG B-cell ELISpot assay for the analysis of vaccine-induced B-cell responses. *J Immunol Methods, 391*(1-2), 50-59. doi:10.1016/j.jim.2013.02.009

Jiang, B., Himmelsbach, K., Ren, H., Boller, K., & Hildt, E. (2015). Subviral Hepatitis B Virus Filaments, like Infectious Viral Particles, Are Released via Multivesicular Bodies. *J Virol, 90*(7), 3330-3341. doi:10.1128/JVI.03109-15

Jung, J. K., Arora, P., Pagano, J. S., & Jang, K. L. (2007). Expression of DNA methyltransferase 1 is activated by hepatitis B virus X protein via a regulatory circuit involving the p16INK4a-cyclin D1-CDK 4/6-pRb-E2F1 pathway. *Cancer Res, 67*(12), 5771-5778. doi:10.1158/0008-5472.CAN-07-0529

Kah, J., Koh, S., Volz, T., Ceccarello, E., Allweiss, L., Lutgehetmann, M., . . . Dandri, M. (2017). Lymphocytes transiently expressing virus-specific T cell receptors reduce hepatitis B virus infection. *J Clin Invest, 127*(8), 3177-3188. doi:10.1172/JCI93024

Kaluza, B., Betzl, G., Shao, H., Diamantstein, T., & Weidle, U. H. (1992). A general method for chimerization of monoclonal antibodies by inverse polymerase chain reaction which conserves authentic N-terminal sequences. *Gene, 122*(2), 321-328. doi:10.1016/0378-1119(92)90221-a

Kang, C., Xia, L., Chen, Y., Zhang, T., Wang, Y., Zhou, B., . . . Xia, N. (2018). A novel therapeutic anti-HBV antibody with increased binding to human FcRn improves in vivo PK in mice and monkeys. *Protein Cell, 9*(1), 130-134. doi:10.1007/s13238-017-0438-y

Kim, G. A., Lim, Y. S., An, J., Lee, D., Shim, J. H., Kim, K. M., . . . Suh, D. J. (2014). HBsAg seroclearance after nucleoside analogue therapy in patients with chronic

hepatitis B: clinical outcomes and durability. *Gut, 63*(8), 1325-1332. doi:10.1136/gutjnl-2013-305517

Klein, F., Gaebler, C., Mouquet, H., Sather, D. N., Lehmann, C., Scheid, J. F., . . . Nussenzweig, M. C. (2012). Broad neutralization by a combination of antibodies recognizing the CD4 binding site and a new conformational epitope on the HIV-1 envelope protein. *J Exp Med, 209*(8), 1469-1479. doi:10.1084/jem.20120423

Ko, C., Michler, T., & Protzer, U. (2017). Novel viral and host targets to cure hepatitis B. *Curr Opin Virol, 24*, 38-45. doi:10.1016/j.coviro.2017.03.019

Kodituwakku, A. P., Jessup, C., Zola, H., & Roberton, D. M. (2003). Isolation of antigen-specific B cells. *Immunol Cell Biol, 81*(3), 163-170. Retrieved from http://dx.doi.org/10.1046/j.1440-1711.2003.01152.x

Kohler, G., & Milstein, C. (1975). Continuous cultures of fused cells secreting antibody of predefined specificity. *Nature, 256*(5517), 495-497. Retrieved from http://dx.doi.org/10.1038/256495a0

Kosinska, A. D., Moeed, A., Kallin, N., Festag, J., Su, J., Steiger, K., . . . Knolle, P. A. (2019). Synergy of therapeutic heterologous prime-boost hepatitis B vaccination with CpG-application to improve immune control of persistent HBV infection. *Sci Rep, 9*(1), 10808. doi:10.1038/s41598-019-47149-w

Kramvis, A. (2014). Genotypes and genetic variability of hepatitis B virus. *Intervirology, 57*(3-4), 141-150. doi:10.1159/000360947

Krebs, K., Bottinger, N., Huang, L. R., Chmielewski, M., Arzberger, S., Gasteiger, G., . . . Protzer, U. (2013). T cells expressing a chimeric antigen receptor that binds hepatitis B virus envelope proteins control virus replication in mice. *Gastroenterology, 145*(2), 456-465. doi:10.1053/j.gastro.2013.04.047

Kruse, R. L., Shum, T., Legras, X., Barzi, M., Pankowicz, F. P., Gottschalk, S., & Bissig, K. D. (2017). In Situ Liver Expression of HBsAg/CD3-Bispecific Antibodies for HBV Immunotherapy. *Mol Ther Methods Clin Dev, 7*, 32-41. doi:10.1016/j.omtm.2017.08.006

Kucinskaite-Kodze, I., Pleckaityte, M., Bremer, C. M., Seiz, P. L., Zilnyte, M., Bulavaite, A., . . . Zvirbliene, A. (2016). New broadly reactive neutralizing antibodies against hepatitis B virus surface antigen. *Virus Res, 211*, 209-221. doi:10.1016/j.virusres.2015.10.024

Kurosaki, T., Kometani, K., & Ise, W. (2015). Memory B cells. *Nat Rev Immunol, 15*(3), 149-159. doi:10.1038/nri3802

Kwok, G., Yau, T. C., Chiu, J. W., Tse, E., & Kwong, Y. L. (2016). Pembrolizumab (Keytruda). *Hum Vaccin Immunother, 12*(11), 2777-2789. doi:10.1080/21645515.2016.1199310

Le Bert, N., Salimzadeh, L., Gill, U. S., Dutertre, C. A., Facchetti, F., Tan, A., . . . Bertoletti, A. (2019). Comparative characterization of B cells specific for HBV

nucleocapsid and envelope proteins in patients with chronic hepatitis B. *J Hepatol*. doi:10.1016/j.jhep.2019.07.015

Leach, D. R., Krummel, M. F., & Allison, J. P. (1996). Enhancement of antitumor immunity by CTLA-4 blockade. *Science, 271*(5256), 1734-1736. doi:10.1126/science.271.5256.1734

Leahy, A. B., Elgarten, C. W., Grupp, S. A., Maude, S. L., & Teachey, D. T. (2018). Tisagenlecleucel for the treatment of B-cell acute lymphoblastic leukemia. *Expert Rev Anticancer Ther, 18*(10), 959-971. doi:10.1080/14737140.2018.1512411

Lefranc, M. P. (2007). IMGT, the international ImMunoGeneTics information system for Immunoinformatics. Methods for querying IMGT databases, tools, and Web resources in the context of immunoinformatics. *Methods Mol Biol, 409*, 19-42. doi:10.1007/978-1-60327-118-9_2

Lefranc, M. P., Giudicelli, V., Duroux, P., Jabado-Michaloud, J., Folch, G., Aouinti, S., . . . Kossida, S. (2015). IMGT(R), the international ImMunoGeneTics information system(R) 25 years on. *Nucleic Acids Res, 43*(Database issue), D413-422. doi:10.1093/nar/gku1056

Levrero, M., & Zucman-Rossi, J. (2016). Mechanisms of HBV-induced hepatocellular carcinoma. *J Hepatol, 64*(1 Suppl), S84-S101. doi:10.1016/j.jhep.2016.02.021

Li, D., He, W., Liu, X., Zheng, S., Qi, Y., Li, H., . . . Sui, J. (2017). A potent human neutralizing antibody Fc-dependently reduces established HBV infections. *Elife, 6*. doi:10.7554/eLife.26738

Liang, T. J., Block, T. M., McMahon, B. J., Ghany, M. G., Urban, S., Guo, J. T., . . . Lok, A. S. (2015). Present and future therapies of hepatitis B: From discovery to cure. *Hepatology, 62*(6), 1893-1908. doi:10.1002/hep.28025

Lipson, E. J., & Drake, C. G. (2011). Ipilimumab: an anti-CTLA-4 antibody for metastatic melanoma. *Clin Cancer Res, 17*(22), 6958-6962. doi:10.1158/1078-0432.CCR-11-1595

Liu, Y., Cheng, L. S., Wu, S. D., Wang, S. Q., Li, L., She, W. M., . . . Jiang, W. (2016). IL-10-producing regulatory B-cells suppressed effector T-cells but enhanced regulatory T-cells in chronic HBV infection. *Clin Sci (Lond), 130*(11), 907-919. doi:10.1042/CS20160069

Llovet, J. M., Ricci, S., Mazzaferro, V., Hilgard, P., Gane, E., Blanc, J. F., . . . Group, S. I. S. (2008). Sorafenib in advanced hepatocellular carcinoma. *N Engl J Med, 359*(4), 378-390. doi:10.1056/NEJMoa0708857

Locarnini, S., Hatzakis, A., Chen, D.-S., & Lok, A. (2015). Strategies to control hepatitis B: Public policy, epidemiology, vaccine and drugs. *Journal of Hepatology, 62*(1, Supplement), S76-S86. doi:http://dx.doi.org/10.1016/j.jhep.2015.01.018

Lonberg, N. (2005). Human antibodies from transgenic animals. *Nat Biotechnol, 23*(9), 1117-1125. doi:10.1038/nbt1135

Loomba, R., & Liang, T. J. (2017). Hepatitis B Reactivation Associated With Immune Suppressive and Biological Modifier Therapies: Current Concepts, Management Strategies, and Future Directions. *Gastroenterology, 152*(6), 1297-1309. doi:10.1053/j.gastro.2017.02.009

Lu, L. L., Suscovich, T. J., Fortune, S. M., & Alter, G. (2018). Beyond binding: antibody effector functions in infectious diseases. *Nat Rev Immunol, 18*(1), 46-61. doi:10.1038/nri.2017.106

Lucifora, J., Xia, Y., Reisinger, F., Zhang, K., Stadler, D., Cheng, X., . . . Protzer, U. (2014). Specific and nonhepatotoxic degradation of nuclear hepatitis B virus cccDNA. *Science, 343*(6176), 1221-1228. doi:10.1126/science.1243462

Ma, Z., Zhang, E., Gao, S., Xiong, Y., & Lu, M. (2019). Toward a Functional Cure for Hepatitis B: The Rationale and Challenges for Therapeutic Targeting of the B Cell Immune Response. *Front Immunol, 10*, 2308. doi:10.3389/fimmu.2019.02308

Maini, M. K., Boni, C., Lee, C. K., Larrubia, J. R., Reignat, S., Ogg, G. S., . . . Bertoletti, A. (2000). The role of virus-specific CD8(+) cells in liver damage and viral control during persistent hepatitis B virus infection. *J Exp Med, 191*(8), 1269-1280. doi:10.1084/jem.191.8.1269

Maini, M. K., Boni, C., Ogg, G. S., King, A. S., Reignat, S., Lee, C. K., . . . Bertoletti, A. (1999). Direct ex vivo analysis of hepatitis B virus-specific CD8(+) T cells associated with the control of infection. *Gastroenterology, 117*(6), 1386-1396. doi:10.1016/s0016-5085(99)70289-1

Maini, M. K., & Peppa, D. (2013). NK cells: a double-edged sword in chronic hepatitis B virus infection. *Front Immunol, 4*, 57. doi:10.3389/fimmu.2013.00057

Manigold, T., & Racanelli, V. (2007). T-cell regulation by CD4 regulatory T cells during hepatitis B and C virus infections: facts and controversies. *Lancet Infect Dis, 7*(12), 804-813. doi:10.1016/S1473-3099(07)70289-X

Markham, A. (2016). Atezolizumab: First Global Approval. *Drugs, 76*(12), 1227-1232. doi:10.1007/s40265-016-0618-8

Markham, A., & Duggan, S. (2018). Cemiplimab: First Global Approval. *Drugs, 78*(17), 1841-1846. doi:10.1007/s40265-018-1012-5

Marks, J. D., Tristem, M., Karpas, A., & Winter, G. (1991). Oligonucleotide primers for polymerase chain reaction amplification of human immunoglobulin variable genes and design of family-specific oligonucleotide probes. *European Journal of Immunology, 21*(4), 985-991. doi:10.1002/eji.1830210419

Meijer, P. J., Andersen, P. S., Haahr Hansen, M., Steinaa, L., Jensen, A., Lantto, J., . . . Nielsen, L. S. (2006). Isolation of human antibody repertoires with preservation of the natural heavy and light chain pairing. *J Mol Biol, 358*(3), 764-772. doi:10.1016/j.jmb.2006.02.040

Michailidis, E., Pabon, J., Xiang, K., Park, P., Ramanan, V., Hoffmann, H. H., . . . Rice, C. M. (2017). A robust cell culture system supporting the complete life cycle of hepatitis B virus. *Sci Rep, 7*(1), 16616. doi:10.1038/s41598-017-16882-5

Michler, T., Kosinska, A. D., Festag, J., Bunse, T., Su, J., Ringelhan, M., . . . Protzer, U. (2020). Knockdown of Virus Antigen Expression Increases Therapeutic Vaccine Efficacy in High-Titer Hepatitis B Virus Carrier Mice. *Gastroenterology*. doi:10.1053/j.gastro.2020.01.032

Milich, D., & Liang, T. J. (2003). Exploring the biological basis of hepatitis B e antigen in hepatitis B virus infection. *Hepatology, 38*(5), 1075-1086. doi:10.1053/jhep.2003.50453

Milich, D. R., McLachlan, A., Thornton, G. B., & Hughes, J. L. (1987). Antibody production to the nucleocapsid and envelope of the hepatitis B virus primed by a single synthetic T cell site. *Nature, 329*(6139), 547-549. doi:10.1038/329547a0

Moody, M. A., & Haynes, B. F. (2008). Antigen-specific B cell detection reagents: use and quality control. *Cytometry A, 73*(11), 1086-1092. doi:10.1002/cyto.a.20599

Morgan, R. A., Dudley, M. E., Wunderlich, J. R., Hughes, M. S., Yang, J. C., Sherry, R. M., . . . Rosenberg, S. A. (2006). Cancer regression in patients after transfer of genetically engineered lymphocytes. *Science, 314*(5796), 126-129. doi:10.1126/science.1129003

Murphy, K., Travers, P., Walport, M., & Janeway, C. (2012). *Janeway's immunobiology*. New York: Garland Science.

Murphy, K., & Weaver, C. (2017). *Janeway's immunobiology*.

Neelapu, S. S., Locke, F. L., Bartlett, N. L., Lekakis, L. J., Miklos, D. B., Jacobson, C. A., . . . Go, W. Y. (2017). Axicabtagene Ciloleucel CAR T-Cell Therapy in Refractory Large B-Cell Lymphoma. *N Engl J Med, 377*(26), 2531-2544. doi:10.1056/NEJMoa1707447

Nemerow, G. R., Wolfert, R., McNaughton, M. E., & Cooper, N. R. (1985). Identification and characterization of the Epstein-Barr virus receptor on human B lymphocytes and its relationship to the C3d complement receptor (CR2). *J Virol, 55*(2), 347-351. Retrieved from https://www.ncbi.nlm.nih.gov/pubmed/2410629

Neumann, A. U., Phillips, S., Levine, I., Ijaz, S., Dahari, H., Eren, R., . . . Naoumov, N. V. (2010). Novel mechanism of antibodies to hepatitis B virus in blocking viral particle release from cells. *Hepatology, 52*(3), 875-885. doi:10.1002/hep.23778

Neumann-Haefelin, C., & Thimme, R. (2018). Entering the spotlight: hepatitis B surface antigen-specific B cells. *J Clin Invest, 128*(10), 4257-4259. doi:10.1172/JCI124098

Nimmerjahn, F., & Ravetch, J. V. (2008). Fcgamma receptors as regulators of immune responses. *Nat Rev Immunol, 8*(1), 34-47. doi:10.1038/nri2206

Offner, S., Hofmeister, R., Romaniuk, A., Kufer, P., & Baeuerle, P. A. (2006). Induction of regular cytolytic T cell synapses by bispecific single-chain antibody constructs on MHC class I-negative tumor cells. *Mol Immunol, 43*(6), 763-771. doi:10.1016/j.molimm.2005.03.007

Patient, R., Hourioux, C., & Roingeard, P. (2009). Morphogenesis of hepatitis B virus and its subviral envelope particles. *Cell Microbiol, 11*(11), 1561-1570. doi:10.1111/j.1462-5822.2009.01363.x

Peeridogaheh, H., Meshkat, Z., Habibzadeh, S., Arzanlou, M., Shahi, J. M., Rostami, S., . . . Teimourpour, R. (2018). Current concepts on immunopathogenesis of hepatitis B virus infection. *Virus Res, 245*, 29-43. doi:10.1016/j.virusres.2017.12.007

Perrillo, R. (2009). Benefits and risks of interferon therapy for hepatitis B. *Hepatology, 49*(S5), S103-S111. doi:10.1002/hep.22956

Pinder, C. L., Kratochvil, S., Cizmeci, D., Muir, L., Guo, Y., Shattock, R. J., & McKay, P. F. (2017). Isolation and Characterization of Antigen-Specific Plasmablasts Using a Novel Flow Cytometry-Based Ig Capture Assay. *J Immunol, 199*(12), 4180-4188. doi:10.4049/jimmunol.1701253

Pinna, D., Corti, D., Jarrossay, D., Sallusto, F., & Lanzavecchia, A. (2009). Clonal dissection of the human memory B-cell repertoire following infection and vaccination. *Eur J Immunol, 39*(5), 1260-1270. doi:10.1002/eji.200839129

Pol, S., Nalpas, B., Driss, F., Michel, M. L., Tiollais, P., Denis, J., . . . Multicenter study, g. (2001). Efficacy and limitations of a specific immunotherapy in chronic hepatitis B. *J Hepatol, 34*(6), 917-921. doi:10.1016/s0168-8278(01)00028-9

Pollicino, T., Cacciola, I., Saffioti, F., & Raimondo, G. (2014). Hepatitis B virus PreS/S gene variants: pathobiology and clinical implications. *J Hepatol, 61*(2), 408-417. doi:10.1016/j.jhep.2014.04.041

Poonia, B., Ayithan, N., Nandi, M., Masur, H., & Kottilil, S. (2018). HBV induces inhibitory FcRL receptor on B cells and dysregulates B cell-T follicular helper cell axis. *Sci Rep, 8*(1), 15296. doi:10.1038/s41598-018-33719-x

Przepiorka, D., Ko, C. W., Deisseroth, A., Yancey, C. L., Candau-Chacon, R., Chiu, H. J., . . . Pazdur, R. (2015). FDA Approval: Blinatumomab. *Clin Cancer Res, 21*(18), 4035-4039. doi:10.1158/1078-0432.CCR-15-0612

Qasim, W., Brunetto, M., Gehring, A. J., Xue, S. A., Schurich, A., Khakpoor, A., . . . Bertoletti, A. (2015). Immunotherapy of HCC metastases with autologous T cell receptor redirected T cells, targeting HBsAg in a liver transplant patient. *J Hepatol, 62*(2), 486-491. doi:10.1016/j.jhep.2014.10.001

Quitt, O. (2020). *Generation and functional characterization of bi- and trispecific antibodies for treatment of chronic hepatitis B*. PhD Thesis.

Raza, A., & Sood, G. K. (2014). Hepatocellular carcinoma review: current treatment, and evidence-based medicine. *World J Gastroenterol, 20*(15), 4115-4127. doi:10.3748/wjg.v20.i15.4115

Reed, W. D., Eddleston, A. L., Cullens, H., Williams, R., Zuckerman, A. J., Peters, D. K., . . . Maycock, W. A. (1973). Infusion of hepatitis-B antibody in antigen-positive active chronic hepatitis. *Lancet, 2*(7842), 1347-1351. doi:10.1016/s0140-6736(73)93321-7

Revill, P. A., Chisari, F. V., Block, J. M., Dandri, M., Gehring, A. J., Guo, H., . . . Zoulim, F. (2019). A global scientific strategy to cure hepatitis B. *Lancet Gastroenterol Hepatol, 4*(7), 545-558. doi:10.1016/s2468-1253(19)30119-0

Rijal, P., Elias, S. C., Machado, S. R., Xiao, J., Schimanski, L., O'Dowd, V., . . . Townsend, A. R. (2019). Therapeutic Monoclonal Antibodies for Ebola Virus Infection Derived from Vaccinated Humans. *Cell Rep, 27*(1), 172-186 e177. doi:10.1016/j.celrep.2019.03.020

Robbins, J. B., Schneerson, R., & Szu, S. C. (1996). Specific Acquired Immunity. In th & S. Baron (Eds.), *Medical Microbiology*. Galveston (TX).

Robert, C., Long, G. V., Brady, B., Dutriaux, C., Maio, M., Mortier, L., . . . Ascierto, P. A. (2015). Nivolumab in previously untreated melanoma without BRAF mutation. *N Engl J Med, 372*(4), 320-330. doi:10.1056/NEJMoa1412082

Rothe, A., Sasse, S., Topp, M. S., Eichenauer, D. A., Hummel, H., Reiners, K. S., . . . Engert, A. (2015). A phase 1 study of the bispecific anti-CD30/CD16A antibody construct AFM13 in patients with relapsed or refractory Hodgkin lymphoma. *Blood, 125*(26), 4024-4031. doi:10.1182/blood-2014-12-614636

Safaie, P., Poongkunran, M., Kuang, P. P., Javaid, A., Jacobs, C., Pohlmann, R., . . . Lau, D. T. (2016). Intrahepatic distribution of hepatitis B virus antigens in patients with and without hepatocellular carcinoma. *World J Gastroenterol, 22*(12), 3404-3411. doi:10.3748/wjg.v22.i12.3404

Salazar, G., Zhang, N., Fu, T. M., & An, Z. (2017). Antibody therapies for the prevention and treatment of viral infections. *NPJ Vaccines, 2*, 19. doi:10.1038/s41541-017-0019-3

Salimzadeh, L., Le Bert, N., Dutertre, C. A., Gill, U. S., Newell, E. W., Frey, C., . . . Bertoletti, A. (2018). PD-1 blockade partially recovers dysfunctional virus-specific B cells in chronic hepatitis B infection. *J Clin Invest, 128*(10), 4573-4587. doi:10.1172/JCI121957

Scheid, J. F., Mouquet, H., Feldhahn, N., Seaman, M. S., Velinzon, K., Pietzsch, J., . . . Nussenzweig, M. C. (2009). Broad diversity of neutralizing antibodies isolated from memory B cells in HIV-infected individuals. *Nature, 458*(7238), 636-640. doi:10.1038/nature07930

Scheid, J. F., Mouquet, H., Feldhahn, N., Walker, B. D., Pereyra, F., Cutrell, E., . . . Nussenzweig, M. C. (2009). A method for identification of HIV gp140 binding memory B cells in human blood. *J Immunol Methods, 343*(2), 65-67. doi:10.1016/j.jim.2008.11.012

Scheid, J. F., Mouquet, H., Ueberheide, B., Diskin, R., Klein, F., Oliveira, T. Y., . . . Nussenzweig, M. C. (2011). Sequence and structural convergence of broad and

potent HIV antibodies that mimic CD4 binding. *Science, 333*(6049), 1633-1637. doi:10.1126/science.1207227

Schilling, R., Ijaz, S., Davidoff, M., Lee, J. Y., Locarnini, S., Williams, R., & Naoumov, N. V. (2003). Endocytosis of hepatitis B immune globulin into hepatocytes inhibits the secretion of hepatitis B virus surface antigen and virions. *J Virol, 77*(16), 8882-8892. doi:10.1128/jvi.77.16.8882-8892.2003

Seeger, C., & Mason, W. S. (2015). Molecular biology of hepatitis B virus infection. *Virology, 479-480*, 672-686. doi:10.1016/j.virol.2015.02.031

Seifert, M., & Kuppers, R. (2016). Human memory B cells. *Leukemia, 30*(12), 2283-2292. doi:10.1038/leu.2016.226

Seimetz, D., Lindhofer, H., & Bokemeyer, C. (2010). Development and approval of the trifunctional antibody catumaxomab (anti-EpCAM x anti-CD3) as a targeted cancer immunotherapy. *Cancer Treat Rev, 36*(6), 458-467. doi:10.1016/j.ctrv.2010.03.001

Seto, W. K., Cheung, K. S., Wong, D. K., Huang, F. Y., Fung, J., Liu, K. S., . . . Yuen, M. F. (2016). Hepatitis B surface antigen seroclearance during nucleoside analogue therapy: surface antigen kinetics, outcomes, and durability. *J Gastroenterol, 51*(5), 487-495. doi:10.1007/s00535-015-1128-2

Setten, R. L., Rossi, J. J., & Han, S. P. (2019). The current state and future directions of RNAi-based therapeutics. *Nat Rev Drug Discov, 18*(6), 421-446. doi:10.1038/s41573-019-0017-4

Smith, K., Garman, L., Wrammert, J., Zheng, N. Y., Capra, J. D., Ahmed, R., & Wilson, P. C. (2009). Rapid generation of fully human monoclonal antibodies specific to a vaccinating antigen. *Nat Protoc, 4*(3), 372-384. doi:10.1038/nprot.2009.3

Smith, M. J., Packard, T. A., O'Neill, S. K., Hinman, R. M., Rihanek, M., Gottlieb, P. A., & Cambier, J. C. (2017). Detection and Enrichment of Rare Antigen-specific B Cells for Analysis of Phenotype and Function. *J Vis Exp*(120). doi:10.3791/55382

Smith, S. A., & Crowe, J. E., Jr. (2015). Use of Human Hybridoma Technology To Isolate Human Monoclonal Antibodies. *Microbiol Spectr, 3*(1), AID-0027-2014. doi:10.1128/microbiolspec.AID-0027-2014

Smith, S. L. (1996). Ten years of Orthoclone OKT3 (muromonab-CD3): a review. *J Transpl Coord, 6*(3), 109-119; quiz 120-101. doi:10.7182/prtr.1.6.3.8145l3u185493182

Socinski, M. A., Jotte, R. M., Cappuzzo, F., Orlandi, F., Stroyakovskiy, D., Nogami, N., . . . Group, I. M. S. (2018). Atezolizumab for First-Line Treatment of Metastatic Nonsquamous NSCLC. *N Engl J Med, 378*(24), 2288-2301. doi:10.1056/NEJMoa1716948

Steinitz, M. (2014). Production of human monoclonal antibodies by the epstein-barr virus method. *Methods Mol Biol, 1060*, 111-122. doi:10.1007/978-1-62703-586-6_6

Steinitz, M., Klein, G., Koskimies, S., & Makel, O. (1977). EB virus-induced B lymphocyte cell lines producing specific antibody. *Nature, 269*(5627), 420-422. Retrieved from http://dx.doi.org/10.1038/269420a0

Suffner, S., Gerstenberg, N., Patra, M., Ruibal, P., Orabi, A., Schindler, M., & Bruss, V. (2018). Domains of the Hepatitis B Virus Small Surface Protein S Mediating Oligomerization. *J Virol, 92*(11). doi:10.1128/JVI.02232-17

Suurs, F. V., Lub-de Hooge, M. N., de Vries, E. G. E., & de Groot, D. J. A. (2019). A review of bispecific antibodies and antibody constructs in oncology and clinical challenges. *Pharmacol Ther, 201*, 103-119. doi:10.1016/j.pharmthera.2019.04.006

Tajiri, K., Ozawa, T., Jin, A., Tokimitsu, Y., Minemura, M., Kishi, H., . . . Muraguchi, A. (2010). Analysis of the epitope and neutralizing capacity of human monoclonal antibodies induced by hepatitis B vaccine. *Antiviral Res, 87*(1), 40-49. doi:10.1016/j.antiviral.2010.04.006

Tan, A., Koh, S., & Bertoletti, A. (2015). Immune Response in Hepatitis B Virus Infection. *Cold Spring Harb Perspect Med, 5*(8), a021428. doi:10.1101/cshperspect.a021428

Tan, A. T., & Schreiber, S. Adoptive T-cell therapy for HBV-associated HCC and HBV infection. (1872-9096 (Electronic)).

Tan, W., Meng, Y., Li, H., Chen, Y., Han, S., Zeng, J., . . . Guo, Y. (2013). A bispecific antibody against two different epitopes on hepatitis B surface antigen has potent hepatitis B virus neutralizing activity. *MAbs, 5*(6), 946-955. doi:10.4161/mabs.26390

Terrault, N. A., Lok, A. S. F., McMahon, B. J., Chang, K. M., Hwang, J. P., Jonas, M. M., . . . Wong, J. B. (2018). Update on prevention, diagnosis, and treatment of chronic hepatitis B: AASLD 2018 hepatitis B guidance. *Hepatology, 67*(4), 1560-1599. doi:10.1002/hep.29800

Thimme, R., Wieland, S., Steiger, C., Ghrayeb, J., Reimann, K. A., Purcell, R. H., & Chisari, F. V. (2003). CD8(+) T cells mediate viral clearance and disease pathogenesis during acute hepatitis B virus infection. *J Virol, 77*(1), 68-76. Retrieved from http://www.ncbi.nlm.nih.gov/pubmed/12477811

Tian, C., Chen, Y., Liu, Y., Wang, S., Li, Y., Wang, G., . . . Wu, C. (2018). Use of ELISpot assay to study HBs-specific B cell responses in vaccinated and HBV infected humans. *Emerg Microbes Infect, 7*(1), 16. doi:10.1038/s41426-018-0034-0

Tiller, T. (2011). Single B cell antibody technologies. *N Biotechnol, 28*(5), 453-457. doi:10.1016/j.nbt.2011.03.014

Tiller, T., Meffre, E., Yurasov, S., Tsuiji, M., Nussenzweig, M. C., & Wardemann, H. (2008). Efficient generation of monoclonal antibodies from single human B cells by single cell RT-PCR and expression vector cloning. *J Immunol Methods, 329*(1-2), 112-124. doi:10.1016/j.jim.2007.09.017

Townsend, S. E., Goodnow, C. C., & Cornall, R. J. (2001). Single epitope multiple staining to detect ultralow frequency B cells. *J Immunol Methods, 249*(1-2), 137-146. doi:10.1016/s0022-1759(00)00352-5

Traggiai, E., Becker, S., Subbarao, K., Kolesnikova, L., Uematsu, Y., Gismondo, M. R., . . . Lanzavecchia, A. (2004). An efficient method to make human monoclonal antibodies from memory B cells: potent neutralization of SARS coronavirus. *Nat Med, 10*(8), 871-875. doi:10.1038/nm1080

Tsuge, M., Hiraga, N., Uchida, T., Kan, H., Miyaki, E., Masaki, K., . . . Chayama, K. (2016). Antiviral effects of anti-HBs immunoglobulin and vaccine on HBs antigen seroclearance for chronic hepatitis B infection. *J Gastroenterol, 51*(11), 1073-1080. doi:10.1007/s00535-016-1189-x

Tuaillon, E., Tabaa, Y. A., Petitjean, G., Huguet, M. F., Pajeaux, G., Fondere, J. M., . . . Vendrell, J. P. (2006). Detection of memory B lymphocytes specific to hepatitis B virus (HBV) surface antigen (HBsAg) from HBsAg-vaccinated or HBV-immunized subjects by ELISPOT assay. *J Immunol Methods, 315*(1-2), 144-152. doi:10.1016/j.jim.2006.07.016

Vaillant, A. (2019). REP 2139: Antiviral Mechanisms and Applications in Achieving Functional Control of HBV and HDV Infection. *ACS Infect Dis, 5*(5), 675-687. doi:10.1021/acsinfecdis.8b00156

Valats, J. C., Tuaillon, E., Funakoshi, N., Hoa, D., Brabet, M. C., Bollore, K., . . . Blanc, P. (2010). Investigation of memory B cell responses to hepatitis B surface antigen in health care workers considered as non-responders to vaccination. *Vaccine, 28*(39), 6411-6416. doi:10.1016/j.vaccine.2010.07.058

Valle, A., Zuber, C. E., Defrance, T., Djossou, O., De Rie, M., & Banchereau, J. (1989). Activation of human B lymphocytes through CD40 and interleukin 4. *Eur J Immunol, 19*(8), 1463-1467. doi:10.1002/eji.1830190818

van Nunen, A. B., Baumann, M., Manns, M. P., Reichen, J., Spengler, U., Marschner, J. P., . . . International Study, G. (2001). Efficacy and safety of an intravenous monoclonal anti-HBs in chronic hepatitis B patients. *Liver, 21*(3), 207-212. doi:10.1034/j.1600-0676.2001.021003207.x

van Nunen, A. B., de Man, R. A., Heijtink, R. A., Vossen, A. C., & Schalm, S. W. (2002). Passive immunization of chronic hepatitis B patients on lamivudine therapy: a feasible issue? *J Viral Hepat, 9*(3), 221-228. doi:10.1046/j.1365-2893.2002.00337.x

Velkov, S., Ott, J. J., Protzer, U., & Michler, T. (2018). The Global Hepatitis B Virus Genotype Distribution Approximated from Available Genotyping Data. *Genes (Basel), 9*(10). doi:10.3390/genes9100495

Vidarsson, G., Dekkers, G., & Rispens, T. (2014). IgG subclasses and allotypes: from structure to effector functions. *Front Immunol, 5*, 520. doi:10.3389/fimmu.2014.00520

Villanueva, A. (2019). Hepatocellular Carcinoma. *N Engl J Med, 380*(15), 1450-1462. doi:10.1056/NEJMra1713263

Wallace, L. E., Young, L. S., Rowe, M., Rowe, D., & Rickinson, A. B. (1987). Epstein-Barr virus-specific T-cell recognition of B-cell transformants expressing different EBNA 2 antigens. *Int J Cancer, 39*(3), 373-379. doi:10.1002/ijc.2910390317

Walsh, P. N., Friedrich, D. P., Williams, J. A., Smith, R. J., Stewart, T. L., Carter, D. K., . . . Network, N. H. V. T. (2013). Optimization and qualification of a memory B-cell ELISpot for the detection of vaccine-induced memory responses in HIV vaccine trials. *J Immunol Methods, 394*(1-2), 84-93. doi:10.1016/j.jim.2013.05.007

Wang, W., Sun, L., Li, T., Ma, Y., Li, J., Liu, Y., . . . Tong, S. (2016). A human monoclonal antibody against small envelope protein of hepatitis B virus with potent neutralization effect. *MAbs, 8*(3), 468-477. doi:10.1080/19420862.2015.1134409

Wang, X., Mathieu, M., & Brezski, R. J. (2018). IgG Fc engineering to modulate antibody effector functions. *Protein Cell, 9*(1), 63-73. doi:10.1007/s13238-017-0473-8

Ward, S. M., Phalora, P., Bradshaw, D., Leyendeckers, H., & Klenerman, P. (2008). Direct ex vivo evaluation of long-lived protective antiviral memory B cell responses against hepatitis B virus. *J Infect Dis, 198*(6), 813-817. doi:10.1086/591094

Wardemann, H., Yurasov, S., Schaefer, A., Young, J. W., Meffre, E., & Nussenzweig, M. C. (2003). Predominant autoantibody production by early human B cell precursors. *Science, 301*(5638), 1374-1377. doi:10.1126/science.1086907

Watanabe, T., Sorensen, E. M., Naito, A., Schott, M., Kim, S., & Ahlquist, P. (2007). Involvement of host cellular multivesicular body functions in hepatitis B virus budding. *Proc Natl Acad Sci U S A, 104*(24), 10205-10210. doi:10.1073/pnas.0704000104

Wherry, E. J., & Kurachi, M. (2015). Molecular and cellular insights into T cell exhaustion. *Nat Rev Immunol, 15*(8), 486-499. doi:10.1038/nri3862

Wherry, E. J., & Masopust, D. (2016). Chapter 5 - Adaptive Immunity: Neutralizing, Eliminating, and Remembering for the Next Time. In M. G. Katze, M. J. Korth, G. L. Law, & N. Nathanson (Eds.), *Viral Pathogenesis (Third Edition)* (pp. 57-69). Boston: Academic Press.

Wieland, S. F. (2015). The chimpanzee model for hepatitis B virus infection. *Cold Spring Harb Perspect Med, 5*(6). doi:10.1101/cshperspect.a021469

Wieland, S. F., & Chisari, F. V. (2005). Stealth and cunning: hepatitis B and hepatitis C viruses. *J Virol, 79*(15), 9369-9380. doi:10.1128/JVI.79.15.9369-9380.2005

Wiesner, M., Zentz, C., Mayr, C., Wimmer, R., Hammerschmidt, W., Zeidler, R., & Moosmann, A. (2008). Conditional immortalization of human B cells by CD40 ligation. *PLoS One, 3*(1), e1464. doi:10.1371/journal.pone.0001464

Wisskirchen, K., Kah, J., Malo, A., Asen, T., Volz, T., Allweiss, L., . . . Protzer, U. (2019). T cell receptor grafting allows virological control of Hepatitis B virus infection. *J Clin Invest, 129*(7), 2932-2945. doi:10.1172/JCI120228

Wisskirchen, K., Metzger, K., Schreiber, S., Asen, T., Weigand, L., Dargel, C., . . . Protzer, U. (2017). Isolation and functional characterization of hepatitis B virus-specific T-cell receptors as new tools for experimental and clinical use. *PLoS One, 12*(8), e0182936. doi:10.1371/journal.pone.0182936

Woda, M., & Mathew, A. (2015). Fluorescently labeled dengue viruses as probes to identify antigen-specific memory B cells by multiparametric flow cytometry. *J Immunol Methods, 416*, 167-177. doi:10.1016/j.jim.2014.12.001

Wong, V. C., Ip, H. M., Reesink, H. W., Lelie, P. N., Reerink-Brongers, E. E., Yeung, C. Y., & Ma, H. K. (1984). Prevention of the HBsAg carrier state in newborn infants of mothers who are chronic carriers of HBsAg and HBeAg by administration of hepatitis-B vaccine and hepatitis-B immunoglobulin. Double-blind randomised placebo-controlled study. *Lancet, 1*(8383), 921-926. doi:10.1016/s0140-6736(84)92388-2

World Health Organization. (2019). Hepatitis B Retrieved from https://www.who.int/news-room/fact-sheets/detail/hepatitis-b

Wu, Y. C., Kipling, D., & Dunn-Walters, D. K. (2011). The relationship between CD27 negative and positive B cell populations in human peripheral blood. *Front Immunol, 2*, 81. doi:10.3389/fimmu.2011.00081

Wynne, S. A., Crowther, R. A., & Leslie, A. G. (1999). The crystal structure of the human hepatitis B virus capsid. *Mol Cell, 3*(6), 771-780. doi:10.1016/s1097-2765(01)80009-5

Xia, Y., Stadler, D., Ko, C., & Protzer, U. (2017). Analyses of HBV cccDNA Quantification and Modification. *Methods Mol Biol, 1540*, 59-72. doi:10.1007/978-1-4939-6700-1_6

Yan, H., Zhong, G., Xu, G., He, W., Jing, Z., Gao, Z., . . . Li, W. (2012). Sodium taurocholate cotransporting polypeptide is a functional receptor for human hepatitis B and D virus. *Elife, 3*. doi:10.7554/eLife.00049

Yang, J. D., Hainaut, P., Gores, G. J., Amadou, A., Plymoth, A., & Roberts, L. R. (2019). A global view of hepatocellular carcinoma: trends, risk, prevention and management. *Nat Rev Gastroenterol Hepatol, 16*(10), 589-604. doi:10.1038/s41575-019-0186-y

Yang, S. H., Lee, C. G., Park, S. H., Im, S. J., Kim, Y. M., Son, J. M., . . . Sung, Y. C. (2006). Correlation of antiviral T-cell responses with suppression of viral rebound in chronic hepatitis B carriers: a proof-of-concept study. *Gene Ther, 13*(14), 1110-1117. doi:10.1038/sj.gt.3302751

Yuen, M. F., Schiefke, I., Yoon, J. H., Ahn, S. H., Heo, J., Kim, J. H., . . . Gish, R. G. (2019). RNA Interference Therapy with ARC-520 Results in Prolonged HBsAg

Response in Patients with Chronic Hepatitis B Infection. *Hepatology*. doi:10.1002/hep.31008

Zhang, T. Y., Yuan, Q., Zhao, J. H., Zhang, Y. L., Yuan, L. Z., Lan, Y., . . . Xia, N. S. (2016). Prolonged suppression of HBV in mice by a novel antibody that targets a unique epitope on hepatitis B surface antigen. *Gut, 65*(4), 658-671. doi:10.1136/gutjnl-2014-308964

Zoulim, F., & Durantel, D. (2015). Antiviral therapies and prospects for a cure of chronic hepatitis B. *Cold Spring Harb Perspect Med, 5*(4). doi:10.1101/cshperspect.a021501

Acknowledgements

First of all I would like to thank Prof. Ulrike Protzer for giving me the opportunity to do my PhD thesis in her lab on this very exciting and challenging project. You provided support and advices when necessary and always found time for urgent questions and help, but you also allowed me to develop into an independent scientist.

I would like to thank Prof. Aphrodite Kapurniotu, my second supervisor, you provided valuable input during my thesis committee meetings. Additionally, I want to thank Prof. Jane McKeating and Dr. Felix Bohne as members of my thesis committee. Without you Dr. Bohne, I would not have started this PhD thesis.

Moreover, I would like to thank the members of the former AG Bohne, Oliver Quitt, Sebastian Altstetter and Lili Zhao and Dr. Francesca Pinci as well as Fenna Kolbe, Sophia Schreiber and Anindita Chakraborty for help with experiments and fruitful discussions.

Special thanks go to Theresa Asen and Romina Bester, you are among the most important people in this lab, without your organizational help, no orders, replacements and repairs would take place.

Furthermore, I would like to thank all other current and former lab members especially naming Dr. Julia Festag, Dr. Wen-Min Chou, Dr. Anna Konsinska, Antje Malo, Christoph Blossey, Florian Wilsch, Dr. Jochen Wettengel, Dr. Marvin Festag, Dr. Chunkyu Ko, Philipp Hagen, Jinpeng Su, Dr. Karin Wisskirchen, Julia Sacherl, Dr. Kathrin Singethan, Martin Kächele, Stoyan Velkov, Andreas Oswald, Dr. Thomas Michler, Dr. Maarten van der Klundert, Natalie Röder, Hortenzia Imhof and Susanne Miko for their direct or indirect support and help to complete this work and to create a great working atmosphere.

Additionally, I would like to thank all members of the virology diagnostics department, if there were urgent and spontaneous measurements needed. Thank you Raza and Marinka for making our lab life to comfortable! Thank you Doris Pelz, Daniela Rizzi,

Halid Musanovic and Dr. Frank Thiele for your support regarding office work and experiment approvals.

Special thanks go to Immanuel Andrä, Lynette Henkel, Corinne Angerpointer and Dr. Matthias Schiemann from the Flow Cytometry Unit for the continuous support regarding cell sorting.

I would like to thank my cooperation partners, Dr. Valeria Falcone, Dr. Philipp Kolb, Prof. Hartmut Hengel, Dr. Wenshi Wang, Prof. Stephan Urban, Dr. Christoph Kreer and Prof. Florian Klein for providing material, experimental support and scientific advice.

As a member of the IRTG TRR 179 for “Determinants and dynamics of elimination versus persistence of hepatitis virus infection”, I would like to thank all members in Freiburg, Heidelberg and Munich for scientific discussions during seminars, symposia and retreats.

I am grateful to my parents, my brother and my friends. Thank you for all your support throughout my life, for all thoughts, helps, wonderful moments and your encouragement to continue when I needed it.

Lastly and importantly, I would like to thank Felix. You supported me in every possible way during this thesis. You helped me to climb up this high mountain encouraged me to always carry on especially when I was close to drop out. I would not have made it without you. THANK YOU!